The Climate Controls and Process of Groundwater Recharge in a Semi-Arid Tropical Environment: Evidence from the Makutapora Basin, Tanzania

A thesis submitted for the degree of Doctor of Philosophy

David Seddon

UCL

Declaration

I, David Seddon, confirm that the work presented in this thesis is my own. Where information has been derived from other sources, I confirm that this has been indicated in the thesis.

…………….....

David Seddon

24th June 2019

Abstract

Groundwater is a vital source of freshwater in semi-arid sub-Saharan Africa. Climate change, to which this region is particularly vulnerable, and increasing water demand are expected to increase the strategic importance of groundwater. The responses of groundwater systems to these forcings remain unclear. Here, in the intensively monitored and pumped groundwater system in the Makutapora Basin of central Tanzania, an analogue for semi-arid tropical areas underlain by weathered and fractured crystalline rock aquifers, I: (1) assess the relationship between precipitation intensity and groundwater recharge, (2) delineate the predominant recharge processes, and (3) project the impacts of climate change and increasing groundwater abstraction on future groundwater resources. Analysis of one of the longest known groundwater-level records in tropical Africa using a modified water-table fluctuation method, incorporating a numerical flow model to account for transience in response to pumping, shows more intensive precipitation disproportionately generates groundwater recharge. This bias is corroborated by a comparison of the stable-isotope composition of groundwater and precipitation as a function of intensity. Recharge is shown to occur via leakage from ephemeral streambeds through the formation and decay of groundwater 'mounds'. Stable-isotope tracers and hydrometric evidence of streambed inundation confirm the predominance of focused recharge pathways. Projections of groundwater resources, using a fully integrated MIKE SHE/MIKE 11 model, indicate that changes to recharge due to climate change will be small in the context of likely increases in groundwater abstraction. However, the bias of disproportionate groundwater recharge production from intensive precipitation, together with new insight regarding the processes and controls of recharge in this semi-arid environment, suggest that climate change may not only enhance groundwater recharge but also enable strategies (e.g. Managed Aquifer Recharge) to artificially enhance the sustainability of groundwater withdrawals since these events and processes are predictable.

Impact Statement

Ultimately, the aim of this research was to better understand the processes and controls which govern groundwater recharge in semi-arid environments of sub-Saharan Africa. This thesis contributes to diminishing knowledge gaps explicitly highlighted by the IPCC, and aids with pragmatic, local water management and will, accordingly, have impacts both inside and outside academia.

Analysis of the impact of precipitation intensity indicated that more intensive events produce a disproportionate amount of groundwater recharge. This has wide reaching implications for sustainable water management and future research. As the intensification of precipitation is one of the more certain and ubiquitous projected climate changes altering the hydrological cycle, we have improved understanding of the likely impact of climate change on groundwater resources. Accordingly, assessments of groundwater's viability for climate change adaptation, and its use in sustainable water management will be more robust. Furthermore, the importance of explicitly accounting for the intensification of precipitation in academic work projecting groundwater resources has been highlighted. An improved understanding of the processes by which meteoric water is transmitted to the saturated zone also facilitates more robust future work. Delineation of recharge pathways facilitates improved projections of groundwater quantity and quality, groundwater resources assessments, and evaluations of engineering solutions to artificially enhance recharge.

Observational data of groundwater resources in Africa are extremely limited, which has stymied the detection and attribution of climate change impacts on groundwater resources, and therefore, limits projections of groundwater availability. This research required the implementation of a novel, high-resolution groundwater and surface water monitoring array in the Makutapora Basin. This will contribute to reducing the data gap as it has been handed over to the Tanzanian government and will continue to produce high-quality data to aid in monitoring a vital source of water.

In undertaking this research in an actively pumped system, a circumstance which similar research often neglects, new techniques, which can be implemented in other pumped systems, were developed to account for transient recessions of groundwater. These new, or modified, methods proved useful in estimating groundwater recharge, delineating recharge processes, and projecting renewable groundwater resources under scenarios of climate change and water demand. The development of techniques applicable in pumped systems facilitates research in often neglected systems.

The primary benefits of this research outside academia will be pragmatic, local benefits for Dodoma. An improved understanding of the processes that govern groundwater recharge allows for a more comprehensive assessment of sustainable management of the Makutapora Wellfield. Tentative first steps have been made towards assessing the viability of engineering solutions to artificially enhance groundwater recharge to improve sustainability.

The legacy of this research will be greater than the implications of the analysis presented here. The Makutapora Basin is a single study site in the GroFutures project which aims to develop the scientific basis and participatory management processes by which groundwater resources can be used sustainably for poverty alleviation.

Acknowledgements

I would like to thank everyone, directly and indirectly, responsible for the completion of this research. My supervisors: Professor Richard Taylor, Dr Mohammad Shamsudduha, and Dr Mark Cuthbert, deserve the most thanks for their excellent supervision. I would also like to thank: members of the GroFutures team; members of the Banking the Rains team; our colleges from Sokoine University of Agriculture: Professor Japhet Kashaigili, Richard Festo, and Hezron Philipo; Dodoma Urban Water Supply And Sewerage Authority and its staff: Lucas Mihale, Catherine Kongola, and Alloice Kaponda; WAMI/RUVU Basin Water Office and its staff: Praxeda Kalugendo and Rosemary Masikini; and the Tanzanian Ministry of Water and Irrigation. This research was funded by the Natural Environment Research Council.

Table of Contents

List of Figures

List of Tables

List of Initialisms and Acronyms

CMB (Chloride Mass Balance)

CMIP5 (Coupled Model Intercomparison Project – Phase 5)

DEM (Digital Elevation Model)

DUWASA (Dodoma Urban Water and Sewerage Authority)

ESA (European Space Agency)

ET_o (Reference Evapotranspiration)

GCM (General Circulation Model)

IPCC (Intergovernmental Panel on Climate Change)

JICA (Japan International Co-operation Agency)

LAI (Leaf Area Index)

LEL (Local Evaporation Line)

LMWL (Local Meteoric Water Line)

MAR (Managed Aquifer Recharge)

MRC (Master Recession Curve method)

NSE (Nash Sutcliffe Efficiency)

RCP (Representative Concentration Pathway)

RD (Root Depth)

RMSE (Root Mean Square Error)

SHE (Système Hydrologique Européen)

SMOW (Standard Mean Ocean Water)

SRTM (Shuttle Radar Topography Mission)

WMO (World Meteorological Organization)

WTF (Water Table Fluctuation method)

Chapter 1

Introduction

1.1 Freshwater in Africa

Superficially, Africa has abundant freshwater resources. The continent is home to some of the largest lakes and longest rivers in the world, and average precipitation is commensurate with Europe and North America (FAO, 2018a). Renewable freshwater resources account for 9% of the global total (WWP, 2017), absolutely more than Australia, and more per capita than Asia (FAO, 2018b). Additionally, Africa's groundwater storage is estimated to be more than 100 times greater than its renewable freshwater resources (MacDonald et al., 2012). Despite this apparent abundance of water, water supplies across much of Africa are inadequate (ECA, 2006; UN, 2015a; WHO/UNICEF, 2008). There are more water-stressed countries in Sub-Saharan Africa than any other region on the planet (Bureau and Strobl, 2016). 42% of its residents are without access to basic drinking water services, and 72% are without access to basic sanitation services (WHO/UNICEF, 2017).

The physical genesis of this water scarcity, "the reliable availability of an acceptable quantity and quality of water for health, livelihoods and production, coupled with an acceptable level of water-related risks" (Grey and Sadoff, 2007), is the uneven distribution of exploitable water resources in both space and time (Wang et al., 2014). Africa's climate is characterised by erratic precipitation (UNEP, 2010), which is markedly variable at intra-annual (Peel et al., 2001), annual (Nicholson, 1998), and decadal to millennial (Nicholson, 2000) timescales. Some areas additionally experience stark seasonal differences, with little or no precipitation for consecutive months during dry seasons (UNEP, 2010). Accordingly, soil moisture and surface water resources are neither perennial nor ubiquitous (UNECA/AU/AfDB, 2003). This is particularly pertinent in arid and semi-arid regions where potential evaporation is high. Accordingly, these environments are susceptible to drought. Africa has the highest drought frequency of all continents (Gautam, 2006).

Due to land availability, natural disaster risk, disease, conflict, and historical geographic boundaries, the spatial distribution of Africa's population does not correspond with the distribution of water as well as other biodiversity (UNEP, 2010). For example, Central Africa (Economic Community of Central African States members) accounts for 22% of Africa's land area, 15% of its population, but over 50% of the continent's renewable water resources (FAO, 2018a). This is concomitantly compensated by more poorly resourced areas. Eastern Africa's share is less than one tenth of the resources of Central Africa, despite a much larger population (UN, 2015a). These regional and international differences are driven by variations in endogenous precipitation and exogenous incoming flows, which are governed by climate and geography.

Synoptic scale (~1000 km), cloud-cluster scale (~300 – 1000 km), mesoscale (~10 – 300 km), and cumulus scale (~1 – 10 Km) controls determine the spatiotemporal distribution of precipitation (Houze and Cheng, 1977) and result in highly changeable climatic patterns over short distances (Nicholson, 1996). Atmospheric controls are superimposed on variable regional geographic controls, such as surface water, topography, and maritime influences (Nicholson, 1996). Accordingly, transitions from arid desert to humid forest can occur over small changes in location and altitude (Nicholson, 1996). This uneven distribution of water in time and relative to population inhibits water security (UNEP, 2002).

Human well-being, socioeconomic development, livelihoods, and protection against water-related disasters are all hampered by water insecurity (UN, 2013). Accordingly, poverty and underdevelopment are rife (Beegle et al., 2016), which has left Africa languishing as the poorest and least developed continent (UNEP, 2010). Inadequate water provision and stunted development have reinforced one another, establishing a ‘poverty trap’ (Azariadis and Stachurski, 2005). Deficient access to water is simultaneously a cause and consequence of poverty. Insufficient quantity or inadequate quality of water limits food security through low productivity, inhibits poverty alleviation, constrains health, and hinders economic development, growth, and recovery (UNEP, 2010). Lack of development constrains the development of water supplies (UNECA/AU/AfDB, 2003), which incites economic water scarcity (FAO, 2009). This feedback loop has left the population as one of the most vulnerable in the world (Hunter et al., 2010). Sub-Saharan Africa has struggled to effectively rectify these problems despite the implementation of various schemes, such as Africa Water Vision 2025 (UNECA/AU/AfDB, 2003), the Millennium Development Goals (UN, 2015b), and the Sustainable Development Goals (UN, 2018a). At the turn of the millennium, poverty was predicted to rise in Africa, while decreasing on every other continent (UNECA/AU/AfDB, 2003). 16 years later, Sub-Saharan Africa failed to make “good progress” on several water-related Millennium Development Goals, such as reducing extreme poverty by half, reducing hunger by half, and halving the proportion of the population without sanitation (UN, 2015b).

As a result of insufficient developmental progress, domestic water supplies in Africa remain the least adequate in the world. Just over half the rural population has access to ‘improved’ drinking water (Carter et al., 2017). The urban water supply is markedly better with 87% having access to ‘improved’ drinking water (Carter et al., 2017). The proportion of urban dwellings connected to reticulated supplies, however, has been in decline. In 2005, considerably fewer households were connected to piped water than in the early 1990s (50% to 39%) (Banerjee et al., 2008). This is due, in part, to the highest urban growth rate in the world (Jacobsen et al., 2012). Due to inadequate planning and lack of investment, population growth has outpaced improvements to municipal supplies (Banerjee et al., 2008). Rapidly growing populations are one of the primary driving forces constraining progress towards improved water provision and sanitation (UNEP, 2010). This stasis has left only 58% of sub-Saharan Africans with access to improved water sources (Carter et al., 2017), and 43% in extreme poverty (Beegle et al., 2016). Shortcomings to the domestic water supply have contributed to Africans having a life expectancy of 60 years (UN, 2015b). Moreover, of the 34 countries with the highest rates of ‘under-5 mortality’, 32 are African nations (CIA, 2016). Short life spans are a stark illustration of the ramifications of Africa’s water crisis as the probability of death between birth and the age of 5 is seen as a good indicator of the development and well-being of children (UN, 2015b).

Water security is inherently linked to food security and the economic prosperity of sub-Saharan Africa (Conway et al., 2009; Rockstrom and Karlberg, 2009). Shortages of water results in chronic food insecurity throughout Africa. 23.3% of the sub-Saharan African population is undernourished (FAO, 2015) and population growth is outpacing improvements to food security

(UN, 2015b). Moreover, suboptimal agricultural production has negative consequences for the economic outlook of the continent. The agricultural sector is the single most important driver of economic growth (Conway et al., 2009), it employs 60% of Africa's workforce (UNECA, 2008), and 90% of rural dwellers' income is derived from farming (UNECA, 2008). Accordingly, economic prosperity depends on the water supply.

Poorly performing economies lead to considerable fiscal constraints, which cause frugal budgetary allocations for, amongst others, health, education, and development of water resources (UNECA/AU/AfDB, 2003). Ironically, the necessary expenditure to improve water supplies in order to achieve all of the Millennium Development Goals is estimated to be less than 10% of the savings associated with improved health and time-saving (Banerjee et al., 2008). Yet due to a poverty trap, Africa succumbs to water scarcity.

1.2 The Importance of Groundwater in Africa

Sustainably managed groundwater appears to be intrinsic to successfully ridding sub-Saharan Africa of several of its most salient developmental impediments (Grey and Sadoff, 2007; Hunter et al., 2010) as it will reduce poverty (Falkenmark et al., 1989), improve food security (FAO, 2009), and stimulate economic growth (Conway et al., 2009). The effectiveness of the response to Africa's socio-economic crisis, and adaptation to impending water demand changes, is contingent on the access to sustainable groundwater resources (UNECA/AU/AfDB, 2003).

Groundwater is seen as fundamental to the future prosperity of Africa because it holds several key advantages over other sources of water. Compared to surface water, groundwater is more extensively distributed (Shiklomanov and Rodda, 2004). In some locations, particularly rural arid or semi-arid regions, it is the only feasible source of water (Robins et al., 2006). This is partly due to the necessary infrastructure for developing groundwater resources as the monetary outlay is usually comparatively small (Pavelic, 2012). This is of great importance in areas with considerable budgetary constraints for development (UNECA/AU/AfDB, 2003). Furthermore, groundwater is generally considered to be of good, and superior quality (Pavelic, 2012) compared to sources with greater exposure to surface contamination (MacDonald et al., 2005). Perhaps most importantly, groundwater is more resilient to climate variability than surface water or soil moisture (Calow et al., 2010). It is less prone to evaporative losses, which is significant in areas which experience such high rates of potential evaporation (Batisani and Yarnal, 2010) and highly variable precipitation (UNEP, 2010). Due to the generally slow movement of groundwater, and storage in aquifers, groundwater has a greater terrestrial residence time than the alternatives (Taylor et al., 2009).

Currently, there is significant dependence on groundwater for domestic use. However, there are differences in rural and urban settings, which are important as Africa is the least urbanised continent with less than 40% of the population residing in cities (World Bank, 2018). The majority of the population of sub-Saharan Africa rely on groundwater for drinking water (Carter et al., 2017). 60% of rural households, but only 30% of urban households, rely on groundwater for domestic purposes (Carter et al., 2017). However, many large cities, such as Lusaka, Windhoek, Kampala, Addis Ababa, and Dodoma (Murray et al., 2018; Pavelic, 2012; Robins et al., 2006), have municipal supplies which are highly, or entirely, dependent on groundwater. As a result of its prevalent use, groundwater is the provenance of 75% of all safe drinking water in Africa (Foster & Loucks, 2006). This is 50% greater than the corresponding global figure. Groundwater use is increasing in rural (Carter et al., 2017) and particularly urban areas (Grönwall, 2016; Okotto et al., 2015; Thompson et al., 2000).

1.3 Population Growth and Increased Freshwater Demand

Demand for water, and specifically groundwater, is set for a bipartite increase due to population growth (UN, 2017), and climate change (Niang et al., 2014). Subsumed within 'population growth' is increases in urban populations, i.e. urbanisation, and the food required to feed a larger population, i.e. agricultural intensification. Currently, the population of Africa is estimated to be growing at 2.6%, the fastest in the world (UN, 2017). By 2050, the population is projected to more than double from its current 1.25 billion to 2.53 billion (UN, 2017), with 28 African countries projected to more than double their populations (UN, 2015b). Moreover, by 2100, ten countries are expected to at least quintuple their populations (UN, 2015b). These increases are expected to be exacerbated by rapid urbanisation. Africa has the fastest growing urban population in the world (2005-2010), at 3.4% (UNFPA, 2009), and the most rapidly urbanising population in the world, at 1.5% (UN, 2014). Population growth is causing a widening gap between water availability and water demand, chiefly in cities (WWP, 2017). Moreover, historical evidence suggests that there is a non-linear relationship between population and water use, associated with an improved standard of living. Between the 1950s and the early 1990s, world population doubled, but global water use more than tripled (ECA, 2006).

It is anticipated that there will be a substantial increase in demand for groundwater to boost agricultural output (Carter and Parker, 2009; MacDonald et al., 2009). The Green Revolution is seen as a central tenet of the poverty alleviation strategies in many African countries (MacDonald et al., 2013). At present, 1% of cultivated land in Africa is irrigated by groundwater (Siebert et al., 2010), leaving significant scope for expansion (Wani et al., 2009). Not only would this improve food security, it would stimulate economic growth (Conway et al., 2009). Despite attempts to diversify economies (Page, 2008), long-term economic prosperity will depend on agricultural performance for the foreseeable future (UNECA/AU/AfDB, 2003).

1.4 Groundwater as a Climate-Resilient Freshwater Source

Climate change will render the use of groundwater increasingly vital. As it is buffered against climate variability (Taylor et al., 2013a), its use is expected to increase in all sectors under continuing climate change. Africa experiences the planet's most variable precipitation and river discharge (McMahon et al., 2007), which is projected to be exacerbated by climate change. Precipitation, surface water, and soil moisture are set to become less reliable and temperatures are projected to continue increasing (Niang et al., 2014). These changes have unfavourable implications for water availability in sub-Saharan Africa due to the prevalent use of surface water and soil moisture.

Transitioning to an increased reliance on groundwater is fundamental to all facets of life and sustainable development in Africa. Access to a sufficient quantity of suitable quality freshwater is integral to poverty reduction, promotion of health, ensuring food security, sustaining economic growth, industrial development, and maintaining healthy ecosystems (UN, 2018b). Currently, groundwater is vital for domestic water supplies throughout sub-Saharan Africa. Changes to demographic structure, population concentrations, agricultural style, and agricultural scale are set to redouble water demand (Wada et al., 2010). Accordingly, increasing the volume of useable water in Africa and moving much of the population out of poverty (Grey and Sadoff, 2007; Hunter et al., 2010), has been deemed contingent on the effective and sustainable utilisation of groundwater (Giordano, 2009).

1.5 Uncertainty in Projections of Renewable Groundwater Resources

Despite present and future importance, the scale of renewable groundwater resources in Africa remains unresolved. The sustainability of current use and reliance, and the viability of any adaptive strategies are unclear. Insufficient study has rendered it nearly impossible to effectively assess the influence of climate change and variability on groundwater recharge (Niang et al., 2014). A lack of studies and data restricted the ability of the Intergovernmental Panel on Climate Change (IPCC) to assess the interactions between ground water and climate change in its third (Arnell et al., 2001), and fourth (Kundzewicz et al., 2007) assessment reports. Prior to the fifth assessment report, there was a marked increase in research (Taylor et al., 2013a). However, the conclusions of the fifth assessment report only served to highlight knowledge gaps:

“Inadequate observational data in Africa remains a systemic limitation with respect to fully estimating future freshwater availability” (Niang et al., 2014, p. 1216).

“Future development of groundwater resources to address direct and indirect impacts of climate change, population growth, industrialization, and expansion of irrigated agriculture will require much more knowledge of groundwater resources and aquifer recharge potentials than currently exists in Africa. Observational data on groundwater resources in Africa are extremely limited and significant effort needs to be expended to assess groundwater recharge potential across the continent” (Niang et al., 2014, p. 1218).

Estimating climate change impacts on groundwater resources in Africa is stymied by 3 issues, a systematic lack of observational data, poor understanding of the climate controls and processes which generate groundwater recharge, and uncertainty and inadequacy in climate projections. A paucity of observational data in Africa restricts the estimation of future groundwater availability (Batisani, 2011; Neumann et al., 2007) because detection and attribution of changes to groundwater resources owing to climate change is difficult (Niang et al., 2014). This is exacerbated by the interaction of multiple drivers, such as land use change, water demand, and natural climate variability (Niang et al., 2014), which obfuscate the relationship between climate change and groundwater.

1.6 Uncertainty in Climate Projections

Considerable uncertainty exists regarding the impacts of climate change on mean annual precipitation from general circulation models (GCMs) (Bates, 2009). As groundwater recharge projections are closely related to projected changes in precipitation (Taylor et al., 2013a), projections of renewable groundwater resources are consequently also uncertain. Uncertainty arises from climate projections derived from GCMs, as the same emissions scenarios are typically translated into very different climate scenarios, particularly for precipitation (Bates, 2009). Projections of precipitation are associated with additional uncertainty due to the necessity of downscaling data (Taylor et al., 2009), which can be greater than the uncertainty associated with the choice of emissions scenarios (Holman et al., 2009; Stoll et al. 2011).

Despite significant uncertainty, there have been assessments of future renewable groundwater resources in Africa. Generally, climate change impacts on groundwater will vary across climatic zones (MacDonald et al., 2009). Changes to precipitation are not expected to appreciably impact the recharge of aquifers in areas receiving less than 200 mm per year, as recharge is negligible due to the balance of precipitation and evapotranspiration. Increases in precipitation in these areas are not expected to be enough to overcome the prevailing rates of evapotranspiration. Similarly, groundwater recharge is also not expected to be significantly affected by climate change in locations that receive more than 500 mm of precipitation per year, as recharge would still occur despite a potential reduction in precipitation. Conversely, arid and semi-arid regions, which generally receive between 200 and 500 mm per year, are anticipated to experience changes related to changes in mean annual precipitation in addition to a reduction in recharge as a result of increased frequency of dry spells and other precipitation anomalies (Allan & Soden, 2008)

1.7 Uncertainty in the Processes and Controls of Groundwater Recharge

Projections of groundwater resources are fundamentally limited by a lack of understanding regarding the climate controls which produce groundwater recharge, and the processes which transmit meteoric water to the saturated zone.

1.7.1 Precipitation Intensity and Groundwater Recharge

Projections of groundwater recharge under climate change commonly do not consider the intensification of precipitation (Taylor et al., 2013a), despite widespread theoretical (Trenberth, 1999; Trenberth et al., 2003), observed (Fischer and Knutti, 2016; Groisman et al., 2005), and projected (Kharin et al., 2013; Kharin et al., 2007; Tebaldi et al., 2006) increases in precipitation intensity as consequence of anthropogenic warming. There have been few studies regarding the effect of precipitation intensity on groundwater recharge in semi-arid sub-Saharan Africa. Accordingly, the impact of intensification remains unclear. However, an association between intensive precipitation and groundwater recharge has been suggested in a few semi-arid locations using stable isotope tracers (Vogel and Van Urk, 1975), soil moisture balance modelling (Eilers et al., 2007), and hydrometric monitoring (Taylor et al., 2013b), whereby groundwater recharge is disproportionately generated by intensive precipitation. Assessing the prevalence and magnitude of this bias is vital for cogent projections of renewable resources. Moreover, the intensification of precipitation is much more certain than changes to mean annual precipitation rendering the implementation of the pertinent processes and controls in hydrological models vital.

1.7.2 Uncertainty in Recharge Process in Semi-Arid Environments in Africa

Equally important for assessments of future groundwater resources is a comprehensive understanding of the processes which transmit meteoric water to the saturated zone. Broadly, both diffuse and focused recharge processes occur in all groundwater systems, with the prevalence of focused recharge generally increasing with aridity (Alley, 2009). Recharge in semi-arid areas predominately occurs via leakage from ephemeral streams (Simmers, 2003; Simmers et al., 1997). Studies throughout Sub-Saharan Africa have shown considerable variation in predominant recharge processes. This is due to the wide range of geological and climatological environments (Scanlon et al., 2006a). Despite its importance, understanding groundwater recharge processes in semi-arid areas remains a major challenge (Wheater et al., 2010), due to a lack of available data, and consequently a lack of studies. This is particularly true in areas where focused recharge occurs (Somaratne and Smettem, 2014). Fundamentally, the processes that transmit precipitation to groundwater systems are not fully understood (Jasechko and Taylor, 2015).

1.8 Aims

The research presented here aims to address the critical gaps in our understanding of the interaction between groundwater and climate, explicitly highlighted by the IPCC, to improve our knowledge of the process and controls of renewable groundwater resources. Understanding the relationship between precipitation and groundwater recharge in tropical semi-arid environments has been hindered by a lack of studies, and a lack of data has prevented more extensive and robust studies being conducted. This thesis aims to contribute to lessening the knowledge gaps by conducting robust analysis on existing data and contributing to the improvement of groundwater monitoring in sub-Saharan Africa. This research will be undertaken in Makutapora, central, semi-arid Tanzania. The reasons for this are discussed in the following chapter. Explicitly, the aims of this research are:

1. Determine whether more intensive precipitation contributes disproportionately to groundwater recharge in a semi-arid environment of sub-Saharan Africa.
2. Resolve the dominant mechanisms which transmit meteoric water to the saturated zone in a semi-arid environment sub-Saharan Africa.
3. Project groundwater resources under scenarios of climate change and increased water demand in a semi-arid environment sub-Saharan Africa.

1.9 Thesis Structure

This thesis is presented as a series of inter-related, but discrete, chapters which address the aims detailed above. Each chapter contains a review of the relevant literature. The thesis is structured as follows:

- Chapter 1 is an introduction detailing the importance of studying the effects of climate change on groundwater and the processes which control groundwater recharge in semi-arid sub-Saharan Africa.

- Chapter 2 is a description of the of the study site; the Makutapora basin, and a rationale of why the location was chosen.
- Chapter 3 is an assessment of the impact of precipitation intensity on groundwater recharge.
- Chapter 4 investigates the groundwater recharge pathways transmitting meteoric water to the saturated zone.
- Chapter 5 details the development of a fully integrated model of the Makutapora Basin which is used to project groundwater resources under scenarios of climate change and groundwater abstraction.
- Chapter 6 comprises overriding conclusions and recommendations for future work.

Chapter 2

Study Area: The Makutapora Basin

2.1 The History of Dodoma and its Water Supply

Dodoma was founded in 1907 during construction of the Tanganyika Railway, which was built to link the capital, Dar es Salaam, to Kigoma, a port on Lake Tanganyika. The location was chosen for its central position in Tanzania, a halfway point between the two termini of the railway, not for its viability as a capital city sustaining a large population (Hayuma, 1980). In 1973, the Tanzanian government announced plans to transfer the *de jure* capital from Dar es Salaam to Dodoma under the premise of bringing the government closer to the people (Hayuma, 1980). In addition to its central location, Dodoma was selected for its favourable transport links to the north, south, east, and west of Tanzania, and considerable scope to stimulate regional development (Mosha, 2004). The decision to instate Dodoma as the new capital, known as The Master Plan, however, failed to adequately address several key issues, including the water supply of the city (Callaci, 2016).

Dodoma's water supply has evolved since the founding of the city. Initially, surface water was exclusively utilised with early water supply infrastructure comprising dams. The first of these, constructed in 1929, was Imagi Dam. By 1943, increased demand from the growing city necessitated the construction of an auxiliary dam, Msalatu dam. It was completed in 1944. Water demand continued to increase, and consequently, Mkonze dam was built to further supplement the supply. By the late 1940s, surface water alone was deemed insufficient to meet the demands of Dodoma.

Exploration, monitoring, and development of the water resources in the Makutapora Basin began in 1948 with the drilling of the first borehole in the Makutapora Wellfield. Following satisfactory yields from initial test boreholes, further investigation was sanctioned by the Geological Survey of Tanzania and the Public Works Department of Tanzania. By 1964, groundwater from the Makutapora Wellfield had become an important source of water for Dodoma. Accordingly, work within the wellfield was simultaneously concerned with building infrastructure to supply water to Dodoma and assessing the suitability and sustainability of the Makutapora Wellfield as a long-term solution to the city's water supply. Initially, the wellfield was considered an interim resource (Shindo et al., 1989), as its full potential was unknown. Infrastructural and exploratory work in the wellfield continued throughout the 1960s with the Water Development and Irrigation Department, United Research Associated and the Office of the Engineering Geologist, Dodoma all undertaking discrete projects.

Upon the inception of The Master Plan in 1973, the need to find a long-term source of water for Dodoma became imperative. The Capital Development Authority ordered a large-scale hydrological and geophysical investigation of the area surrounding Dodoma. Binnie and Partners Consulting Engineers of London carried out a feasibility study of the Makutapora Wellfield while the Ministry of Water Development and Power oversaw a companion study on the groundwater resources of the neighbouring ward, Hombolo. The external consultation concluded that the wellfield could sustain abstraction of 22,000 $m^3 \cdot day^{-1}$. In the late 1970s, the Capital Development Authority, once again, investigated potential water sources for the new capital city to replace groundwater from Makutapora. This work was the most comprehensive to that date, but the Makutapora Wellfield remained Dodoma's primary water source.

In the late 1980s, the Japan International Co-operation Agency (JICA) undertook research within the Makutapora Basin with the primary aim of determining the full potential of the wellfield, and to advise on necessary infrastructure. The research culminated in a revised estimate of the maximum sustainable rate of abstraction, 50,000 $m^3 \cdot day^{-1}$ (Shindo et al., 1990). In late 1987, abstraction from the wellfield started regularly exceeding the sustainable yield estimated by Binnie and Partners, and in mid-2015, abstraction exceeded the JICA estimate. Despite being the exclusive source of water for Dodoma for over 50 years, the Makutapora Wellfield has once again been designated a temporary water source, as it is deemed insufficient by Tanzania's Ministry for Water and Irrigation (Daily News, 2017a).

The Makutapora Wellfield is presently the sole source of Dodoma's municipal water supply (DUWASA, 2015) and in 2016 supplied the city with an average of almost 50,000 $m^3 \cdot day^{-1}$ of water. The aquifer in Makutapora is currently tapped by 24 deep boreholes (DUWASA, 2017). Despite having exceeded previous estimates of maximum sustainable yield, water levels are currently higher than they were in the 1990s, and roughly the same as they were prior to development. It is clear that the renewable volume of groundwater in the Makutapora basin is only loosely constrained.

According to the 2012 Tanzanian census, the population of Dodoma was 410,956, with a growth rate of 2.1% over the preceding 10 years (MOF, 2012). This has subsequently been exacerbated by the transfer of government ministries (The East African, 2017) and international organisations (XinhuaNet, 2017) from Dar es Salaam to Dodoma. Several new strategies to address water demand in Dodoma have been proposed. During the 2010 presidential campaign, President Jakaya Kikwete announced a dam would be built in Bahi district, ~60 km north of Dodoma. However, this plan was abandoned in favour of building Farkwa Dam in Chema District, ~130 km north of Dodoma (The Citizen, 2014). Early designs suggest the dam would inundate an area of approximately 48 km^2, and store between 290,000 m^3 and 850,000 m^3 of water (The Citizen, 2014), allowing 120,000 $m^3 \cdot day^{-1}$ of additional water to be supplied to Dodoma (Daily News, 2017b). Given the size of the dam, and the distance water will be transmitted, the project is anticipated to cost US$420 million, and will be funded by the World Bank (Construction Review Online, 2017). More recently, it has been suggested that the construction of Farkwa Dam maybe inadequate, and the possibility of transporting water from Lake Victoria, ~500 km away, to Dodoma has been mooted (Daily News, 2017c).

2.2 Rationale

The Makutapora Basin in semi-arid central Tanzania has been chosen as the study site as it facilitates the achievements of the aims of this research.

2.2.1 Historical Observations

In its Fifth Assessment Report, the IPCC explicitly states that inadequate observational data in Africa remains a systemic limitation with respect to fully estimating future freshwater availability (Niang et al., 2014). The same lack of data means there are very few long-term studies which assess the impact of climate on groundwater. One of the longest known groundwater records in sub-Saharan Africa comprises observations from Makutapora. Furthermore, proximate precipitation data has been recorded for almost 100 years, and long-term surface water monitoring has taken place within the basin. Makutapora represents a rare and excellent opportunity to study historical records and contextualise them with contemporary monitoring and analysis. More robust analyses can be conducted in Makutapora than would be possible in other locations.

2.2.2 Pragmatically Important to Dodoma

Makutapora represents an unusual opportunity to study a vital source of groundwater. In addition to any theoretical outcomes, the findings of this research will have an immediate local impact. The sustainable management of the Makutapora Basin will be contingent on any research carried out here. Such an important source of water would usually be deemed too precious for external researchers to intrusively monitor, but existing relationships with the Tanzanian government, and in-country colleagues have facilitated this research opportunity. Furthermore, as an actively pumped system, which are often neglected from research due to their complexity, new and modified techniques can be developed to accurately assess groundwater dynamics.

2.2.3 Makutapora Represents Important Areas in Africa

Makutapora is proposed to act as an analogue of geological and climatological conditions more widely in sub-Saharan Africa. Like Makutapora, approximately 40% of sub-Saharan Africa is underlain by weathered crystalline rock aquifers (MacDonald et al, 2012), which are the product of deep weathering and stripping of basement rocks by geomorphic activity and meteoric water.

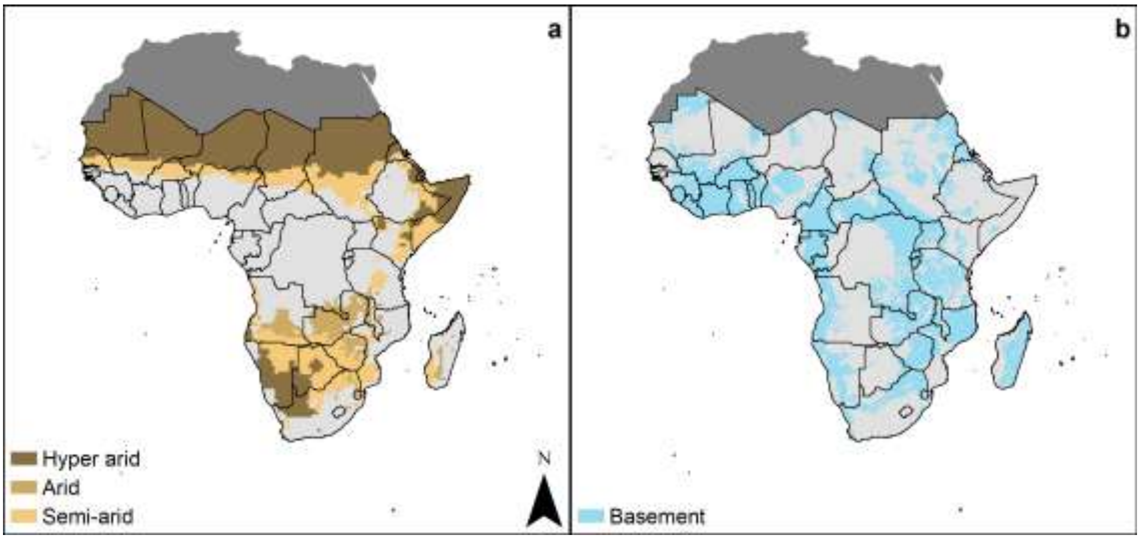

Figure 2.1 Maps of sub-Saharan Africa highlighting (a) areas with dryland climates and (b) areas underlain by basement aquifers (MacDonald et al., 2012).

Furthermore, semi-arid environments, which are growing (Hassan, 2005), account for 21% of Africa's area, including Makutapora. While the relationship between climate and the saturated zone is strongly modulated by land cover, Makutapora can act as a reasonable analogue for large areas of the most vulnerable regions of Africa. Unlike wetter, or drier regimes, semi-arid regions fall in an 'unstable' zone (De Wit & Stankiewicz, 2006; MacDonald et al., 2009). Terrestrial water balances have been found to respond non-linearly to climate variability and change (De Wit & Stankiewicz, 2006; MacDonald et al., 2009; Taylor et al., 2013b). These regions are most susceptible to climate change, yet there is a paucity of research based on semi-arid regions of sub-Saharan Africa.

2.3 Site description

2.3.1 Location and physiography

The Makutapora Basin is situated in central Tanzania, approximately 20 km north of the capital city, Dodoma (Shindo et al., 1989) (Figure 2.2). The catchment occupies an area of 698 km^2 upstream of the Chihanga outlet (35.84E, 5.90S) on the River Little Kinyasungwe, which forms the upper section of the Hombolo Basin (Shindo et al., 1989). The Makutapora and Hombolo Basins are separated by a normal fault with the Makutapora side forming an upthrown foot wall, whilst the Hombolo Basin is the corresponding downthrown hanging wall (Nkotagu, 1996).

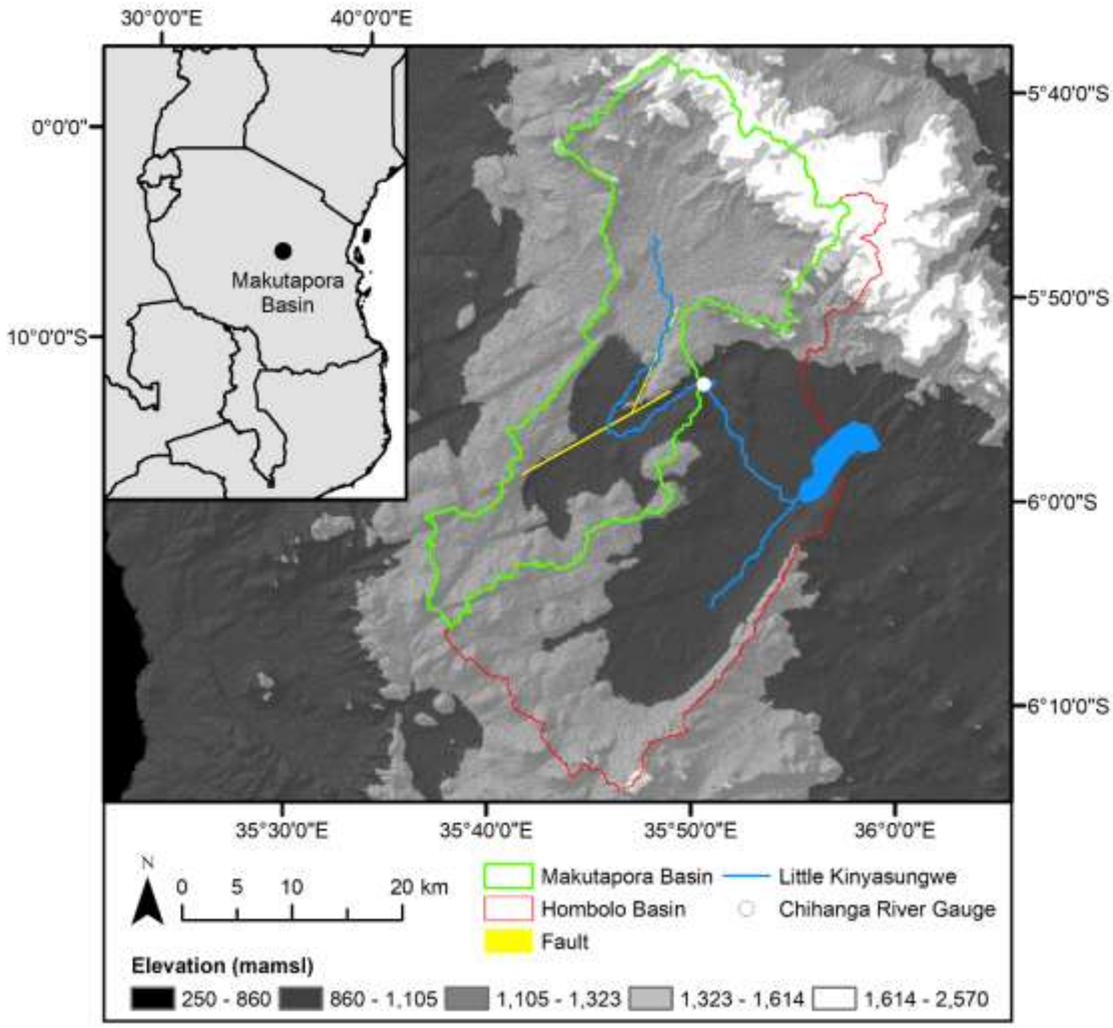

Figure 2.2 Location of the Makutapora Basin in East Africa (inset). Makutapora and Hombolo basins delineated using NASA Shuttle Radar Topography Mission (SRTM) data (90 m resolution) with ArcSWAT. Location of surface water, comprising the River Little Kinyasungwe and Hombolo Reservoir, is highlighted. Locations of major faults in the Makutapora Basin are also shown. White areas coincide with ‘mountains’, light grey with ‘uplands’ and dark grey with ‘lowlands’.

The catchment is situated on the East African Plateau, at the southern end of the Gregory Rift, the eastern branch of the East African Rift System. There is evidence of recent tectonic activity. The catchment is an eastward sloping, warped, asymmetric plateau, punctuated by steep escarpments, rectilinear slopes of tectonic origin, and inselbergs. Linear features generally trending SW-NE and NW-SE, such as the River little Kinyasungwe River, Hombolo Reservoir and the Makutapora swamp, indicate extensive faulting. The Chenene Hills, a mountain range which defines the NE boundary of the basin, is a fault block forming part of a horst and graben structure, which extends more than 100 km NW-SE, perpendicular to the major faults within the basin (Shindo et al., 1990). The largest faults in the basin are the Mlemu and Kitope faults (Shindo et al., 1989), which trend NE-SW (Figure 2.2). Elevation within the catchment ranges from 1066 mamsl to 2035 mamsl, however, 89% of the basin lies below 1400 mamsl (appendix a). Higher elevations are associated with the Chenene Hills and inselbergs.

The most comprehensive description of the Makutapora Basin to date classified three areas within the catchment: mountains, uplands, and lowlands (Shindo et al., 1990). These areas can be defined by their elevation (Figure 2.2), surface geology (Figure 2.4), and location in the basin. The mountains encompass the Chenene Hills and inselbergs. The Chenene Hills are characterised by their high altitude relative to most of the plateau, steep slopes, and table-top summits. Inselbergs are scattered across the plateau and often have steep slopes, and some have distinct footslopes. The uplands comprise areas of low relief including pediplains and pediment, which, along with the Chenene Hills, define the boundaries of the basin. The uplands surround the lowlands in the centre of the catchment. The lowlands consist of fluvial lowland and seasonal swamp, which is generally flat (Onodera et al., 1995).

2.3.2 Geology

For the first time, a three-dimensional model of the geology of the Makutapora Wellfield has been created. 44 well logs, from Shindo (1989), the Drilling & Dam Construction Agency, and China Guangdong International Cooperation, were interpolated using inverse distance weighting in RockWorks 14 to produce the model. Cross sections extracted from the model are shown in Figure 2.3. Lithological data used to create the model, in addition to borehole construction information, are compiled and listed in Appendix D.

The Makutapora Basin is underlain by fractured crystalline basement rocks, which are predominantly granites, forming part of the Tanzania Craton (Kashaigili et al., 2003). Outcrops of the deeply weathered granite (Kashaigili, 2010) are found at the topographic highs of the Chenene Hills. The granites are commonly grey, non-schistose and rarely porphyritic (De Pauw et al., 1983). They are believed to be late Precambrian age but their exact age and mode of emplacement are unknown (De Pauw et al., 1983). The granites enclose disconnected fragments of older basement rocks, which outcrop in the inselbergs south of the Chenene Hills. They are predominantly amphibolites, schists and gneisses, and generally have a more basic mineralagy than the granites which envelope them. Younger intrusions are also present in the form of basic and ultrabasic dykes (Nkotagu, 1996).

In the uplands and lowlands, basement rocks are covered by a regolith of unconsolidated and cemented superficial deposits (Figure 2.3). The nature of unconsolidated sediments is strongly determined by the underlying parent rock. Unconsolidated material is generally coarse and weathered (Nkotagu, 1996), consisting of detrital sediments of granitic origin (Kashaigili et al., 2003) including sand, gravel and silt. The cemented deposits are mostly calcareous. The abundance of calcium is thought to be due to the persistent presence of freshwater swamps (Wades and Oates, 1938).

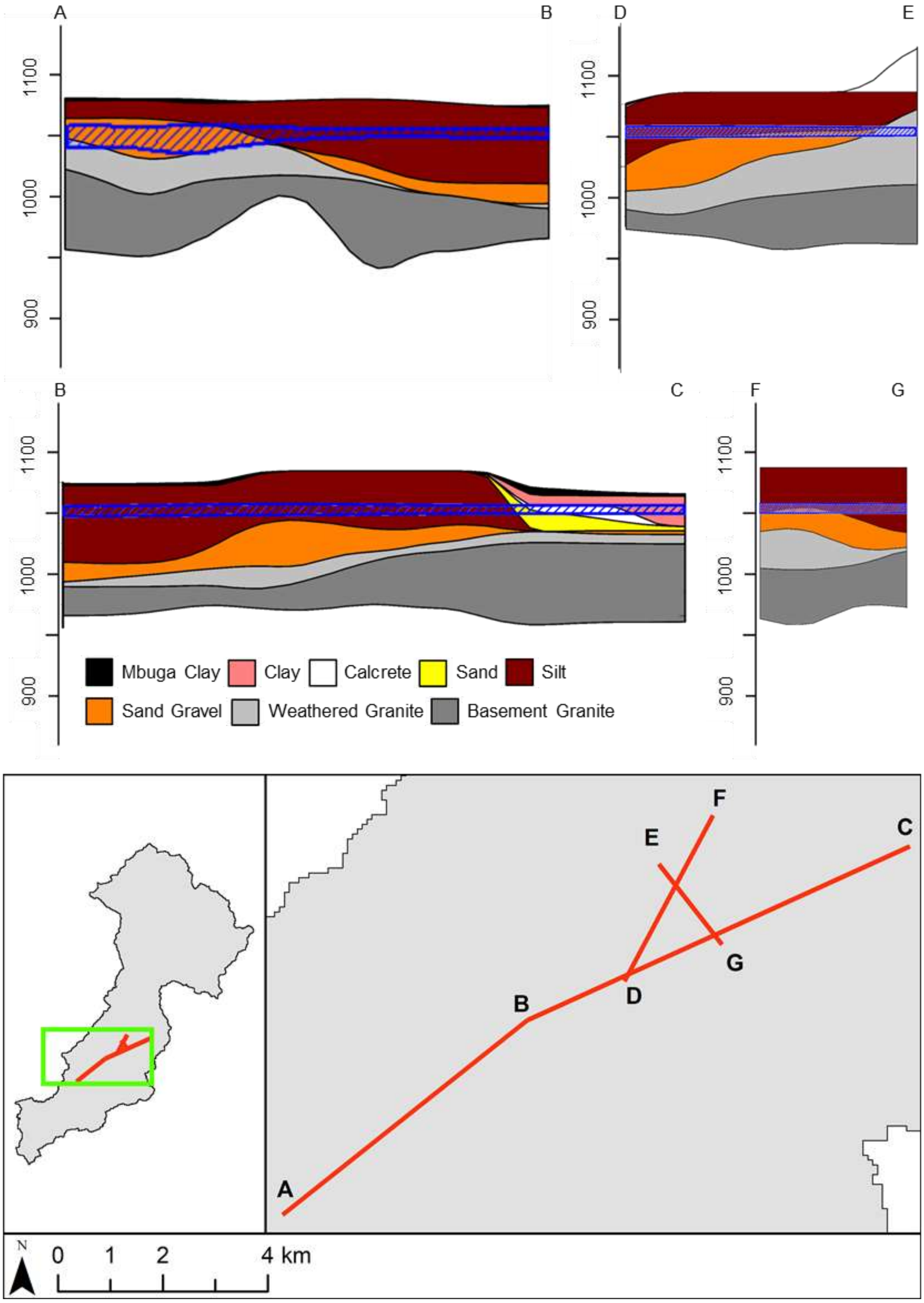

Figure 2.3 Geological cross sections from the Makutapora Wellfield extracted from a 3D geological model. The range of groundwater-level fluctuations recorded since 1955 is highlighted on the sections (blue). The locations of the sections are indicated on the map.

The composition of the regolith varies throughout the basin (Figure 2.4). Except for minor soil cover, there is little regolith covering the basement outcrops of the Chenene Hills and the inselbergs. The uplands are generally underlain by coarse grained, unconsolidated decomposed granite. The thickness of the regolith varies between 50 m and 100 m (Nkotagu, 1996). Uplands are generally covered in sandy soil (Shindo et al., 1990). The centre of the basin, the lowland areas, are generally underlain by a similar geology to the upland areas with the addition of layers of Mbuga clay and calcrete, both associated with the swamp (Figure 2.3). Mbuga clay is a black, clay-like deposit (Onodera et al., 1995). Mbuga clay deposits is generally very thin, consistently less than 10 m (Figure 2.3).

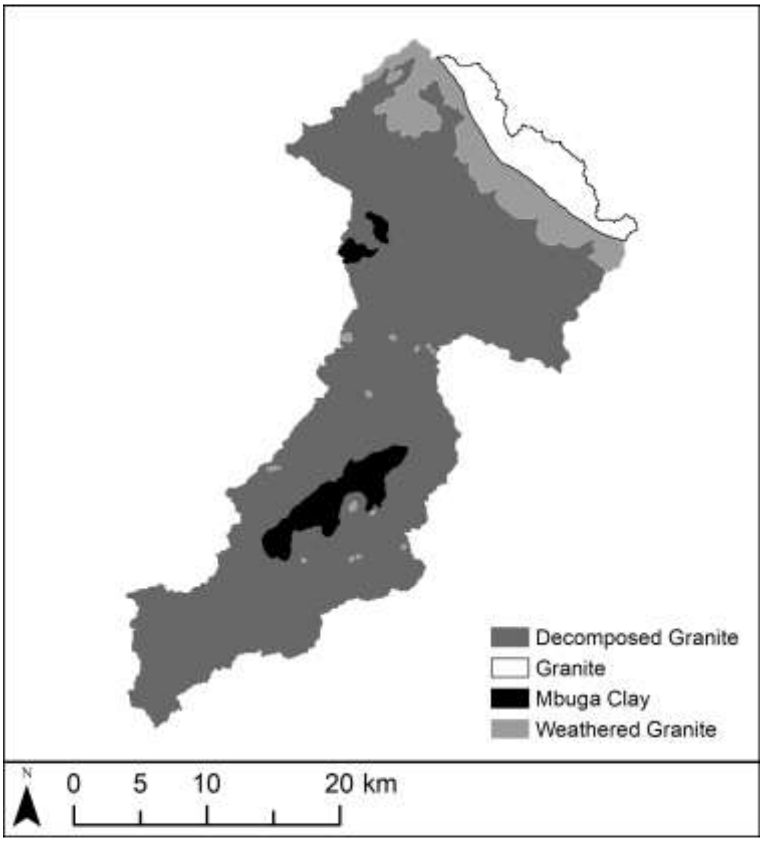

Figure 2.4 Map of surface geology in the Makutapora Basin, after Geological Survey of Tanganyika quarter degree sheet 143 (GST, 1955).

2.3.3 Hydrogeology

The water bearing formations are unconsolidated silt, sand and gravel overlying weathered and fractured granite (Kashaigili et al., 2003) (Figure 2.3). Dense, unfractured granite bedrock, is thought to form the lower boundary of the aquifer (Hayashi and Chiba, 1994). In the lowlands, sand and gravel layers are sometimes overlain by a layer of calcrete (Figure 2.3). Mbuga clay covers approximately 4% of the basin surface, but the thickness of the clay deposits and the depth of the water table means the aquifer remains unconfined over its range of water levels since 1955 (Figure 2.3). Tectonic activity associated with the East African Rift system has left the area fractured and faulted (Nkotagu, 1996). The anomalously high transmissivities found in the Makutapora Basin are thought to be a consequence of enhanced weathering associated with the complex network of faults present in the saturated zone (Maurice et al., 2018; Taylor et al., 2013b). Deeply weathered crystalline rock aquifer systems generally feature low transmissivities (MacDonald & Calow, 2009; Taylor & Howard, 2000) that commonly range from 1 to 10 $m^2 \cdot d^{-1}$. However, pumping tests in the Makutapora Wellfield indicate that transmissivities are vastly greater than that, ranging from 400 to 4000 $m^2 \cdot d^{-1}$ (Maurice et al., 2018). Accordingly, the Makutapora aquifer is characterised by high yielding wells. These are generally proximate to the Mlemu fault, which runs through the wellfield. It is thought that the faults help to rapidly transmit water throughout the saturated zone (Taylor et al., 2013b). The degree to which coarse-grained horizons within the alluvium provide storage to, and enhance the yield of, wells drawing from the unconsolidated weathered bedrock remains unclear (Shindo et al., 1989).

2.3.4 Hydrology

Drainage within the Makutapora Basin is influenced by ENE-trending faults associated with horst and grabens of the East African Rift System (Taylor et al., 2013b). There are no perennial streams in the catchment. The largest ephemeral stream, the River Little Kinyasungwe (Shindo et al., 1989), drains the upland areas and flows in the direction of the Kitope fault into the wellfield (Figure 2.2). Ephemeral stream flow occurs throughout the basin but is spatially dynamic. The size and location of ephemeral stream channels are highly variable at intra- and inter-annual timescales. Surface water flowing out of the Makutapora Basin ultimately drains into the Hombolo Reservoir, the only permanent water body in the area (Figure 2.2). The reservoir is man-made and generally very shallow, with a maximum depth of approximately 2.5 m.

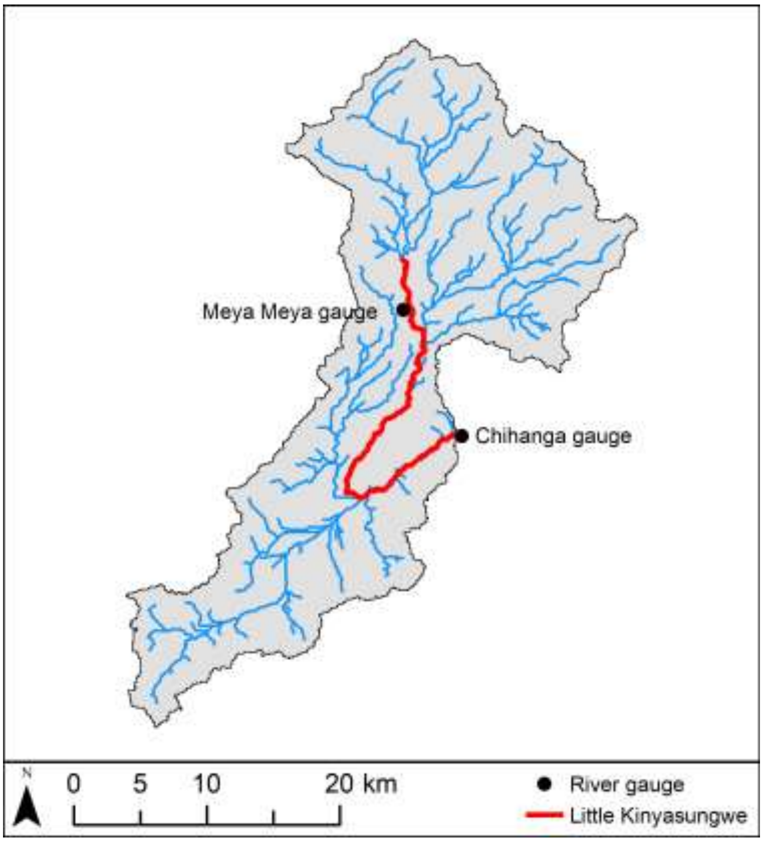

Figure 2.5 Ephemeral drainage channels within the Makutapora Basin. Streams are defined by a drainage area threshold of 1 km^2 based on SRTM 90m DEM data (Jarvis et al., 2008) using ArcSWAT. The location of the River Little Kinyasungwe and two gauging stations, Meya Meya and Chihanga, are highlighted.

Generally, surface drainage routes all water from the edges of the basin towards the lowland (Figure 2.5). The lowlands are thought to have originated from a former lake bed and have very low relief. They are perennially waterlogged and flooded in the wet season.

2.3.5 Climate

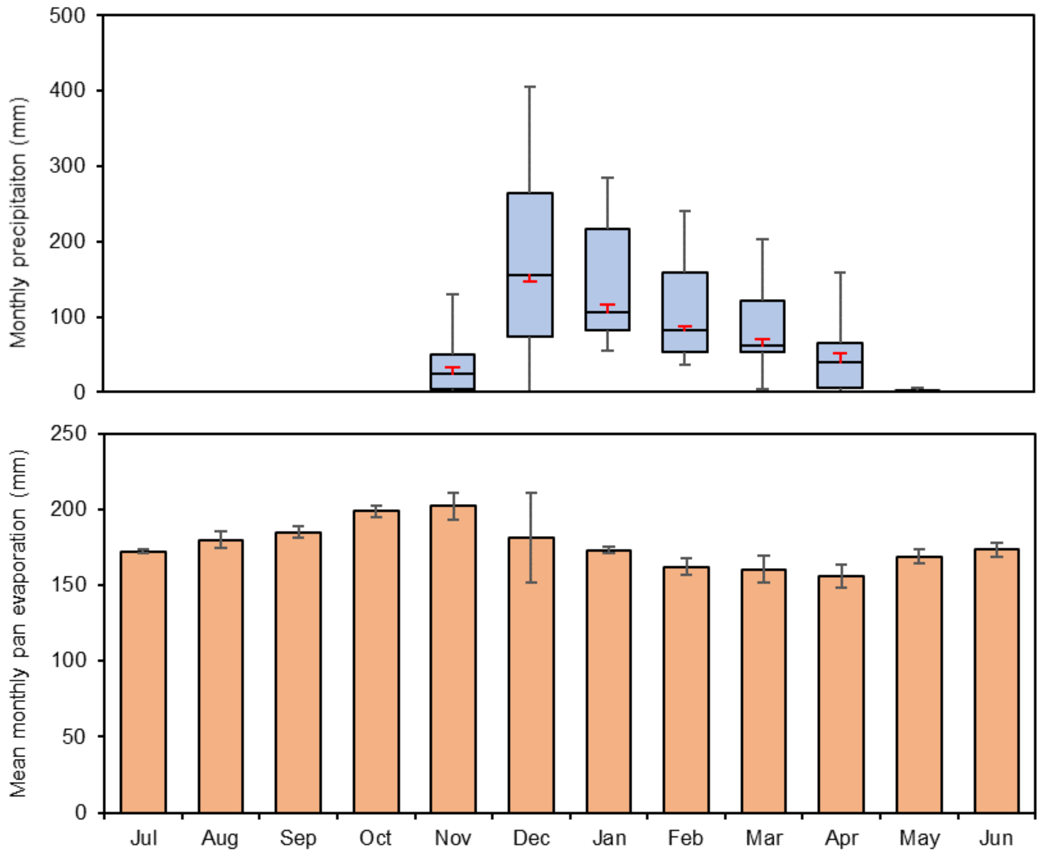

Figure 2.6 Box and whisker plot of monthly precipitation at the Makutapora Meteorological Station 2007 – 2016 (top). The plot indicates maximum, minimum, first quartile, median, third quartile and mean (red) precipitation for each month. Mean monthly pan evaporation, and associated standard deviation, recorded at the Makutapora Meteorological Station (2003, 2004 and 2006) (bottom).

Makutapora and Dodoma feature a 'hot semi-arid' climate characterised by distinct wet and dry seasons and perennially high temperatures. Makutapora has a unimodal wet season with more than 99% of precipitation falling between November and April. Recent monitoring (2007 – 2016) shows that mean annual precipitation in Makutapora is 527 mm·year^{-1} (Figure 2.6), falling on average over 28 rain days per year. Over the same observation period, average precipitation in Dodoma was similar, 539 mm·year^{-1}, which fell on 32 rain days per year. The hydrological year is defined as starting on 1st July and ending on 30th June to ensure that no wet season is split across hydrological years. Short-lived observations in the basin suggest that precipitation in the upland areas may be greater than on the floor of the basin (Onodera et al., 1995), but the extent of this effect is unclear. There has never been systematic temperature monitoring in Makutapora, but in nearby Dodoma, average highs range from 26.5 ºC in July to 30.5 ºC in October, and lows from 13.6 ºC in July to 18.8 ºC in December (WMO, 2018). There have been several estimates of potential evapotranspiration in Makutapora and Dodoma. An early estimate based on evaporative losses from reservoirs in Dodoma was 73 inches per year (1854 mm·yr^{-1}) (Fawley, 1958). Subsequent estimates have generally been similar, ranging from 1700 mm·yr^{-1} (Kashaigili et al., 2003) to 2460 mm·yr^{-1} (Shindo et al., 1990) to 2500 mm·yr^{-1} (Onodera, 1993). The most robust estimate is 2120 mm·yr^{-1}, based on 3 non-consecutive years of data (recorded between 2003 and 2006) observed at the Makutapora Meteorological Station (35.72E, 5.97S) (Figure 2.6).

2.3.6 Land Cover

Land cover is dominated by grassland and dwarf shrubs (Taylor et al., 2013b) with typical vegetation types including Acacia shrubs, Baobab trees, and Euphorbia (Hayashi and Chiba, 1994). Land cover varies throughout the catchment (Figure 2.7). The Chenene Hills are mostly covered by thick shrubland on the lower slopes and forest at higher altitude. The inselbergs have a generally dense cover of forest and thicket. In the uplands, grassland is the primary vegetation type, followed by shrubland. Thickets and forest occur less commonly. The natural vegetation of lowlands is grassland and infrequently forest (De Pauw et al., 1983).

In the semi-arid climate of central Tanzania, pastoralism is the dominant form of agriculture. Within the Makutapora Basin, however, agriculture is limited due to the importance of the wellfield and a nearby military base (Taylor et al., 2013b). Furthermore, as a result of erosion and vegetation degradation in the basin, agricultural productivity is generally low. There is little evidence of substantial land-use change over the last several decades (Taylor et al., 2013b). Change has been limited since the 1990s by a soil preservation policy (Kangalawe, 2009).

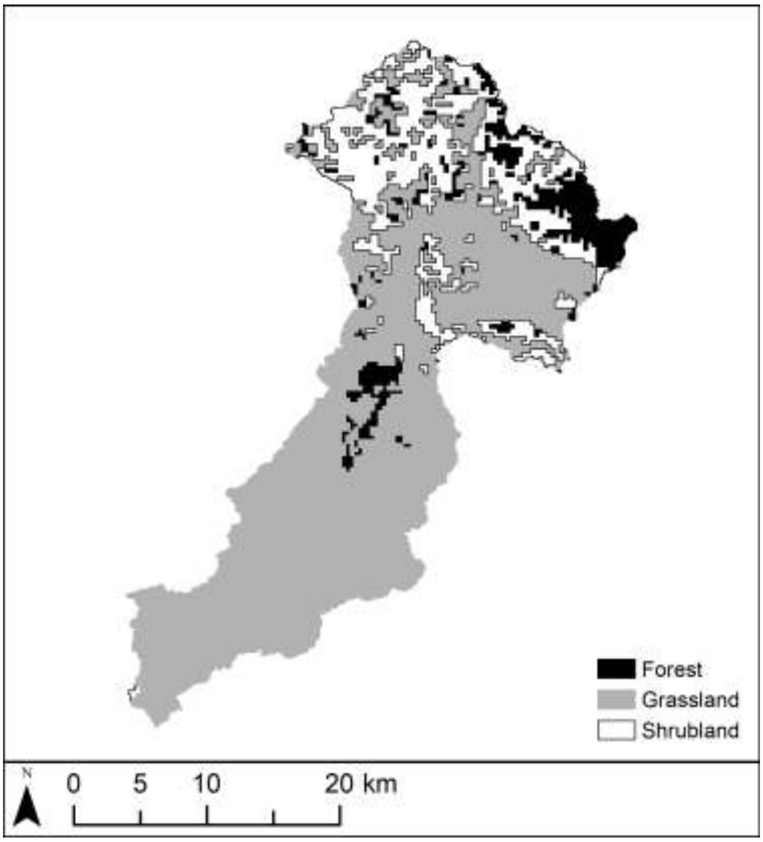

Figure 2.7 Land cover within the Makutapora Basin. Data is a simplified version of the Global Land Cover Map, GlobCover Version 2.3, 2009 (Arino et al., 2012), produced by the European Space Agency (ESA) as part of the Globcover Project.

2.3.7 Groundwater Abstraction

Groundwater abstraction from the Makutapora Basin has increased since it was established as a source of water for Dodoma. This has been facilitated by the construction of improved pumping and transmissions infrastructure. Pumping wells are located in what is generally termed the 'wellfield', which is proximate to the Mlemu Fault, in the lowlands. The locations of all production wells known to have ever been in use are shown in Figure 2.8. Timeseries of pumping data for each of those wells are shown in appendix b.

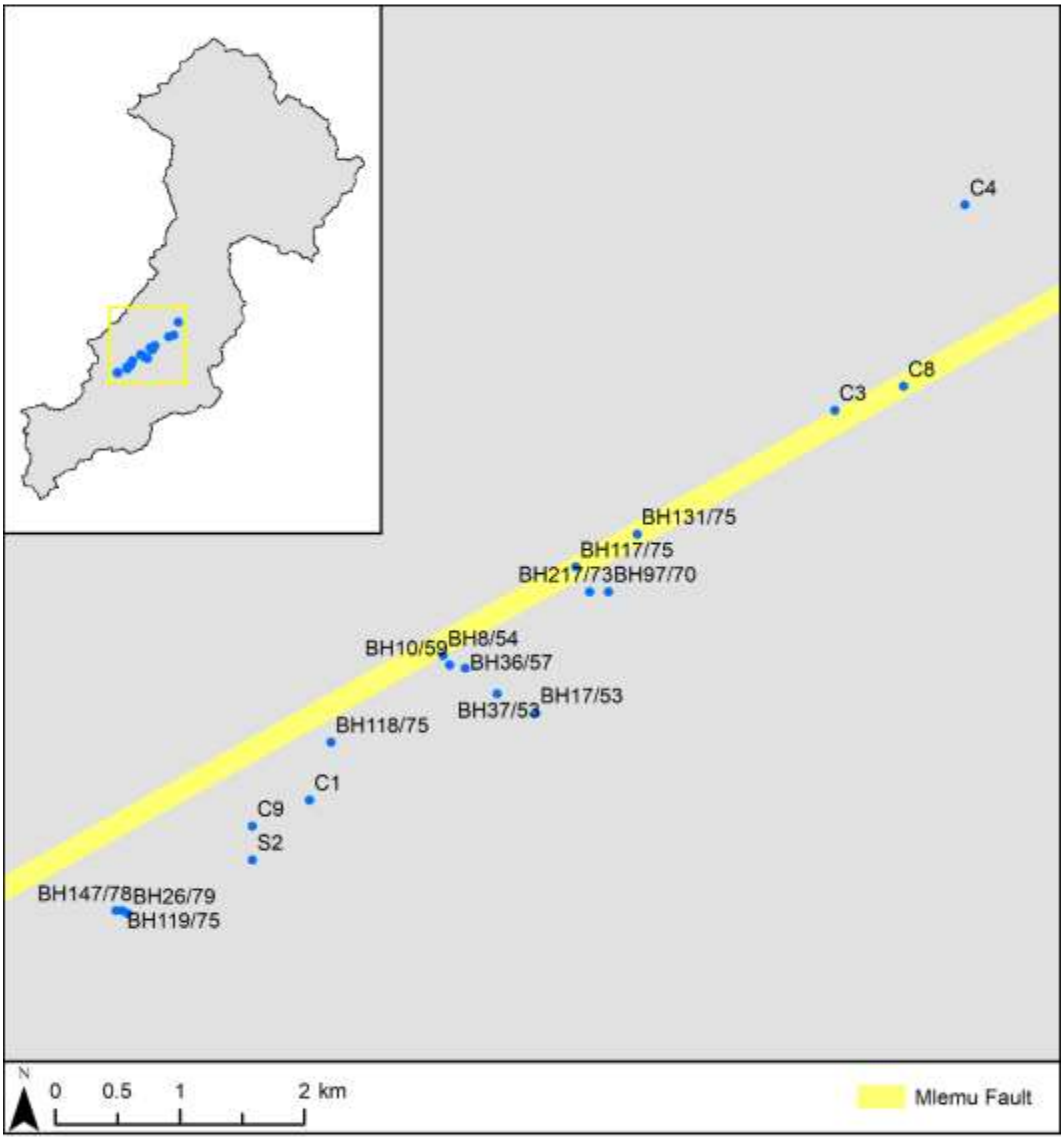

Figure 2.8 Location of all pumping wells known to be active between 1964 and present in the Makutapora Basin, and the location of the Mlemu fault.

2.3.8 Historical Data

Groundwater-level data have been recorded in eight monitoring wells in Makutapora since 1955 (figure 2.9a). Precipitation data has been sporadically recorded in Dodoma since the 1920s, and consistently since the 1940s, at the Dodoma Meteoritical Station (35.75 E, 6.17S). More recently, precipitation has been recorded at the Makutapora Meteorological Station (35.72E, 5.97S), and stream stage data have been recorded at the Meya Meya gauge (35.80E, 5.82S) on the River Little Kinyasungwe (figure 2.9c). Six high-resolution groundwater monitoring wells and two high-resolution river gauges were installed in November 2015 (figure 2.9b). These datasets are incorporated into analyses in subsequent chapters.

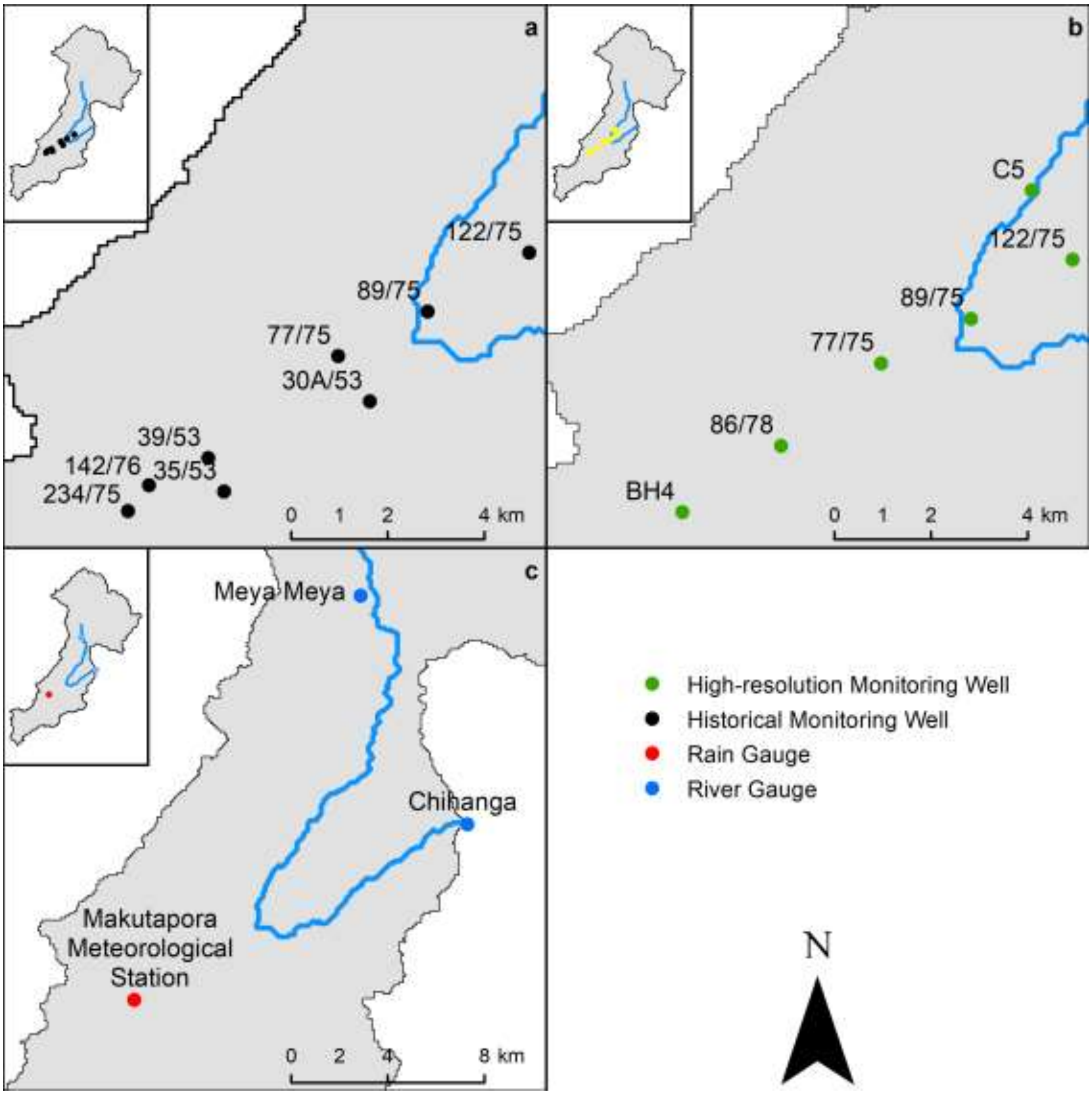

Figure 2.9 Maps of the Makutapora Basin showing detailed locations of (a) historical monitoring wells, (b) newly installed high-resolution monitoring wells, and (c) river gauges and the meteorological station.

2.3.9 Conceptual model of groundwater recharge

Natural groundwater recharge, the addition of water from an overlying unsaturated zone or surface water body to the saturated zone (Scanlon et al., 2006b), generally occurs via two mechanisms. Focused recharge is the leakage of water from the inundation of topographic depressions such as streams, lakes, and playas, to the groundwater system. Diffuse recharge is the areally distributed transmission of water from the land surface to the water table as a result of in situ infiltration and percolation of meteoric water. Infiltration is the movement of water from the surface into the subsurface, and percolation is the downward movement of water through the unsaturated zone. Percolation occurs via two primary mechanisms: (1) piston flow, the uniform movement of water that displaces existing water without bypassing it; and (2) preferential flow, the movement of water along preferred pathways, such as fractures, cracks, wormholes and roots. Preferential flow allows water that infiltrated relatively later to reach the saturated zone before water that infiltrated relatively earlier, as it is bypassed. Both diffuse and focused recharge processes can occur in all groundwater systems.

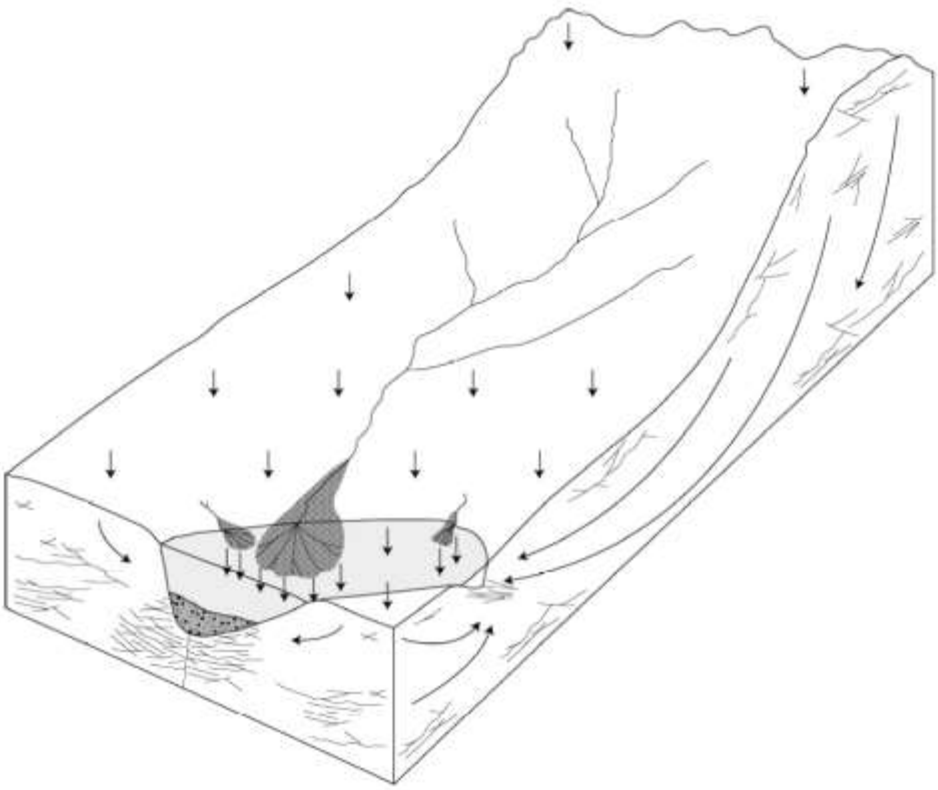

Figure 2.10. Conceptual diagram highlighting diffuse and focused groundwater recharge pathways (vertical arrows) to the aquifer underlying the Makutapora Basin. Figure adapted from Fig. S3. in (Taylor et al., 2013b).

Understanding groundwater recharge processes in semi-arid areas remains a major challenge (Wheater et al., 2010), due to a lack of available data, and consequently a lack of studies. This is particularly true in areas where focused recharge occurs (Somaratne and Smettem, 2014). Fundamentally, the processes that transmit precipitation to groundwater systems are not fully understood (Jasechko and Taylor, 2015). Focused recharge is generally believed to increase with increasing aridity (Alley, 2009) with limited evidence suggesting that leakage from ephemeral streams is important in semi-arid regions (Simmers, 2003; Simmers et al., 1997). The relationship between climate and recharge mechanism, however, is modified by land cover and underlying geology (Taylor et al., 2013a). Studies throughout Sub-Saharan Africa have shown considerable variation in predominant recharge processes. This is due to the wide range of geological and climatological environments (Scanlon et al., 2006a).

Various groundwater recharge mechanisms have been proposed to occur in the Makutapora Basin. Previously, groundwater recharge was proposed to predominantly occurred via a diffuse mechanism (Nkotagu, 1996; Shindo et al., 1989), in the uplands and mountains (Shindo et al., 1989) with macropores rapidly transmitting the bulk of the water through the unsaturated zone (Shindo et al., 1989). More recent research (e.g. Taylor et al., 2013b), however, has indicated the importance of focused recharge. Leakage from streambeds of ephemeral streams, as they flow over coarser-grained soils in alluvial fans at the margin of the wellfield depression, is now believed to contribute significantly to groundwater recharge. This focused recharge pathway features substantially greater infiltration capacities than those in upland and mountain environments and the depression and may dominate (Taylor et al., 2013b). Spatially heterogenous leakage results in groundwater mounding, whereby mounds of groundwater form and grow under leaking streambeds and ultimately decay. The design of this research seeks to explore more fully the possibility that groundwater recharge occurs via leakage from ephemeral streams; this focus does not preclude the potential contribution of diffuse recharge. The size, location and discharge of ephemeral streams are known to be highly dynamic in space and time within the Makutapora Basin. The mechanism producing runoff, either infiltration excess runoff or saturation excess runoff, is unknown. Focused recharge is, therefore, understood to potentially occur throughout the basin, wherever ephemeral streamflow occurs. Large streams, the largest being the River Little Kinyasungwe, are expected to contribute the most recharge via leakage, but all streams may contribute based on wetted perimeter and duration of ephemeral flow. Therefore, there may be well distributed focused recharge occurring through the basin during certain periods.

Chapter 3

Precipitation Intensity and Groundwater Recharge in the Makutapora Basin: A Revised Analysis Accounting for Transience in a Pumped System

3.1 Abstract

Changes in the intensity of precipitation have been observed and are projected to continue under climate change. Changes are projected to be most severe in the tropics. The impact of increased precipitation intensities on groundwater recharge remains unclear. In the Makutapora Basin, analysis of long-term hydrometric and stable-isotope data indicates that groundwater recharge is disproportionately generated by more intensive precipitation. Hydrometric data are reanalysed by estimating groundwater recharge from groundwater-level fluctuations in an actively pumped system by employing a saturated zone numerical flow model to account for transience in groundwater-level recessions. These findings indicate that climate change may enhance groundwater recharge in the Makutapora Basin and similar environments in semi-arid sub-Saharan Africa.

3.2 Introduction

Sub-Saharan Africa is particularly vulnerable to climate change due to high exposure, low adaptive capacity, and projected greater than average warming (Niang et al., 2014). Increased temperatures have been observed to, and are expected to continue to, greatly affect the hydrological cycle (Hegerl et al., 2015). Projected changes to annual precipitation over sub-Saharan Africa are varied and uncertain (Niang et al., 2014), but an increase in precipitation intensity is a widespread theoretical, observed, and projected consequence of anthropogenic warming. Precipitation intensity could increase exponentially with temperature, at a rate determined by the Clausius–Clapeyron relation (Trenberth, 1999; Trenberth et al., 2003) as intensive precipitation is thought to increase with moisture availability (Trenberth, 1999). However, in the tropics, precipitation is primarily driven by latent heat of condensation released by precipitation, which influences intensity (Houghton et al., 2001), potentially producing larger increases than those defined by the Clausius–Clapeyron relation (Trenberth, 1999). Observational data show an almost ubiquitous increase in precipitation intensity and frequency of heavy precipitation events (Fischer and Knutti, 2016; Groisman et al., 2005). Heavy precipitation events increase in frequency whereas light and moderate precipitation events decline in frequency (Allan and Soden, 2008). Consequently, more precipitation falls during intensive events (Huntington et al., 2009), a disproportionate amount of annual precipitation is contributed by intensive events (Easterling et al., 2000), and dry spells are longer. Global and regional climate models, driven with scenarios of increasing CO_2 concentrations, project a continued increase in precipitation intensity over most of the globe as warming continues (Kharin et al., 2013; Kharin et al., 2007; Tebaldi et al., 2006).

Intensification of precipitation is expected to increase variability in surface water, precipitation, and soil moisture (Jiménez Cisneros et al., 2014), rendering groundwater, and our understanding thereof, vital to water and food security. Despite the heightened vulnerability of water resources in semi-arid areas (De Wit & Stankiewicz, 2006; MacDonald et al., 2009), there have been few studies regarding the effect of precipitation intensity on groundwater recharge in sub-Saharan Africa. Accordingly, the response to intensification remains unclear. An association between intensive precipitation and groundwater recharge has been suggested in a few locations using stable-isotope tracers (Vogel and Van Urk, 1975), soil moisture balance modelling (Eilers et al., 2007), and hydrometric monitoring (Taylor et al., 2013b).

Generally, recharge investigations have relied on the use of a single investigatory technique, and lack corroborating evidence to substantiate recharge estimates (Taylor & Howard, 1996). Although a paucity of meteorological and hydrological observations has inhibited accurate evaluation of recharge in Africa (Niang et al., 2014), two commonly implemented methods are the observation of recharge from water-table fluctuations and tracing the origins of groundwater using stable-isotope ratios of O and H. The water table fluctuation method (WTF) has been used, and modified, to estimate groundwater recharge from groundwater-level fluctuations, in numerous studies (Yang et al., 2018) for almost 100 years (Meinzer, 1923), but is commonly predicated on the assumption that observed well hydrographs depict water-table fluctuations caused by natural ground-water recharge and discharge (Yang et al., 2018).

The WTF has several important variations (Yang et al., 2018), of which, the three most well-established are: the graphical method, the Master Recession Curve method (MRC), and the RISE method. The graphical method estimates recharge by correcting for unrealized recession (Delin et al., 2007), whereby antecedent recessions are extrapolated beyond the onset of observed recharge. Groundwater recharge is estimated as the difference between the peak observed water-table elevation and the corresponding extrapolated water table elevation. The graphical method operates on the temporal scale of hydrological episodes, and therefore functions at a variable time-step. Unlike the graphical method, MRC does not identify single recharge episodes, but calculates recharge for each timestep. Rates of unrealized recessions are assumed to be solely a function of water table elevation, generally, with more rapid declines occurring at greater elevations (Nimmo et al., 2015). The form of the relationship is based on observed declines which took place in the absence of recharge. Once the MRC is established, positive deviations are attributed to recharge. The simplest iteration of WTF is the RISE method in which unrealized recessions are not considered. Recharge is estimated to be any positive deflection of the water table (Rutledge, unpublished manuscript). Negative deflections are assumed to represent groundwater-level declines. The assumptions embedded in these iterations of WTF render their implementation in pumped systems impossible (Yang et al., 2018). The explicit assumption of the RISE method, that unrealised recessions are negligible, is unjustifiable in an area with an observably non-trivial recession rate, under natural and pumped conditions. Similarly, the assumption that recessionary rates are entirely head dependant, explicit in the MRC method, inhibit accurate incorporation and assessment of the effect of pumping. Finally, the assumption of the graphical method that unrealized recessions are defined by their antecedent recessions, is not necessarily valid under conditions of variable abstraction.

Methods used to trace the origins of groundwater using stable-isotope tracers are generally unaffected by pumping and are therefore useful for validation. It is, however, not possible to derive a time series of recharge estimates from analysis of tracers. Accordingly, any comparison between findings from water-table fluctuations and stable-isotope tracers seeks to trace general, steady-state associations. Stable-isotope ratios of oxygen ($^{18}O/^{16}O$) and hydrogen ($^{2}H/^{1}H$) in precipitation and groundwater can be used to identify intensity-based selection (Gat, 1971) that occurs prior to groundwater recharge. Cogent comparison is predicated on the relationship between isotope ratios and site-scale intensity of precipitation, the 'amount effect'. The cause of the amount effect is contentious (Scholl et al. 2009), with various proposed mechanisms. Nevertheless, empirical relationships, whereby more intensive precipitation events are significantly depleted in heavy isotopes (^{18}O and ^{2}H), are well established in many locations in tropical latitudes (Dansgaard, 1964; Jasechko & Taylor, 2015; Risi et al., 2008; Taylor & Howard, 1999; Taylor & Howard, 1996) where there is little correlation between temperature and precipitation isotopic composition (Dansgaard, 1964; Gonfiantini, 1986; Rozanski et al., 1993). Accordingly, comparison of isotope ratios found in samples of groundwater and precipitation of varying intensities can identify the intensity of precipitation that is most strongly associated with the generation of groundwater recharge.

Here, I examine the relationship between groundwater recharge and precipitation intensity in the Makutapora Basin, using hydrometric techniques and stable-isotope tracers. This revised analysis builds upon a previous study by Taylor et al. (2013b), who presented empirical evidence of the relationship between precipitation and groundwater recharge in semi-arid tropical East Africa. The key findings of which were: (1) groundwater recharge in the Makutapora Basin is highly episodic, with none occurring in most years, (2) seasonal groundwater recharge increases non-linearly with seasonal precipitation intensity, and (3) the largest recharge events have coincided with strong El Niño events. I revisit this analysis addressing a key simplification employed in the application of the water-table fluctuation method (Healy & Cook, 2002; Taylor et al., 2013b), that recessionary trends, in observed hydrographs, are linearly related to cumulative total wellfield groundwater abstraction. This assumption denies transient responses in groundwater-levels to changes in abstraction. The reanalysis comprises: (1) the implementation of a modified WTF, which accounts for transience in a pumped system, (2) examination of the relationship between precipitation intensity and groundwater recharge at a finer temporal resolution than before (daily instead of monthly (appendix c)), and (3) testing of the hydrometric study, and assessing the efficacy of the modified WTF, with stable-isotope tracers.

3.3 Hydrometric Methods and Data

To assess the relationship between precipitation intensity and groundwater recharge, I (1) updated a long-term dataset of groundwater-level observations and compiled a proximate, coincident dataset of daily precipitation, (2) quantified annual groundwater recharge events using a modified WTF method, incorporating a saturated-zone numerical flow model developed in MIKE SHE, and (3) examined the effect of precipitation intensity, over variable temporal scales, on the magnitude of groundwater recharge events.

3.3.1 Data

Systematic groundwater monitoring in the Makutapora Basin commenced in 1955, following the exploration of the Makutapora Wellfield as a water source for Dodoma, and is currently carried out by Dodoma Urban Water and Sewerage Authority (DUWASA). Active monitoring wells have changed throughout the duration of the record. Observations from 8 wells have been collated to produce an updated composite record of groundwater-levels (Figure 3.1). Monitoring resolution and completeness vary considerably between wells and with time. Missing groundwater data prevented recharge estimation associated with 14 wet seasons. Proximate precipitation data (Figure. 3.1) have been collected since 1911 at the Dodoma Airport Meteorological Station, which has since been subsumed into the World Meteorological Organization (WMO) network of synoptic weather stations (WMO: 63862). Aggregated wellfield abstraction has been recorded since the Makutapora Wellfield became an appreciable source of water for Dodoma in 1964 (Figure 3.1).

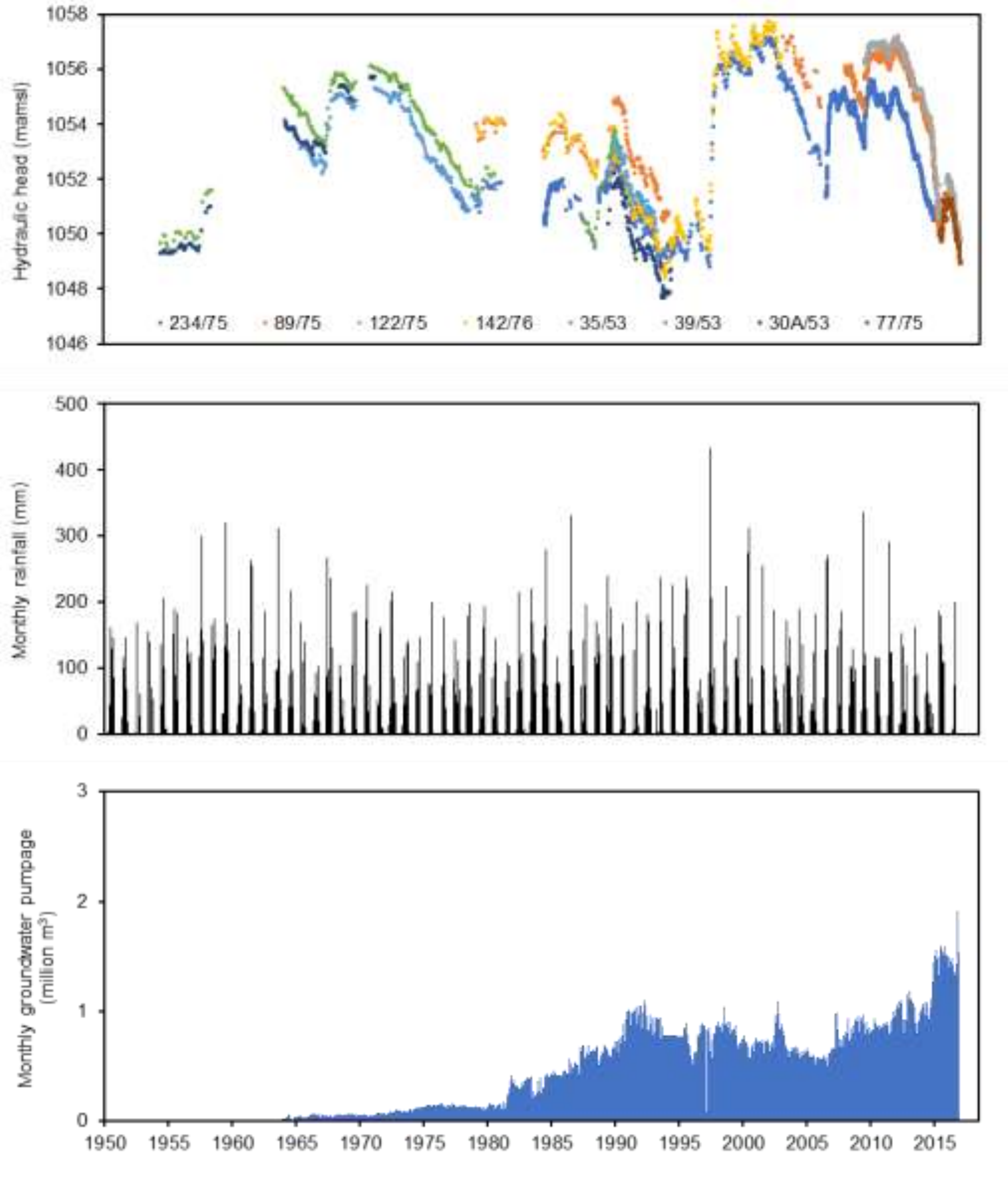

Figure 3.1 Time series of groundwater-level observations from 8 monitoring wells in the Makutapora Wellfield (top), monthly precipitation from the Dodoma Airport Meteorological Station (middle) and monthly groundwater abstraction in the Makutapora Basin (bottom).

3.3.2 A Modified WTF Method

Groundwater recharge events were quantified using a modified WTF method (Equations 3.1, 3.2 and 3.3) in which changes in groundwater-level (δh [L]) through time (δt [T]) are assumed to result from the balance of recharge (q [LT^{-1}]) and net groundwater drainage (D [LT^{-1}])

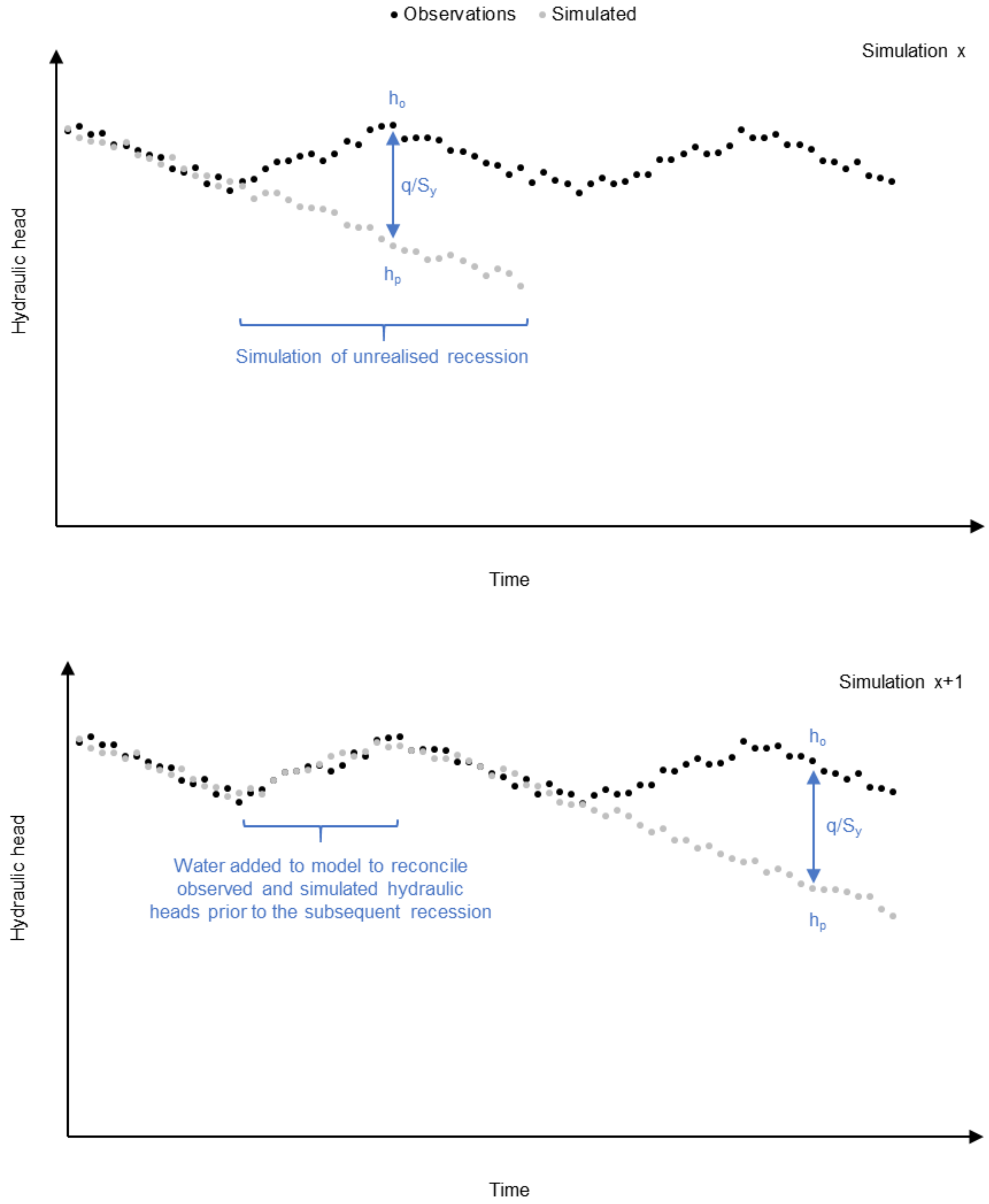

Figure 3.2 Schematic diagram of the modified WFT, incorporating a saturated zone model, used to estimate the magnitude of groundwater recharge events.

(Healy and Cook, 2002). In this case, drainage comprises both groundwater abstraction and hydraulic gradient induced groundwater flow. Groundwater recharge was quantified as:

$$\frac{\delta h}{\delta t} = \frac{q - D}{S_y} \qquad \text{(Equation 3.1)}$$

$$q = S_y * \frac{\delta h}{\delta t} + D \qquad \text{(Equation 3.2)}$$

$$q = S_y * \frac{(h_o - h_p)}{\delta t} \qquad \text{(Equation 3.3)}$$

where h (L) is water-table elevation, h_o (observed) is observed hydraulic head at time = t, and h_p (predicted) is the unrealised hydraulic head value that would have occurred in the absence of recharge at time = t. h_p values are simulated using a saturated-zone numerical flow model developed in MIKE SHE. Recharge for each event was estimated when the difference between h_o and h_p was maximum, which is not necessarily coincident with the peak h_o value, which is typical of other iterations of WTF.

Observed and simulated hydraulic head values were reconciled at the onset of a groundwater level recession (figure 3.2) by the addition of water to the model. Subsequently, groundwater levels observed during the recession were simulated. The unrealised recessions which would have occurred in the absence of groundwater recharge were subsequently simulated allowing recharge events to be estimated as the difference between observed hydraulic head values and hydraulic head values predicted to have occurred in the absence of recharge. The same procedure is followed for all subsequent recharge events. To estimate q/S_y in 'simulation x+1', groundwater recharge is added to the model to reconcile hydraulic head levels following the recharge event estimated in 'simulation 1'. Water is added, areally equally, as a fraction of daily rainfall via a process of trial and error until observed and simulated hydraulic head values at the onset of the recession are equal. Therefore, a simulation was run for each recharge event to be estimated, in each monitoring well in which it was observed. Water is added as a function of rainfall in an attempt to represent the timing of water reaching the saturated zone.

As the addition of all recharge is not instantaneous and the saturated zone is not at steady state, the amount of water added to reconcile groundwater levels does not necessarily equal estimates of q/S_y as described above. Hydraulic gradients within the saturated zone will redistribute water towards the wellfield, the location of the monitoring wells. Accordingly, on average the amount of water added to the model will be less than the R/S_y values estimated. The difference between h_p and h_o is taken as the magnitude of the recharge event rather than the amount of water added to the model to reconcile hydraulic head as this allows for cogent comparison with previously published work which employed this methodology.

3.3.3 Characterisation of Wet Spells and Precipitation Intensity

Following the approach of Owor et al. (2009), the magnitude of annual recharge events was compared to, both, the annual sum of all daily precipitation, and the annual sum of 'wet spell precipitation' which comprised the sum of daily precipitation that comprised wet spells that exceed an intensity threshold. The annual sum of all daily precipitation was calculated using Equation 3.4 where P_i is the amount of precipitation on any day. The duration of wet spells and the threshold of intensity were varied to maximise the correlation between annual 'wet spell precipitation' and annual recharge. Wet spells were varied in duration between daily (1 day) and monthly (30 days). Intensity thresholds were varied between 1 mm and 250 mm. For example, the sum of precipitation comprising 5 day wet-spells exceeding an intensity threshold of 50 mm would include all days which comprise a period of 5 consecutive days where a total of 50 mm, or more, of precipitation fell. In this example, the annual sum of 'wet spell precipitation' comprising wet spells of 5 days exceeding 50 mm of precipitation is given by Equation 3.4 where P_i is the precipitation on any day where: $(P_{i-4} + P_{i-3} + P_{i-2} + P_{i-1} + P_i) > 50$mm, or $(P_{i-3} + P_{i-2} + P_{i-1} + P_i + P_{i+1}) > 50$mm, or

$(P_{i-2} + P_{i-1} + P_i + P_{i+1} + P_{i+2}) > 50$mm, or $(P_{i-1} + P_i + P_{i+1} + P_{i+2} + P_{i+3}) > 50$mm, or $(P_i + P_{i+1} + P_{i+2} + P_{i+3} + P_{i+4}) > 50$mm.

Annual sum of precipitation = $\sum_{i=1}^{n} P_i$ (Equation 3.4)

3.3.4 Numerical Modelling of Recessionary Trends from Pumping in MIKE SHE

The MIKE SHE modelling system (Graham and Butts, 2005) is based on the Système Hydrologique Européen (SHE) (Abbott et al., 1986a, 1986b). It is a deterministic, fully distributed and physically based modelling system that simulates the land-phase processes of the hydrologic cycle.

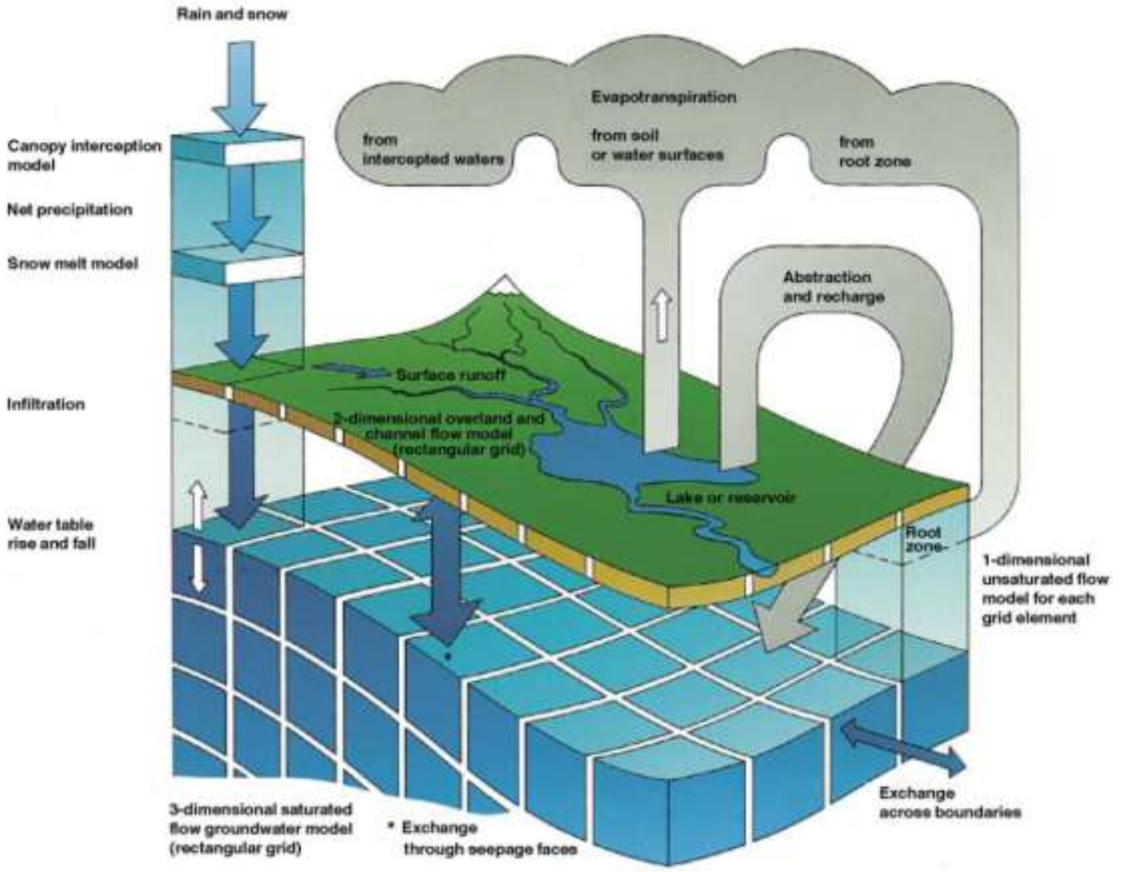

Figure 3.3 Schematic representation of the MIKE SHE model (Refsgaard and Storm, 1995).

The dynamically coupled MIKE SHE/MIKE 11 hydrological model allows for exchange of fluxes between MIKE 11 river channels and MIKE SHE overland flow, saturated zone and unsaturated zone components (Figure 3.3). It has successfully been employed under diverse climatological and hydrological regimes, across a range of scales (Thompson et al., 2013). MIKE 11 is a fully dynamic, one-dimensional hydraulic modelling system with comprehensive capabilities for modelling stream channel networks (Havnø et al., 1995). The primary components of the coupled model are: evapotranspiration/interception, overland flow/channel flow, unsaturated zone, saturated zone and the exchange between aquifers and rivers. Dynamic coupling of MIKE SHE and MIKE 11 is achieved using river links (line segments) between adjacent grid squares in MIKE SHE. Locations of river links are determined from the specified co-ordinates of river points that define coupled reaches in MIKE 11. During simulations, water levels are transferred from H-points

(points in the hydraulic model where water levels are calculated) to adjacent MIKE SHE river links. MIKE SHE calculates overland flow into river links from adjacent grid squares and the river-aquifer exchange, which are then fed back into MIKE 11 as lateral inflows or outflows for the next computational time step (Thompson et al., 2004).

The model developed for use in this chapter utilises only the saturated zone component of MIKE SHE which is not coupled with a MIKE 11 model. In chapter 5, the model developed here is expanded upon and forms the basis of a fully integrated hydrological model. Accordingly, an introduction to the main components of MIKE SHE/MIKE 11 is detailed below.

3.3.4.1 Domain

Variations in the characteristics of the catchment are represented by the discretisation of the domain horizontally into a computational grid. Spatial variability in parameters such as elevation, soil hydraulic parameters, and land cover are represented at the resolution of the grid. Within grid squares, vertical variations are represented by horizontal layers of variable depths. Lateral flow between grid squares can occur as overland flow or subsurface saturated zone flow. The method employed to represent flow in the unsaturated zone assumes that horizontal flow is negligible.

3.3.4.2 Climate

MIKE SHE requires two climatological inputs, precipitation and reference evapotranspiration. The spatial distribution of climatological variables can be uniform throughout the domain, station based, or fully distributed. Furthermore, precipitation data can be corrected for elevation and temperature by defining a lapse rate. MIKE SHE uses the Kristensen and Jensen (1975) model to calculate actual evapotranspiration from ET_o, computed soil moisture in the root zone, leaf area index (LAI), and root depth (RD).

3.3.4.3 Overland Flow

Overland flow is simulated by diffusive wave approximation of two-dimensional Saint-Venant equations (Havnø et al., 1995) once ponding depth exceeds detention storage in a grid cell. The velocity of overland flow is determined by values of Manning's M roughness. Variations in Manning's M roughness and detention storage can be represented at the resolution of the computational grid.

3.3.4.4 Land Use

Land cover data comprises leaf area index, canopy interception and root depths data, which can be parameterised at the resolution of the computational grid. Leaf area index and root depths are used in the calculation of actual evapotranspiration from ET_o.

3.3.4.5 River Flow

Flow in open channels is simulated by a fully dynamic finite difference solution of complete non-linear one dimensional Saint-Venant equations (Havnø et al., 1995). The channel leakage coefficient, which governs the bi-directional flow exchange between streams and groundwater, can be parameterised to vary throughout the network of river links. Leakage from streams uses a leakage coefficient in addition to a wetted perimeter, which is a function of stream stage and the architecture of the channel.

3.3.4.6 Unsaturated Zone

Unsaturated-zone fluxes are simulated by a fully implicit finite-difference solution of one-dimensional Richards' equation. This approach assumes that horizontal flow is negligible. Unsaturated zone parameters, Van Genuchten (1980) model parameters, soil moisture retention curves and specific yield, can be parameterised at the resolution of the computational grid.

3.3.4.7 Saturated Zone and Groundwater Abstraction

A finite-difference approach is used to solve the partial differential equations describing the saturated subsurface flows, which are simulated by 3D Darcy equations.

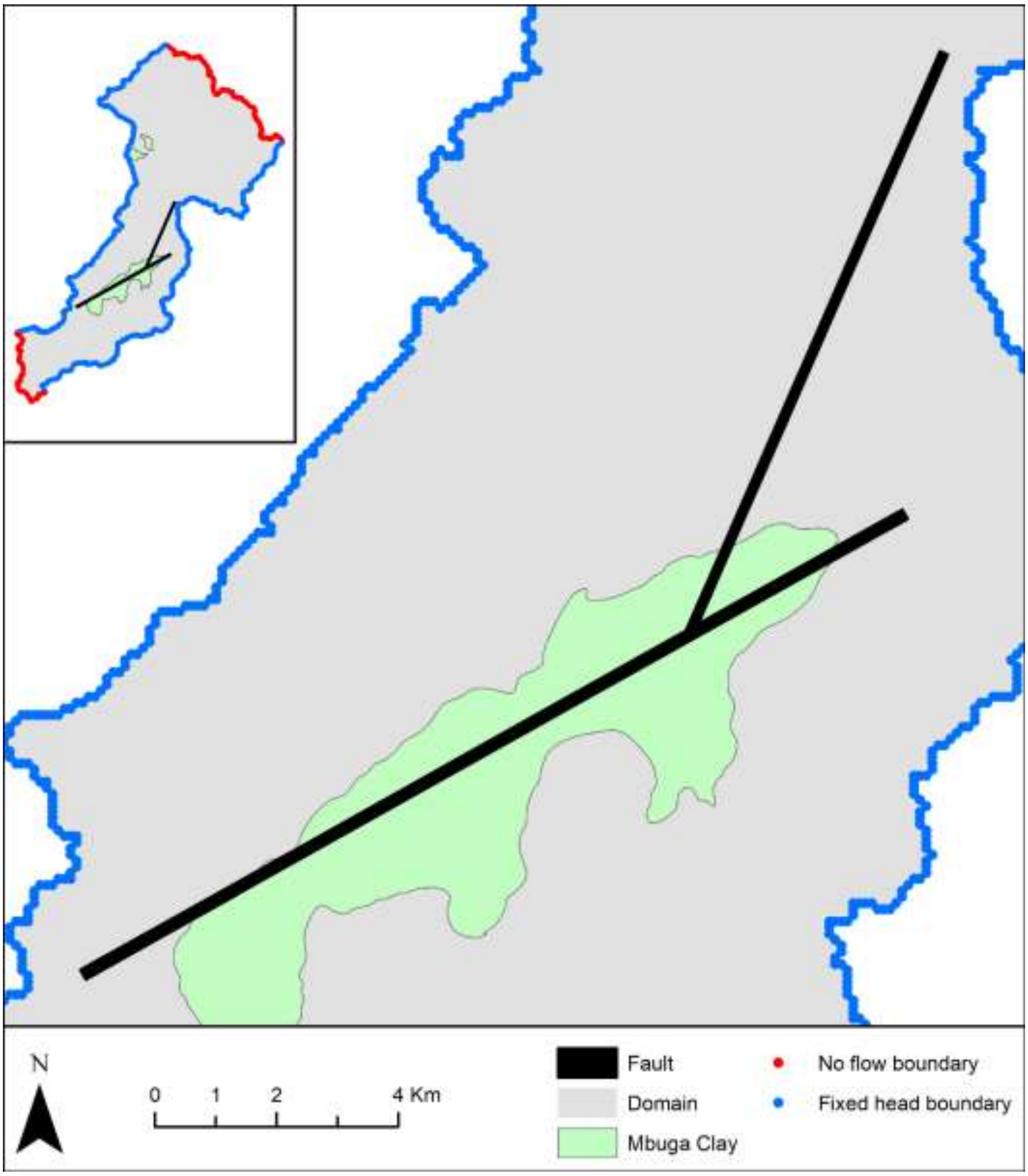

Figure 3.4 A representation of the saturated zone in MIKE SHE of the Makutapora wellfield within the Makutapora basin. The domain, boundary conditions, location of faults, and location of Mbuga Clay are shown.

The aquifer can be discretised vertically and horizontally and parameterised with specific yield and hydraulic conductivity values. Saturated zone boundaries can either allow flow in and out of the model, in the form of fixed head boundaries or fixed flow boundaries or prevent flow in the form of a no flow boundary.

Time-varying rates of groundwater abstraction can be applied to spatially distributed well locations throughout the domain. Water is abstracted at the specified rate, where possible, from the screened depth defined for each well in the model.

3.3.4.8 Saturated Zone Model

The model developed here employed a 100 m x 100 m computational grid, which was chosen as a compromise between model accuracy and logistically appropriate computation times. Additionally, the model was temporally discretised to run at a 24-hour time step. The model domain, comprising the Makutapora Basin, was defined topographically using SRTM 90m DEM data (Jarvis et al., 2008). The Chihanga gauge on the River Little Kinyasungwe River, originally established by Shindo et al. (1989), was designated as the outlet, consistent with Taylor et al. (2013b). Here, the model domain was defined as the entire Makutapora Basin as this model will subsequently be developed into a fully integrated hydrological model of the Makutapora Basin (chapter 5) and is therefore useful to carry out calibration on the entire basin. The modelling carried out in the chapter, however, is primarily concerned with the area encompassing the wellfield where groundwater pumping and monitoring take place (figure 3.4). Within the saturated zone, vertical discretization of aquifer parameters is based on the depth of geological layers and lenses defined in the model, Mbuga clay and fault zones. Accordingly, there is a single calculation node associated with each layer and lens. Based on well logs from the Drilling & Dam Construction Agency and China Guangdong International Cooperation, the bottom of the saturated zone was designated to be 200 m below ground as that was generally the depth at which basement granite was encountered. High hydraulic conductivity zones, representing the Mlemu and Kitope faults, extending from the surface to 100 m depth, were discretised as the faults are believed to be important in transmitting the effects of pumping throughout the wellfield (Taylor et al., 2013b). A lens of low storage, low hydraulic conductivity Mbuga clay (GST, 1955) was added over a small portion of the aquifer to a depth of 3 m, based on the average thickness of Mbuga Clay in the basin (figure 2.3). During pre-processing of the model input data, these features were resampled to the resolution of the computational grid. Accordingly, the fault zone was resampled to 100 m x 100 m grid squares (Figure 3.5).

The saturated zone was bounded by no-flow boundaries on the north-east and south-west edges of the basin due to the lack of conspicuous, proximate discharge areas to the north-east and south-west of the Makutapora Basin (Figure 3.4). Fixed-head boundaries were applied to the south-east and north-west boundaries (Figure 3.4), to simulate drainage towards proximate surface discharge areas, Hombolo Reservoir and Singida Lake, to the west, respectively. The relative elevations of hydraulic head values in the Makutapora Wellfield, and the presumed discharge areas guided initial values for the elevations of the fixed-head boundaries, with final values determined through calibration.

Specific yield (S_y) of the aquifer was guided by literature values from Makutapora (Taylor et al., 2013b), and another weathered crystalline aquifer in sub-Saharan Africa (Taylor et al., 2010). Initial hydraulic conductivity (K) values were taken from pumping tests conducted by Shindo et al. (1990). Pumped wells and observation wells, used in these tests, were situated sufficiently close to major faults in the wellfield to have influenced the results. Accordingly, the bulk properties interpreted from these tests were used as very loose constraints on the hydraulic conductivity of the aquifer and the faults. Measured soil texture (% sand, silt, clay) for Mbuga Clay elsewhere in Tanzania (Tanganyika) (Muir et al., 1957) was used in ROSETTA (Schaap et al., 2001) to determine initial values of hydraulic conductivity. Soil texture was also used to determine an initial value of specific yield for Mbuga Clay (Johnson, 1967). Final values of S_y and K for the aquifer, the clay, and the faults were determined by calibration, with all 3 assumed to be isotropic.

3.3.4.9 Representation of the fault

The faults within the Makutapora Basin, represented within the model as high transmissivity areas, are understood to be important in the rapidly transporting water throughout the wellfield (Taylor et al., 2013b). It is, therefore, important that the faults are represented appropriately at various resolutions. In this chapter, the computation grid resolution is 100 m. Accordingly, the discretised fault zones are resampled to that resolution. Following pre-processing, the faults occupy an area within the model equating to 4.36 km^2. At a computation grid resolution of 500 m, the resolution used in the iteration of the model used in chapter 5, the fault zone is resampled to occupy an area of 4.25 km^2. As the fault zones extend to the same depth in both versions of the model, the volume of the high hydraulic conductivity areas is similar in both iterations of the model. Further, the performance of MIKE SHE has been found to be insensitive to changes in resolution (Vázquez et al., 2002).

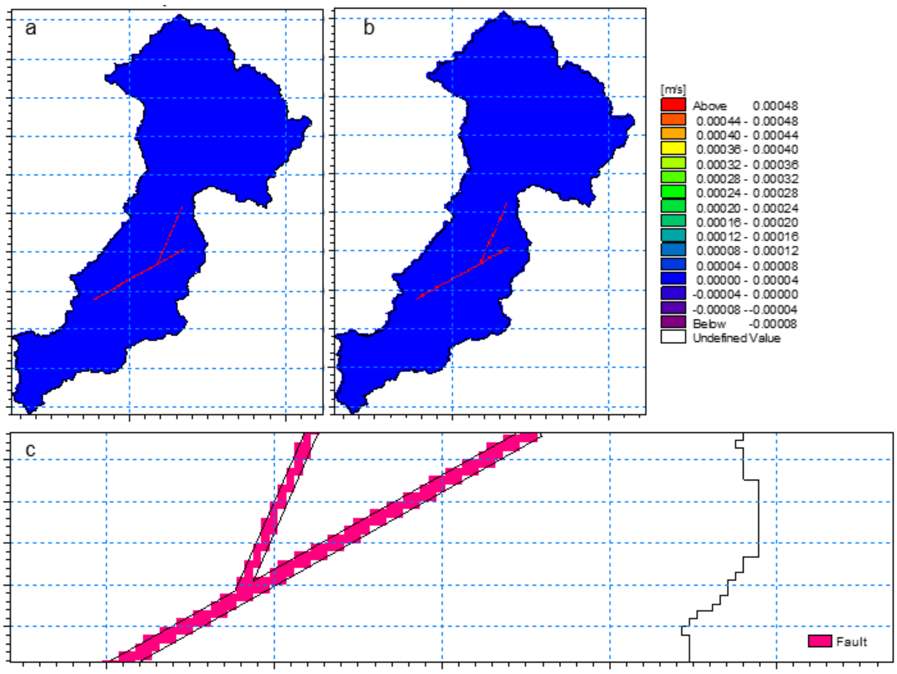

Figure 3.5 Representation of the fault zones in the saturated zone at (a) 100 m computation grid resolution and (b) 500 m computation grid resolution. Resampling of the fault to the resolution of the computation grid is shown in panel c.

3.3.4.10 Validity of Boundary Conditions

The validity of the boundary conditions defined within the model developed in MIKE SHE was assessed by determining the extent to which the boundaries interacted with drawdown arising from groundwater abstraction.

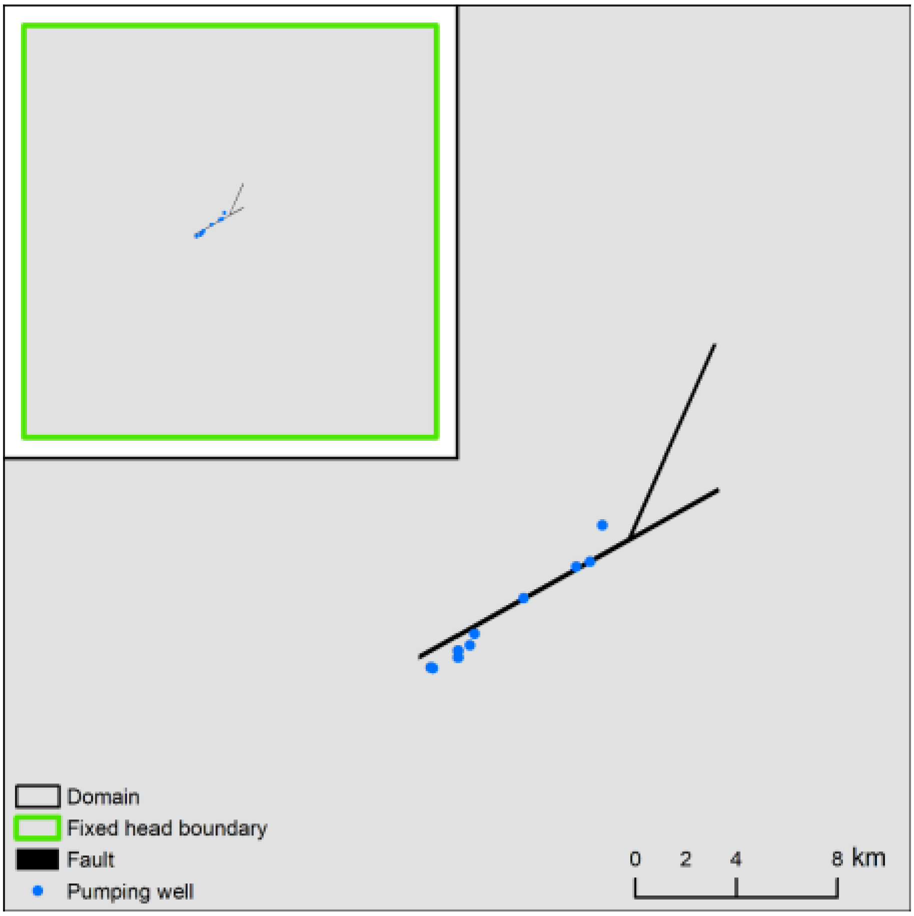

Figure 3.6 Model developed in MIKE SHE to assess the validity of boundary conditions. The size of the domain, the boundary conditions and the relative location of the fault and pumping wells are shown in the inset maps. The location of the pumping wells relative to the fault are shown in more detail in the main panel.

Calculating drawdown using the Theis method (1935) was deemed unsuitable due to the assumption of isotropy, which is irreconcilable with the importance of the fault zones which rapidly transmit water throughout the wellfield (section 2.3.3). Consequently, the model developed in MIKE SHE, described in section 3.3.4.8, was modified to best facilitate an assessment of the suitability of the boundary conditions. The domain was changed from the Makutapora Basin (figure 3.4) to a larger 100 km x 100 km square to increase the distance between pumping and the boundaries (figure 3.6). The boundaries surrounding the domain were defined as fixed head boundaries with the same elevation as the initial potentiometric surface which was set to 1000 m, the approximate average elevation of hydraulic head values observed in the wellfield (1955 – 2016). Drawdown was simulated using contemporary pumping rates i.e. the average pumping rate of each active well during the period April 2015 – April 2016, the period of highest observed abstraction rates. These constant pumping rates were used to simulated drawdown until equilibrium was reached. The equilibrium potentiometric surface was subsequently superimposed onto a map of the Makutapora Basin to assess the extent to which the boundary conditions defined within the model interact with drawdown based on drawdown calculated at the edges of the basin (figure 3.10).

3.3.4.11 Groundwater Abstraction

Groundwater abstraction is a significant component of the current water balance in the Makutapora Wellfield. A continuous dataset exists for aggregated wellfield abstraction from 1964 to present, though a full record of daily abstraction for individual pumping wells does not. Records for individual wells exist between 1985 and 1990, at a monthly resolution, and daily records exist from the middle of 2015 to present. A daily record of abstraction for individual wells was synthesised based on these periods of detailed observations, as well as records of well yields, dates wells came online or went offline, and the long-term aggregated wellfield pumping record. From 1964 to 1985, daily pumping records for individual wells were synthesised based on the relative maximum yields of active wells (Fawley, 1955; Shindo, 1989), and scaled to the corresponding total wellfield abstraction data. Data from 1985 to 1990 comprised monthly pumping data for individual production wells, which were downscaled to a daily resolution. Subsequent data, 1990 to 2001, are based on the fractional input of each well between 1985 and 1990 and scaled to the corresponding total wellfield abstraction. 2001 was defined as the end of this period due to the implementation of several newly built production wells. Data from 2001 to 2015 are based on the fractional inputs of each well between 2015 and 2017 and scaled. The period between 2015 and 2017 employs the observed daily data for individual wells.

It is worth noting, however, that a few wells, used for small-scale abstraction in local villages, are not accounted for in this dataset as they are no longer under DUWASA jurisdiction. Additionally, wellfield pumping is not actually a measure of the volume of water abstracted from the wellfield during the specified timeframe. Rather, it is the volume of water transmitted to Dodoma. In specific instances, these values will deviate as there is storage infrastructure embedded in the pumping system. At a greater temporal scale, however, these data still reflect changes in abstraction.

3.3.4.12 Model Calibration and Validation

The model was calibrated and validated on sections of the groundwater record deemed to have occurred in the absence of recharge, i.e. sustained groundwater-level recessions (Figure 3.7). As groundwater-level changes are recorded in a variable number of wells, at variable temporal resolutions, and at variable levels of completeness, the chosen groundwater-level declines were characterised by a single recessionary rate in each active well, defined by initial and final hydraulic head values. Calibration and validation were conducted using these values. The early part of the record is dominated by ‘natural drainage’ whereas latterly it is more strongly influenced by pumping. To encompass a sufficient range of behaviour within the calibration period (Gan et al., 1997), chosen recessions were ordinally numbered, with even numbered recessions used for calibration, and odd numbered recessions used for validation. Therefore, neither the calibration period, nor the validation period, are continuous. Auto-calibration was deemed unsuitable due to the necessity of reconciling simulated hydraulic head values with observed data prior to the periods of groundwater-level decline.

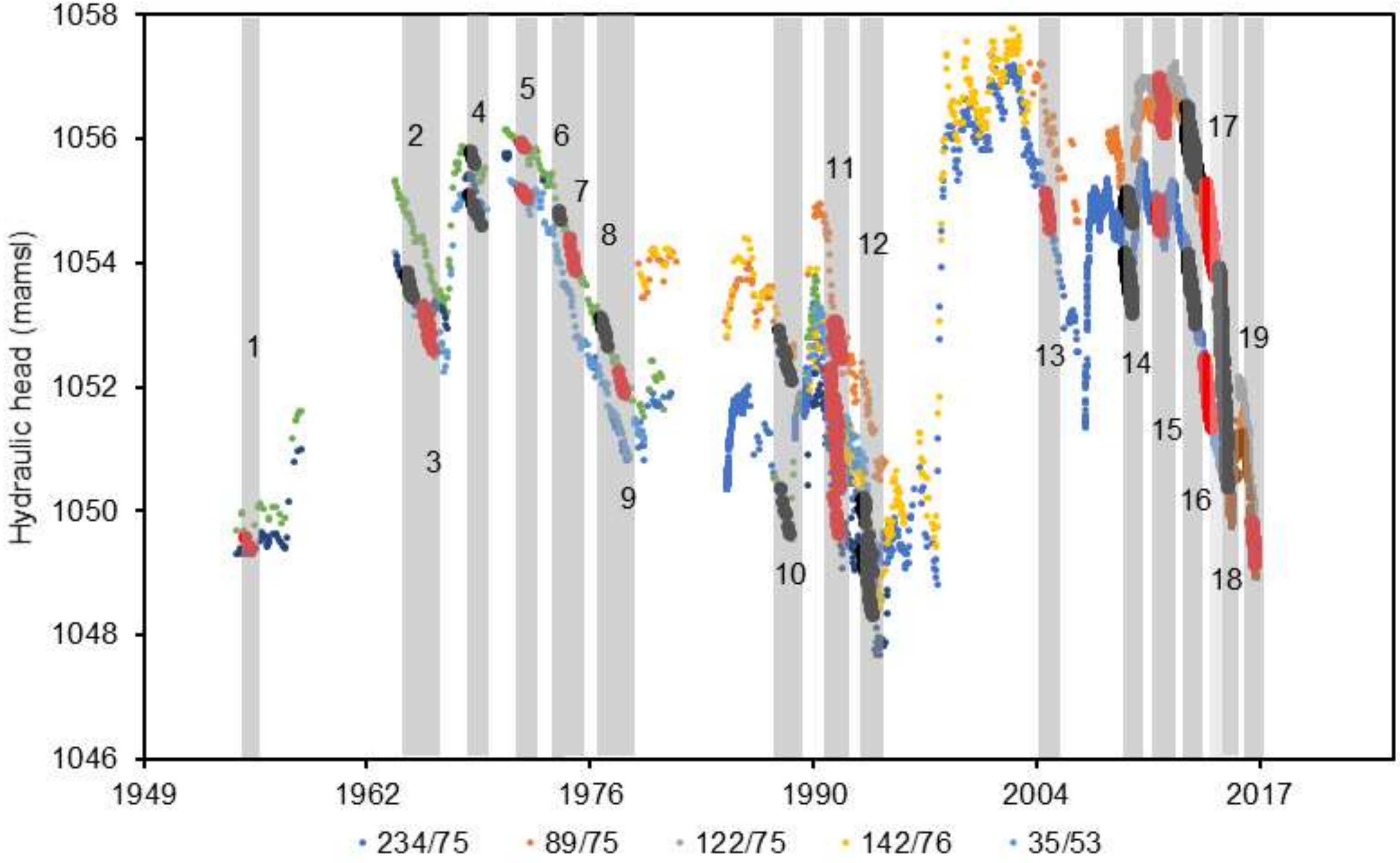

Figure 3.7 Composite record of groundwater level fluctuations in the Makutapora Basin. Recessions used for calibration (black) and validation (red) are numbered.

Accordingly, the calibration process was carried out by manually modifying model parameters. Model performance was evaluated using Nash Sutcliffe Efficiency (NSE) (Nash and Sutcliffe, 1970), Root Mean Square Error (RMSE), Index of Agreement (d) (Willmott, 1981), and percent bias (PBIAS). In this study, model performance was rated based on the scheme of Moriasi et al. (2007) where NSE values between 0.65 and 0.75 indicates "good" model performance while NSE values greater than 0.75 indicates "very good" model performance. Final values of parameters subject to calibration are detailed in Table 3.1.

3.4 Stable-Isotope Tracer Methods and Data

To assess the relationship between daily precipitation intensity and groundwater recharge using stable-isotope tracers, I: (1) collected and analysed precipitation samples, and recorded precipitation data from within the Makutapora Basin; (2) compiled and reconciled a secondary, supplementary dataset comprising daily precipitation and stable-isotope ratios of O and H in daily precipitation, and groundwater from the Makutapora Basin; (3) assessed the relationship between daily precipitation intensity and stable-isotopic composition of precipitation; and (4) compared precipitation and groundwater stable-isotopic compositions to assess any biases in groundwater recharge related to precipitation intensity.

Primary data were collected over 3 wet seasons (2015/2016 – 2017/2018) at the Makutapora Meteorological Station, established by Shindo et al. (1989). Precipitation samples for isotopic analysis were collected in accordance with IAEA (2014) precipitation sampling guidelines for event-based sampling using a buried sampler. Stable-isotopic analysis was undertaken by Elemtex LTD.

Table 3.1. Parameter values for the model developed in MIKE SHE. Calibrated values are highlighted in bold.

Parameter	Value
Aquifer	
Specific yield	**0.07**
Hydraulic conductivity	**$5\text{x}10^{-6}$ $m \cdot s^{-1}$**
Mbuga clay	
Specific yield	**$1\text{x}10^{-4}$**
Hydraulic conductivity	**$1\text{x}10^{-11}$ $m \cdot s^{-1}$**
Faults	
Specific yield	**0.1**
Hydraulic conductivity	**0.001 $m \cdot s^{-1}$**
Fixed head boundary elevation	**1033.3 mamsl**

A supplementary secondary dataset of precipitation, corresponding stable-isotopic compositions, and groundwater stable-isotopic compositions was compiled from previously published studies and the IAEA TWIN database (Table 3.2).

Herein, the ratios of $^{18}O/^{16}O$ and $^{2}H/^{1}H$ are referred to in delta notation ($\delta^{18}O$ and $\delta^{2}H$, respectively), expressed in units of per mille (‰), where $\delta = \left(\left(R_{sample}/R_{VSMOW}\right) - 1\right) \cdot 1000$ and R is the ratio of $^{18}O/^{16}O$ or $^{2}H/^{1}H$ in Vienna standard mean ocean water ("VSMOW") and the sample ("sample").

I followed the approach of Jasechko and Taylor (2015) to calculate amount weighted precipitation oxygen isotopic compositions ($\delta^{18}O_{paw}$), above various intensity thresholds, as:

$$\delta^{18}O_{paw} = \frac{\sum_{i=1}^{n} P_i * \delta^{18}O_{p_i}}{\sum_{i=1}^{n} P_i} \qquad \text{(Equation 3.5)}$$

where P represents daily precipitation (mm·day^{-1}), $\delta^{18}O_p$ represents the corresponding measured stable isotope ratio of O in daily precipitation, and n is the total number of precipitation events included in the calculation. For example, the amount weighted precipitation isotopic composition corresponding to a threshold above x mm·day^{-1}, is equivalent to the result of Equation 3.5 where precipitation events less than x mm·day^{-1} are excluded from the calculation. These calculations facilitate the assessment of the relationship between precipitation intensity and stable-isotopic composition. The average unevaporated ($\delta^{18}O_{ugw}$), or pristine, isotopic composition of the precipitation, from which groundwater derived, was determined from the intersection of the local meteoric water line and the local evaporation line (Gonfiantini, 1986). I then compared $\delta^{18}O_{ugw}$ values with $\delta^{18}O_{paw}$ associated with varying intensity thresholds to assess precipitation intensity-based recharge biases.

Table 3.2. Type, amount, and source of secondary precipitation and stable-isotope data.

Type	n	Reference
Precipitation	1 season	(Shindo et al., 1989)
Precipitation	1 season	(Shindo et al., 1990)
Precipitation	1 season	(Onodera et al., 1995)
Precipitation composition	33	(Nkotagu, 1996)
Precipitation composition	26	(Onodera, Kitaoka, Hayashi, et al., 1995)
Groundwater composition	16	URT8003 (IAEA/WMO, 2018)
Groundwater composition	6	URT8004 (IAEA/WMO, 2018)
Groundwater composition	6	URT8006/1 (IAEA/WMO, 2018)
Groundwater composition	11	URT-EXT/01 (IAEA/WMO, 2018)
Groundwater composition	23	URT-RAF8029 (IAEA/WMO, 2018)
Groundwater composition	47	(Shindo et al., 1990)

3.5 Results and Discussion

3.5.1 Model Evaluation

A comparison of simulated and observed hydraulic head values is shown in figure 3.8 and figure 3.9 and model performance statistics are provided in Table 3.3. Overall, model performance can be classified as ‘good’, based on the NSE score and the performance rating of Moriasi (2007), calculated using data from all recessions. This indicates that the model accurately replicated the magnitude of observed water-level changes. During calibration, the NSE score indicated ‘very good’ performance. Residual variance was small compared to measured variance. Calibration and validation periods exhibited similar RMSE, 0.65 m and 0.59 m, respectively. Average RMSE, 0.62 m, represents 50% of the standard deviation in the observed data. Accounting for all groundwater declines, model prediction error, d, was 0.92. PBIAS varied considerably between calibration and validation periods, with the calibration period displaying greater bias. Positive PBIAS indicates that the model over-predicted hydraulic head levels during calibration, whereas hydraulic head levels were generally under-predicted during validation, albeit to a lesser extent. The recessionary periods used for calibration and validation, despite being objectively mixed, encompassed different conditions, which appears to have resulted in different model performance statistics and ratings based on calibration and validation periods.

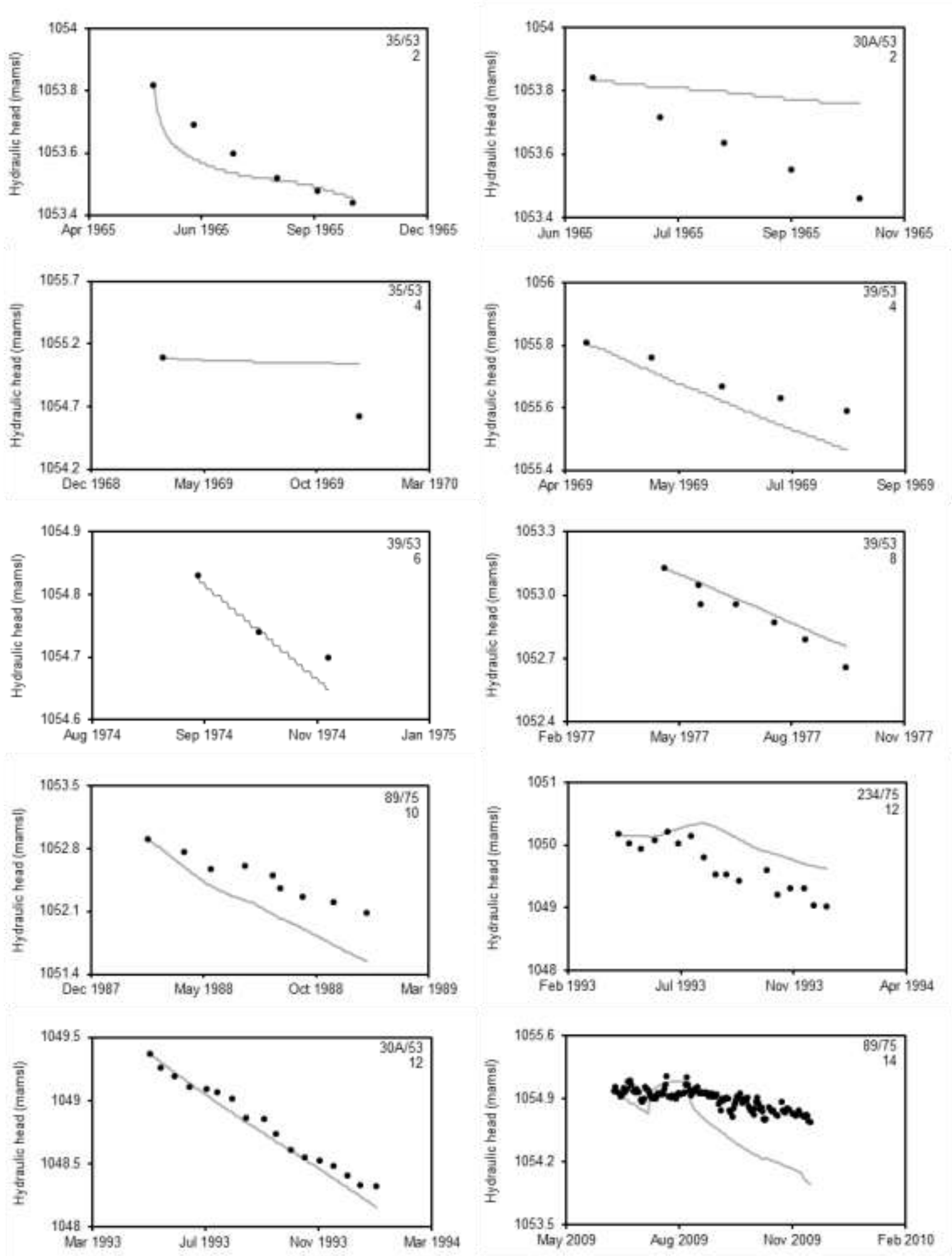

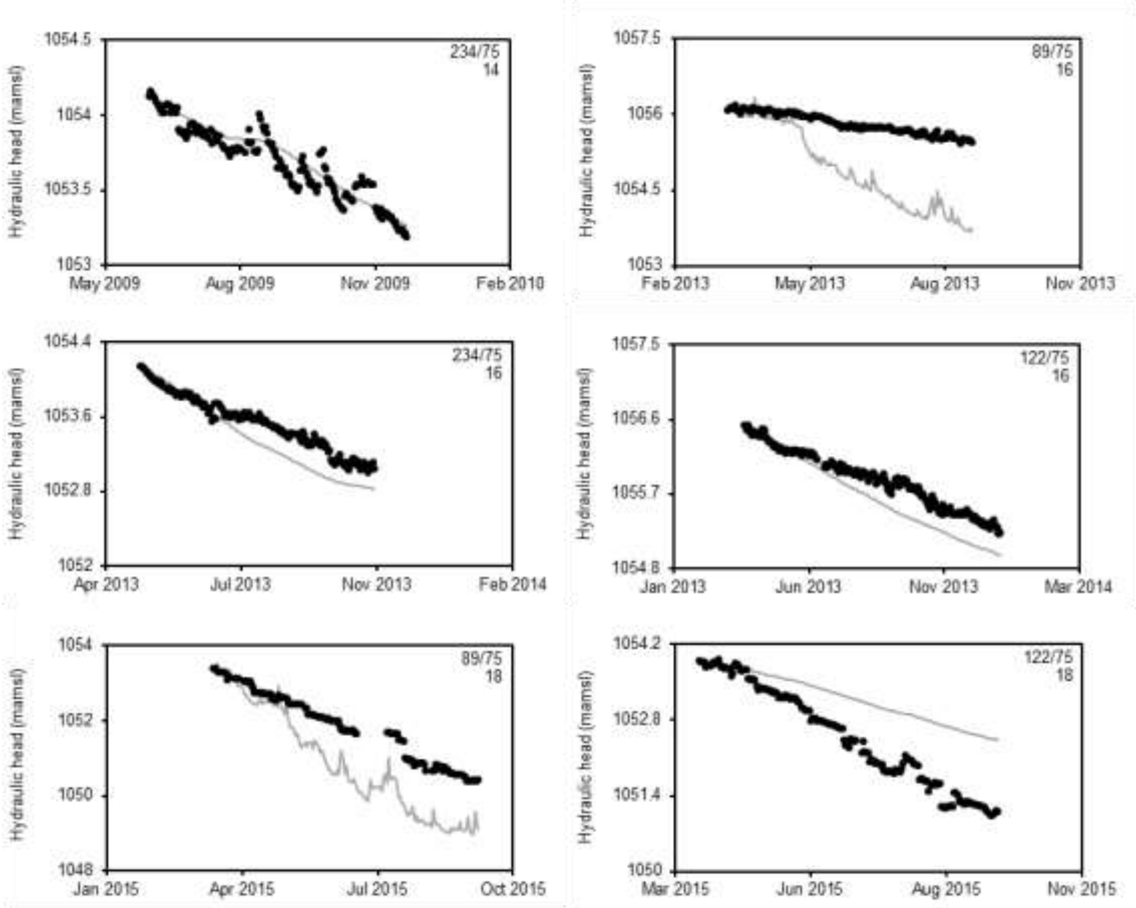

Figure 3.8 Observed (black dots) and simulated (grey line) hydraulic head values for simulations used to calibrate the MIKE SHE saturated zone model. Numbers in the top right corner of each graph correspond to the observation well (top) (figure 2.9) and recession number (bottom) (Figure 3.7).

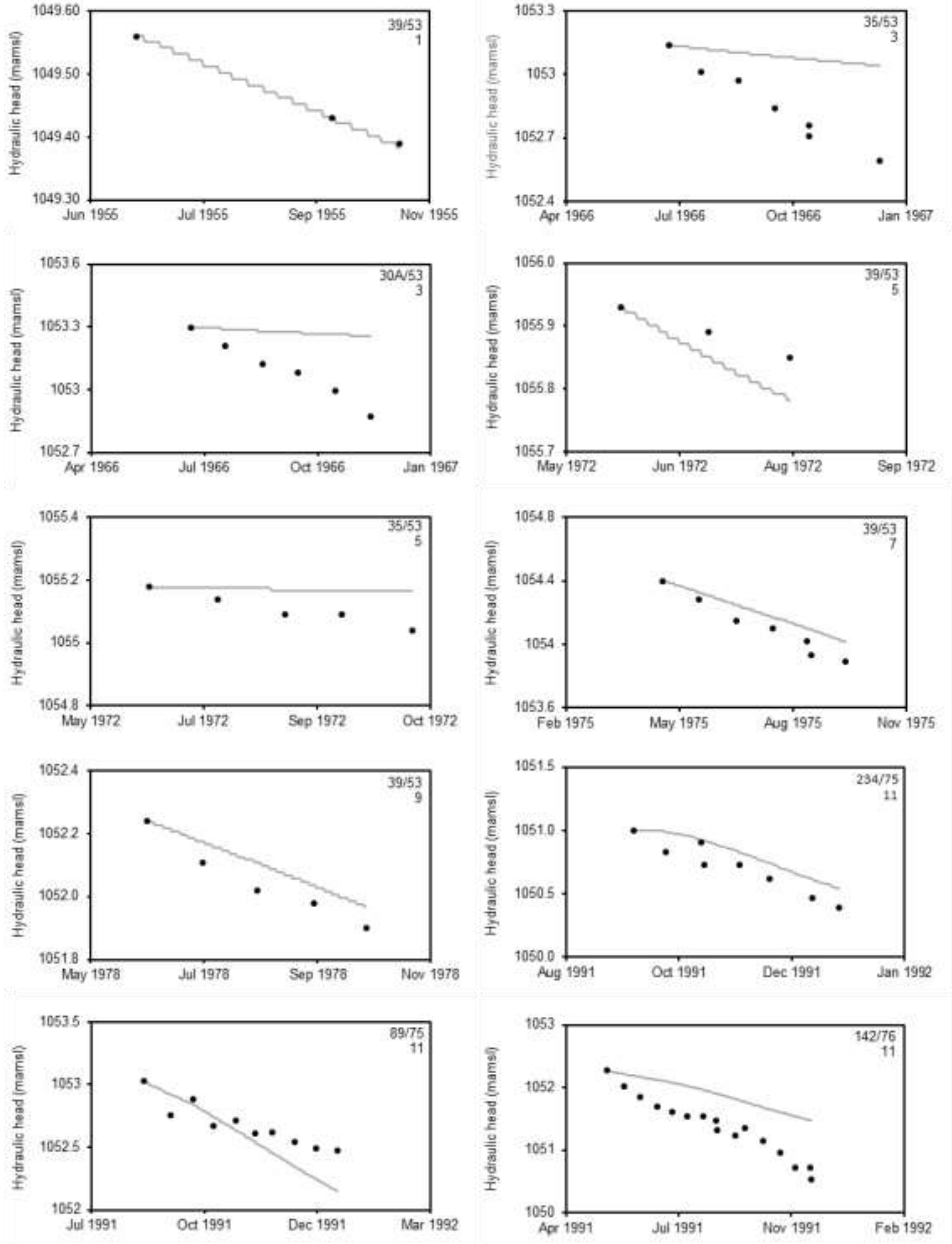

Hydraulic head (mamsl)
39/53
1
1049.60
1049.50
1049.40
1049.30
Jun 1955
Jul 1955
Sep 1955
Nov 1955
35/53
3
1053.3
1053
1052.7
1052.4
Apr 1966
Jul 1966
Oct 1966
Jan 1967
30A/53
3
1053.6
1053.3
1053
1052.7
Apr 1966
Jul 1966
Oct 1966
Jan 1967
39/53
5
1056.0
1055.9
1055.8
1055.7
May 1972
Jun 1972
Aug 1972
Sep 1972
35/53
5
1055.4
1055.2
1055
1054.8
May 1972
Jul 1972
Sep 1972
Oct 1972
39/53
7
1054.8
1054.4
1054
1053.6
Feb 1975
May 1975
Aug 1975
Nov 1975
39/53
9
1052.4
1052.2
1052.0
1051.8
May 1978
Jul 1978
Sep 1978
Nov 1978
234/75
11
1051.5
1051.0
1050.5
1050.0
Aug 1991
Oct 1991
Dec 1991
Jan 1992
89/75
11
1053.5
1053
1052.5
1052
Jul 1991
Oct 1991
Dec 1991
Mar 1992
142/76
11
1053
1052
1051
1050
Apr 1991
Jul 1991
Nov 1991
Feb 1992

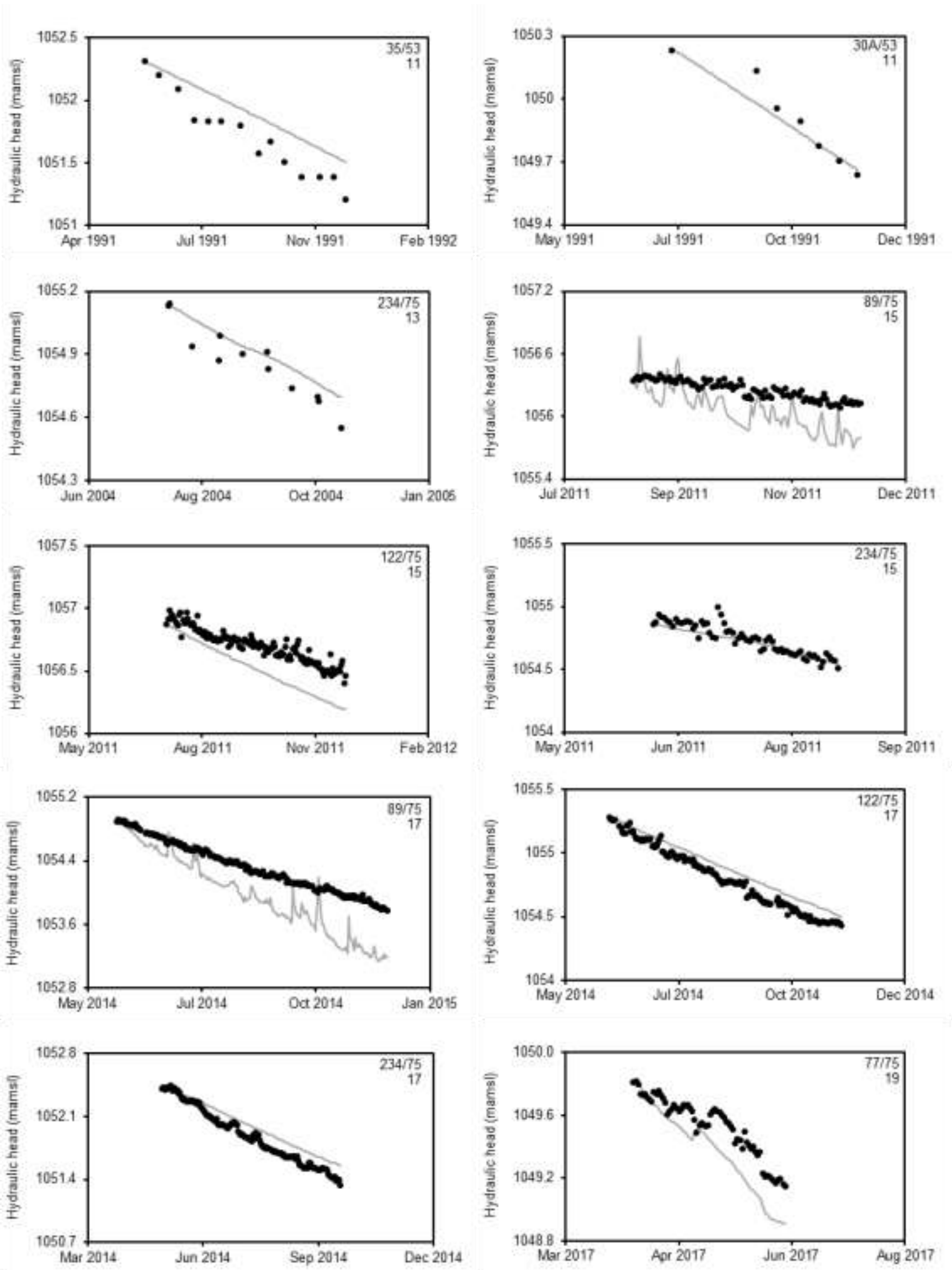

Figure 3.9 Observed (black dots) and simulated (grey line) hydraulic head values for simulations used to validate the MIKE SHE saturated zone model. Numbers in the top right corner of each graph correspond to the observation well (top) (figure 2.9) and recession number (bottom) (Figure 3.7).

Overall model performance was 'good', but replication of observed recessions in individual wells was varied. Recession 1, the only recession caused by 'natural' water table fluctuations, i.e. in the absence of abstraction, was replicated very well. The Pearson correlation coefficient between observed and simulated hydraulic head values is 0.99, and the difference between observed and simulated average recessionary rates is less than 6%. Recessions 7,8,9,12,13 and 17 are all reproduced well by the model, all falling within ±25% of the observed recession rate. Other observed recessions were reproduced well when averaged across active wells. Examples of this include recessions 4,5,10,11,14,15,16 and 18. Recessions early in the record, such as 2 and 3, which coincide with the largest relative abstraction changes in the entire record, the onset of pumping, are less well reproduced.

Table 3.3. MIKE SHE model performance statistics for hydraulic head values in the Makutapora Basin for calibration and validation periods. Overall statistics are also given.

Period	Target	NSE	RMSE	d	PBIAS
Calibration	Groundwater recessions (2,4,6,8,10,12,14,16,18)	0.81	0.65	0.95	19.91
Validation	Groundwater recessions (1,3,5,7,9,11,13,15,17,19)	0.55	0.59	0.92	-2.38
Overall	Groundwater recessions (all)	0.74	0.62	0.94	8.75

3.5.1.1 Validity of Boundary Conditions

Simulated drawdown for contemporary abstraction rates at equilibrium is shown in figure 3.10.

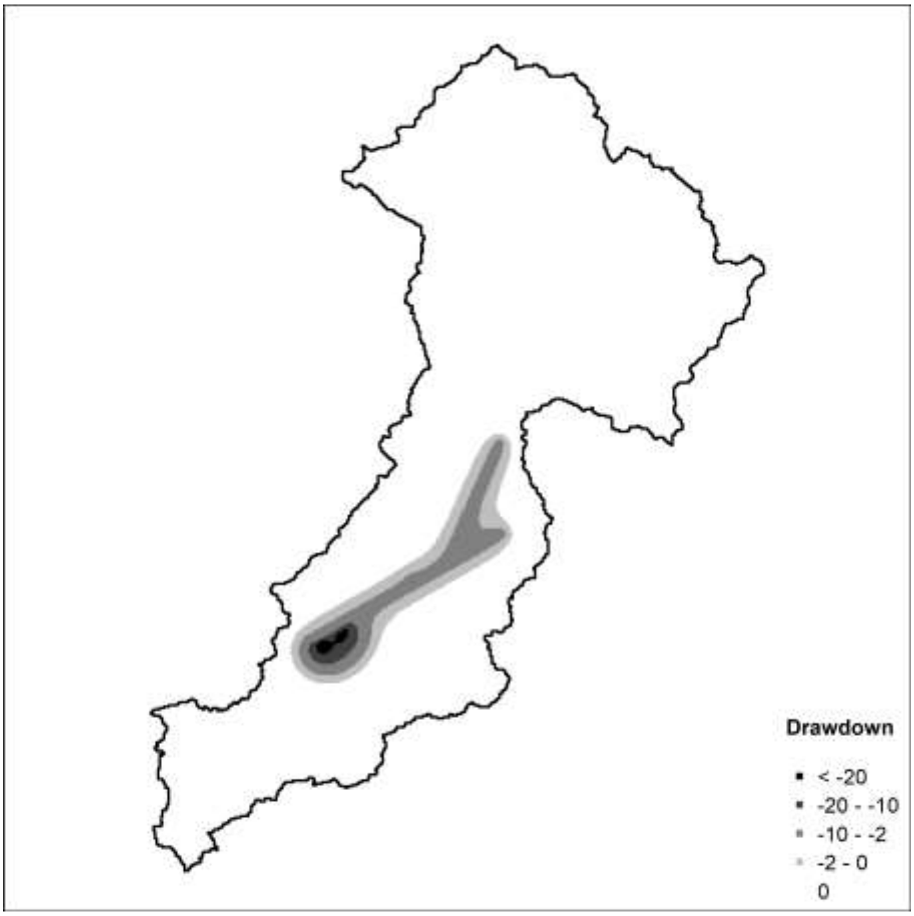

Figure 3.10 A map of the domain of the model developed in MIKE SHE showing drawdown due to contemporary groundwater abstraction rates at equilibrium.

Superimposition of the Makutapora Basin on the computed drawdown shows that the largest drawdown occurs in the south west of the wellfield, the area with the highest concentration of production wells. The combined effect of all active production wells has minimal interaction with the model boundaries as no drawdown is computed at the boundary of the basin. Using the surface water divide as the model domain appears to be valid.

3.5.2 Hydrometric Results

Groundwater-levels from the Makutapora Basin exhibit prolonged periods of decline, signifying little or no recharge, punctuated by considerable, but infrequent recharge events (Figure 3.1). The original analysis of this record by Taylor et al. (2013b), based on a steady-state relationship between recessionary trends and abstraction, suggested that nearly two-thirds of the wet seasons were not associated with any groundwater recharge. After accounting for dynamic recessionary trends in groundwater-levels due to abstraction, far fewer years (6 of 49) exhibit no recharge, revealing that groundwater recharge occurs more frequently than the previously thought (Figure 3.11). The original analysis indicated that, with the exception of years comprising anomalously intensive months, more than 670 mm·year^{-1} of rainfall was required to produce groundwater recharge. This reanalysis indicates that the annual precipitation threshold to produce groundwater recharge is lower. The reanalysis shows that many seasons originally associated with "little or no recharge" are now associated with non-trivial amounts of recharge despite as little as 400 mm of precipitation. As a result of these changes, while the estimated magnitude of the largest recharge events remained similar, there is a more pronounced non-linearity between precipitation and recharge in the original analysis. A non-linear relationship between annual precipitation and groundwater recharge is, however, still observed with large (q/S_y > 3.5 m) recharge events exclusively occurring when annual precipitation exceeds 750 mm (Figure 3.11); very little or no recharge is recorded when annual precipitation is below 400 mm.

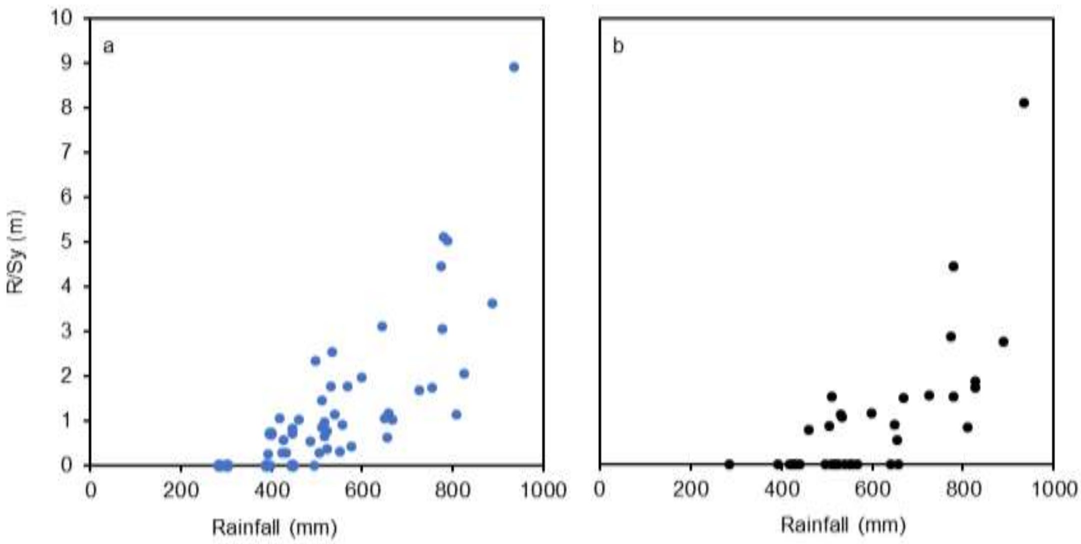

Figure 3.11 Cross plots of estimated groundwater recharge versus wet season precipitation, from (a) this thesis assuming dynamic recessions and (b) figure adapted from Figure 2 in (Taylor et al., 2013b) assuming steady state recessions.

Taylor et al. (2013b) demonstrated a strong association between large recharge events and El Niño conditions. The 2015/2016 wet season, associated with one of the strongest El Niño events on record (Becker, 2016a), aligned with this trend as it produced the third largest recharge event since groundwater monitoring began in the Makutapora Basin.

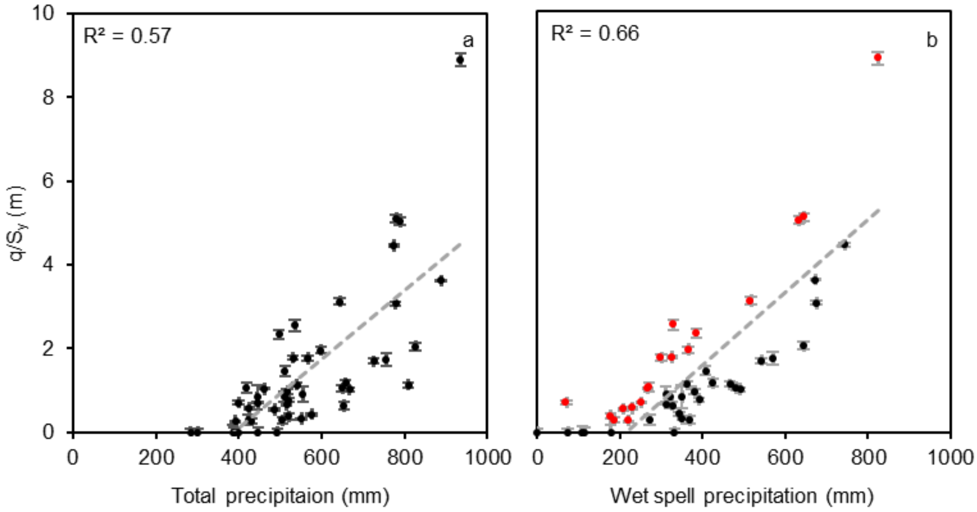

Figure 3.12 Cross plot of estimated groundwater recharge and total annual precipitation (a). Cross plot of estimated groundwater recharge and the sum of annual wet spell precipitation greater than 70 mm in 9 days (b). Error bars are the RMSE associated with the recession prior to each recharge events. In graph b, recharge events with positive residuals are highlighted in red.

Linear regressions of estimated recharge and annual precipitation, and estimated recharge and wet spell precipitation, show that recharge magnitude is significantly ($p < 0.05$) (Steiger, 1980) more strongly correlated to precipitation comprising wet spells ($R^2 = 0.66$) than the sum of all precipitation ($R^2 = 0.55$) (Figure 3.12). R^2 values are greater than 0.55 for various combinations of duration and intensity threshold between 4 days and 16 days and 45 mm and 84 mm, respectively. a 9-day wet spell with a threshold of 70 mm produces the greatest correlation (Figure 3.12). The importance of prolonged periods of higher intensity have previously been noted in Makutapora (Taylor et al., 2013b). The statistically significant ($p < 0.05$) intercept indicates that, on average over 200 mm of precipitation comprising wet spells is required before recharge occurs.

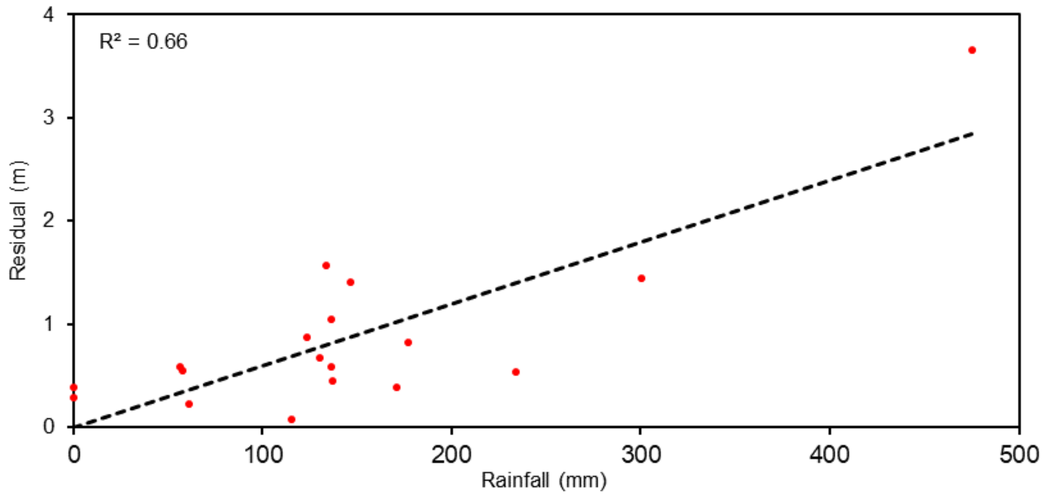

Figure 3.13 Plot of residuals calculated using the regression model shown in Figure 3.12, against the sum of all precipitation events exceeding the 96.3th intensity percentile in the corresponding wet season.

Seasons with positive residuals, i.e. years where observed recharge is greater than recharge predicted by the regression model (Figure 3.12), were examined to determine their genesis. The magnitude of positive residuals is significantly ($p < 0.05$) correlated to the sum of extremely intensive daily precipitations in the corresponding wet season. The strongest relationships ($r > 0.7$) exist for the sums of precipitation events between the 99.3th (105 mm·day^{-1}) and 93.2rd (39 mm·day^{-1}) intensity percentiles. The strongest of these relationships occurs at the 96.3th (51 mmday^{-1}) percentile (Figure 3.13). Discrete heavy precipitation events have previously been implicated in producing groundwater recharge in other regions of sub-Saharan Africa (Owor et al., 2009).

3.5.3 Stable-Isotope Tracer Results

Fundamental to this analysis is the presence of the 'amount effect' (Dansgaard, 1964) in the Makutapora Basin. Figure 3.14 shows a non-linear relationship whereby amount-weighted $\delta^{18}O$ of precipitation varies as a function of daily precipitation intensity, with heavy precipitation events relatively depleted in heavy isotopes. The lower 3 quartiles of precipitation intensity exhibit a shallow decline, with all amount-weighted $\delta^{18}O$ values falling between -4.7‰ and -4.2‰. A more severe declining trend occurs at intensities greater than the 75th percentile with the heaviest 1% of daily precipitation events, for which data was collected, comprising an amount-weighted composition of less than -7.1‰. The dependence of $\delta^{18}O$ content of precipitation on precipitation intensity, in the Makutapora Basin, has previously been observed, by studies with smaller sample sizes (Nkotagu, 1996; Onodera et al., 1995). The general form of the relationship closely matches many locations across the tropics analysed by Jasechko and Taylor (2015), employing the same statistical methods.

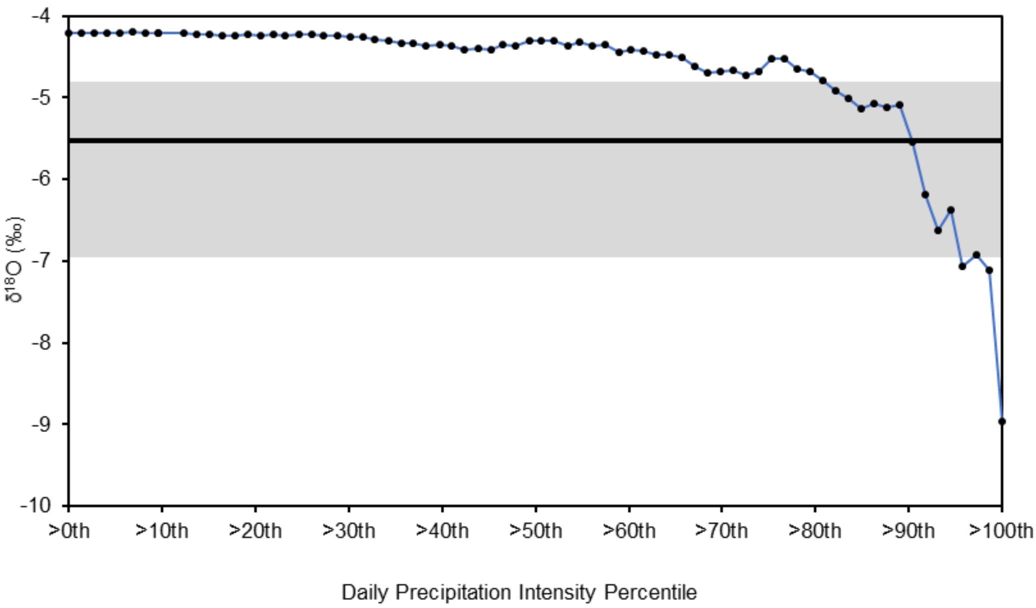

Figure 3.14 Amount-weighted precipitation $\delta^{18}O$ using data exceeding progressive daily precipitation intensity thresholds (blue line) and mean groundwater $\delta^{18}O$ value (black line). Grey shaded area represents limits of the estimated average groundwater value (Figure 3.15).

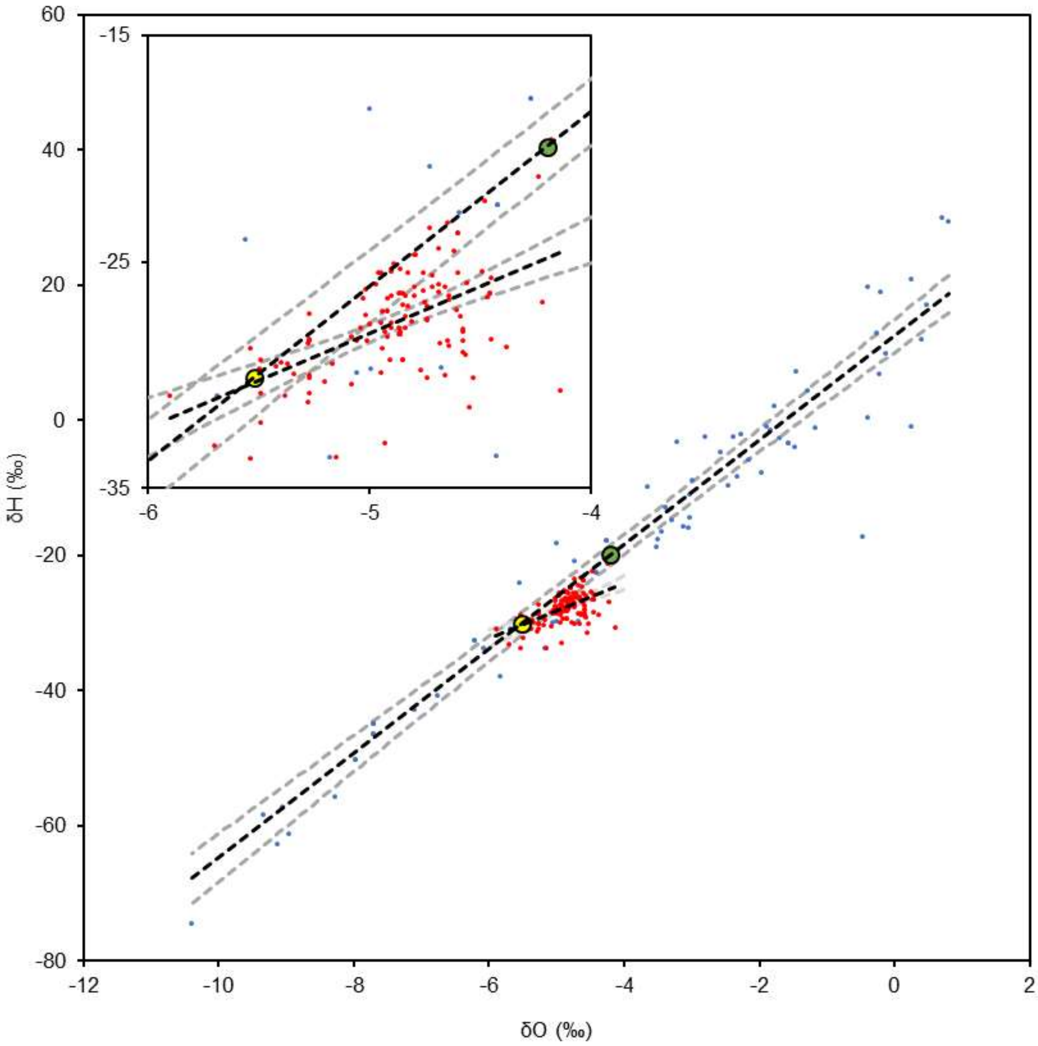

Figure 3.15 Linear trends (black dotted lines) and 95% confidence bands (grey dotted lines) for $\delta^{18}O$ and $\delta^{2}H$ of precipitation (blue dots) and groundwater (red dots) samples from the Makutapora Basin. Mean amount weighted precipitation (green circle) and the intercept of the local meteoric water line and the local evaporation line (yellow dot) are highlighted.

There are statistically significant ($p<0.05$) linear relationships between the $\delta^{18}O$ and $\delta^{2}H$ values of precipitation (Equation 3.6) and groundwater (Equation 3.7) samples collected in Makutapora Wellfield (Figure 3.15).

$$\delta^{2}H = 7.7\pm0.3\cdot\delta^{18}O + 12.5\pm1.2‰ \qquad \text{(Equation 3.6)}$$

$$\delta^{2}H = 4.1\pm0.6\cdot\delta^{18}O - 7.5\pm2.7‰ \qquad \text{(Equation 3.7)}$$

The local meteoric water line (LMWL) (Equation 3.6), characterised by the linear trend derived from precipitation data, is similar to the global meteoric water line (Craig, 1961). The trend defined by groundwater samples (Equation 3.7) is significantly ($p<0.05$) (Cohen et al., 2013) distinct from the LMWL and is characterised by a shallower gradient, signifying the local evaporation line (LEL). The LMWL and LEL intersect when $\delta^{18}O$ = -5.52‰. 95% confidence bands for both linear regressions intersect at an upper $\delta^{18}O$ value of -5.02‰, and a lower $\delta^{18}O$ value of -6.76‰. The point of intersection represents the average composition of precipitation, after selection, but prior to fractionation (Gonfiantini, 1986), which ultimately became groundwater. This average pristine groundwater δ^{18}O is lower than amount-weighted precipitation δ^{18}O for all precipitation (Figure 3.14), and is, therefore, relatively depleted in ^{18}O. Given the presence of an observable 'amount effect', this comparison indicates that more intensive precipitation produces a disproportionate amount of groundwater recharge.

Considering isotopic composition as a function of precipitation intensity, the intensity threshold most closely related to groundwater was estimated. Mean isotope composition of groundwater corresponds to the amount-weighted composition of daily precipitation exceeding the 90th percentile (Figure 3.14), equivalent to 41 mm·day^{-1}. Calculated upper and lower limits of groundwater composition correspond to precipitation exceeding the 84th intensity percentile (30 mm·day^{-1}) and the 95th percentile (53 mm·day^{-1}), respectively. This bias is consistent with the few previous isotope studies in Africa (Jasechko & Taylor, 2015; Taylor & Howard, 1999; Taylor & Howard, 1996; Vogel & Van Urk, 1975), which utilised cumulated monthly precipitation samples.

In addition to exploring the presence of the 'amount effect' within the Makutapora Basin, other observed isotope effects in precipitation were examined (Gat et al., 2001). Figure 3.16 shows the seasonality of stable-isotope composition of precipitation. Raw data and monthly averages show no conspicuous trend or pattern. No 'seasonal effect' based on temperature, as observed at temperature latitudes, is observed (Fricke and O'Neil, 1999; Yurtsever, 1975).

On comparison with average Dodoma temperatures (1971-2000), isotopic composition does not conform in the manner expected if composition was strongly determined by temperature. This concurs with general findings in the tropics where the isotopic composition of precipitation has shown poor correlation with surface temperature (Dansgaard, 1964; Gonfiantini et al., 2001; Rozanski et al., 1993). Further, in some locations, the 'seasonal effect' has been attributed to an 'amount effect'

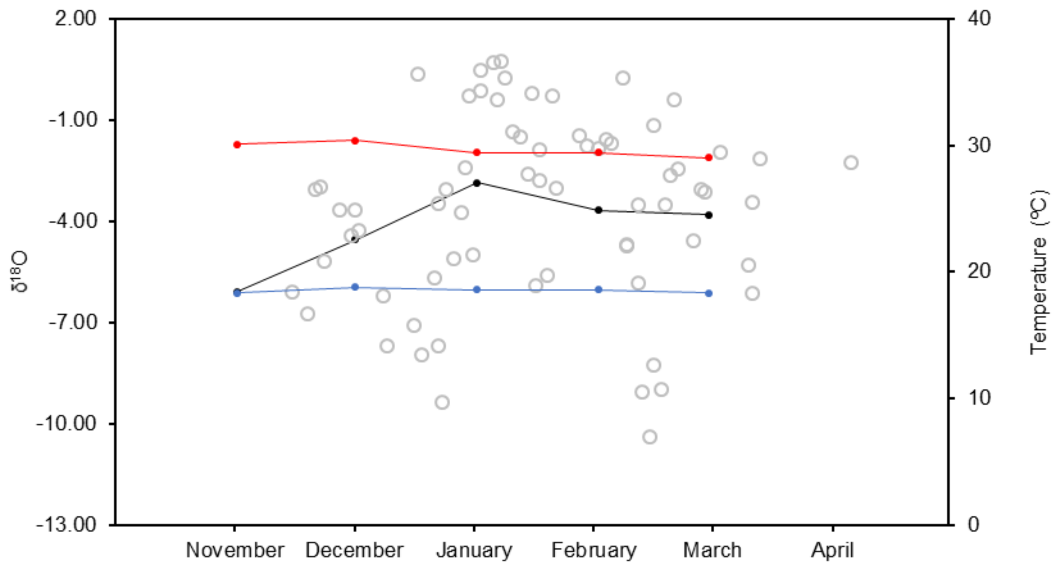

Figure 3.16 Seasonal variation in δ^{18}O of precipitation samples. Grey circles are raw data representing individual samples, collected over 5 wet seasons (1989/1990, 1990/1991, 2015/2016, 2016/2017, and 2017/2018). Black dots and lines are monthly averages of those data (April is excluded due to a shortage of samples collected in April). Red dots and lines, and blue dots and lines, are monthly average daily temperature highs and lows in Dodoma (1971-2000), respectively (WMO, 2018).

whereby more intensive precipitation events generally occur in the wet season (Gonfiantini et al., 2001; Jones & Banner, 2003; Jones et al., 2000; Lachniet et al., 2007). Due to the latitude of Makutapora, there is limited temperature variation throughout the year (fig 3.9), and little deviation in $\delta^{18}O$ (Gat et al., 2001). Additionally, Makutapora does not receive any precipitation for more than half the year. Again, due to its latitude, and the passage of the inter tropical convergence zone, central Tanzania experiences a unimodal wet season. Accordingly, any 'seasonal effect' is unlikely to arise from variations in surface temperatures or changes in precipitation any throughout the year.

3.6 Discussion

The analyses presented here reveal several important findings. Firstly, groundwater derives preferentially from more intensive precipitation in the Makutapora Basin. Intensity over 2 distinct timescales was shown to be important in this regard. Prolonged intensity, over multiple days, and extremely intensive precipitation, on discrete single days, are both associated with groundwater recharge. This intensity bias was evident in both the hydrometric and stable-isotope data. Secondly, groundwater recharge is more frequent and less episodic than previously assessed. The reanalysis of the long-term groundwater-level record from the Makutapora basin shows that many years that were previously thought to exhibit no groundwater recharge, experienced small events. The non-linearity in the relationship between precipitation and groundwater recharge is, however, confirmed. Thirdly, while this study was not primarily concerned with the processes transmitting precipitation to the saturated zone, they were incidentally, partially elucidated. Before precipitation becomes groundwater, it undergoes selection and fractionation. Selection appears to be based on the intensity of precipitation, and fractionation is presumed to be due to evaporation. Finally, stable isotope analysis was predicated on the presence or absence of a variety of isotope effects in precipitation. There is a clear 'amount effect' in the Makutapora Basin and there is no evidence of a 'seasonal effect'.

3.6.1 Conceptual Model of Recharge Generation

The importance of more intensive precipitation on discrete days could be the result of recharge occurring via a diffuse mechanism whereby in-situ precipitation temporarily exceeds high rates of prevailing transpiration and soil moisture deficits (Taylor et al., 2013b), or precipitation producing infiltration excess overland flow resulting in focused recharge. Alternatively, an increase in the number of intensive precipitation events can cause a higher fraction of precipitation to runoff (Wang et al., 2017) due to saturation excess overland flow, or the cumulative saturation of soil to incite diffuse recharge. The importance of precipitation intensity for diffuse recharge has been highlighted by soil-moisture balance modelling studies (Eilers et al., 2007; Mileham et al., 2009; Taylor & Howard, 1996). Observed rapid transmission of recharge is expected to involve preferential pathways (Jasechko and Taylor, 2015), such as soil macropores that bypass soil matrices and whose role in soil hydrology has long been neglected (Beven and Germann, 2013). To fully understand the impacts of climate change on groundwater recharge in the Makutapora Basin, further research into predominant recharge mechanisms is required. Recharge mechanisms in the Makutapora Basin are explored in Chapter 4.

3.6.2 Model Performance

The performance of a modified WTF method to account for transient recessions of groundwater-levels using a numerical model in MIKESHE was 'good' and groundwater recessions under, both, natural and pumped conditions are generally well reproduced. Inaccuracies may result from improperly apportioned abstraction in the synthesised abstraction data inputted in the model. Not only was the distribution of abstraction amongst active wells estimated for much of the record, there is also no definitive record of active wells. Furthermore, some wells have been ceded to nearby villages, and are no longer under the jurisdiction of DUWASA, and are therefore not included in the records of total wellfield abstraction. These wells, however, are not pumped on the same scale as those used for the municipal supply of Dodoma. Here, I have demonstrated that WTF method can be implemented in a highly pumped location with a numerical model to account for transience in groundwater-level responses, to good effect. The performance of this modified procedure would benefit from more comprehensive data, if it were to be implemented in other areas, or in Makutapora in the future.

3.6.3 Climate Change Impact

Annual precipitation shows highly variable responses to climate change (Zhang et al., 2007), however, the intensity of precipitation has been observed to increase almost ubiquitously, with the greatest increases occurring in the tropics, including sub-Saharan Africa (Westra et al., 2012). These changes are anticipated to continue with further warming (Niang et al., 2014), despite generally being underestimated by models (Allan and Soden, 2008). The replacement of lower intensity precipitation events with higher intensity precipitation events, implies that groundwater recharge will increase in Makutapora and analogous areas. Accurate projections of future groundwater resources are, therefore, reliant on explicitly considering changing precipitation intensities (Owor et al., 2009). However, direct and indirect changes to groundwater resources, such as, human overuse (Richey et al., 2015), changes in the total volume of precipitation (Jiménez Cisneros et al., 2014; Zhang et al., 2007), changes to evaporation (McCarthy, 2001), and land-use change (Favreau et al., 2009), may negate or exacerbate increased rates of groundwater recharge. The relative magnitudes of the impacts of these drivers is explored in Chapter 5.

3.7 Conclusions

The efficacy of a modified WTF method, accounting for transient effects of dynamic abstraction using a numerical model, is demonstrated in an intensively pumped wellfield. Rare, long-term datasets of coincidental groundwater and precipitation data from semi-arid central Tanzania are reanalysed. This analysis indicates a non-linear relationship between precipitation intensity and groundwater recharge but suggests that groundwater recharge is less episodic than previously computed as the revised analysis is more sensitive to the resolution of small recharge events. Groundwater recharge was shown to be better related to wet spells of higher intensity precipitation than total precipitation and is also influenced by discrete days of extremely high intensity.

This intensity bias is corroborated by analysis of stable-isotope ratios of O and H of precipitation and groundwater. Climate change is projected to increase the variability, and reduce the availability of surface water and soil moisture through the intensification of precipitation and amplification of potential evapotranspiration (Jiménez Cisneros et al., 2014). These changes and potential impacts are particularly acute in sub-Saharan Africa where more than 95% of farmed land is rainfed (Wani et al., 2009). Overall, the results show, that an intensification of the hydrological cycle may enhance groundwater recharge in the semi-arid Makutapora Basin. Groundwater may thus prove to be a more climate-resilient source of freshwater than surface water, facilitating adaptive strategies including groundwater-fed irrigation and sustaining domestic and industrial water supplies. It is worth noting that these findings merely indicate a bias of increased groundwater recharge associated with more intensive precipitation, and not necessarily that groundwater resources will increase in the future.

Locally, this research has potentially important implications for Dodoma. Currently, the city is seeking to supplement its water supply with a large-scale water transfer project. If the renewable groundwater resources in Makutapora are set increase drastically, this expensive infrastructure project may be unnecessary. Before an assessment of the future viability of Makutapora as the sole source of water for Dodoma can be made, it is necessary to assess the relative magnitudes of all direct and indirect changes pertinent to groundwater recharge. In addition to the research presented here concerning precipitation intensity, it will be necessary to assess the impact of concomitant climate changes such as increased temperatures and changes to annual precipitation. Additionally, the water demand of Dodoma is growing with the population of the city. Increases in water demand need to be assessed in the context of any potential increases in recharge. The sustainability of the Makutapora Wellfield is assessed in Chapter 5.

Chapter 4

Groundwater Recharge Processes in the Makutapora Basin

4.1 Abstract

To investigate the predominant recharge mechanisms transmitting meteoric water to the saturated zone in the Makutapora Basin, a high-resolution groundwater monitoring network was constructed prior to the 2015/2016 El Niño wet season. A novel method of observing the formation and decay of groundwater 'mounds' in an actively pumped system was developed to identify the location and prevalence of focused recharge. Long-term surface water dynamics and stable-isotope analyses support the conclusion that groundwater recharge primarily occurs via leakage from ephemeral streambeds. These analyses indicate that groundwater recharge may increase as a result of climate change if runoff and ephemeral stream flow increase. Furthermore, an improved understanding of processes within the basin is a first step towards assessing the viability of MAR solutions and developing a fully integrated hydrological model of the basin.

4.2 Introduction

Natural groundwater recharge, the addition of water from an overlying unsaturated zone or surface water body to the saturated zone (Scanlon et al., 2006b), generally occurs via two mechanisms. Focused recharge is the leakage of water from inundated surface topographic depressions, such as streams, lakes, and playas, to the groundwater system. Diffuse recharge is the areally distributed transmission of water from the land surface to the water table as a result of in situ infiltration and percolation of meteoric water. Infiltration is the movement of water from the surface into the subsurface, and percolation is the downward movement of water through the unsaturated zone. Percolation occurs via two primary mechanisms: (1) piston flow, the uniform movement of water that displaces existing water without bypassing it; and (2) preferential flow, the movement of water along preferred pathways, such as fractures, cracks, wormholes and roots. Preferential flow allows water that infiltrated relatively later to reach the saturated zone before water that infiltrated relatively earlier, as it is bypassed. Broadly, both diffuse and focused recharge processes occur in all groundwater systems, with the prevalence of focused recharge generally increasing with increasing aridity (Alley, 2009).

Recharge in semi-arid areas predominately occurs via leakage from ephemeral streams (Scanlon et al., 2006b; Simmers, 2003; Simmers et al., 1997), however, the relationship with climate is modified by land cover and underlying geology (Taylor et al., 2013a). Studies throughout sub-Saharan Africa have shown considerable variation in predominant recharge processes. This is due to the wide range of geological and climatological environments (Scanlon et al., 2006a), but may also be an artefact of inappropriate application of methodologies (Somaratne and Smettem, 2014).

Estimating groundwater recharge and assessing renewable groundwater resources require a conceptual understanding of the processes that link precipitation to the saturated zone (Somaratne and Smettem, 2014). Many methods of estimation have been developed (Nimmo et al., 2006; Scanlon et al., 2002) as no single method has emerged as a universal standard due to the incompatibility of certain methods with certain locations (Cuthbert et al., 2013). Groundwater studies have commonly relied on the use of a single technique and have lacked corroborating evidence to substantiate results (Taylor & Howard, 1996), despite the general recommendation that multiple methods should be applied in all cases (Healy, 2010; Lerner et al., 1990; Scanlon et al., 2002). The chloride mass balance (CMB) approach has become the most widely applied technique for estimating recharge in arid and semi-arid regions (Scanlon et al., 2006b) and is often used in isolation. Yet, the conventional CMB method is valid only when diffuse recharge occurring via piston flow is the sole recharge pathway (Wood, 1999), as focused recharge and preferential flow are not considered (Somaratne and Smettem, 2014). Without sufficient understanding of recharge processes, recharge estimations relying on partial methods are equivocal. Only when processes are well understood, can appropriate methods be selected to undertake accurate renewable groundwater resources assessments.

Climate change will impact the quantity and quality of groundwater resources (Gleick, 1989) through the alteration of the hydrological cycle (Hegerl et al., 2015). Climate is directly linked to precipitation, soil moisture and surface water, which are subsequently related to groundwater via the processes that govern recharge (Jyrkama and Sykes, 2007). Therefore, quantifying the impact of climate change on groundwater resources requires not only reliable forecasting of climate changes but also delineation of groundwater recharge pathways (Jyrkama and Sykes, 2007). Furthermore, understanding recharge processes is necessary to properly assess aquifer vulnerability to contamination (Jyrkama and Sykes, 2007).

Transport of most groundwater contaminants occurs in the aqueous phase as part of the recharge process. Assessing aquifer pollution vulnerability is, therefore, inextricably linked to understanding groundwater recharge mechanisms (Foster, 1998). This is particularly important in areas where the underlying aquifers are exploited extensively for drinking water purposes (Jyrkama and Sykes, 2007), such as Makutapora (DUWASA, 2017). Accordingly, knowledge of recharge processes are embedded in simulations of recharge responses to projected climate changes (Scanlon et al., 2006b) and assessments of contamination vulnerability. They are thereby integral to sustainable water development to meet human and ecosystem needs (Gates et al., 2008).

Despite the importance of focused recharge, diffuse processes are more widely understood and are more extensively incorporated in large-scale hydrological models (Cuthbert et al., 2016). Therefore, projections of groundwater resources are uncertain in areas where recharge from surface water bodies, such as ephemeral streams, dominates (Döll and Fiedler, 2008; Wheater et al., 2010). This knowledge gap is a consequence of lack of data, and lack of appropriate studies (Cuthbert et al., 2016).

Managed aquifer recharge (MAR), the purposeful recharge of water to an aquifer for subsequent recovery or environmental benefit (Dillon et al., 2009), can increase storage to secure and enhance municipal water supplies to better cope with climate change and variability as well as increased demand. An understanding of the hydrogeology and of recharge processes facilitates assessment of the feasibility and viability of MAR solutions such as infiltration ponds, infiltration galleries, percolation tanks, recharge weirs, and reservoirs for recharge releases. Although some MAR solutions, such as injection wells, will work regardless of predominant recharge processes, solutions which rely in the infiltration and percolation of water, will greatly rely on recharge processes, that, in turn, rely on soils and underlying geology. As such, understanding how meteoric water reaches the saturated zone, greatly assists in choosing the most effective engineering intervention.

Despite its obvious importance, understanding groundwater recharge processes in semi-arid areas remains a major challenge (Wheater et al., 2010), due to a lack of available data, and consequently a lack of studies. This is particularly true in areas where focused recharge occurs (Somaratne and Smettem, 2014). Fundamentally, the processes that transmit precipitation to groundwater systems are not fully understood (Jasechko and Taylor, 2015). This includes the Makutapora Basin (Taylor et al., 2013b). Previously, specific but unsubstantiated processes have been proposed. The Chenene Hills were hypothesised to be an important recharge area, but with little evidence (Shindo et al., 1989). Additionally, termite mounds were once thought to transmit the bulk of the water through the unsaturated zone by acting as macropores (Shindo et al., 1989). Further, it has also been suggested that meteoric water reaches the saturated zone predominantly via diffuse recharge, which only occurs late in the wet season after soil moisture deficits have been overcome (Nkotagu, 1996; Shindo et al., 1989). There is, however, a consensus that groundwater recharge is endogenous, i.e. it derives from precipitation falling within the basin and is not the result of regional scale groundwater flow. Clearly, the primary recharge mechanisms occurring in the Makutapora Basin are not well constrained as findings from previous studies have been varied and contradictory. Accordingly, it has not been possible to accurately project groundwater quantity and quality, evaluate the viability of potential engineering interventions to enhance recharge, and assess the impacts of climate change on groundwater resources in an aquifer vital to Tanzania’s capital city.

Previous research conducted in the Makutapora Basin indicated that groundwater storage is replenished by infrequent, episodic recharge events, which occur, on average, three or four times per decade. The largest episodes of recharge were shown to be associated with strong El Niño events (Taylor et al., 2013b). Accordingly, the 2015/2016 El Niño event which was anticipated as early as January 2014 (WMO, 2014) was considered a promising, and potentially the only, opportunity to observe recharge in Makutapora during the duration of this research. A monitoring array was, therefore, emplaced prior to the first precipitation of the season to comprehensively monitor the surface water and groundwater dynamics associated with an El Niño event. By the time of the implementation of the monitoring array, values within NOAA's Oceanic Niño Index peaked at +2.4 °C, which surpassed the record of December 1997 by 0.2 °C (Becker, 2016a). In retrospect, the event is considered to be one of the strongest El Niño events since records began, by a variety of metrics (Becker, 2016b).

This chapter features a detailed study of recharge processes observed during a period predicted to produce substantial groundwater recharge and uses these findings to contextualise the long-term records of groundwater and surface water dynamics. Here, I examine the dominant recharge mechanisms in the semi-arid Makutapora Basin of Central Tanzania in three discrete ways: (1) direct observation of groundwater-level fluctuations; (2) tracing sources of groundwater using stable-isotope ratios of O and H; and (3) examining the spatiotemporal relationship between ephemeral streamflow and groundwater recharge. This study utilises a rare pair of proximate, coincident, long-term groundwater-levels and stream stage datasets in conjunction with a dense network of wells for high-resolution monitoring of groundwater-levels, implemented to observe the 2015/2016 El Niño wet season. Groundwater-level fluctuation observations provide insight into recharge dynamics due to direct observation of water added to the saturated zone. By accounting for recession characteristics under a dynamic abstraction regime, groundwater responses to proximate ephemeral streamflow are observed. Consequently, the presence or absence of groundwater ‘mounds’ is explored to assess the prevalence of focused recharge. The validity of any groundwater mounding interpretation, given current estimates of groundwater hydraulic parameters in the Makutapora Basin, was tested using a numerical model developed in MIKE SHE by comparing observed and simulated groundwater responses to focused recharge. These results were compared with evidence from stable isotope tracers.

4.3 Methods and Data

The methodological design of this research was predicated on the conceptual model of the Makutapora Basin formulated on available data, literature, and site visits (section 2.3.9). Focussed recharge is assumed to predominate in the basin. Accordingly, the methodology was designed to facilitate the observation of focussed groundwater recharge leaking from ephemeral streambed at the boundaries of the wellfield near the centre of the basin.

4.3.1 Daily Hydrometric Records (2006 - 2016)

To assess the effect of climate and surface hydrology on groundwater recharge in the Makutapora Basin, long-term ephemeral stream stage, precipitation and groundwater-level datasets were analysed. Ephemeral stream flow in the Makutapora Basin is highly variable in space and time. The River Little Kinyasungwe, the largest ephemeral stream in the catchment, is monitored at the Meya Meya gauge (Figure 4.1, 4.3), established by Shindo et al. (1989). Daily stream stage data have been manually recorded using a staff gauge by DUWASA under the supervision of Wami/Ruvu Basin Water Office (WRBWO), since January 2006 (Figure 4.2). Daily precipitation data has been collected since January 2007 at the Makutapora Meteorological Station (Figure 4.2).

Figure 4.1 Photographs of the Meya Meya gauge on the Little Kinyasungwe, showing staff gauges and unused automated gauges, during a relatively dry wet season (February 2013) (left) and relatively wetter wet season (April 2016) (right).

Groundwater-level fluctuations were used to estimate values of groundwater recharge using a modified WTF, accounting for transience in the pumped Makutapora wellfield (Chapter 3).

To assess the relationships between climatological and hydrological variables and groundwater recharge, linear regressions were performed. The duration of ephemeral stream flow, representing the duration of streambed inundation and potential leakage, was assessed in relation to estimates of groundwater recharge. In lieu of stream discharge or a rating curve, seasonal cumulative stream stage, i.e. the sum of daily stream stage, was additionally compared to estimates of groundwater recharge. To assess the relative importance of precipitation and stream flow in controlling groundwater recharge, two precipitation variables were assessed in relation to groundwater recharge. The duration of precipitation, i.e. the number of rain days, and the seasonal total precipitation were compared to estimates of groundwater recharge. These precipitation-based variables represent a sample of the more comprehensive analysis concerning the relationship between precipitation and groundwater recharge conducted in Chapter 3.

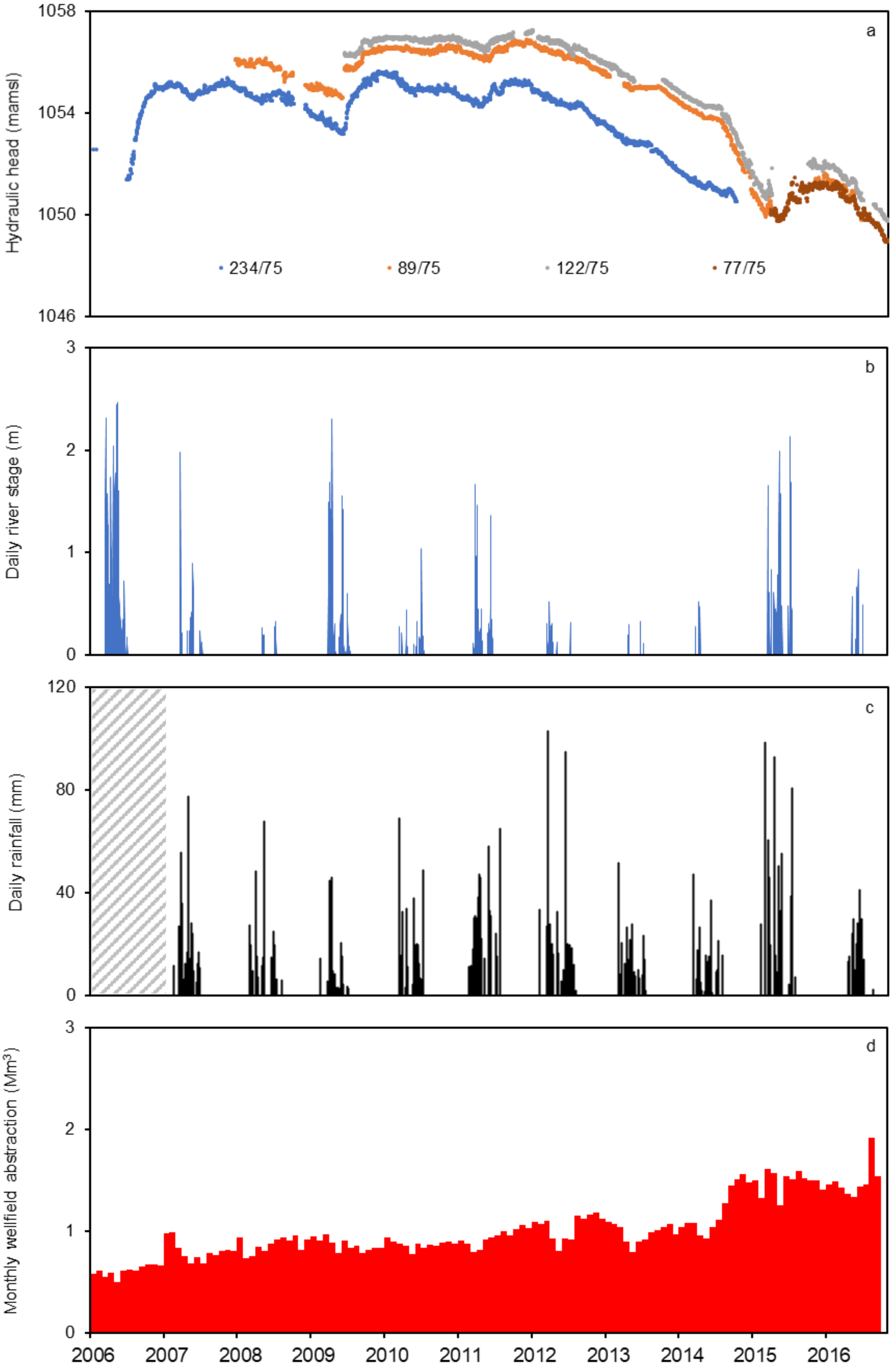

Figure 4.2 Observations from July 2006 to June 2017 of: (a) hydraulic head values observed in wells 234/75, 122/75, 89/75 and 77/75; (b) daily stream stage at the Meya Meya gauge on the River Little Kinyasungwe; (c) daily precipitation recorded at the Makutapora Meteorological Station; and (d) total monthly wellfield abstraction from the Makutapora Basin. Precipitation data collection commenced on 1st January 2007, so all precipitation data from the 2006/2007 wet season was removed from the plot.

4.3.2 Hourly Hydrometric Records (November 2015 - present)

In advance of the 2015-2016 wet season, which coincided with one of the strongest El Niño events on record, an automated high-resolution monitoring array was installed in the Makutapora Basin (Figure 4.3). Hourly, temporally coincident groundwater-levels, stream stage, and atmospheric pressure data were collected using six piezometers, one bespoke stream gauge, and one barometer. The piezometers were established in boreholes originally drilled as pumping wells that were no longer in use. Hourly monitoring of water levels (pressure) was conducted using InSitu RuggedTROLL 100 Data Loggers, which have a range of 30 ft (9.14 m). Accordingly, dataloggers were placed at ~2 m below the static water level to ensure the upcoming potentially large recharge event was fully captured in addition to any groundwater decline occurring prior to the onset of the wet season. Manual measurements were taken each time the loggers were physically accessed (e.g. to download data) to recalibrate the depth of the loggers relative to ground level to negate the potential effects of drift. Dipped values were additionally used to convert logged depth values to hydraulic head values.

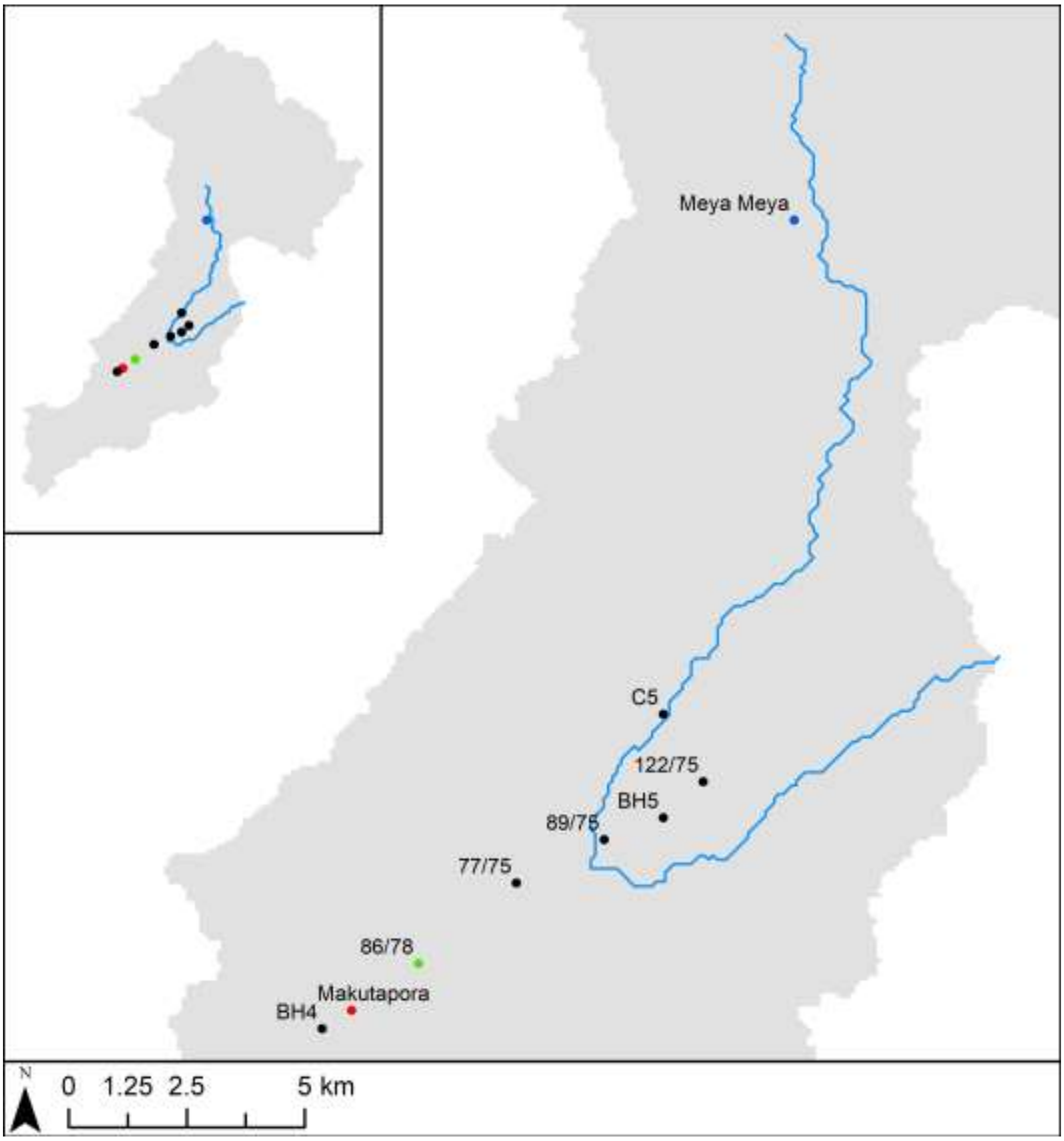

Figure 4.3 Map of the Makutapora Basin showing the location of the River Little Kinyasungwe, based on the topography and drainage modelling. The location of the high-resolution monitoring array of piezometers (black dots), stream gauge (blue dot), barometer (green dot), and meteorological station (red dot).

Hourly stream stage data were collected at the previously established Meya Meya gauge on the River Little Kinyasungwe. The stream stage gauge was constructed using an InSitu RuggedTROLL 100 Data Logger suspended inside 2-inch perforated PVC piping, screened with wire mesh, and sealed at the top using a torquer locking well plug (Figure 4.4). Water could freely flow into, and out of, the gauge through the screened section and the open base. The gauge was attached to the existing staff gauge and buried beneath the streambed. The depth of the sensor, relative to the staff gauge, was measured at the time of installation, and subsequently calibrated using manually collected stream stage data. Groundwater-levels and stream stage data were compensated using data from a barometric logger (InSitu BaroTROLL) situated close to the centre of the monitoring array, in borehole 86/78. The logger was installed 2 mbgl to reduce the effect of atmospheric temperature variability to minimize diel artefacts in the pressure data (Cuthbert et al., 2016).

Figure 4.4 Photographs of: the stream stage gauge (a), location of installation, at the Meya Meya gauge on the River Little Kinyasungwe (b), demonstration of how the datalogger is suspended within the casing (c), and the method by which the gauge was attached to the existing staff gauge (d).

Due to data logger malfunctions and piezometer vandalism, gaps are present in the records of C5, BH4, BH5, and 77/75. Figure 4.5 shows the full dataset from six piezometers after atmospheric corrections. Groundwater-level data was additionally corrected for recessionary behaviour and groundwater abstraction using the saturated zone model described in Chapter 3. Abstraction rates are dynamic at a sub-daily scale and this was observable in the corrected groundwater data. Accordingly, the data was smoothed over a 24-hour period to negate this effect and highlight groundwater mounding.

The monitoring array is designed to observe relative changes in hydraulic head in space and time, observing the formation and decay of groundwater 'mounds' that can result from streambed inundation. Accordingly, five piezometers (89/75, 122/75, BH4, BH5, and 77/75) were located at variable distances perpendicular from the River Little Kinyasungwe, with 89/75 situated very close to the stream. To facilitate an upstream/downstream comparison, C5 was installed close to the stream but in the upland section of the basin to contrast with the lowland location of 89/75. To assess the extent to which mounding occurs, particular attention was paid to episodes of streambed inundation which occurred in isolation, i.e. periods where newly formed 'mounds' did not experience superposition from previously formed decaying 'mounds' or subsequently forming 'mounds'. Furthermore, periods that coincided with stable abstraction rates, both in the wellfield as a whole, and in individual production wells, especially those proximate to the monitoring array were preferred. Transient changes to local groundwater-levels are interpreted as representing an uneven spatial distribution of recharge, i.e. focused recharge. Accordingly, this analysis will also facilitate the identification of locations experiencing focused recharge.

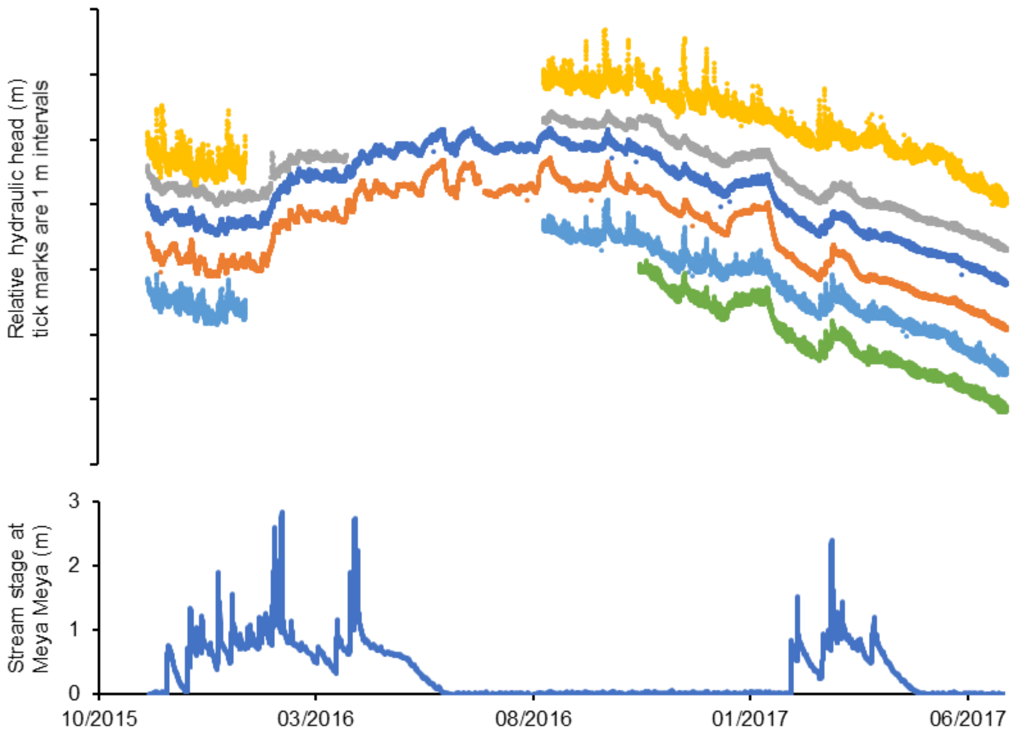

Figure 4.5 Groundwater hydrographs from BH4 (yellow), C5 (grey), 122/75 (dark blue), 89/75 (orange), 77/75 (light blue), and BH4 (green) and stream stage. Hydraulic heads are given on the same vertical scale, but with the absolute values shifted to facilitate comparison of the hydrographs.

4.3.3 Stable-Isotope Ratios of O and H

To trace the origins of groundwater using stable-isotope ratios of O and H, daily precipitation data and samples were recorded and collected at the Makutapora Meteorological Station over 3 wet seasons (2015/2016 – 2017/2018). Precipitation samples for isotopic analysis were collected in accordance with IAEA (2014) precipitation sampling guidelines for event-based sampling using a buried sampler. Stable-isotope analysis was undertaken by a commercial laboratory, Elemtex Limited. A supplementary, secondary dataset of stable-isotope values of precipitation, groundwater, surface water, and soil water, in additional to precipitation data, was compiled from previously published studies and the IAEA TWIN database (Table 4.1). The locations of collected water samples, analysed for stable-isotope ratios, are shown in Figure 4.6.

Table 4.1 Type, amount, and source of secondary data.

Type	n	Reference
Precipitation	1 season	(Shindo et al., 1989)
Precipitation	1 season	(Shindo et al., 1990)
Precipitation	1 season	(Onodera et al., 1995a)
Precipitation composition	33	(Nkotagu, 1996a)
Precipitation composition	26	(Onodera et al., 1995a)
Groundwater composition	16	URT8003 (IAEA/WMO, 2018)
Groundwater composition	6	URT8004 (IAEA/WMO, 2018)
Groundwater composition	6	URT8006/1 (IAEA/WMO, 2018)
Groundwater composition	11	URT-EXT/01 (IAEA/WMO, 2018)
Groundwater composition	23	URT-RAF8029 (IAEA/WMO, 2018)
Groundwater composition	47	(Shindo et al., 1990)
Soil water composition	14	(Nkotagu, 1996a)
Soil water composition	8	(Senguji, 1999)
Surface water composition	32	URT8004 (IAEA/WMO, 2018)
Surface water composition	11	(Nkotagu, 1996a)

The origin of average groundwater was assessed with reference to precipitation, streamflow, soil water, and lake water using the ratios of $\delta^{18}O$ to $\delta^{2}H$ and average values of $\delta^{18}O$ (Gat, 1971). Ratios of $\delta^{18}O$ to $\delta^{2}H$ were calculated using linear regression and the significance of their differences to the linear trend defined by groundwater samples was tested (Cohen et al., 2013). Samples which were not expected to undergo fractionation, i.e. their $\delta^{18}O$ to $\delta^{2}H$ ratios were not anticipated to change before entering the saturated zone, were excluded as possible sources of groundwater if a significant difference existed in the ratio of $\delta^{18}O$ to $\delta^{2}H$. Samples were not anticipated to undergo fractionation if their exposure to the atmosphere was limited. Differences between average values of $\delta^{18}O$ were also used to eliminate possible source of groundwater. $\delta^{18}O$ was chosen instead of $\delta^{2}H$ simply because a greater number of samples have associated $\delta^{18}O$ values.

Qualitative (histograms and Q-Q plots) and quantitative (Shapiro-Wilk tests) tests indicated that it is a reasonable assumption that $\delta^{18}O$ and $\delta^{2}H$ of precipitation and groundwater are normally distributed ($p > \alpha$ for $\alpha = 0.05$). As the water source and the ultimate state of the

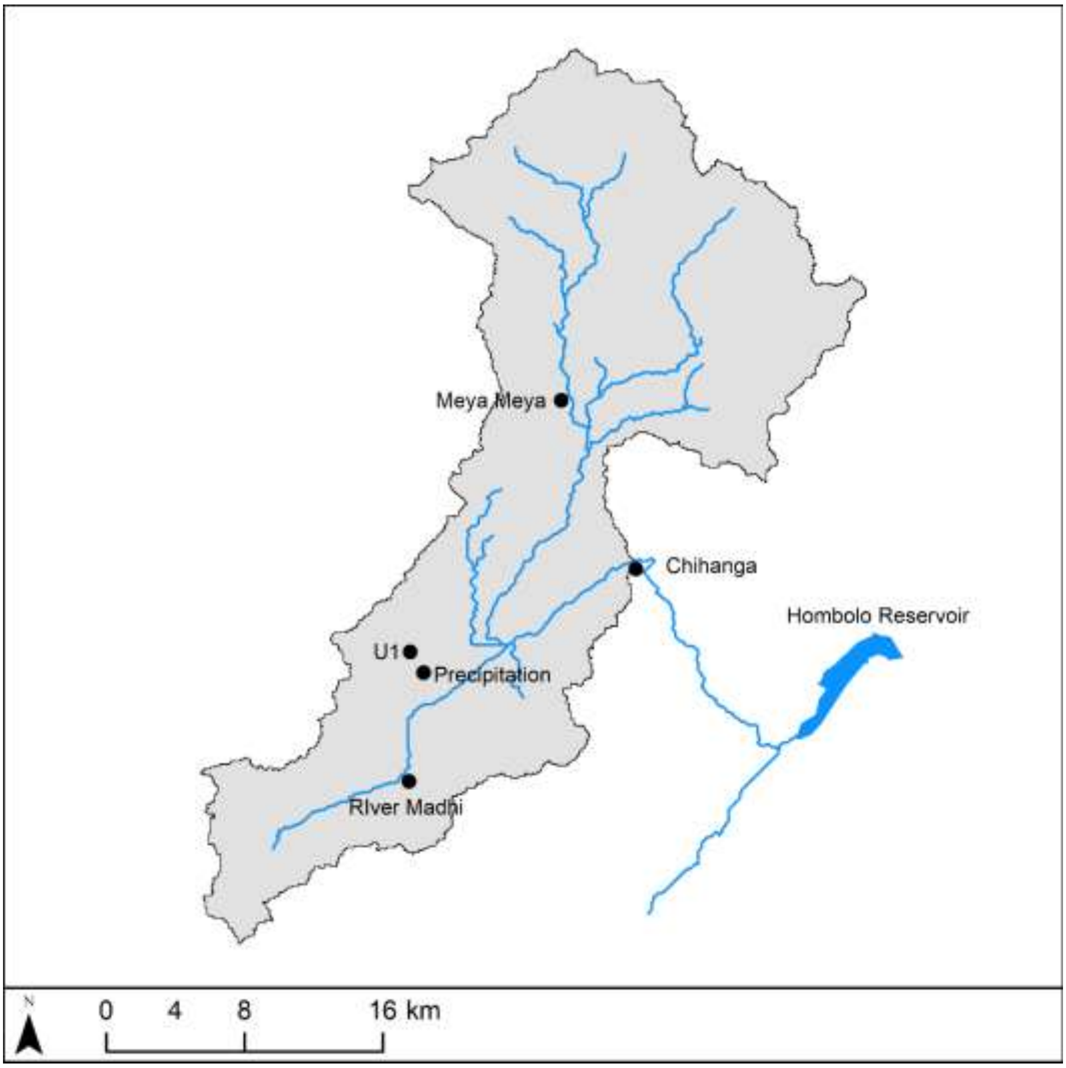

Figure 4.6 Map showing the location of water samples used for stable-isotope analysis. Surface water samples were taken from the Meya Meya and Chihanga gauges on the River Little Kinyasungwe, the River Madhi and the Hombolo Reservoir. Soil water was sampled at U1. Precipitation samples were collected at the Makutapora Meteorological Station. Groundwater was sampled throughout the basin.

water, after selection and fractionation, are both normally distributed, it is assumed that all intermediate states (surface water and soil water) are also normally distributed.

F-test of equality of variances indicated that isotope samples from intermediate states have unequal variances. Accordingly, Welsh's t-tests were carried out to determine if the means of the $\delta^{18}O$ samples were likely to be drawn from a population with the same mean as groundwater samples. Sample averages that are significantly different and are not expected to undergo fractionation are excluded in addition to sample with averages that are significantly more positive, regardless of the potential for further fractionation. These tests will not directly indicate sources of groundwater recharge within the Makutapora Basin, but they will constrain which source do not deviate significantly from groundwater in their stable-isotope ratios.

4.3.4 Numerical Modelling of Groundwater Mounding

To test the validity of any interpretation of groundwater mounding from field observations, a simulation of the decay of a groundwater mound originating from the River Little Kinyasungwe

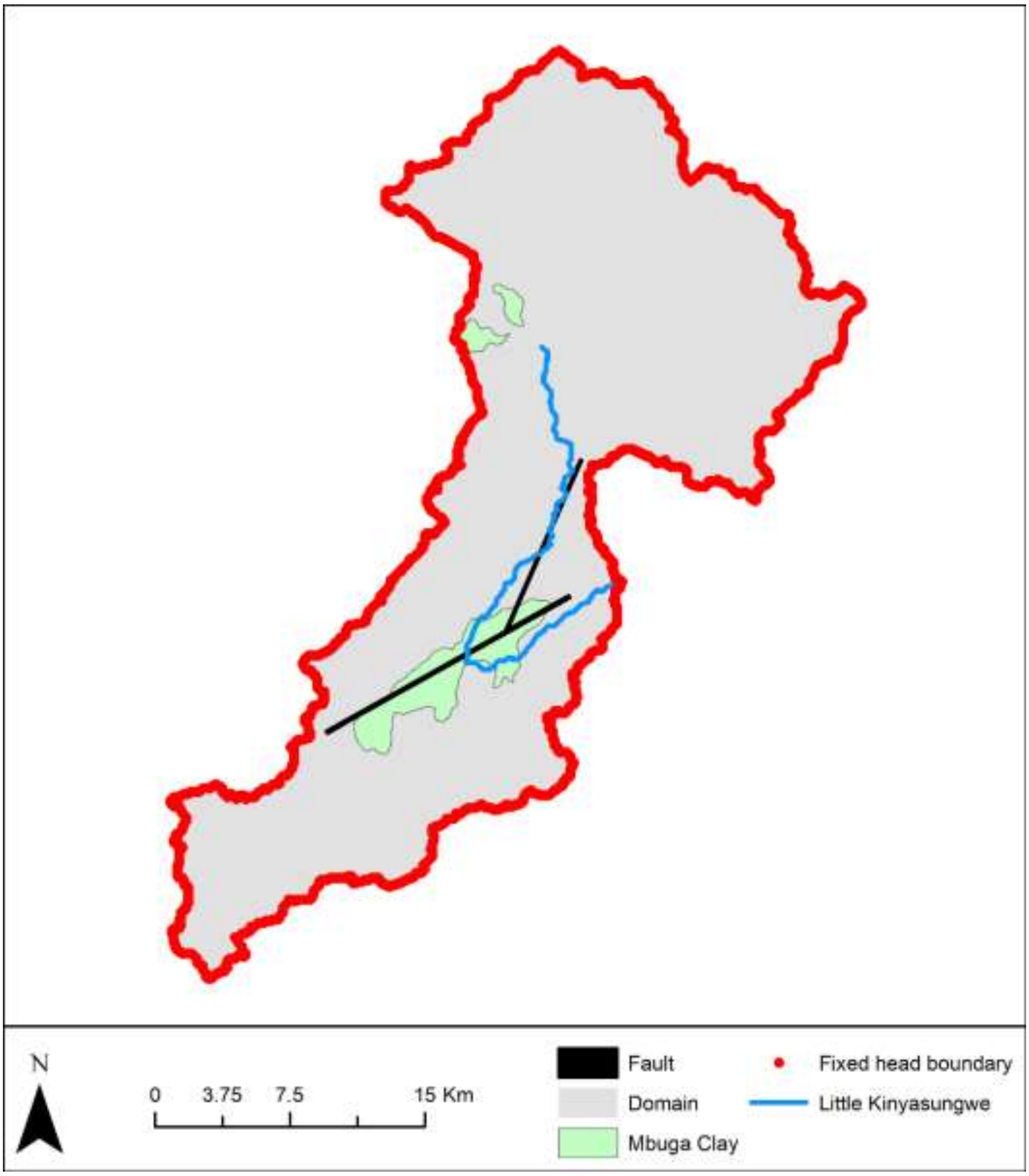

Figure 4.7 A representation of the numerical model developed in MIKE SHE of the Makutapora basin. The domain, boundary conditions, location of faults, location of Mbuga Clay, and location of the River Little Kinyasungwe are shown.

was carried out with a numerical model. Observations of groundwater fluctuations, interpreted to show a groundwater mound forming and decaying, were then compared with simulated groundwater responses to groundwater mounding.

The model described in section 3.3.4.8 was modified to best observe groundwater fluctuations associated with groundwater mounding. To obviate the need to account for background groundwater recessions and dynamic recessions resulting from groundwater abstraction, the initial potentiometric surface and external boundary conditions were changed. The potentiometric surface was prescribed as uniform throughout the domain at an elevation of 1000 mamsl. 1000 mamsl was approximately the average hydraulic head value observed in the high-resolution monitoring wells. Therefore, the faults should affect simulated mounds similarly to observed mounds. All four external boundaries were changed to constant head boundaries with the same elevation as the potentiometric surface (figure 4.7). Additionally, pumping wells were removed from the model, so groundwater abstraction does not occur. Accordingly, no hydraulic gradients, other than those caused by groundwater mounds themselves, were simulated to impact the decay of those mounds.

Current conceptual understanding indicates that the ephemeral stream network is highly dynamic in space and time (section 2.3.9). As such, attempting to replicate the conditions which produced the groundwater fluctuations shown in figure 4.9, figure 4.10 and figure 4.11, was deemed impossible as the location and channel architecture of all inundated streams is unknown. Accordingly, only focused recharge emanating from the River Little Kinyasungwe was considered in the model. Due to the size and location of the River Little Kinyasungwe, it is the most important ephemeral stream in terms of leakage and recharge production (section 2.3.9). Accordingly, the salient groundwater responses to groundwater mounding are observable. To test the validity of groundwater mounding as an interpretation of the observed hydrogeological dynamics, a pulse of recharge was added directly to the saturated zone under the location of the River Little Kinyasungwe. This pulse simulated the formation of a groundwater mound, and its decay was observed through groundwater fluctuations in observation wells. To approximate recharge resulting from leakage beneath the River Little Kinyasungwe in figure 4.9, figure 4.10 and figure 4.11, 175 $mm \cdot day^{-1}$ of recharge was added to the saturated zone for 2 days. These values are considered appropriate given the duration of streambed inundation in figure 4.9, figure 4.10 and figure 4.11 and the leakage coefficient on the streambed (section 5.3.8). Water table fluctuations resulting from the decay of the mound were simulated in the same locations field observations were taken (figure 4.14).

Groundwater fluctuations in C5 were not simulated despite the existence of field observation. Streambed leakage in the vicinity of C5 is expected to be significantly less due to its upstream location (section 2.3.9), remote from the wellfield.

4.4 Results

4.4.1 Stream Stage and Groundwater Recharge

Between 2006 and 2017, groundwater-levels in the Makutapora basin, represented by observations from 89/75, 122/75, 234/75 and 77/75, experienced a slight decline (Figure 4.2). Generally, recessionary rates, in the absence of recharge, increased during this period as a result of increases in groundwater abstraction. These increasingly rapid declines are punctuated by three large groundwater-level rises in 2006/2007, 2009/2010 and 2015/2016 (all El Niño years). Distinct wet and dry seasons are observable in records of precipitation and stream flow. There appears to be greater variation in stream flow than precipitation, with little apparent correspondence between the two. The largest positive groundwater fluctuations appear to coincide with the seasons of greatest stream flow, but not necessarily the greatest precipitation, e.g. 2009/2010.

Climatological and hydrological variables were assessed to constrain the controls of groundwater recharge events. The relationships between annual groundwater recharge and total precipitation, number of rain days, duration of streambed inundation, and cumulative stream stage are shown in Figure 4.8. Of the variables tested, duration of stream flow in the River Little

Kinyasungwe is the most strongly linearly related to the magnitude of groundwater recharge ($R^2 = 0.85$) (Fig 4.8b). The x-intercept is not significant ($p > 0.05$) and groundwater-levels increase linearly, at a rate of approximately 50 mm·day^{-1}. There are, however, 5 seasons which experienced no recharge despite experiencing stream flow. Furthermore, there are 2 seasons associated with observed groundwater recharge which experiences shorter flow durations than other seasons which experiences no recharge. This ambiguity indicates that the amount of groundwater recharge is not entirely determined by streamflow duration. The robustness of the linear relationship established here is constrained by the limited duration of observations (11 wet seasons), however, this analysis encompasses wet seasons which were associated with a large range of groundwater recharge magnitudes. 97.5% (39/40) of all recharge events recorded in the Makutapora Basin since 1955, when systematic groundwater records began, fall within the range of 0 m - 5.11 m.

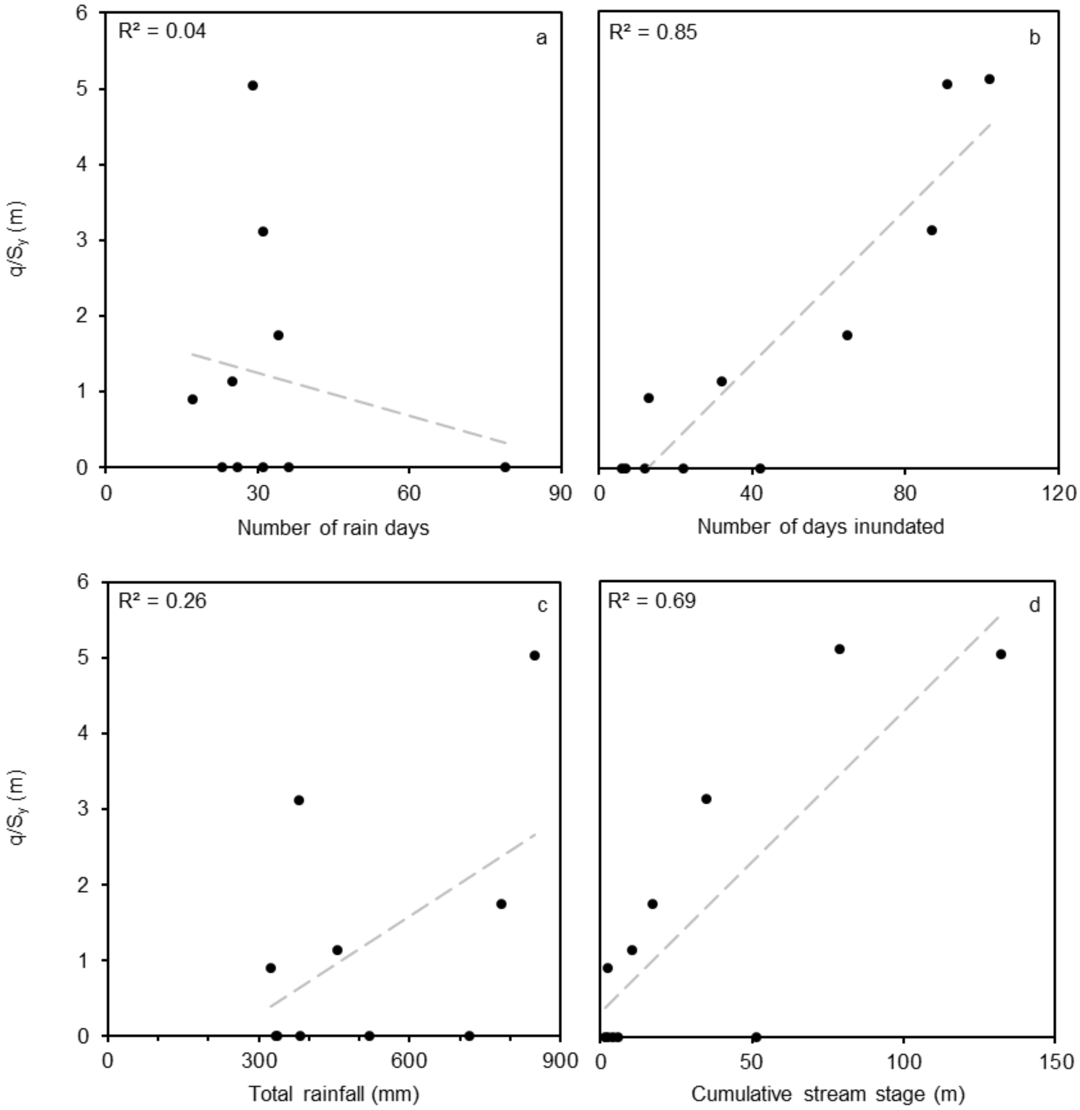

Figure 4.8 Cross-plots of recharge magnitude versus: (a) number of rain days, (b) duration of ephemeral flow of the River Little Kinyasungwe at the Meya Meya gauge, (c) total precipitation, (d) and cumulative daily stream stage of the River Little Kinyasungwe at the Meya Meya gauge. Plots a and c comprise data from hydrological years 2007/2008 – 2016/2017, whereas plots b and d comprise data from hydrological years 2006/2007 – 2016/2017.

In lieu of stream discharge data, the magnitude of groundwater recharge events was compared to cumulative stream stage (Figure 4.8d), i.e. the annual sum of daily stream stage. The relationship ($R^2 = 0.69$) is significant ($p < 0.05$), but weaker than the relationship between groundwater recharge and duration of stream flow. Channel architecture strongly influences stream stage. Accordingly, the significance of this relationship is uncertain. However, the concave downward shape of the cross-plot is the shape that would be expected if a linear relationship existed between discharge and groundwater recharge, assuming that the rating curve at Meya Meya was also concave downwards.

The magnitude of groundwater recharge events was also compared to total seasonal precipitation (Figure 4.8c) and the number of rain days per season (Figure 4.8a). The relationship between recharge magnitude and total precipitation shows a non-significant ($p > 0.05$) linear relationship ($R^2 = 0.26$). This is contrary to the relationship found in Chapter 3 via the same analysis. Presumably, this is an artefact of the smaller sample size, and an anomalously high number of years experiencing zero recharge. Furthermore, there is no significant linear relationship ($p > 0.05$) between number of rain days and groundwater recharge magnitude ($R^2 = 0.04$).

4.4.2 High-Resolution Groundwater Dynamics Monitoring

High-resolution hydraulic head data from 6 piezometers in the Makutapora Basin (Figure 4.3) show very similar behaviour throughout the monitoring array with relative changes in hydraulic head matching closely throughout the duration of monitoring (Figure 4.5). The record shows two complete wet seasons, one complete dry season, and 2 partial dry seasons. A brief groundwater-level decline in November and December 2015 was observed in all active piezometers. Groundwater-levels started to increase in early 2016 and peaked in the middle of the year. Peak groundwater-levels were approximately 2 m greater than they had been 6 months previously. Subsequently, a groundwater recession associated with the dry season is observed from late 2016 until early 2017. The recession results in a lowering of hydraulic head values to approximately the level prior to the preceding wet season. The generally linear decline is punctuated by periods of sharp increases and decreases presumed to be associated with dynamic abstraction. In early 2017, a small positive deflection, of approximately 0.5 m, punctuates the groundwater decline. Subsequently, the linear decline continues. Groundwater-levels at the end of the record are approximately 1.5 m lower than they were at the start.

The record of stream stage at the Meya Meya gauge on the River Little Kinyasungwe shows two discrete periods of stream flow. A brief period of no flow immediately after installation lasts less than one month. Early in December 2015 stream stage rapidly increases to almost 1 m. Shortly after, stream stage declines before rapidly increasing once again. Subsequently, the River Little Kinyasungwe is consistently flowing until the middle of June 2016. During this time, there are 2 significant peaks of stream stage, both reaching almost 3 m, which both rise and recede rapidly. The River Little Kinyasungwe ceases to flow again until early February 2017. This period of streamflow is continuous until the end of April the same year. Duration of stream flow associated with the 2016/2017 wet season is shorter than the previous year and the maximum stage is also less.

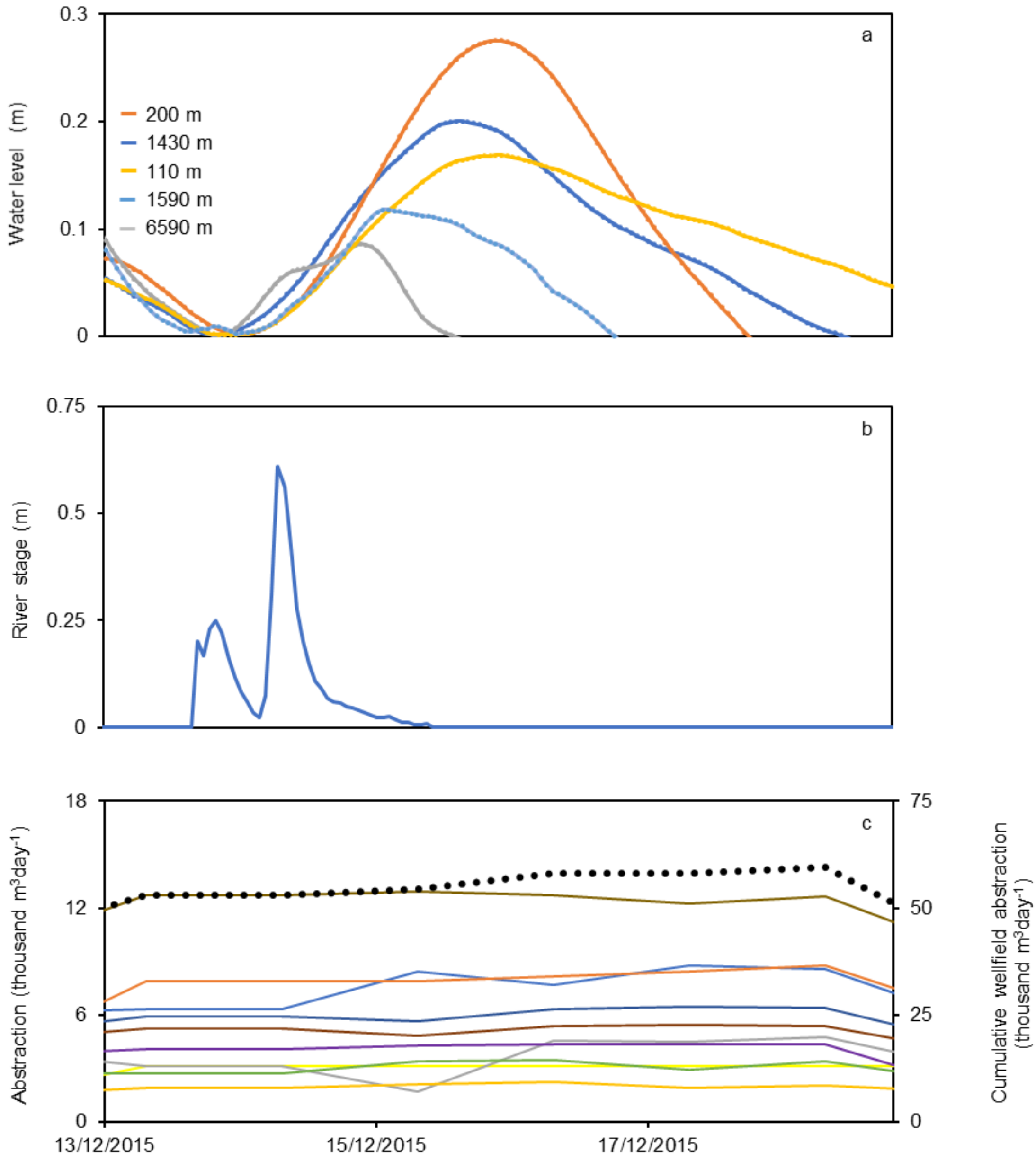

Figure 4.9 Observations from 13th to 19th December 2015 of: (a) hourly groundwater-level fluctuations in 89/75 (orange), 122/75 (dark blue), C5 (yellow), 77/75 (light blue), and BH4 (grey) normalised at 1600h on 14/12/2015; (b) hourly stream stage at the Meya Meya gauge on the River Little Kinyasungwe; (c) daily groundwater abstraction from entire wellfield (black dotted line), 26/79 (light brown), C3 (dark orange), C1 (light blue), C9 (dark blue), 117/75 (dark brown), 188/75 purple, C4 (yellow), 147/78 (green), C8 (grey), S2 (light orange). Distance between piezometer and the River Little Kinyasungwe are given in (a).

Three episodes of short-lived, isolated stream flow were identified within the full record and explored to assess the presence or absence of groundwater mounds as a results of streambed inundation. Figure 4.9 shows a period from 13th to 19th December 2015, associated with the first stream flow of the 2015/2016 wet season. The stream stage hydrograph at the Meya Meya gauge shows a rapid rise from 0 m to approximately 0.25 m within 1 hour. Stream stage gradually receded over the subsequent 10 hours, almost returning to 0 m, before rapidly increasing to over 0.6 m before again receding over the next 24 hours. The first pulse of

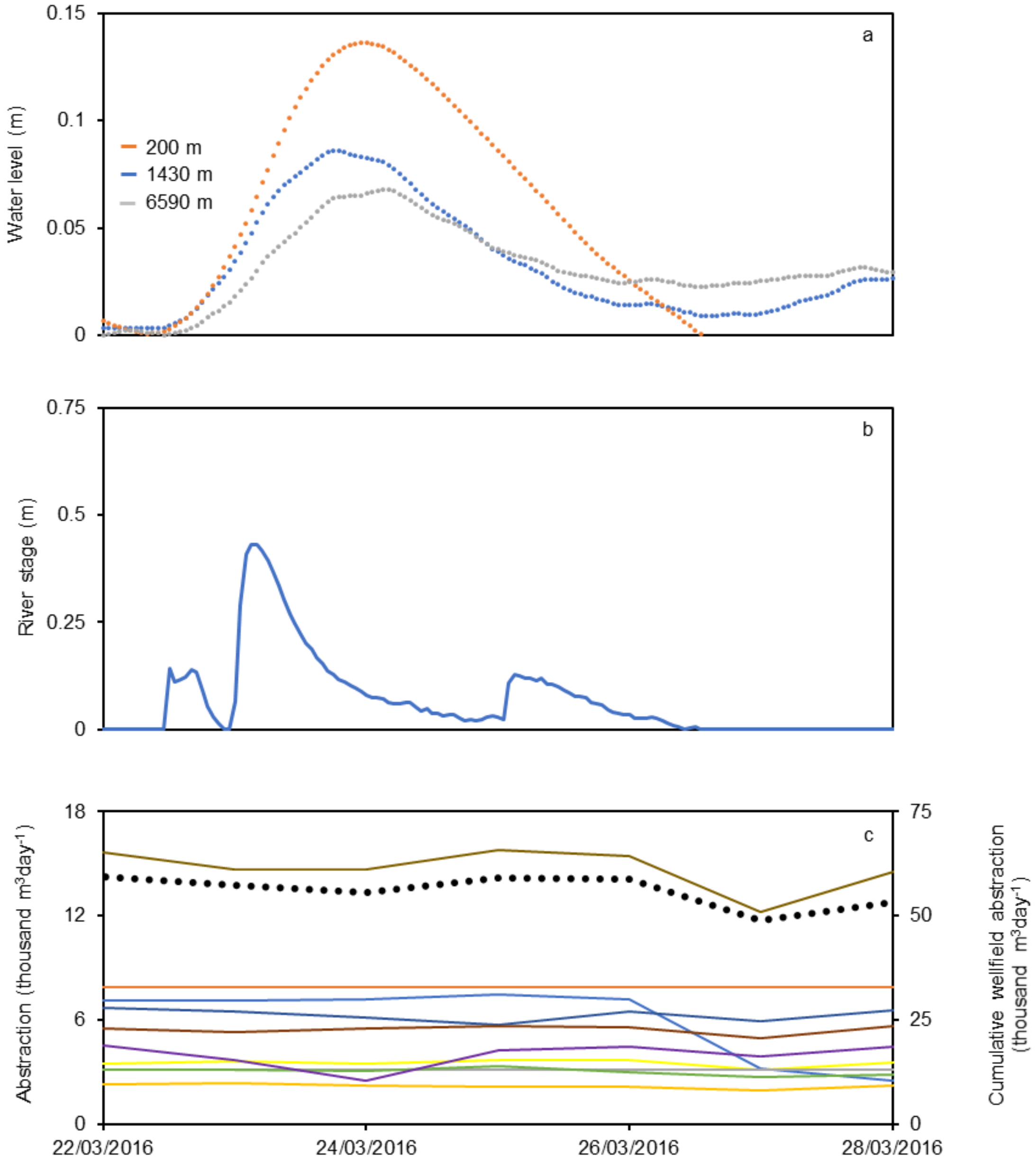

Figure 4.10 Observations from 22nd to 28th March 2016 of: (a) hourly groundwater-level fluctuations in 89/75 (orange), 122/75 (dark blue), and BH4 (grey) normalised at 0900h on 22/03/2016; (b) hourly stream stage at the Meya Meya gauge on the River Little Kinyasungwe; (c) daily groundwater abstraction from entire wellfield (black dotted line), 26/79 (light brown), C3 (dark orange), C1 (light blue), C9 (dark blue), 117/75 (dark brown), 188/75 purple, C4 (yellow), 147/78 (green), C8 (grey), S2 (light orange). Distance between piezometer and the River Little Kinyasungwe are given in (a).

ephemeral streamflow was rapidly followed by an increase in groundwater-level in all 5 active piezometers. The rapidity of the initial response of the water table to streamflow indicates rapid infiltration and percolation, in a matter of hours. These positive groundwater deflections were generally linear; however, the duration and magnitude of the groundwater-level rises varied between piezometers. The largest peak, observed in 89/75, was the culmination of a 48-hour groundwater-level rise, and ultimately achieved a magnitude of almost 0.3 m. By comparison, the increase observed in BH4 lasted for less than 12 hours, and reached a peak amplitude of less than 0.1 m. The relative magnitudes of these increases generally correspond to the distance

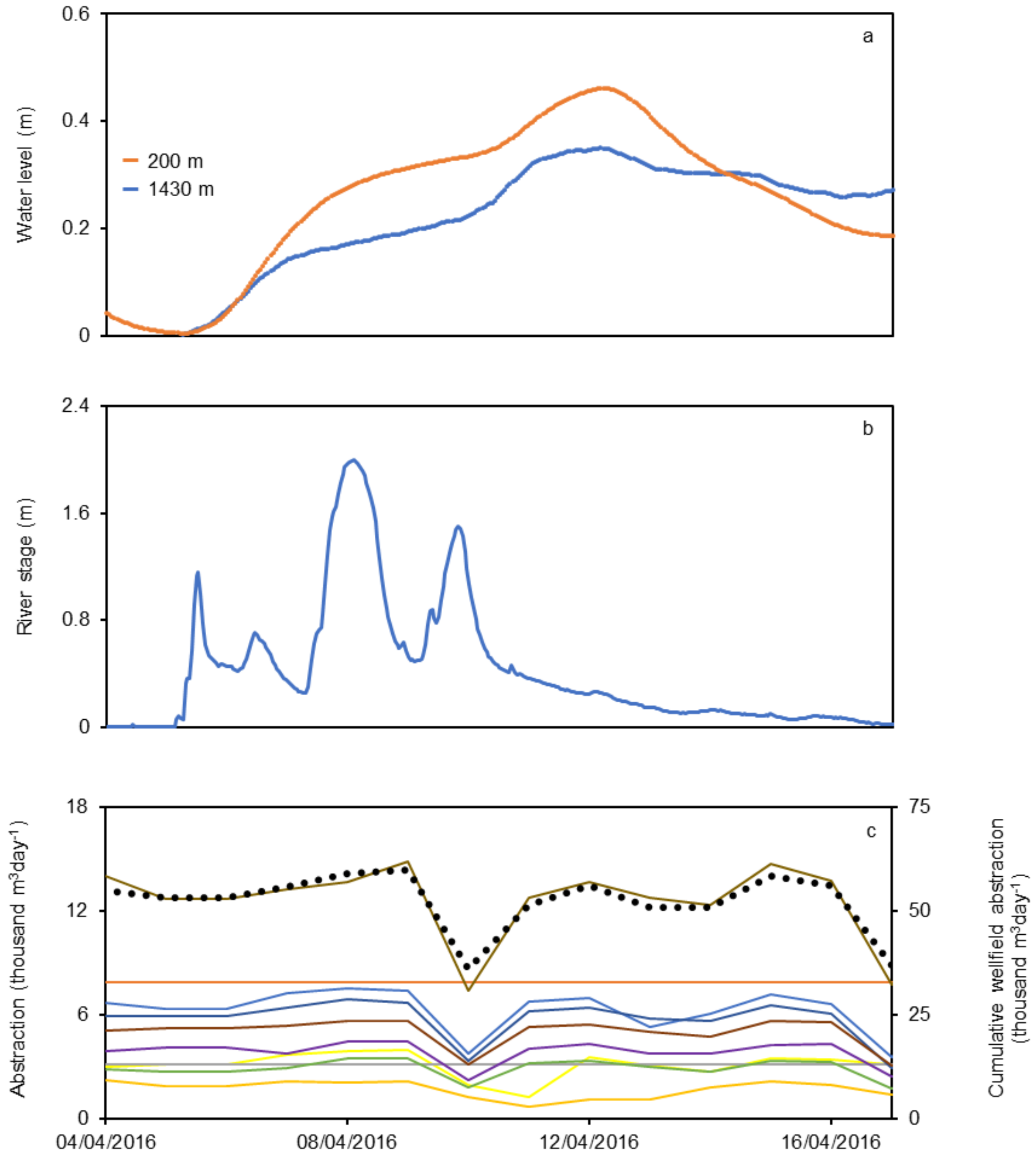

Figure 4.11 Observations from 4th to 16th April 2016 of: (a) hourly groundwater-level fluctuations in 89/75 (orange), and 122/75 (dark blue) normalised at 0500h on 05/04/2016; (b) hourly stream stage at the Meya Meya gauge on the River Little Kinyasungwe; (c) daily groundwater abstraction from entire wellfield (black dotted line), 26/79 (light brown), C3 (dark orange), C1 (light blue), C9 (dark blue), 117/75 (dark brown), 188/75 purple, C4 (yellow), 147/78 (green), C8 (grey), S2 (light orange). Distance between piezometer and the River Little Kinyasungwe are given in (a).

between the piezometer and the River Little Kinyasungwe in the section of the monitoring array perpendicular to the stream, i.e. all monitoring wells except C5. C5, the piezometer considerably upstream of the rest of the array, exhibits a response smaller than its proximity to the River Little Kinyasungwe would suggest. This is consistent with the conceptual model of recharge occurring in the Makutapora Basin (section 2.3.9) Piezometers in the east, close to the River Little Kinyasungwe, 89/75 and 122/75, experience conspicuously larger increases in groundwater-levels than piezometers in the west of the basin, 77/75 and BH4. This is consistent with the formation and decay of groundwater mounds as a result of leakage from an ephemeral streambed.

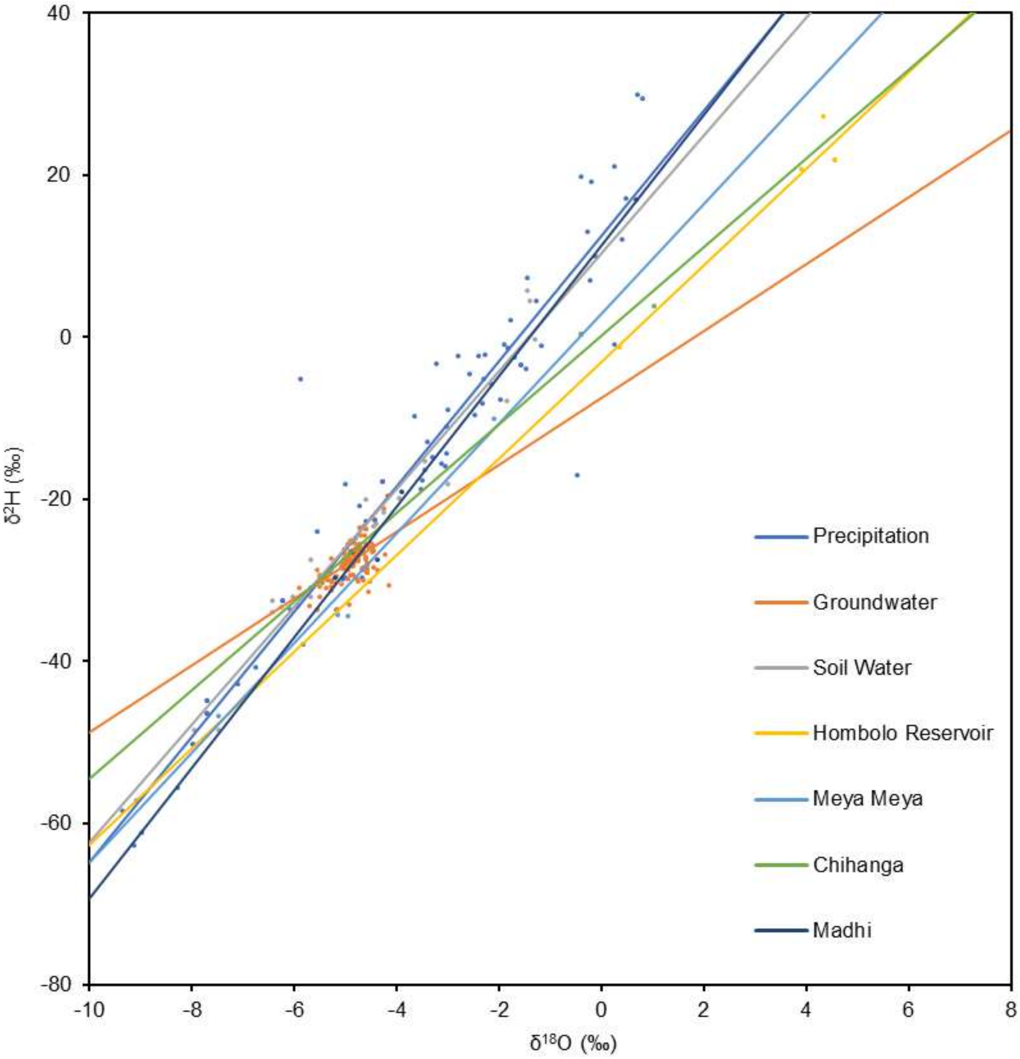

Figure 4.12 Relationships between $\delta^{18}O$ and $\delta^{2}H$ in precipitation, groundwater, soil water, Hombolo Reservoir water, stream water from the River Madhi and the River Little Kinyasungwe, in the Makutapora and Hombolo Basins.

Figure 4.10 and Figure 4.11 similarly show the formation and decay of groundwater mounds associated with streamflow, albeit observed in fewer piezometers. They show a rapid water table response to streambed inundation, larger water table responses closer to the River Little Kinyasungwe, and generally linear increases in hydraulic head. Figure 4.10 shows a decrease in abstraction that appears to be associated with groundwater-level recovery, not fully accounted for by the saturated zone model. An increase in the rate of water level rise, observed in 89/75 and 122/75, coincides with a decrease in total wellfield abstraction. Accordingly, the water level rise is attributed to water table recovery, which is superimposed on the rise attributed to leakage from the River Little Kinyasungwe.

4.4.3 Stable-Isotope Tracers

The linear trends defined by $\delta^{18}O$ and $\delta^{2}H$ of water samples from Makutapora groundwater, precipitation, Hombolo Reservoir water, soil water, surface water from 2 locations on the River Little Kinyasungwe (which flows into Hombolo Reservoir), and surface water from the River Madhi (a tributary of the River Little Kinyasungwe) were assessed to trace the origins of Makutapora groundwater (Figure 4.12). Of the samples which are not expected to undergo further evaporation, the ratio of $\delta^{18}O$ to δ^2H excluded soil water as a source of groundwater. The regression calculated from groundwater samples defines a line with equation $\delta^2H = 4.1 \pm 0.6 \cdot \delta^{18}O - 7.5 \pm 2.7$, which is significantly ($p < 0.05$) different from the linear trend defined by soil water $\delta^2H = 7.3 \pm 0.4 \cdot \delta^{18}O + 10.4 \pm 1.8$ (Figure 4.13). Soil water was sampled at a depth greater than 2 m below the surface and therefore it is assumed it would not have undergone further fractionation. Samples from Hombolo Reservoir and the River Little Kinyasungwe taken at the Chihanga gauge were not found to be significantly different ($p > 0.05$). Samples from the River Little Kinyasungwe taken at the Meya Meya gauge, and samples from the River Madhi were found to significantly different but are expected to undergo fractionation prior to reaching the saturated zone as they remain exposed to the atmosphere. Accordingly, these locations were not discounted as possible sites of focused recharge based on this evidence.

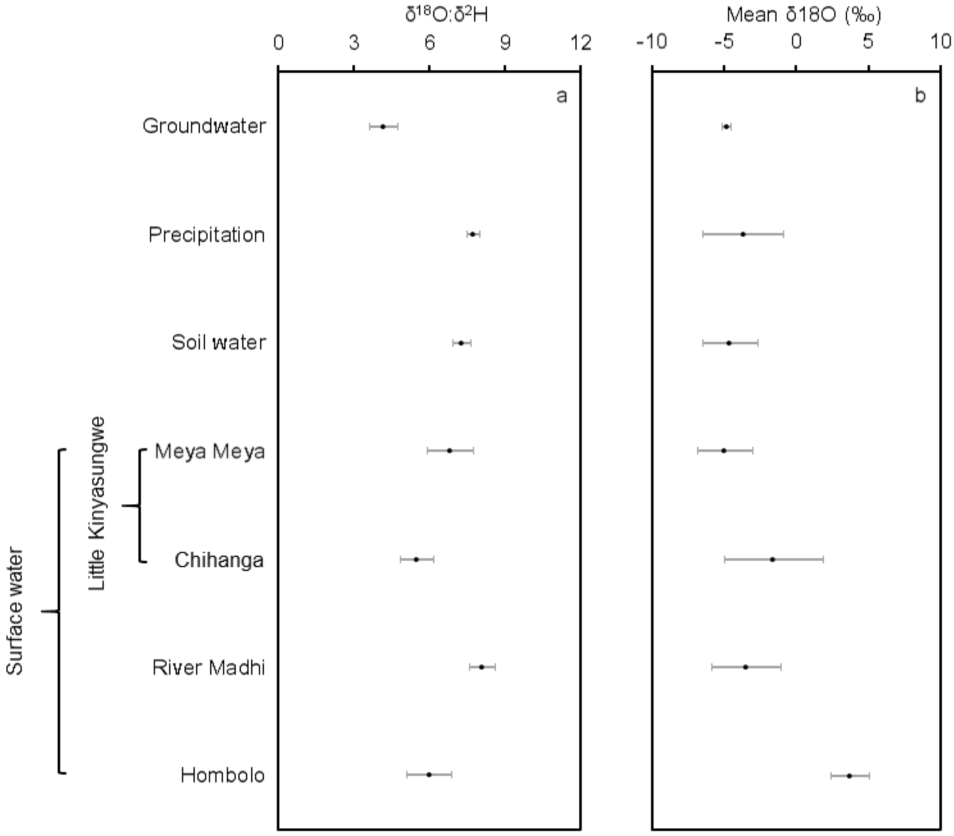

Figure 4.13 $\delta^{18}O$ to δ^2H ratios (black dots) with standard error associated with the ratio (grey bars) based on linear regressions (a), and mean $\delta^{18}O$ values and their associated standard deviations (grey bars) (b).

All isotope samples were tested to determine whether it was likely they were drawn from populations with the same mean $\delta^{18}O$ as groundwater. Only mean $\delta^{18}O$ of samples from Hombolo Reservoir, $\delta^{18}O = +3.7 \pm 1.3$, was found to be significantly ($p < 0.05$) different from the Mean $\delta^{18}O$ of groundwater, $\delta^{18}O = -4.9 \pm 0.3$. All other samples were found not to be significantly different and can therefore not be discounted as possible sources of groundwater.

Based on comparisons of $\delta^{18}O$ to δ^2H ratios and mean $\delta^{18}O$ values, it is unlikely that groundwater derives directly from precipitation, even when accounting for selection, as it has not undergone the requisite fractionation. This confirms the findings in Chapter 3. Similarly, water from Hombolo Reservoir has undergone too much fractionation to be the source of groundwater in Makutapora. Conversely, soil water samples indicate they did not fractionate under the same conditions as the source of groundwater. These statistical tests were unable to exclude ephemeral streamflow from the River Little Kinyasungwe and the River Madhi as possible sources of groundwater recharge in the Makutapora Basin based on their stable-isotopic composition.

4.4.4 Numerical Modelling of Groundwater Mounding

The magnitude of simulated water table fluctuations corresponds well with the distance between monitoring wells and the River Little Kinyasungwe (figure 4.14). The largest response, over 0.3 m, occurs

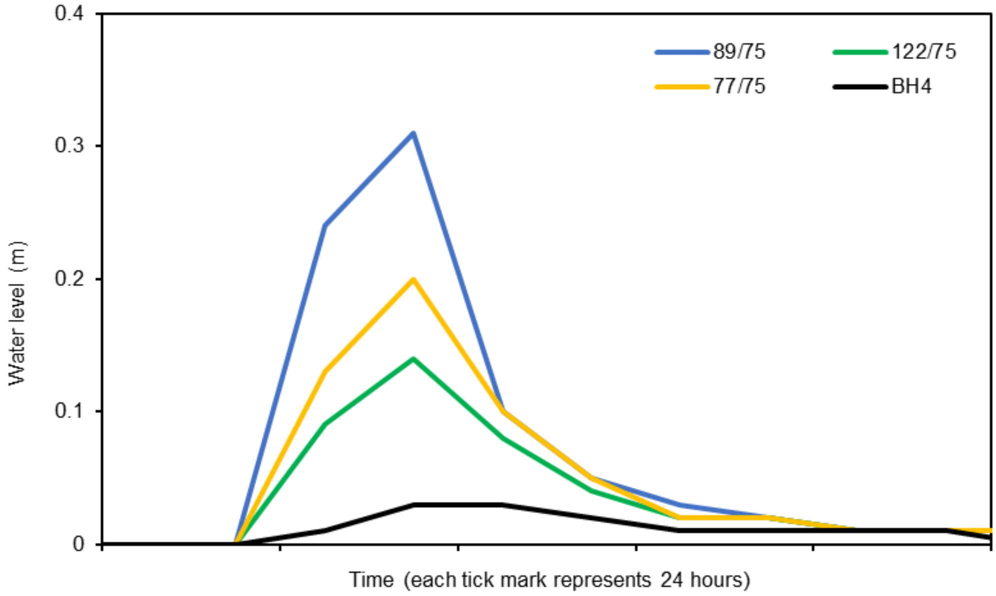

Figure 4.14 Simulated groundwater-level fluctuations in 89/75, 122/75, 77/75, and BH4 resulting from a recharge pulse under the River Little Kinyasungwe.

in the closest well, 89/75 and the magnitude of fluctuations decrease farther away. The peak fluctuation magnitude in the farthest well, BH4, is less than 0.1 m. The propagation of groundwater mounds is rapid. Dissipation of the mound, i.e. water level returning to its prior elevation, takes approximately 6 days.

4.5 Discussion

4.5.1 Recharge Mechanisms

Analysis of a long-term stream stage and groundwater-level fluctuations, high-resolution observations of groundwater mounding, numerical modelling and stable-isotope tracers indicate that significant focused groundwater recharge occurs in the Makutapora Basin.

Associating climatological and hydrological variables indicate that recharge is more strongly related to stream flow than precipitation. Strong relationships between the duration of streambed inundation and groundwater recharge magnitude suggests that leakage may be the source of focused recharge. This fits a conceptual model whereby groundwater recharge increases with inundation duration as the duration of infiltration would be directly proportional to groundwater recharge amount (section 2.3.9). The association simply shows that stream flow and groundwater recharge are produced under the same conditions. However, in combination with high-resolution observation of groundwater-level fluctuations and stream stage, it is clear that focused recharge emanates from streambed leakage. Further, the feasibility of the mounding interpreted from high-resolution observations, given current estimated of groundwater hydraulic parameters, was confirmed using a numerical model. Observation of transient groundwater-level fluctuations demonstrate that groundwater-levels respond to streambed inundation. Furthermore, positive groundwater fluctuations were generally larger in piezometers closer to inundated streambeds, i.e. mounds of groundwater formed under the streambed and subsequently decayed. The magnitude of the observed responses, however, deviates from this pattern in some instances. C5, the closest monitoring well to the River Little Kinyasungwe experiences an anomalously small response. The prior conceptual understanding of leakage form the River Little Kinyasungwe indicted that maximum leakage was believed to occur at the edge of the wellfield. The location of C5 is upstream of the wellfield and would, therefore, expect to experience less recharge. The location of C5 was chosen to explore variability along the River Little Kinyasungwe and results from C5 indicate that leakage increases at the edges of the wellfield. Despite the focus on the leakage from the River Little Kinyasungwe, it is well recognised that leakage from other ephemeral streams is expected to occur and has been observed without measurements (e.g. R. Taylor pers. Comm.) throughout lowland areas of the Makutapora Basin. Accordingly, due to spatial variability in precipitation, infiltration or percolation, recharge may occur remotely from the River Little Kinyasungwe prior to leakage occurring from the stream itself. An example of this is observable in figure 4.9. BH4, the monitoring well farthest from the River Little Kinyasungwe appears to respond first. This may have been a response to early leakage from another ephemeral stream close to BH4.

In tandem, these two findings, the relationship between the inundation duration of ephemeral streambeds and groundwater recharge magnitude and the observation of mounding in high-resolution groundwater monitoring wells, suggest that focused recharge occurs due to leakage from the River Little Kinyasungwe. To further assess the provenance of average groundwater, stable-isotope tracers were used to trace its origin. Average stable-isotopic composition of groundwater in the Makutapora basin does not match the composition of precipitation falling in the basin, which is strong evidence that significant diffuse recharge does not occur (Gat, 1971). Furthermore, the ratio of $\delta^{18}O$ and $\delta^{2}H$ in groundwater and precipitation, even when selection is accounted for, do not match. This discrepancy suggests that groundwater does not derive directly from precipitation, and that it also undergoes significant fractionation prior to reaching the saturated zone. The only potential source of groundwater which was tested and was not excluded, based on stable-isotopic composition, was surface water from ephemeral streams. Soil water, distant from ephemeral streams, and lake water from Hombolo Reservoir were both discounted, along with precipitation due to differences in average stable-isotope composition or the relationship between stable-isotope ratios of O and H. Synthesizing these three separate findings, there is considerable evidence to conclude that the predominant recharge pathway in the Makutapora Basin is focused recharge via leakage from ephemeral streams.

Given the prevailing climate of Makutapora, the results of these analyses are consistent with the understanding that the prevalence of focused recharge is associated with aridity (Alley, 2009). Moreover, the apparent importance of leakage from ephemeral streams is consistent with limited evidence from other semi-arid regions (Simmers, 2003; Simmers et al., 1997). Previous research in the Makutapora Basin proposed that groundwater recharge predominantly occurred via a diffuse mechanism (Nkotagu, 1996; Shindo et al., 1989). Accordingly, this research invalidates those assertions. There is not sufficient evidence to definitively conclude that diffuse recharge does not occur, but it appears that focused recharge is the dominant pathway.

High-resolution observations of stream stage and groundwater-level fluctuations provide new evidence of recharge processes in the Makutapora Basin. The rapidity of groundwater-level responses to stream flow and the thickness of the unsaturated zone suggests that percolation is not occurring via matrix flow. Percolation via macropores or fractures, allowing water to bypass the matrix, would reconcile better with these observations. It is worth noting that there is no evidence indicating mechanisms of percolation elsewhere in the basin. As focused recharge appears to be the predominant mechanism, and the River Little Kinyasungwe is the largest ephemeral stream, it seems unlikely that a significant amount of water is reaching the saturated zone via matrix flow. Rapid percolation through the unsaturated zone was proposed as possibly occurring in the Makutapora Basin previously (Shindo et al., 1989). Termite mounds acting as macropores were suggested as conduits for water.

4.5.2 Climate Change Impacts

An improved understanding of recharge processes has several important implications. Our findings indicate that groundwater recharge is strongly controlled by the duration of ephemeral streamflow. Accordingly, it is indicated that renewable groundwater resources are controlled by runoff and consequently stream flow. Moreover, given the importance of precipitation intensity (Chapter 3) and stream flow on groundwater recharge, it is follows that the former may produce the latter. Infiltration excess overland flow occurs when the rate of precipitation exceeds the infiltration rate of the ground and saturation excess overland flow occurs when precipitation continues to fall after soil has become saturated. Both mechanisms producing runoff due to more intensive precipitation aligns with the findings of Chapter 3. This allows for a more comprehensive assessment of the potential effects of climate change.

Changes to mean annual precipitation in sub-Saharan Africa are variable and uncertain in current climate projections, but an increase in precipitation intensity is widely projected and has already been observed. Accordingly, projected changes to precipitation could increase runoff. However, significantly more research is required to fully understand the conditions which produce runoff in the Makutapora Basin before a robust assessment is possible. In addition to increased precipitation producing runoff, climate change is expected to increase runoff via the physiological forcing (Cao et al., 2010) whereby reduced transpiration is caused by increased CO_2

concentrations (Sellers et al., 1996). Previous research in semi-arid sub-Saharan Africa has highlighted an historical example of increased runoff increasing groundwater recharge (Leblanc et al., 2008). In this case, however, increased runoff resulted from land cover change. Accordingly, climate change may increase groundwater recharge in the Makutapora Basin.

4.5.3 Implications for Modelling

Understanding the processes that transmit meteoric water to the saturated zone is vital for cogent modelling. Accordingly, projections of groundwater quality and quantity can embed more accurate characterisations of the processes known to occur in the basin. Without an understanding of the primary recharge processes, modelling work is limited to empirical models. The chapter which follows explores the implementation of this improved understanding in a process-based model to project groundwater resources. For example, the importance of accurately simulating ephemeral stream flow, particularly its duration and timing, have been highlighted and will become a central feature of the model. Furthermore, accurate parameterisation of streambed leakage is clearly vital for an accurate representation of processes within the catchment. Similarly, limiting diffuse recharge will become an important feature of the hydrological model representing the Makutapora Basin. While not explored further in this thesis, the processes which govern aquifer contamination are now significantly better understood.

Delineation of primary recharge mechanisms allows for better recharge estimations and assessments of renewable groundwater resources. The most widely used estimation method in arid and semi-arid regions is the CMB, which would not be appropriate here in its conventional form, due to the heterogeneity in recharge. While this has limited impact in Makutapora as recharge has generally been estimated by other means, it highlights the need to move away from widely used partial methods in areas where recharge mechanisms are unknown.

4.5.4 Water management

From a pragmatic standpoint, the prevalence of focused recharge has important implications for water management in Makutapora. Population and concomitantly water demand are increasing and are expected to carry on doing so. Sustainably managing the sole water source of a capital city may become impossible without artificially enhancing groundwater recharge. It is clear that water is able to rapidly infiltrate and percolate into the saturated zone in certain locations within the basin. This may aid in the assessment of viable engineering solutions. If, for example, construction of infiltration ponds, or a dam for recharge release, could inundate the pertinent areas for a greater duration than would naturally occur, recharge could greatly increase. The findings from this study indicate that recharge is linearly related to the duration of inundation. This study encompassed two anomalously large recharge seasons which produced approximately 100 days of streambed inundation, leading to up to 5 m of groundwater head increase. If this could be artificially replicated, it would greatly increase the renewable water resources at the disposal of Dodoma’s water managers and increase the sustainable population of the city.

While it has not been possible to conclusively show that groundwater recharge occurs exclusively as the result of precipitation falling within the catchment, and that regional scale groundwater flow has little influence, this analysis indicates that recharge is predominantly endogenous. This concurs with previous research and hypotheses (Fawley, 1955; Nkotagu, 1996;

Taylor et al., 2013b). This is additionally important for implementation of engineering solutions. As recharge is generated within the basin, engineering solutions can also be implemented internally. If recharge was found to be primarily generated outside the basin, the scale of any MAR solutions may have to be significantly larger and costlier.

4.5.5 Limitations

There are some caveats associated with this study. which need to be appreciated. The River Little Kinyasungwe is not the only ephemeral stream in the Makutapora Basin. The high-resolution monitoring array was positioned in such a way to observe potential groundwater mounds originating from the River Little Kinyasungwe, however, focused recharge may have been occurring elsewhere within the basin. Therefore, relating the timing and magnitude of groundwater-level fluctuations relative to distance from the River Little Kinyasungwe may be somewhat specious. Piezometers may be more strongly influenced by focused recharge from other, closer, smaller streams, which are unmonitored.

Some groups of isotope samples are small. There is no indication of whether water samples represent long term average isotopic compositions of water present in the corresponding locations. For this reason, potential sources of groundwater were discounted as less likely to be the source of groundwater, rather than definitively included or excluded. The stable-isotope analysis in this chapter would be greatly improved with additional data from the locations already sampled, but also additional locations throughout the basin.

4.6 Conclusions

This chapter has shown that groundwater recharge predominantly occurs via leakage from ephemeral streambeds in the Makutapora Basin. Three discrete methods of investigation, high-resolution groundwater-level fluctuation monitoring, stable-isotope tracers, and long-term surface water monitoring, all independently highlighted the importance of focused recharge. Additionally, percolation was also shown to be very rapid, implying that water may be transmitted through the unsaturated zone via bypass flow. The conceptual model developed from findings here and in Chapter 3 will be tested with a fully integrated groundwater, surface water hydrological model in the chapter which follows.

This research entailed the development and implementation of several novel techniques. A high-resolution monitoring array was installed prior to the 2015/2016 El Niño wet season and will continue to monitor groundwater and surface water dynamics in the basin to the benefit of Dodoma’s water supply. The dataset produced for this research is rivalled in very few basins elsewhere on the continent. Analysis of high-resolution groundwater data required the development of a novel method to account for transient groundwater recessions in an actively pumped system. These techniques can be implemented in other pumped systems and will allow for research to be carried out in locations which have generally been avoided due to their complexity.

This research is an important first step for various further research. To assess how climate change may impact renewable groundwater resources, the conditions and processes which produce runoff need to be explored. Currently, there is little understanding of the specifics of how streamflow originates in the Makutapora Basin. Additionally, research is required to determine how competing changes, such as increased temperature and increased groundwater abstraction, may interact with changes to precipitation and runoff.

The improved understanding of the primary processes associated with groundwater recharge allows for much more comprehensive evaluations of MAR solutions. Moreover, these analyses will form the basis of a physically based model to assess renewable groundwater recharge in the basin.

Chapter 5

Projection of Groundwater Resources in the Makutapora Basin Under Scenarios of Climate Change and Groundwater Abstraction

5.1 Abstract

This chapter projects changes in groundwater resources under scenarios of climate change and groundwater abstraction in the Makutapora Basin. Specific climate change impacts include the intensification of precipitation as well as changes in mean annual precipitation and evapotranspiration. A coupled MIKE SHE/MIKE 11 model was developed to encompass the processes which were found to be important for the generation of groundwater recharge in Chapters 3 and 4. A 3% reduction in mean annual precipitation in conjunction with a 2.7% increase in evapotranspiration were found to disproportionately reduce groundwater recharge. These impacts, however, are negated and exceeded by the effect of the intensification of precipitation, which significantly increased groundwater recharge. The dominant factor which will determine future groundwater resources in the Makutapora, however, is groundwater abstraction. Pumping at a rate which the infrastructure within the wellfield is designed to transmit to Dodoma will result in a catastrophic reduction in groundwater-levels and is unsustainable. A 'business as usual' scenario of groundwater abstraction also resulted in a significant reduction in groundwater-levels.

5.2 Introduction

Groundwater is the most voluminous and pervasive water resource in Africa (MacDonald et al., 2012). This has led to widespread development of groundwater resources in service of municipal water supplies across sub-Saharan Africa (Lapworth et al., 2017). Many urban areas in sub-Saharan Africa, such as Lusaka, Windhoek, Kampala, Addis Ababa, and Dodoma (Murray et al., 2018; Pavelic, 2012; Robins et al., 2006), are partially or entirely dependent on groundwater for their domestic water supply (Adelana et al., 2008). The future sustainability of groundwater dependant municipal water supplies is contingent on the net influences of climate change and human activity on groundwater resources (Taylor et al., 2013a). Water demand in African cities is set to increase due to the growth of urban populations. In Africa, this is most rapid in the world (UNFPA, 2009) due to the fastest growing population (UN, 2017), and the most rapidly urbanising population (UN, 2014). These factors are widening the gap between water availability and water demand (WWP, 2017).

Despite the importance of groundwater, the renewability of this resources in Africa, now and in the future, remains unresolved. Projecting the impacts of climate change on groundwater recharge is an example of the propagation of uncertainty (Taylor et al., 2009). Uncertainty arises from many interconnected and uncertain procedures which are all required to project groundwater resources. Accordingly, projections of groundwater are known to be highly uncertain, yet modelling is the only technique which can be used to predict future recharge rates and is invaluable for isolating impacts of different controls on groundwater recharge (e.g. Keese et al., 2005; Salama et al., 1999; Zhang et al., 1999).

Projection of future climate by GCMs is generally considered the dominant source of uncertainty in projecting water resources as different emissions scenarios translate into significantly different climate scenarios (Bates, 2009). This is particularly true for precipitation, projections of which are much more uncertain than temperature projections (Kundzewicz et al., 2009). As groundwater recharge projections are closely related to projected changes in precipitation (Taylor et al., 2013a), this uncertainty translates directly to uncertain groundwater recharge. The use of GCMs to project future climates is an unavoidable uncertainty associated with groundwater projections.

Groundwater resources assessments require scenarios of climate change and water demand, which are interrelated and difficult to predict. Climate change projections rely on emissions scenarios to define radiative forcing. The IPCC currently uses Representative Concentration Pathways (RCPs), which are associated with emissions scenarios which increase radiative forcing by a specified value in the future, relative to pre-industrial levels. Previously, emissions scenarios were accompanied by storylines of socio-economic development. The IPCC does not indicate that any scenarios are more or less likely to occur. Accordingly, there is no "best guess" of future emissions or climate. Despite this, climate change projections are often framed as “reliable forecasts” (Kundzewicz et al., 2009).

Further uncertainty derives from scenarios of water demand, which is determined by a rapidly evolving demographic and economic environment, which is hard to predict. Moreover, water demand is, in part, determined by the impacts of climate change on the hydrological cycle. Projections of water demand, and more specifically groundwater use are consequently highly uncertain.

Further uncertainty is added by the necessity of downscaling precipitation data. The scale of CGM outputs is generally too large to be compatible with basin scale hydrological models. Accordingly, projected precipitation, the principal forcing of hydrological models, is downscaled. Uncertainty from downscaling is considerable. It can be greater than uncertainty deriving from the choice of emissions scenario (e.g. Holman et al., 2009; Stoll et al., 2011). Simply, downscaling is the procedure of taking information known at large scales to make predictions at local, basin relevant scales (Taylor et al., 2009). Vitally, there is no standard method of downscaling. Commonly, historical daily precipitation distributions are used to downscale monthly precipitation projections. Unfortunately, the increased greenhouse gas concentration which increase temperatures and alter precipitation, concomitantly alter the distribution of precipitation in a way which is generally not accounted for by downscaling procedures. Warming increases the water-holding capacity of atmosphere which is projected to increase the frequency of more intensive precipitation events, i.e. those in the uppermost quantiles of the precipitation distribution (Allan & Soden, 2008; Trenberth, 1999). Failure to account for precipitation intensification can misrepresent the direction and magnitude of the climate change signal (Taylor et al., 2009). There is a growing body of research which suggests that precipitation intensity significantly effects the production of groundwater recharge (Jasechko & Taylor, 2015; Owor et al., 2009; Taylor et al., 2013b; Chapter 3).

Hydrological model parameters and hydrological model structure are also sources of uncertainty (Taylor et al., 2009). Groundwater recharge is derived from the hydrological balance of a basin, which means, in addition to accurately projected precipitation, evapotranspiration, surface runoff, infiltration and storage also need to be accurately simulated. Furthermore, the hydrological model developed needs to encompass all important processes in the catchment in question. For example, despite the importance of focused recharge (Simmers, 2003; Simmers et al., 1997), diffuse processes are more widely understood and are more extensively incorporated in large-scale hydrological models (Cuthbert et al., 2016). Therefore, projections of groundwater recharge are uncertain in areas where recharge from surface water bodies, such as ephemeral streams, dominates (e.g. Döll & Fiedler, 2008; Wheater et al., 2010).

Here, a fully integrated hydrological model is developed for the Makutapora Basin, the sole source of water for the capital city of Tanzania (DUWASA, 2017). The model is forced with projections of climate change and groundwater abstraction to assess plausible projections of future groundwater resources. Climate projections derive from an ensemble mean of phase 5 of the Coupled Model Intercomparison Project (CMIP5) under RCP 8.5. Furthermore, given the importance of more intensive precipitation found in the analysis of Chapter 3, climate change projections will be downscaled to explicitly consider for the intensification of precipitation. Additional climate change scenarios will be simulated to assess the impacts of changes to mean precipitation and increased evapotranspiration. Scenarios of increased groundwater abstraction will also be assessed and will be based on a well constrained estimates based on the infrastructural limits of the wellfield and contemporary pumping rates.

There has been a single previous attempt to create a hydrological model of the Makutapora Basin to assess the effects of different scenarios of recharge and abstraction (Kashaigili et al., 2003). Previous work was limited by the lack of integrated surface water-groundwater modelling as it neglected interactions with, and potential contributions from, surface water. Modelling systems that exclusively consider groundwater (e.g. MODFLOW) are of limited utility when surface hydrology has been found to strongly impact groundwater recharge (Chapter 4). Use of an integrated, physically based model, which incorporates surface and subsurface flows, such as MIKE SHE/MIKE 11 (Figure 5.1) is better suited to simulate groundwater flow, recharge, and surface water flows in response to different scenarios of groundwater abstraction and climate change. Integrated hydrologic modelling requires extensive records of long-term climate, hydrogeology, land use, surface flows and groundwater-levels (Sishodia et al., 2017), but very few catchments in sub-Saharan Africa have the requisite data (Feyen et al., 2000; Jones et al., 2008) to constrain such dynamics.

The aim of this chapter is to project groundwater resources under climate change and increased water demand in a semi-arid, fractured crystalline aquifer in central Tanzania. This will facilitate an assessment of the impact of: (1) the intensification of precipitation, (2), changes to mean annual precipitation, (3) changes to evapotranspiration, and (4) increased groundwater abstraction.

5.3 Hydrological Modelling

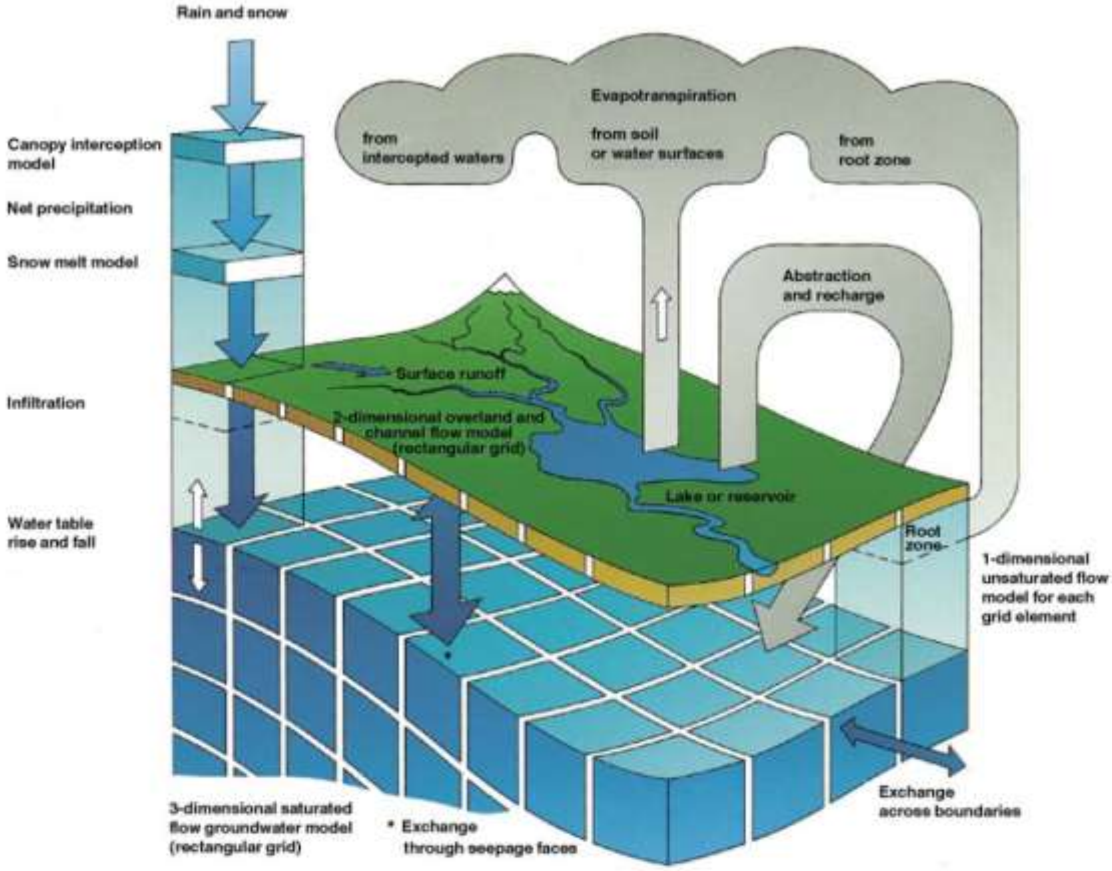

Figure 5.1 Schematic representation of the MIKE SHE model (Refsgaard and Storm, 1995).

The dynamically coupled MIKE SHE/MIKE 11 hydrological model allows for exchange of fluxes between MIKE 11 river channels and MIKE SHE overland flow, saturated zone and unsaturated zone components (Figure 5.1). The MIKE SHE modelling system (Graham and Butts, 2005) is based on the Système Hydrologique Européen (SHE) (Abbott et al., 1986a, 1986b). It is a deterministic, fully distributed and physically based modelling system that simulates the land-phase processes of the hydrologic cycle. It has successfully been employed under diverse climatological and hydrological regimes, at various scales (Thompson et al., 2013). MIKE 11 is a fully dynamic, one-dimensional hydraulic modelling system with comprehensive capabilities for modelling stream channel networks (Havnø et al., 1995). The primary components of the coupled model are: evapotranspiration/interception, overland flow/channel flow, unsaturated zone, saturated zone and the exchange between aquifers and rivers. Dynamic coupling of MIKE SHE and MIKE 11 is achieved using river links (line segments) between adjacent grid squares in MIKE SHE. Locations of river links are determined from the specified co-ordinates of river points that define coupled reaches in MIKE 11. During simulations, water levels are transferred from H-points (points in the hydraulic model where water levels are calculated) to adjacent MIKE SHE river links. MIKE SHE calculates overland flow into river links from adjacent grid squares and the river-aquifer exchange, which are then fed back into MIKE 11 as lateral inflows or outflows for the next computational time step (Thompson et al., 2004).

The model developed here is based on the saturated zone model developed in chapter 3. The saturated zone component of the model used here is the same as the saturated zone component previously developed with the exception of the resolution of the computation grid. The computational grid resolution has been increased from 100 m to 500 m for use in this chapter to ensure logistically appropriate computation times. The impact of changes in resolution is discussed in section 3.3.4.9 and an example is given in figure 3.5.

Unlike the saturated zone model developed in chapter 3, the model developed here incorporates evapotranspiration/interception, overland flow/channel flow, unsaturated zone, saturated zone and the exchange between aquifers and rivers. Once coupled with MIKE 11, this forms a fully integrated hydrological model. MIKE 11 is a fully dynamic, one-dimensional hydraulic modelling system with comprehensive capabilities for modelling stream channel networks (Havnø et al., 1995). Dynamic coupling of MIKE SHE and MIKE 11 allows for exchange of fluxes between MIKE 11 river channels and MIKE SHE overland flow, saturated zone and unsaturated zone components (Figure 5.1). The setup of the all the components comprising the MIKE SHE/MIKE 11 model are detailed below.

5.3.1 Domain

The domain of the model is the Makutapora Basin, which has a catchment area of 698 km^2 upstream of the Chihanga outlet on the River Little Kinyasungwe (Shindo et al., 1989). The basin is defined by topography using 90 m SRTM data (Jarvis et al., 2008). Variations in the characteristics of the catchment are represented by the discretisation of the domain horizontally into a computational grid. The model employs a 500 m x 500 m grid, which was chosen as a compromise between model accuracy and logistically appropriate computation times. Spatial variability in parameters such as elevation, soil hydraulic parameters, and land cover are represented at the resolution of the grid. Within grid squares, vertical variations are represented by horizontal layers of variable depths. Lateral flow between grid squares can occur as overland flow or subsurface saturated zone flow. The method employed to represent flow in the unsaturated zone assumes that horizontal flow is negligible.

5.3.2 Climate

MIKE SHE requires two climatological inputs, precipitation and reference evapotranspiration. Meteorological data for the period 1st July 1955 to 30th June 2016 were provided by the Dodoma Meteorological Station. A complete record of daily precipitation exists for the entire duration of the simulation. It is assumed precipitation is spatially uniform throughout the basin. An almost complete record of daily temperature highs and lows was used to calculate daily potential evapotranspiration. Where data are missing, average high or low values from the corresponding month are substituted. Where no values are available for the entire month, average high and low values taken from the entire record for that month are substituted. As recommended by the FAO (Allen et al., 1998), the Hargreaves and Samani method (1982) (Equation 5.1) was used to calculate ET_o, as there was insufficient data to employ the Penman-Monteith method.

$$\mathrm{ET}_0 = \mathrm{a} + \mathrm{b} \cdot \left(\frac{T_{max} - T_{min}}{2} + 17.8\right) \cdot \sqrt{T_{max} - T_{min}} \cdot R_a \qquad \text{(Equation 5.1)}$$

T_{max} (°C) is daily maximum air temperature, T_{min} (°C) is the daily minimum air temperature, R_a ($MJ \cdot m^{-2} \cdot d^{-1}$) is extra-terrestrial solar radiation. Parameters a and b are calibration coefficients determined for individual sites (Berti et al., 2014). Daily extra-terrestrial radiation, R_a is calculated using Equation 5.2.

$$R_a = \frac{24(60)}{\pi} \cdot G_{sc} \cdot d_r[\omega_s \cdot \sin(\varphi) \cdot \sin(\delta) + \cos(\varphi) \cdot \sin(\omega_s)] \qquad \text{(Equation 5.2)}$$

G_{sc} is the solar constant (0.0820 $MJ \cdot m^{-2} \cdot min^{-1}$), d_r is inverse relative distance Earth-Sun, ω_s is the sunset hour angle, φ is latitude of the site (rad), δ is solar declination (rad). The inverse relative distance Earth-Sun, d_r, the solar declination, δ, and sunset hour angle, $\omega_{s,}$ are calculated using Equations 5.3, 5.4 and 5.5, respectively.

$$d_r = 1 + 0.033 \cdot cos\left(\frac{2\pi}{365} \cdot J\right) \qquad \text{(Equation 5.3)}$$

$$\delta = 0.409 \cdot sin\left(\frac{2\pi}{365} \cdot J - 1.39\right) \qquad \text{(Equation 5.4)}$$

$$\omega_s = arccos[-tan(\varphi) \cdot tan(\delta)] \qquad \text{(Equation 5.5)}$$

J is the number of the day in the year between 1 (1 January) and 365 or 366 (31 December). Parameters a and b were calibrated on 3 years of pan evaporation data. This necessitated the estimation of a pan coefficient to translate recorded pan data to ET_o values. Pan coefficient (K_{pan}) was determined using the procedure described in Allen at al. (1998) based on prevailing conditions and the site of the pan. ET_o. MIKE SHE uses the Kristensen and Jensen (1975) model to calculate actual evapotranspiration from ET_o, computed soil moisture in the root zone, leaf area index (LAI), and root depth (RD).

5.3.3 Overland Flow

In MIKE SHE, overland flow is simulated by diffusive wave approximation of two-dimensional Saint-Venant equations (Havnø et al., 1995) once ponding depth exceeds detention storage in a grid cell. The velocity of overland flow is determined by values of Manning's M roughness, which is assumed to be spatially uniform. An initial value of Manning's M roughness was taken from Thompson (2012), who specified values for analogous vegetation types. The final value was determined via calibration. Detention storage was also assumed to be spatially uniform and final values were determined via calibration; initial values were constrained by field observations. Overland flow time step is set at 24 hours.

5.3.4 Land Use

The spatial distribution of vegetation cover is based on a simplified version of the Global Land Cover map, GlobCover Version 2.3, 2009 (Arino et al., 2012), produced by the European Space Agency (ESA) as part of the GlobCover Project (Figure 5.2d). There are three land cover types within the Makutapora Basin: forest, shrubland and grassland, which are associated with individual, time varying leaf area index and root depth values. Leaf area index data comprises monthly average LAI values, derived from TERRA/MODIS LAI data (Myneni et al., 2015), associated with each vegetation type between July 2002 and June 2016. Root depths were taken from a database of root depths for various land cover types (Foxx et al., 1984). LAI and RD values for each vegetation type are given in Appendix F.

5.3.5 River Flow

In MIKE 11, flow in open channels is simulated by a fully dynamic finite difference solution of complete non-linear one dimensional Saint-Venant equations (Havnø et al., 1995). The location of river links, representing ephemeral streams in MIKE 11, were assumed to be constant, in locations determined by topography. River links in MIKE 11 were specified in locations defined by a drainage area threshold of 10 km^2 based on SRTM 90m DEM data (Jarvis et al., 2008) using ArcSWAT (Figure 5.2c). The channel leakage coefficient, which governs the bi-directional flow exchange between streams and groundwater, was determined through calibration. Initial values were constrained by analysis in Chapter 4. Cross sections used in MIKE 11 to represent channel architecture were approximated from field observations. The MIKE 11 river flow model has a fixed time step of 24 hours.

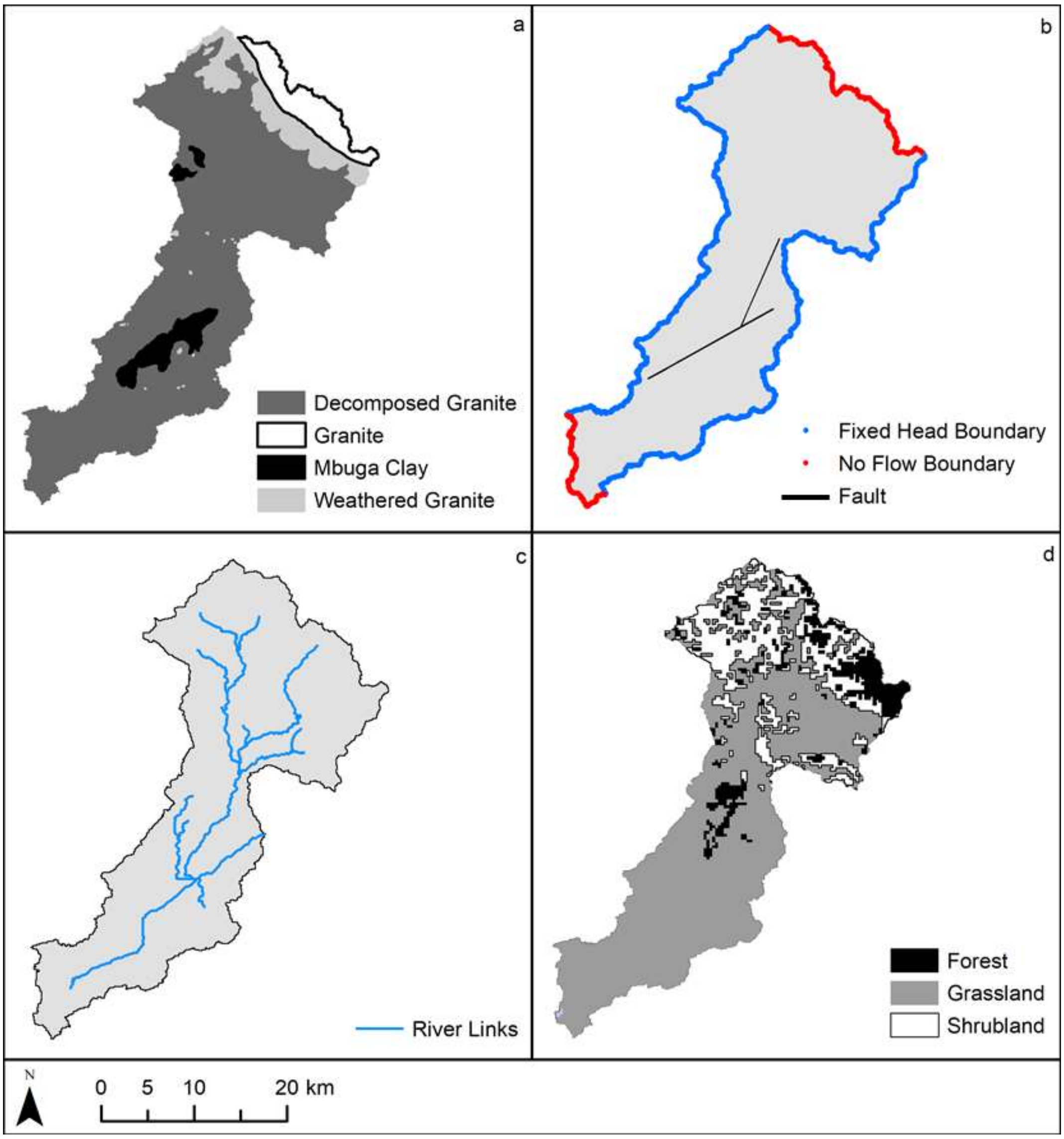

Figure 5.2 Distributions of soil zone profiles (a), saturated zone features (b), river links (c), and distribution of land cover types (d) defined in the MIKE SHE/MIKE 11 model.

5.3.6 Unsaturated Zone

Unsaturated-zone fluxes are simulated by a fully implicit finite-difference solution of one-dimensional Richards' equation. This approach assumes that horizontal flow is negligible. Soils in the unsaturated zone were assumed to spatially vary. The basin was separated in 4 areas defined by their soil profiles: decomposed granite, granite, weathered granite, and Mbuga clay over decomposed granite (Figure 5.1a). Van Genuchten (1980) model parameters and soil moisture retention curves for each soil type were estimated using ROSETTA (Schaap et al., 2001) based on estimates of soil texture (% sand, silt, clay) (De Pauw et al., 1983; Muir et al., 1957), bulk density, specific retention (Heath, 1983) and specific yield (Heath, 1983). Soil texture was also used to determine an initial values of specific yield (Johnson, 1967). The unsaturated zone component of the model operates on a 24-hour time step. Tables of soil zone profiles and their associated parameters are included in Appendix E along with details of the vertical discretisation of the unsaturated zone.

5.3.7 Saturated Zone and Groundwater Withdrawals

A finite-difference approach is used to solve the partial differential equations describing the saturated subsurface flows, which are simulated by three-dimensional Darcy equations. Specific yield and hydraulic conductivity of the aquifer, faults and Mbuga Clay, and the elevation of fixed head boundaries were retained from Chapter 3, section 3.3.4.8 (Figure 5.2b). Groundwater withdrawals for the historical baseline scenario comprise the same data detailed in section 3.3.4.11 in Chapter 3.

5.3.8 River-aquifer exchange

River-aquifer exchange is governed by the conductance between river and grid node which is a function of both the aquifer conductivity and the conductivity of the river bed. Conductance, C, is given as:

$$c = \frac{1}{\frac{d_s}{K \cdot d_a \cdot d_x} + \frac{1}{L_c \cdot w \cdot d_x}} \qquad \text{(Equation 5.6)}$$

where K is the horizontal hydraulic conductivity in the grid cell, d_a is the vertical surface available for exchange flow, d_x is the grid size used in the saturated zone, d_s is the average flow length, L_c is the leakage coefficient [1/T] of the stream bed, and w is the wetted perimeter of the cross-section. The average flow length, ds, is the distance from the grid node to the middle of the river bank in the river-link cross-section. Wetted perimeter, w, is assumed to be equal to the sum of the vertical and horizontal areas available for exchange flow. da is calculated as either: 1) if the water table is higher than the river water level, da is the saturated aquifer thickness above the bottom of the river bed, or 2) if the water table is below the river level, then da is the depth of water in the river. In Makutapora, ephemeral streams are separated from the aquifer by an unsaturated zone and are therefore understood to be losing reaches.

5.3.9 Climate Change and Groundwater Abstraction Scenarios

To assess the discrete and combined impacts of climate change and varying rates of groundwater abstraction, the hydrological model was used to simulate water resources in the Makutapora Basin under varying scenarios. Climate change scenarios were designed to assess the impacts of plausible changes to mean annual precipitation, precipitation intensity, and evapotranspiration. Accordingly, both climate change scenarios used perturbed historical precipitation data that accounted for changes to mean annual precipitation, but only one accounted for the intensification of daily precipitation. Therefore, three climate scenarios (two climate change scenarios and one baseline scenario) were simulated in conjunction with baseline groundwater abstraction data, and two future groundwater abstraction scenarios. A summary of simulated scenarios is shown in Table 5.1.

Table 5.1 The climate and groundwater abstraction scenarios for each simulation.

Name	Climate	Groundwater Abstraction
HB-HB	Historical Baseline	Historical Baseline
CCni-HB	Climate Change without intensification	Historical Baseline
CCi-HB	Climate Change with intensification	Historical Baseline
HB-IA	Historical Baseline	Increased Abstraction
CCni-IA	Climate Change without intensification	Increased Abstraction
CCi-IA	Climate Change with intensification	Increased Abstraction
HB-CA	Historical Baseline	Contemporary Abstraction
CCni-CA	Climate Change without intensification	Contemporary Abstraction
CCI-CA	Climate Change with intensification	Contemporary Abstraction

Projections of precipitation and temperature-based ET_o under climate change scenarios are based on CMIP5 ensemble mean projections for the grid square, 35E – 37.5E, 5S – 7.5S, which contains the Makutapora Basin. Precipitation projections are based on an ensemble mean of 32 GCMs, whereas temperature projections are derived from 31 GCMs. Differences between baseline hindcasts (1955 – 2016) and projections (2040 – 2070) under RCP 8.5 were used to scale historical precipitation. RCP 8.5 was chosen to assess the more severe plausible impacts of climate change. This represents a cautious approach from a water management perspective, however, it additional makes the attribution of climate change impacts more definitive. Historical mean annual precipitation, for all climate scenarios, was scaled based on the relative difference between mean annual precipitation for hindcasts and projections. In the climate change scenario not accounting for the intensification of precipitation (CCni), historical daily precipitation was simply uniformly scaled based on projected changes to mean annual precipitation. The procedure was different for the climate change scenario which accounted for the intensification of precipitation (CCi). To capture the intensification of precipitation, daily precipitation values were selectively scaled. Downscaling was achieved using a statistical delta change approach. This ensured that precipitation was explicitly intensified. Daily precipitation events exceeding the 95^{th}

intensity percentile ($P_{>95}$) were scaled based on the relative change between $P_{>95}$ in hindcasts and projections. To maintain annual precipitation values, lower intensity events, i.e. > 70th intensity percentile ($P_{<70}$), were scaled in a compensatory manner. The 70th intensity percentile was chosen due to the pan-tropical importance of precipitation greater than 70th intensity percentile for producing groundwater recharge (Jasechko and Taylor, 2015). The downscaling method of the climate change scenario accounting for intensification (CCi) is expressed in Equations 5.6 and 5.7.

$$MAP_d = MAP_o \cdot \frac{MAP_p}{MAP_h} = \frac{\sum \delta \cdot P_{o\,<70} + \sum P_{o\,70-95} + \sum \Delta \cdot P_{o>95}}{n} \qquad \text{(Equation 5.6)}$$

$$\Delta = \frac{\sum P_{p>95}}{\sum P_{h>95}} \qquad \text{(Equation 5.7)}$$

MAP is mean annual precipitation, subscripts d, p, o and h signify downscaled, projected, observed and hindcast, respectively, P is daily precipitation, subscripts <70, 70-95 and >95 signify daily precipitation less than the 50th intensity percentile, between the 70th and 95th intensity percentile, and greater than the 95th intensity percentile, respectively, and δ is a scaler which depends on Δ.

Projections of ET_o were calculated in the same manner as described in section 5.3.2. Scaling was based on the relative changes between hindcasts and projections for both temperature highs and lows. Average monthly changes were used to scale daily historical temperature data using a delta change approach. Temperature downscaling is described mathematically in equations 5.8 and 5.9.

$$T_d = \Delta_m \cdot T_o \qquad \text{(Equation 5.8)}$$

$$\Delta_m = \frac{\overline{T_{pm}}}{\overline{T_{hm}}} \qquad \text{(Equation 5.9)}$$

T is daily temperature, where subscripts d, o, p, m, and h are downscaled, observed, projected, month and hindcast. Δ_m is the delta factor for the month m. The procedure for downscaling highs and lows is the same.

The groundwater abstraction scenario, IA (increased abstraction), was based on the current maximum rate of transmission from the wellfield to Dodoma, i.e. the amount of groundwater which the recently upgraded infrastructure can transmit. On 1st June 2017, 81,439 m^3 of groundwater was transmitted from Makutapora to Dodoma. This projection assumes new transmission infrastructure will not be built in the future. Accordingly, abstraction data for the scenario of increased abstraction is a constantly daily rate of 81,439 m^3, distributed between the wells in the same proportions as recorded on 1st June 2017. The 'business as usual' groundwater abstraction scenarios, CA (contemporary abstraction) was based on average baseline groundwater abstraction from 1st July 2015 to 30th June 2016. The average for each monitoring well was applied as a constant daily rate. This equated to slightly less than 50,000 m^3 per day.

5.3.10 Model Calibration and Validation

Following Refsgaard and Storm (1995), the number of parameters subject to calibration was minimised by relying on literature values. This is the general recommendation for distributed hydrological models, such as MIKE SHE. The model was calibrated and validated on daily stream stage and groundwater-levels. As groundwater-levels are recorded in a variable number of wells, at variable temporal resolutions, and at variable levels of completeness, an 'active well average' was calculated. 'Active well average' is the average of the average hydraulic head values in each active well for each month, weighted equally between all active monitoring wells. Averaging over all available hydraulic head values allows calibration and validation to be conducted over the largest possible spatial scale and ensures performance metrics are not to unfairly weighted to periods of more active monitoring. Given the importance of the duration of ephemeral stream flow (Chapter 4), and the poor constraints on dynamic stream-channel architecture, model performance statistics were calculated using the duration of stream flow, not stream stage or stream discharge. In order to include both stream stage and groundwater-levels in the calibration and validation periods, the traditional spilt-sample approach was used on the period for which stream stage data were collected (2006 – 2016). Accordingly, calibration was carried out on groundwater-level data from 1st January 1955 to 30th June 2011, and stream stage data from 1st January 2007 to 30th June 2011. Validation was carried out on groundwater-levels and stream stage from 1st July 2011 to 30th June 2016. Model performance was evaluated with Nash Sutcliffe Efficiency (NSE) (Nash and Sutcliffe, 1970), Root Mean Square Error (RMSE), Index of Agreement (d) (Willmott, 1981), and percent bias (PBIAS). In this study, model performance was rated based on the scheme of Moriasi et al. (2007) where NSE values between 0.5 and 0.65 indicates satisfactory performance, between 0.65 and 0.75 indicates "good" model performance, and NSE values greater than 0.75 indicates "very good" model performance. Final calibrated values are detailed in Table 5.2

Table 5.2 Calibrated values for MIKE SHE/MIKE 11 parameters.

Parameter	Value
Detention Storage (m)	0.07
Manning's M roughness ($m^{1/3} \cdot s^{-1}$)	30
Leakage coefficient (s^{-1})	2.0×10^{-4}

5.4 Results

5.4.1 Model Evaluation

A comparison of simulated and observed stream stage at the Meya Meya gauge is shown in Figure 5.3. Associated model performance statistics are provided in Table 5.3. Overall, during calibration and during validation, model performance for simulating ephemeral stream flow can be classified as 'very good', based on NSE scores and the performance rating of Moriasi (2007). Residual variance was small compared to measured variance, and the model accurately replicated the duration of stream flow. Calibration and validation periods exhibited varied RMSE, 16 days and 6 days, respectively. Overall RMSE, 12 days, represents 32% of the standard

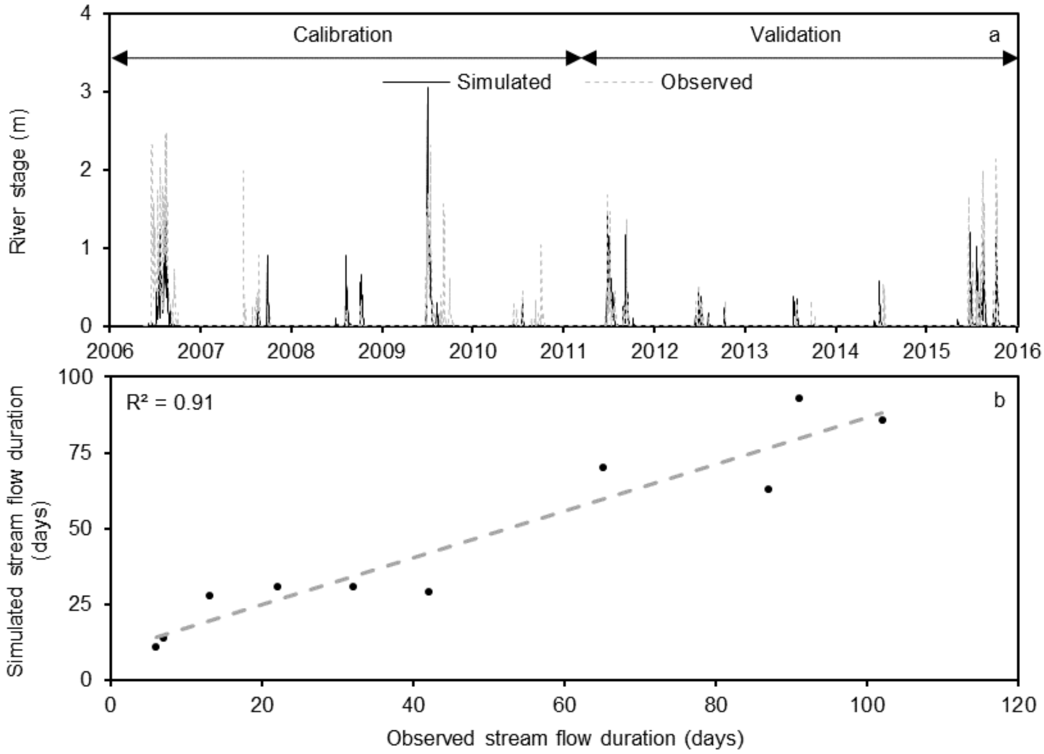

Figure 5.3 Observed and simulated stream stage at the Meya Meya gauge on the River Little Kinyasungwe between 1st July 2006 and 30th June 2016 (a). Observed seasonal stream flow duration, in days, plotted against simulated stream flow duration (b).

deviation in the observed data. Model prediction error was generally low (d = 0.96), and similar during calibration and validation. PBIAS varied considerably between calibration and validation periods. The magnitude of the bias in the two periods were similar, but stream flow duration was underestimated during calibration, PBIAS = -14%, and overestimated during validation, PBIAS = 15%.

Comparison of simulated and observed hydraulic head in the Makutapora Basin is shown in Figure 5.4. Corresponding model performance statistics are provided in Table 5.4. Overall, model performance for simulating groundwater-levels can be classified as ‘satisfactory’, based on the NSE score and the performance rating of Moriasi (2007). NSE values associated with calibration and validation periods varied considerably, 0.52 and 0.79, respectively. Calibration and validation periods exhibit similar RMSE, 1.55 m and 1.01 m, respectively. Overall RMSE, 1.49 m, represents 66% of the standard deviation in the observed data. Model prediction error was generally low. Overall, d = 0.90, and was similar during calibration and validation. PBIAS was consistently low.

Table 5.3 Calibration, validation, and overall model performance statistics for stream stage at the Meya Meya gauge on the River Little Kinyasungwe.

	NSE	RMSE	PBIAS	d
Calibration	0.80	15.67	-14.13	0.92
Validation	0.97	6.07	14.66	0.99

Overall	0.88	11.88	-2.36	0.96

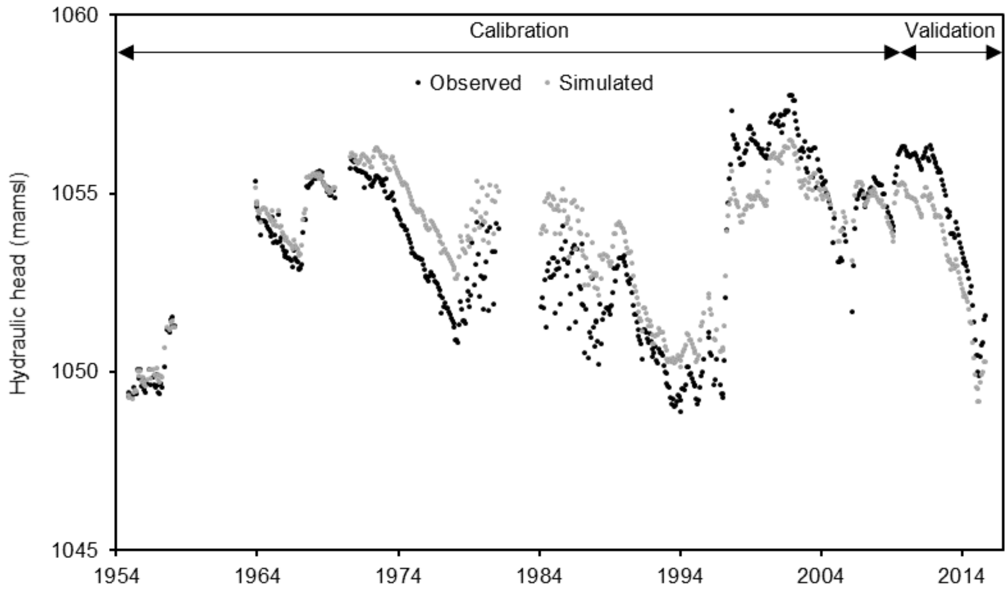

Figure 5.4 A comparison of observed and simulated 'active well average' hydraulic head values in the Makutapora Wellfield between 1st July 1955 and 30th June 2016.

Groundwater-levels simulated during the calibration period exhibited minimal bias, PBIAS = 0.01. PBIAS associated with the validation periods was greater, and more negative, but still small, PBIAS = -0.09. The considerable difference evident in model performance during calibration and validation is assumed to be due to the duration of the periods and the behaviour of the saturated zone during that time. The much shorter validation period is primarily characterised by a single groundwater-level recession whereas the much longer calibration period encompasses considerably more varied behaviour. An uneven split of groundwater-level data between calibration and validation was unavoidable due to the inconsistent duration of stream stage data.

Table 5.4 Calibration, validation, and overall model performance statistics for hydraulic head values in the Makutapora Basin between 1^{st} July 1955 and 30^{th} June 2016.

	NSE	RMSE	PBIAS	d
Calibration	0.52	1.55	0.01	0.89
Validation	0.79	1.01	-0.09	0.95
Overall	0.56	1.49	0.00	0.90

5.4.2 Water Balance of the Makutapora Basin

The historical water balance of the Makutapora Basin was assessed at the scale of the basin between 1^{st} July 1955 to 30^{th} June 2016. Figure 5.5 shows the accumulated water balance simulated using historical meteorological data and groundwater abstraction rates (HB-HB) (table 5.1). All water inputted into the model derives from precipitation; the depth of which simply equates to the total rainfall observed between 1955 and 2016 as rainfall in the model is spatially uniform. No water flows into the model from the fixed head boundaries in the saturated zone, nor through the internal surface water boundary defined in MIKE 11. A large proportion of precipitation is returned to the atmosphere through evaporation and transpiration due to high rates of potential evapotranspiration and extensive vegetation cover during the wet season. Accordingly, a smaller

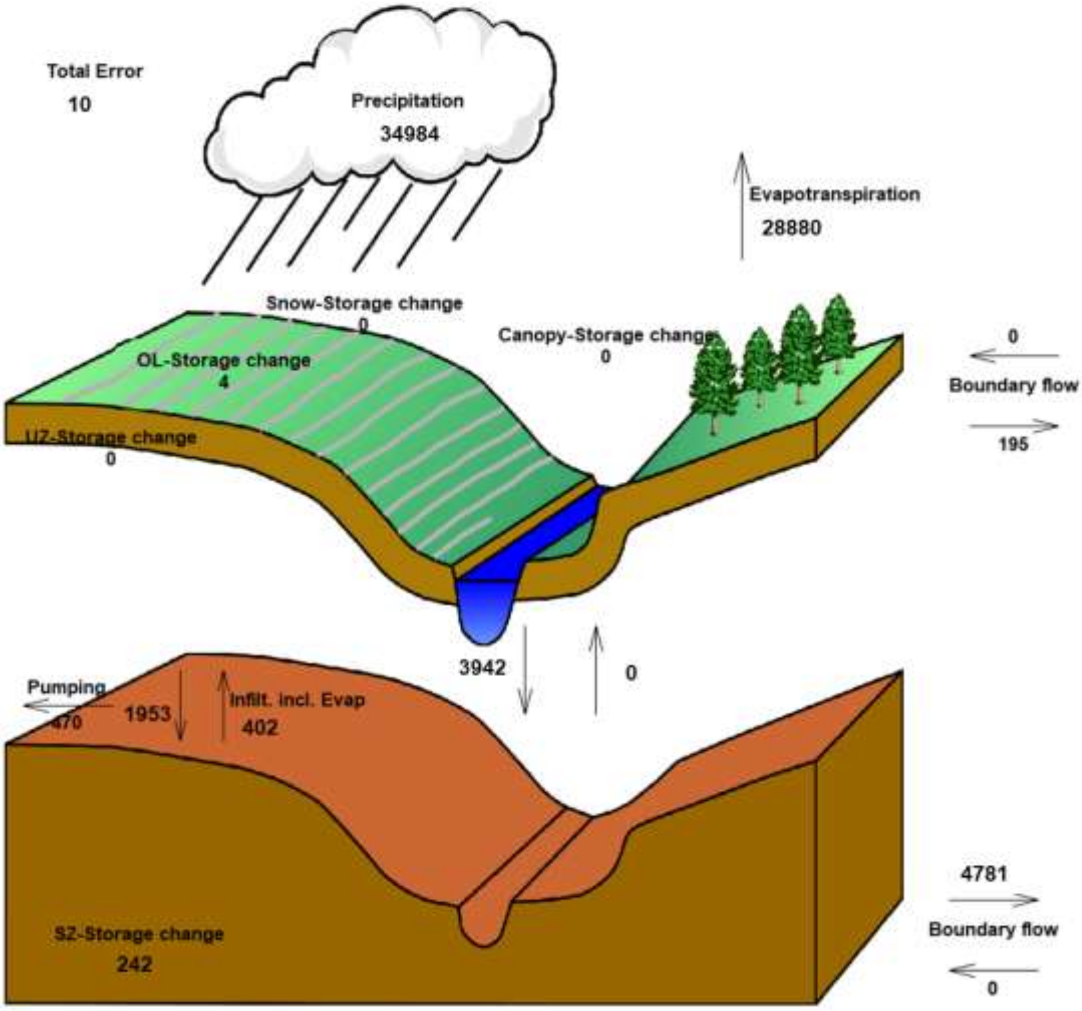

Figure 5.5 MIKE SHE figure of accumulated water balance for HB-HB (table 5.1) simulation from 1st July 1955 to 30th June 2016 for the Makutapora Basin. Storage depth are shown in mm.

proportion of precipitation infiltrates and percolates. The total depth of water that reaches the saturated zone, given the S_y defined in MIKE SHE, is equivalent to a cumulative groundwater level rise of 84 m or 1.4 m·year^{-1}. Infiltration predominately occurs via leakage from river links defined in MIKE 11 rather than diffuse processes on the ground surface. Leakage of streamflow contained in MIKE 11 river links is determined by the geometry of the channel and the leakage coefficient defined in the model. Water is additionally lost via the internal surface water boundary defined in MIKE 11, i.e. surface water, in river links, flowing out the model. Considerably more streamflow is lost from the stream via leakage than is lost from the basin as streamflow flowing out of the basin at the Chihanga gauge. None of the infiltrated water is returned to the river as baseflow. Of the water that enters the saturated zone, the majority exits the model through the boundaries. Flow out the boundaries in the saturated zone represents hydraulic gradient driven drainage which is known to occur in the Makutapora Basin (figure 3.1). A relatively small portion of the water is lost to groundwater abstraction. While the observed and simulated hydrographs (figure 3.1 and figure 5.7) appear to be strongly influenced by groundwater pumping, particularly in more recent years, production wells and observation wells are concentrated in the small area of the basin. Accordingly, at the scale of the basin, groundwater abstraction has a relatively small influence on storage despite strongly influencing the closely monitored wellfield. Over the duration of the simulation, groundwater storage increases despite the simulated hydrographs showing an overall decline (figure 5.7). Again, this is due to the simulated hydrographs representing an unusual portion of the basin where groundwater abstraction strongly controls groundwater storage. Changes in overland storage is negligible as the water balance calculation starts and ends at the same time of year, i.e. when there is close to zero overland storage. Canopy storage change is also negligible as there is very little during the dry season due to high rates of evaporation. Similarly, snow storage does not change as there is no snow storage at any point in the simulation.

5.4.3 Inundation of River Links

Streambed inundation has been shown to be important in the generation of groundwater recharge in the Makutapora Basin (figure 4.8). It is, therefore, important to understand how inundation

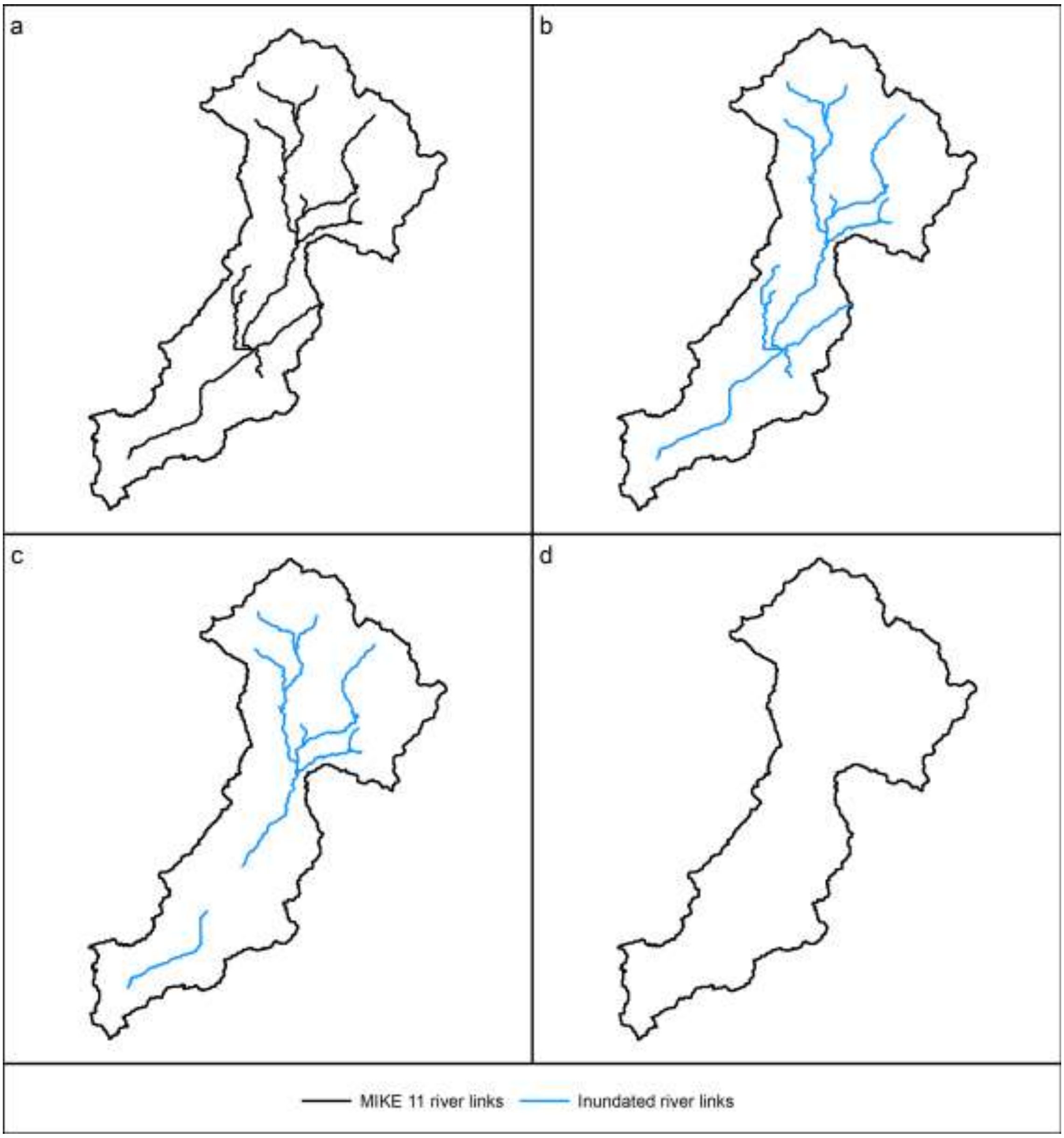

Figure 5.6 Maps showing snapshots of the extent of river links inundated at monthly intervals at the end of the 2006 – 2007 wet season. Panel a shows the extent of river links defined within

MIKE 11. Panes b, c and d show the MIKE 11 river links inundated on 15th February 2007, 15th March 2007 and 15th April 2007, respectively.

changes are simulated in response to changes climatological conditions. Snapshots of the extent of river links inundated at intervals at the end of the 2006 – 2007 wet season are shown in figure 5.6. The 2006 – 2007 wet season was chosen as an example as it was associated with one of the largest recharge events in the record and one of the longest seasonal streambed inundation durations. Accordingly, in the chosen examples, conditions associated with focused groundwater recharge and conditions not associated with focused groundwater recharge, in addition to the transition between the two, are illustrated. As rainfall and potential evapotranspiration in the MIKE SHE model are spatially uniform, runoff generation and streamflow responses are also generally spatially uniform. Run off generation is, however, affected by spatially variable vegetation and soil. The channels rapidly dry on the cessation of rainfall and runoff generation as water is lost along the length of the losing stream. Further, there is no baseflow contribution to streamflow in the Makutapora Basin (figure 5.5). Accordingly, there are no delayed streamflow responses. Streamflow is very directly related to precipitation.

In the middle of February 2007, all river links defined in MIKE 11 were inundated. In the preceding month, the Makutapora Basin experienced anomalously high precipitation of 340 mm. This amount of precipitation was enough to overcome interception, evapotranspiration and detention storage to produce large amounts of run off throughout the basin. Significant inundation of ephemeral streams has been found to be important in the generation of recharge from observations (figure 4.8) and simulations (figure 5.5). Generally, precipitation in Makutapora is at its highest in February and declines in March and April before stopping in May, except rare instances. The 2006 – 2007 wet season followed this pattern. Precipitation in the month preceding March 15th was considerably less, 103 mm. At that time, no surface water flowed out of the basin. Upstream sections of the streams, which drain large, steeply sloping areas of lower permeability (figures 2.2, figure 2.4), are, however, inundated. Due to leakage through the stream channel, the water is lost before it can discharge from the basin. Precipitation in the month preceding April 15th was 42 mm. This was not enough to produce streamflow anywhere within the basin. Following drying of the streambeds in April, no streamflow occurred until the subsequent wet season.

5.4.4 Projected Impact of Climate Change on Groundwater Storage

Projections of groundwater storage changes in the Makutapora Basin under three climate scenarios are generally similar (Figure 5.7). Figure 5.7 shows 'wellfield average' hydraulic head values which represents the daily average of hydraulic heads simulated in all monitoring wells in the Makutapora wellfield. It is clear that recharge varies in time and magnitude between simulations. Accordingly, hydraulic head values at the end of the simulation vary by 1.92 m.

Compared to HB-HB, CCi-HB employed an overall reduction in annual precipitation equivalent to 3%. $P_{>95}$ increased by 30%, and $P_{<70}$ were concomitantly reduced by 52%. Additionally, due to increased temperatures, ET_o increased by 2.7%. Increases in temperature were smaller during the wet season (southern hemisphere summer) than the average of the year. These changes to climatic variables effected the generation of runoff and ephemeral streamflow. Relative to HB-HB, CCi-HB produced 2% more days of ephemeral stream flow. Changes to precipitation amount, distribution, temperate and consequently evapotranspiration, and ephemeral stream flow have resulted in changes to groundwater recharge. Final hydraulic head

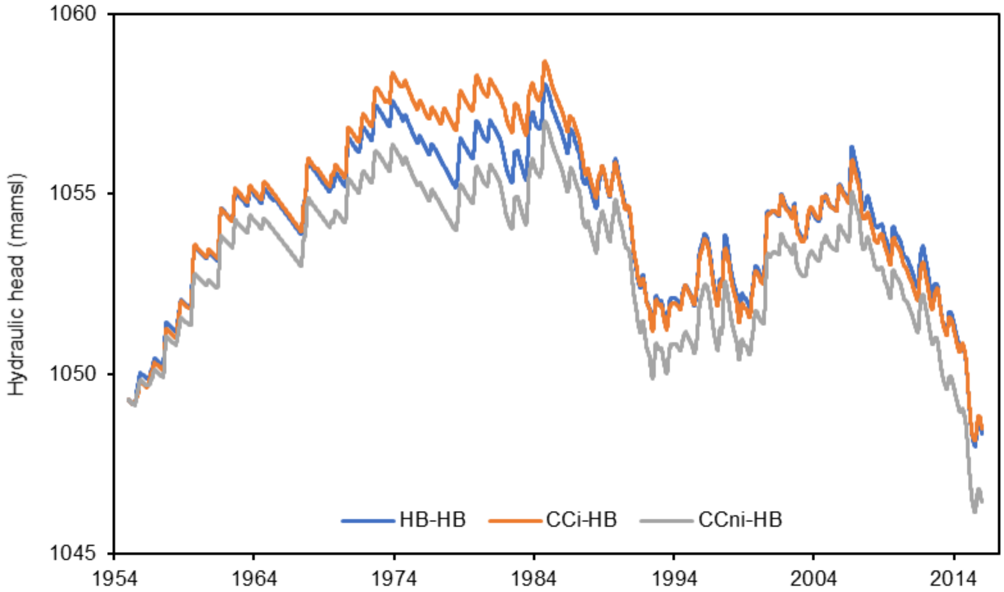

Figure 5.7 Simulated 'wellfield average' hydraulic heads for 3 climate scenarios with historical groundwater abstraction. HB-HB is a historical baseline of climate. CCi-HB is a climate change scenario which incorporates the intensification of precipitation. CCni-HB is a climate change scenario which does not incorporate the intensification of precipitation.

values for the HB-HB and CCi-HB were almost identical, with CCi-HB being 0.13 m greater. This difference was caused by a 1.0% increase in recharge over the duration of the simulation. Despite the similarities, there are, however, differences throughout the record. The 1.0% increase in recharge is clearly not temporally uniform as HB-HB has a greater hydraulic head value for significant parts of the simulation.

The differences between HB-HB and CCni-HB were much greater. Daily precipitation was uniformly reduced by 3%, consistent with a projected decline in mean annual precipitation of 3% and ET_o increased by an average of 2.7% compared to the historical baseline. These changes to atmospheric variables resulted in a reduction of ephemeral stream flow duration by 9.1%. This resulted in significant changes to groundwater recharge and subsequently groundwater storage. The final hydraulic head value associated with CCni-HB was 1.92 m lower than the historical baseline. This was the result of a 9.3% reduction in recharge compared to HB-HB and a 10.1% reduction in recharge relative to CCi-HB. Again, it is clear that changes in recharge are not temporally uniform as the differences in hydraulic heads corresponding to the three climate scenarios do not steadily increase.

5.4.5 Projected Impact of Increased Groundwater Abstraction on Groundwater Resources

Changes to groundwater storage owing to projected changes in groundwater abstraction (HB-IA and HB-CA) were considerable relative to baseline conditions (HB-HB) (Figure 5.8). Increasing abstraction to a rate equivalent to the maximum volume of transmission from the wellfield resulted in a catastrophic reduction in groundwater-levels. In the first year of the simulation, groundwater-levels declined by approximately 13.5 m. Over the duration of the 51-year HB-IA simulation, 425% more groundwater would be abstracted relative to baseline. The simulation, however, was not completed as specified because well drying began to restrict pumpage. The first well to dry out was unable to sustain the specified rate of abstraction less than 6 years into the simulation. While

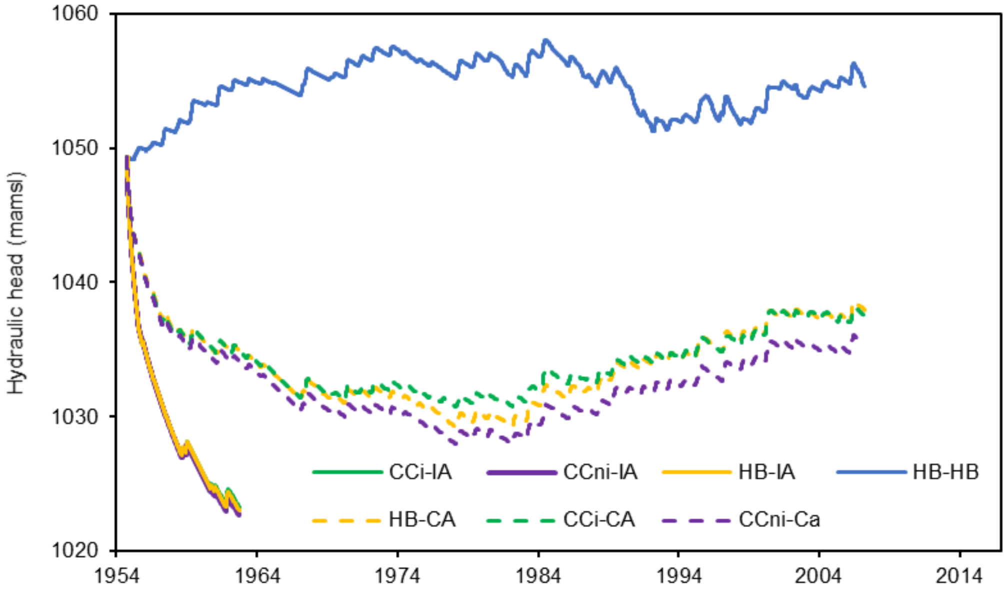

Figure 5.8 Simulated hydraulic heads for 7 simulations. A historical baseline of climate and abstraction (HB-HB) is included for reference. 6 combinations of 3 climate scenarios (HB, CCi, CCni) and 2 abstraction scenarios (IA, CA) are also shown.

the rate of drawdown did start to reduce, suggesting the cone of depression was moving towards equilibrium, the depth of the wells ultimately prevented this from happening. Reductions in groundwater-levels were highly localised to the areas around the active production wells (Figure 5.9).

Constant abstraction at a rate equivalent to average pumping between July 2015 and June 2016 also results in significant declines in groundwater-levels (Figure 5.8). Similar to HB-IA, HB-CA simulated a severe decline early in the record, however, it was not significant enough for wells to dry. Accordingly, the cones of depression which formed were able to move closer to equilibrium and stabilise. Ultimately this allowed groundwater-levels to increase again. ‘Contemporary abstraction’ is equivalent to an increase in 316% relative to the baseline. As a result, groundwater-levels at the termination of the simulation were more than 11 m lower than baseline levels.

5.4.6 Combined Projected Impact of Climate Change and Increased Groundwater Abstraction on Groundwater Resources

It is clear that projected changes to groundwater storage owing to climate change are small compared to the potential changes occurring as a result of increased water demand. Regardless of the climate change scenario specified in the model, increases in groundwater abstraction dwarfed their impact even when abstraction was specified at a contemporary rate. However, the ‘business as usual’ scenario of pumping appears to reach equilibrium approximately 10 m below baseline levels, and subsequently responds to recharge in a similar way.

The severe declines in groundwater levels were shown to be highly localised to the areas surrounding the active pumping wells, and do not actually represent a significant reduction in groundwater storage throughout the basin.

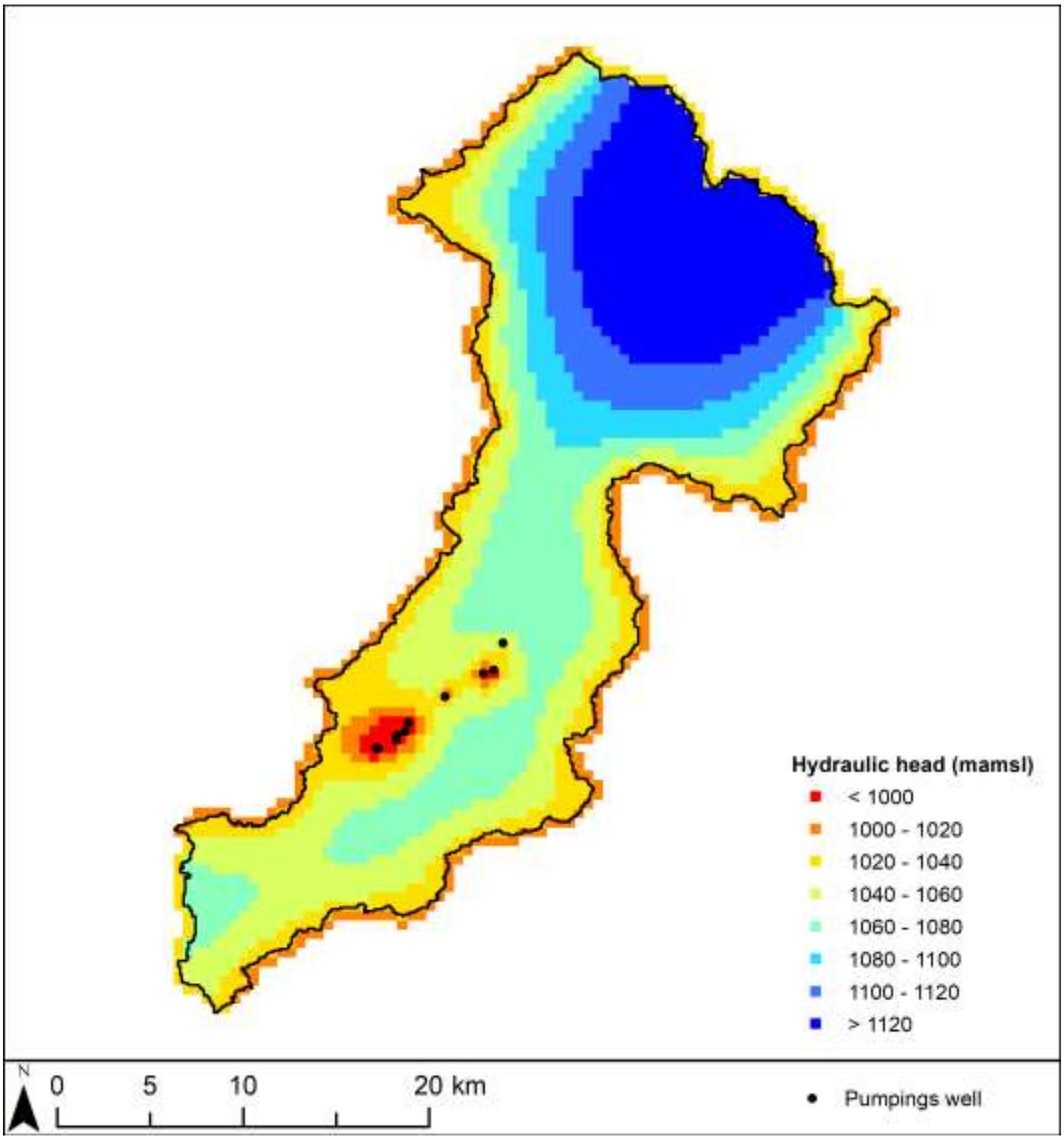

Figure 5.9 Elevation of the potentiometric surface in the Makutapora Basin on 1st July 1962, the point at which abstraction became limited, during HB-IA.

Generally in Africa, non-climatic drivers, such as population growth, urbanization, land use change, and increased irrigation are expected to impact groundwater resources much more than climate change (Calow & MacDonald, 2009; Carter & Parker, 2009; MacDonald et al., 2009; Taylor et al., 2009). The situation in Makutapora aligns with this understanding.

5.5 Discussion

5.5.1 Climate Change Impacts

Simulating groundwater resources in the Makutapora Basin, using a coupled MIKE SHE/MIKE 11 model, highlighted several important findings. Changes to mean annual precipitation were shown to have a disproportional impact on groundwater recharge. A 3% reduction in precipitation in conjunction with a 2.7% increase in ET_o reduced groundwater recharge by 10.1%. Reduced input to the saturated zone resulted in a general lowering of the water table. Reduced recharge resulting from less precipitation is widely expected as groundwater recharge projections are closely related to projected changes in precipitation (Taylor, et al., 2013a). Semi-arid regions of Africa have previously been deemed 'unstable' due to the fine balance of precipitation and evapotranspiration which results in non-linear responses of the terrestrial hydrological system to climate change (De Wit & Stankiewicz, 2006; MacDonald et al., 2009; Taylor et al., 2013a).

The reduction in groundwater recharge resulting from reduced mean annual precipitation and increased evapotranspiration was negated and exceeded by recharge amplified through an increase in precipitation intensity. This indicates that groundwater recharge was simulated to disproportionately derive from more intensive precipitation, as demonstrated in Chapter 3. With the same rate of increased ET_o, groundwater recharge increased 11.3% when the intensification of precipitation was considered. This additionally resulted in more recharge than had been simulated during the baseline period when annual precipitation is greater. The bias of more intensive precipitation disproportionately producing groundwater recharge, shown in Chapter 3, has previously been indicated in hydrometric (Taylor et al., 2013b), stable isotope (Jasechko and Taylor, 2015; Vogel and Van Urk, 1975) and modelling (Eilers et al., 2007) studies in semi-arid areas in Africa. It is worth noting that only precipitation more intensive than the 95^{th} intensity percentile was intensified, not all precipitation. This is due to the data available from CMIP5 model simulations. However, it is also worth noting that precipitation more intensive than the 95^{th} intensity percentile has been observed to strongly influence groundwater recharge in Makutapora (Chapter 3).

5.5.2 Groundwater Abstraction Impacts

Despite an overall increase in groundwater recharge due to climate change, these increases were dwarfed by the impact of projected increases in groundwater abstraction. The onset of high rates of abstraction for which pumping infrastructure is designed, resulted in a catastrophic reduction in groundwater-levels. Historical observations of the saturated zone response to abstraction indicate that this rate of drawdown was not unexpected. Between April and October 2015, pumping in the well field averaged 46113.6 $m^3 \cdot day^{-1}$, 56.6% of the abstraction specified in the simulation, yet the rate of drawdown was greater than 6.5 $m \cdot year^{-1}$. Considering abstraction during that time only represented an increase of 38.8% over the previous year, i.e. significant pumping had already produced a cone of depression around the wells, observing a 13.5 m decline from projected abstraction is consistent with these observations. It is worth noting that the declines observed during simulations of high groundwater abstraction were highly localised and determined by the spatial distribution of active production wells. Clearly the faults in the Makutapora Basin are responsible for the unusually high yielding production wells, but there is also clearly a limit to the volume of water that can sustainably be abstracted from this small area. To increase the sustainability of groundwater abstraction it may be necessary to explore opportunities to drill production wells distant from the faults and compensate for low yields with an increased number of wells.

The way the saturated zone responds to dynamic pumping is a consequence of the assumptions embedded in the model. Contemporary abstraction scenarios showed that the cones of depression move towards equilibrium and allow groundwater levels to stabilise and consequently increase. This, however, is strongly influenced by the boundary conditions imposed on the model.

5.5.3 Projections of Groundwater Resources

The implications regarding these findings are ultimately ambiguous. Clearly, groundwater resources in the Makutapora Basin are sensitive to changes in mean annual precipitation, evapotranspiration and precipitation intensity, however, climate changes are highly uncertain (Niang et al., 2014). Consequently, groundwater resources projections remain uncertain. Ultimately, the amount of groundwater recharge occurring in the Makutapora Basin in the future is no better understood despite an improved understanding of the process and controls on recharge, and a demonstrable ability to simulate those processes accurately.

The intensification of precipitation has already been observed and is projected to continue, at a much higher level of certainty than changes to mean annual precipitation (Allan and Soden, 2008; Niang et al., 2014). Accordingly, groundwater recharge may increase as atmospheric temperature increases, as the increases in recharge from intensification appear to outweigh reductions due to increased evapotranspiration. Furthermore, the relationship between reduced recharge due to increased ET_o and increased recharge due to the intensification of precipitation is not directly proportional as intensification will increase exponentially with global warming (Trenberth, 1999; Trenberth et al., 2003). Importantly, however, the interaction between total precipitation and precipitation distribution remains unclear. In the scenarios simulated here, the impact of intensification effectively nullified the impact of changes to total precipitation.

Ultimately, it appears that groundwater resources in the Makutapora Basin will be most strongly impacted by groundwater abstraction, and not climate change. Infrastructure currently exists in the wellfield which could deplete the wellfield of its resources. Changes resulting from groundwater abstraction render changes due to climate trivial. Groundwater abstraction rates have generally increased for the last 50 years. If this trend continues, which one would expect, there is a serious risk of groundwater depletion. Even if groundwater abstraction does not increase at such a rapid rate, the inevitable reduction in groundwater levels will increase the cost of pumping significantly.

5.5.4 Improving Sustainability

The Tanzanian government is actively looking to supplement/replace Makutapora as the source of water for Dodoma. This research indicates that this is a necessary step. Unless highly effective engineering solutions are devised to artificially enhance recharge within the basin, it appears that the rate of recharge, regardless of climate change, will be insufficient to meet the needs of Dodoma. An MAR solution has previously been implemented in a location highly analogous to Dodoma (Murray et al., 2018). Windhoek, the capital city of Namibia, experiences a 'hot semi-arid' climate. Dodoma's population is slightly larger, with both cities rapidly growing. Like Dodoma, Windhoek relies on a fractured crystalline aquifer, the Windhoek aquifer, as there are no proximate, perennial rivers. Presently, groundwater abstraction for Windhoek is 27 $Mm^3 \cdot year^{-1}$, while it is 17 $Mm^3 \cdot year^{-1}$ in Dodoma. Due to these high rates of abstraction, from the onset of large-scale pumping in the 1950s, to the early 1990s, groundwater-levels declined 40 m. Windhoek undertook the first major MAR scheme in the world in a fractured, crystalline aquifer. In 2006, six injection wells were constructed with a combined recharge capacity of 10,000 $m^3 \cdot day^{-1}$. Injections of water continued until the tapped aquifer could no longer accommodate additional water. Groundwater-levels returned close to their elevation prior to pumping. The success of the initial MAR phase has led to the scheme being extended with the drilling of additional injection wells in other parts of the aquifer (Murray et al., 2018). This will increase total injection capacity to 26,000 $m^3 \cdot day^{-1}$. The example set in Namibia illustrates that large-scale MAR projects are possible in semi-arid regions underlain by fractured crystalline aquifers. The water security of Windhoek has been greatly improved by this scheme, and it appears that Dodoma could benefit from a similar approach. Windhoek chose MAR over a large water transfer project as it was more cost effective (Murray et al., 2018). Comprehensive viability assessments would need to be undertaken to determine the most appropriate solution for Dodoma.

5.5.5 Model discussion

The coupled MIKE SHE/MIKE 11 hydrological model of the Makutapora Basin incorporated findings from Chapters 3 and 4. From empirical observations, groundwater recharge in the Makutapora Basin was found to disproportionately derive from more intensive precipitation (Chapter 3). This behaviour was simulated by the model. Accounting for the intensification of precipitation resulted in a significant increase in groundwater recharge. Moreover, analysis in Chapter 4 highlighted the importance of ephemeral streamflow on the magnitude of groundwater recharge. Simulated durations of stream flow showed good concurrence with the amount of recharge, indicating the implementation of streambed leakage was appropriate. Additionally, the non-linear response to a reduction in mean annual precipitation aligns with historical observations of precipitation and groundwater recharge whereby the two are non-linearly related (Taylor et al., 2013b). Accurate replication of known behaviours allowed important questions to be addressed which, so far, have not been answered by empirical analysis. The model facilitated an assessment of the relative magnitudes of recharge increases owing to the intensification of precipitation and the presumed reduction in recharge owing to increased evapotranspiration. Furthermore, the relative impacts of climate change and increased abstraction were assessed.

The model performed satisfactorily based on performance metrics, and in the replication of expected behaviour in simulations of climate change scenarios. It remains, however, a simplistic representation of the Makutapora Basin. Within the model, many parameters do not vary in space or time, when they do in reality. For example, LAI was specified to vary periodically over 12 months, yet it would presumably vary closely with prevailing climatic conditions in any given year, which would consequently affect rates of evapotranspiration and recharge. Given the importance of land use on groundwater recharge (Leblanc et al., 2008), dynamic vegetation would be an important potential improvement to the model. Simulations would benefit from the inclusion of dynamic vegetation and two-way coupling between vegetation and the water cycle as both critically impact soil water balance, deep drainage and recharge (Foley et al., 2000). Furthermore, the model does not account for the effect of the physiological forcing of CO_2. Under higher atmospheric CO_2 concentrations, terrestrial plants open their stomata less, which is projected to reduce evapotranspiration and increase continental runoff (Cao et al., 2010). This is particularly pertinent in Makutapora as runoff has been observed to strongly influence groundwater recharge (Chapter 4). The implementation of the effects of the physiological forcing would be an additional improvement.

5.6 Conclusion

Water resources in the Makutapora Basin are very sensitive to climate change. Disproportionate responses were observed to a decrease in mean annual precipitation and an increase in evapotranspiration. These changes were, however, negated and exceeded by concomitant changes in precipitation intensity. All of these changes were immaterial in the context of feasible increases in groundwater abstraction. Future rates of groundwater abstraction are unknown, and the scenarios imposed in the model represent a huge increase relative to baseline conditions. These increases dwarf the changes to the climate, so it is maybe unsurprising that the impacts of increase abstraction dwarf the impacts of climate change.

A coupled MIKE SHE/MIKE 11 model demonstrated efficacy in replicating empirically observed phenomenon, i.e. increased recharge from increased precipitation intensity (Chapter 3) and good concurrence between the duration of stream flow and groundwater recharge magnitude (Chapter 4). This facilitated an assessment of the impact of changes in mean annual precipitation and increased evapotranspiration on groundwater recharge.

The findings indicate that the water demand of Dodoma could become unsustainable. Groundwater abstraction, at a rate which current infrastructure in the basin is designed to transmit, will result in a catastrophic reduction in groundwater-levels and well drying. Moreover, abstraction at ‘contemporary’ rates also resulted in significant reductions in groundwater storage. Accordingly, the Tanzanian government should seek to enhance groundwater recharge in the Makutapora Basin artificially or look to replace or supplement the current water source for Dodoma.

Chapter 6

Conclusions and Future Directions

6.1 Conclusions

This thesis aims to lessen a key knowledge gap explicitly highlighted by the IPCC in its most recent assessment report. The improved understanding of groundwater recharge controls and processes detailed here is locally important and is, in some instances, more widely applicable. Discrete sections of this thesis develop a cohesive narrative given their interrelatedness and progressive nature. The semi-arid setting of the research was chosen as these areas are considered 'unstable' in relation to the potential effects of climate change on water resources. First, the best observed hydrological consequence of climate change, the intensification of precipitation, was explored with regards to its impact of groundwater recharge. The analysis comprised an empirical assessment of how groundwater recharge has been affected by precipitation intensity. Second, the processes which translate changes in precipitation distribution into changes in renewable groundwater resources were explored through highly detailed monitoring of the passage of meteoric water to the saturated zone. This research facilitated a better understanding of how and why groundwater has and will respond to climate change and variability. Finally, the knowledge garnered from empirical studies was synthesised in a hydrological model to project the impact of climate change on groundwater resources. An improved understanding of how and why climate change impacts groundwater resources allowed for a significantly more comprehensive assessment of future groundwater resources than was possible previously. Understanding of the processes and relationships detailed here has relevance for other tropical semi-arid regions.

6.1.1 Groundwater Recharge and Precipitation Intensity

Groundwater recharge in the Makutapora Basin is disproportionately generated by statistically extreme daily to seasonal precipitation.

A bias in the generation of groundwater recharge to more intensive precipitation is observed via hydrometric and stable-isotope analyses. Intensity over two-time scales is shown to be important and includes discrete days of high intensity precipitation (>95th percentile), and prolonged intensity over 9-day periods exceeding the 80th percentile. The observed dependence on episodic, extreme seasonal precipitation is less striking in this reanalysis than had previously been determined (Taylor et al., 2013b); fewer wet seasons are associated with zero groundwater recharge. Accordingly, the water resources of the Makutapora Basin, are maintained by infrequent, large recharge events, and also by more frequent, small events. As the intensification of precipitation is a widely and confidently projected impact of climate change, the results suggest groundwater recharge may increase as a result of this change to the hydrological cycle. Locally, this has potentially important implications for Dodoma, which is currently assessing options to supplement or replace the Makutapora Basin as its source of water.

6.1.2 Estimating Groundwater Recharge in a Pumped System

Transience in groundwater-level recessions associated with pumping are successfully represented by a numerical model.

A common limitation of the computation of recharge using the WTF is a simplified, often steady state, representation of groundwater-level declines, which limits the use of the WTF in pumped systems. A method of estimating groundwater recharge which accounts for the effects of variable groundwater abstraction improved the justifiability of groundwater recharge estimation in pumped systems. The model developed in MIKE SHE demonstrated ‘very good‘ performance in replicating groundwater-level declines under natural and variable pumping conditions. In addition to the event-based approach used to estimate seasonal groundwater recharge, the modified WTF method was used to produce a time series of groundwater recharge in piezometers throughout the wellfield to determine the heterogeneity of recharge to assess recharge pathways.

6.1.3 Recharge Pathways

The predominant recharge pathway in the Makutapora Basin is leakage from ephemeral streambeds.

Recharge mechanisms in the Makutapora Basin were delineated using three discrete methods of analysis: high-resolution groundwater-level fluctuation monitoring, stable-isotope tracers, and long-term surface water monitoring. High-resolution groundwater-level observation facilitated the observation of the formation and decay of groundwater mounds beneath inundated ephemeral streambeds. A strong linear relationship between the duration of streambed inundation and groundwater recharge magnitude was found in long-term records of surface water and groundwater dynamics. The stable-isotope composition of ephemeral stream flow was not distinct from average groundwater found in the Makutapora Basin. Focused recharge, emanating from leakage from ephemeral streambeds, was universally indicated by these discrete analyses, which provides good evidence that it is the source of groundwater.

6.1.4 Climate Change impacts on Groundwater resources

Increased precipitation intensity negates the impacts on groundwater recharge of declining annual precipitation and rising temperatures based on ensemble mean climate change projections.

Projected groundwater recharge in the Makutapora Basin reduced disproportionately in response to reduced mean annual precipitation and increased evapotranspiration. A projected 3% reduction in mean annual precipitation and a projected 2.7% increase in evapotranspiration resulted in a projected reduction of 10.1% in groundwater recharge. The impact of these factors, however, was outpaced by the impact of increases in recharge owing to the intensification of precipitation. Using a simplified intensification procedure, the projected increase of 30% in precipitation above the

95th percentile increases annual groundwater recharge by over 10%. Climate projections from an ensemble mean of over 30 CMIP5 GCMs under RCP 8.5, indicate that the net impact of all three of these projected impacts will be small, equivalent to a 1% increase in groundwater recharge.

6.1.5 Groundwater Abstraction Impacts on Groundwater resources

The impact of projected increases in groundwater withdrawals on groundwater storage greatly outweigh the projected impacts of climate change.

Groundwater abstraction at the limit of recently upgraded infrastructure is unsustainable. Projected groundwater levels suffer a catastrophic decline, which results in well drying due to increased abstraction. Similarly, a 'business as usual' abstraction scenario also results in significant groundwater level declines. The impact of increased groundwater abstraction outweighs the changes resulting from climate change. Dodoma should assess the viability of artificially enhancing groundwater recharge in the Makutapora Basin if it is not replaced as the source of Dodoma's water supply.

6.2 Future Directions

6.2.1 Improved Monitoring of Makutapora Basin

It is clear that the water resources of Makutapora are at the mercy of Dodoma's water demand. To ensure the groundwater resources are optimally and sustainably exploited, groundwater-levels and abstraction rates need to be monitored closely. Such scrutiny will also aid in the assessment and forewarning of the need to supplement/replace the Makutapora wellfield. Improved monitoring within the basin will also assist in improving our understanding of recharge dynamics and wellfield storage responses to pumping. More detailed records of groundwater-levels, abstractions, and precipitation would facilitate improved analyses. Part of the high-resolution monitoring array has been retrofitted with telemetry equipment, facilitating the availability of real-time groundwater-level data for the Ministry of Water and Irrigation, so that water management decisions can be made instantly. Additional monitoring of other ephemeral streamflow would allow greater certainty regarding the viability of MAR solutions. Furthermore, additional collection of water samples for isotopes analysis would allow for a much more comprehensive analysis of basin-scale processes.

6.2.2 Assess the Pervasiveness of Findings in Semi-Arid Sub-Saharan Africa

The semi-arid regions of sub-Saharan Africa are considered to have particularly vulnerable water resources. The findings presented here have important implications for these areas. Yet it is necessary to assess the ubiquity of these results. Two keys findings regarding direct climate change impacts on groundwater resources are (1) increased precipitation intensity will increase groundwater recharge and (2) leakage from ephemeral streambeds is the primary pathway by which recharge occurs. Before cogent large-scale assessments of climate change impacts on groundwater resources can be conducted, it is vital to determine the prevalence of these findings.

Makutapora acts as an appropriate analogue for large portions of sub-Saharan Africa due to its climate, geology and water use. Accordingly, the methods used and developed here should be widely applicable. 21% of sub-Saharan Africa experience semi-arid climates like Makutapora (figure 2.1). A continental scale study in Africa suggests that the non-linearity of the relationship between groundwater recharge and precipitation found in Makutapora exists in many dryland areas (Cuthbert et al., 2019). Focused recharge pathways, the mechanism from which the non-linearity is thought to arise, are also prevalent in many dryland areas and would therefore be suitable areas for the implementation of similar methods to observe and analyse leakage from ephemeral streambeds. More than 40% of Africa is underlain by fractured crystalline aquifers, which facilitates translation of the methods used in Makutapora to similar studies elsewhere. The water balance of the Makutapora wellfield is influenced by groundwater abstraction and novel techniques were developed to facilitate cogent research in an actively pumped system. By definition, many of the most important aquifer systems globally are actively pumped, and many cities in sub-Saharan Africa are reliant on groundwater abstraction. The methodology applied here is suitable for many of these locations. Specifically, the techniques applied here, for a pumped system, are particularly relevant to the Limpopo Basin where semi-arid, weathered “basement” crystalline rocks occur and will increasingly be important as development of groundwater in semi-arid Sub-Saharan Africa progresses in the coming decades.

6.2.3 Assess the Processes Which Govern Runoff Generation

An obvious next step, which was not addressed in this thesis would be to finely assess the conditions and processes which govern the generation of runoff and consequently streamflow. A synthesis of the results of Chapters 3 and 4 would imply that precipitation intensity plays a key role in generating run off; understanding of existing thresholds are poor and warrant further study. Accurate projection of future groundwater recharge requires a comprehensive understanding of the processes and climate conditions which produce recharge. Additionally, an assessment of streambed infiltration capacities would significantly aid model accuracy and viability assessments of MAR solutions.

6.2.4 Assessment of MAR

The balance of projected impacts of climate change and groundwater abstraction indicates that groundwater use in the Makutapora Basin may become unsustainable. Maximum sustainable yield could be artificially increased by the implementation of engineering solutions. Windhoek, a highly analogous situation to Dodoma, has successfully implemented a managed aquifer recharge scheme. While there would need to be a viability assessment of different solutions, Makutapora could consider closely the example set in Namibia. Indeed, successfully implemented MAR scheme may obviate the need to replace/supplement the Makutapora water supply.

References

Abbott, M.B., Bathurst, J.C., Cunge, J.A., O'Connell, P.E., Rasmussen, J., 1986a. An introduction to the European Hydrological System — Systeme Hydrologique Europeen, "SHE", 1: History and philosophy of a physically-based, distributed modelling system. J. Hydrol. 87, 45–59. https://doi.org/10.1016/0022-1694(86)90114-9

Abbott, M.B., Bathurst, J.C., Cunge, J.A., O'Connell, P.E., Rasmussen, J., 1986b. An introduction to the European Hydrological System — Systeme Hydrologique Europeen, "SHE", 2: Structure of a physically-based, distributed modelling system. J. Hydrol. 87, 61–77. https://doi.org/10.1016/0022-1694(86)90115-0

Adelana, S.M.A., Abiye, T.A., Nkhuwa, D.C.W., Tindimugaya, C., Oga, M.S., 2008. Urban groundwater management and protection in Sub-Saharan Africa, in: Applied Groundwater Studies in Africa, IAH Selected Papers on Hydrogeology. CRC Press, pp. 1–7.

Allan, R.P., Soden, B.J., 2008. Atmospheric warming and the amplification of precipitation extremes. Science 321, 1481–1484. https://doi.org/10.1126/science.1160787

Allen, R.G., Pereira, L.S., Raes, D., Smith, M., 1998. Crop evapotranspiration-Guidelines for computing crop water requirements, in: FAO Irrigation and Drainage Paper 56.

Alley, W.M., 2009. Ground Water, in: Likens, G.E. (Ed.), Encyclopedia of Inland Waters. Academic Press, Oxford, pp. 684–690.

Arino, O., Ramos, J., Kalogirou, V., Defourny, P., Van Bogaert, E., 2012. Global Land Cover Map for 2009 (GlobCover 2009 ver. 2.3 released on 21st December 2010). © Eur. Space Agency ESA Univ. Cathol. Louvain UCL. https://doi.org/10.1594/PANGAEA.787668

Arnell, N.W., Canziani, O.F., Leary, N.A., Dokken, D.J., White, K.S., 2001. Hydrology and Water Resources, in: McCarthy, J.J. (Ed.), Climate Change 2001: Impacts, Adaptation, and Vulnerability: Contribution of Working Group II to the Third Assessment Report of the Intergovernmental Panel on Climate Change. Cambridge University Press.

Azariadis, C., Stachurski, J., 2005. Poverty traps, in: Handbook of Economic Growth. Elsevier, pp. 295–384. https://doi.org/10.1016/S1574-0684(05)01005-1

Banerjee, S., Skilling, H., Foster, V., Briceño-Garmendia, C., Morella, E., Chfadi, T., 2008. Africa-Ebbing water, surging deficits: urban water supply in sub-Saharan Africa (The World Bank No. 12), Africa infrastructure country diagnostic (AICD) background paper.

Bates, B., 2009. Climate Change and Water: IPCC technical paper VI. World Health Organization.

Batisani, N., 2011. Spatio-temporal ephemeral streamflow as influenced by climate variability in Botswana. J. Geogr. Sci. 21, 417–428. https://doi.org/10.1007/s11442-011-0854-5

Batisani, N., Yarnal, B., 2010. Rainfall variability and trends in semi-arid Botswana: Implications for climate change adaptation policy. Appl. Geogr., Climate Change and Applied Geography – Place, Policy, and Practice 30, 483–489. https://doi.org/10.1016/j.apgeog.2009.10.007

Becker, E., 2016a. May 2016 El Niño/La Niña update: Switcheroo! | NOAA Climate.gov [WWW Document]. URL https://www.climate.gov/news-features/blogs/enso/may-2016-el-ni%C3%B1ola-ni%C3%B1a-update-switcheroo (accessed 7.18.18).

Becker, E., 2016b. February 2016 El Niño update: Q & A…and some Thursday-morning quarterbacking [WWW Document]. URL https://www.climate.gov/news-features/blogs/enso/may-2016-el-ni%C3%B1ola-ni%C3%B1a-update-switcheroo (accessed 7.18.18).

Beegle, K., Christiaensen, L., Dabalen, A., Gaddis, I., 2016. Poverty in a rising Africa. The World Bank.

Berti, A., Tardivo, G., Chiaudani, A., Rech, F., Borin, M., 2014. Assessing reference evapotranspiration by the Hargreaves method in north-eastern Italy. Agric. Water Manag. 140, 20–25. https://doi.org/10.1016/j.agwat.2014.03.015

Beven, K., Germann, P., 2013. Macropores and water flow in soils revisited. Water Resour. Res. 49, 3071–3092. https://doi.org/10.1002/wrcr.20156

Bureau, D., Strobl, E., 2016. Conférence “Water Scarcity in Africa: Issues and Challenges” | GIS Climat Environnement Société [WWW Document]. URL https://web.archive.org/web/20160401234042/http://www.gisclimat.fr/manifestation-scientifique/conf%C3%A9rence-%E2%80%9Cwater-scarcity-africa-issues-and-challenges%E2%80%9D (accessed 8.9.18).
Callaci, E., 2016. ‘Chief village in a nation of villages’: history, race and authority in Tanzania’s Dodoma plan. Urban Hist. 43, 96–116. https://doi.org/10.1017/S0963926814000753
Calow, R., MacDonald, A.M., Nicol, A.L., Robins, N.S., 2010. Ground water security and drought in Africa: linking availability, access, and demand. Ground Water 48, 246–256. https://doi.org/10.1111/j.1745-6584.2009.00558.x
Cao, L., Bala, G., Caldeira, K., Nemani, R., Ban-Weiss, G., 2010. Importance of carbon dioxide physiological forcing to future climate change. Proc. Natl. Acad. Sci. https://doi.org/10.1073/pnas.0913000107
Carter, R., Baguma, A., Bizoza, A., Cavill, S., Foster, S., Foster, T., Jobbins, G., Hope, R., Katuva, J., Koehler, J., 2017. Groundwater and poverty in sub Saharan Africa a short investigation highlighting outstanding knowledge gaps. UPGro Work. Pap.
Carter, R., Parker, A., 2009. Climate change, population trends and groundwater in Africa. Hydrol. Sci. J. 54, 676–689. https://doi.org/10.1623/hysj.54.4.676
CIA, W., 2016. World Factbook. CIA Facts File Bangladesh, South Asia.
Cohen, J., Cohen, P., West, S.G., Aiken, L.S., 2013. Applied Multiple Regression/Correlation Analysis for the Behavioral Sciences. Routledge.
Construction Review Online, A., 2017. Duwasa sets aside $450,000 to Boost Dodoma Water Supply. Constr. Rev. Online. URL https://constructionreviewonline.com/2017/08/duwasa-sets-aside-450000-boost-dodoma-water-supply/ (accessed 11.27.17).
Conway, D., Persechino, A., Ardoin-Bardin, S., Hamandawana, H., Dieulin, C., Mahé, G., 2009. Rainfall and Water Resources Variability in Sub-Saharan Africa during the Twentieth Century. J. Hydrometeorol. 10, 41–59. https://doi.org/10.1175/2008JHM1004.1
Craig, H., 1961. Isotopic Variations in Meteoric Waters. Science 133, 1702–1703. https://doi.org/10.1126/science.133.3465.1702
Cuthbert, M., Acworth, R.I., Andersen, M.S., Larsen, J.R., McCallum, A.M., Rau, G.C., Tellam, J.H., 2016. Understanding and quantifying focused, indirect groundwater recharge from ephemeral streams using water table fluctuations. Water Resour. Res. 52, 827–840. https://doi.org/10.1002/2015WR017503
Cuthbert, M., Mackay, R., Nimmo, J.R., 2013. Linking soil moisture balance and source-responsive models to estimate diffuse and preferential components of groundwater recharge. Hydrol Earth Syst Sci 17, 1003–1019. https://doi.org/10.5194/hess-17-1003-2013
Cuthbert, M., Taylor, R., Favereau, G., Todd, M., Shamsudduha, M., Villholth, K.G., MacDonald, A., Scanlon, B., Kotchoni, V., Vouillamoz, J.M., Lawson, F.M.A., Adjomay, P.A., Kashaigili, J., Seddon, D., Sorensen, J.P.R., Ebrahim, G.Y., Owor, M., Nyenj, P., Nazoumou, Y., Goni, I., Ousmane, B.I., Sibanda, T., Ascott, M., Macdonald, D., Agyekum, W., Koussoubé, Y., Wanke, H., Kim, H., Wada, Y., Lo, M.-H., Oki, T., Kukuric, N., 2019. Observed controls on resilience of groundwater to climate variability in sub-Saharan Africa. Nature.
Daily News, 2017a. Mega projects to end water woes [WWW Document]. URL http://dailynews.co.tz/index.php/home-news/50496-mega-projects-to-end-water-woes (accessed 4.7.18).
Daily News, 2017b. Dam set to increase Dodoma water availability [WWW Document]. URL http://www.dailynews.co.tz/index.php/home-news/54024-dam-set-to-increase-dodoma-water-availability (accessed 11.27.17).
Daily News, 2017c. Tap Lake Victoria water, Dodoma told [WWW Document]. URL https://dailynews.co.tz/index.php/home-news/55064-tap-lake-victoria-water-dodoma-told (accessed 4.7.18).
Dansgaard, W., 1964. Stable isotopes in precipitation. Tellus 16, 436–468. https://doi.org/10.1111/j.2153-3490.1964.tb00181.x
De Pauw, E.F., Magoggo, J.P., Niemeyer, W., 1983. Soil survey report of Dodoma Capital City district. Natl. Soil Serv. Tanzan. Rep. I 2.
De Wit, M., Stankiewicz, J., 2006. Changes in surface water supply across Africa with predicted climate change. Science 311, 1917–1921. https://doi.org/10.1126/science.1119929
Delin, G.N., Healy, R.W., Lorenz, D.L., Nimmo, J.R., 2007. Comparison of local- to regional-scale estimates of ground-water recharge in Minnesota, USA. J. Hydrol. 334, 231–249. https://doi.org/10.1016/j.jhydrol.2006.10.010

Dillon, P.J., Pavelic, P., Page, D., Beringen, H., Ward, J., 2009. Managed aquifer recharge. National Water Commission.
Döll, P., Fiedler, K., 2008. Global-scale modeling of groundwater recharge. Hydrol Earth Syst Sci 12, 863–885. https://doi.org/10.5194/hess-12-863-2008
DUWASA, 2017. Needs, Production and Water Supply [WWW Document]. URL http://www.duwasa.go.tz/pages/supply-of-clean-water (accessed 10.16.17).
DUWASA, 2015. Dodoma Urban Water Supply and Sewerage Authority [WWW Document]. URL www.duwasa.or.tz/about (accessed 8.4.18).
Easterling, D.R., Meehl, G.A., Parmesan, C., Changnon, S.A., Karl, T.R., Mearns, L.O., 2000. Climate Extremes: Observations, Modeling, and Impacts. Science 289, 2068–2074. https://doi.org/10.1126/science.289.5487.2068
ECA, 2006. Water in Africa: Management Options to Enhance Survival and Growth. Water Afr. Manag. Options Enhance Surviv. Growth 27.
Eilers, V.H.M., Carter, R.C., Rushton, K.R., 2007. A single layer soil water balance model for estimating deep drainage (potential recharge): An application to cropped land in semi-arid North-east Nigeria. Geoderma 140, 119–131. https://doi.org/10.1016/j.geoderma.2007.03.011
Falkenmark, M., Lundqvist, J., Widstrand, C., 1989. Macro-scale water scarcity requires micro-scale approaches. Nat. Resour. Forum 13, 258–267. https://doi.org/10.1111/j.1477-8947.1989.tb00348.x
FAO, 2018a. AQUASTAT database [WWW Document]. URL http://www.fao.org/nr/water/aquastat/data/query/index.html (accessed 8.12.18).
FAO, 2018b. AQUASTAT - FAO’s Information System on Water and Agriculture [WWW Document]. URL http://www.fao.org/nr/water/aquastat/didyouknow/index.stm (accessed 8.12.18).
FAO, 2015. The State of Food Insecurity in the World 2015: Meeting the 2015 international hunger targets: taking stock of uneven progress. FAO.
FAO, 2009. Water at a Glance. Relatsh. Water Agric. Food Secur. Poverty 8.
Favreau, G., Cappelaere, B., Massuel, S., Leblanc, M., Boucher, M., Boulain, N., Leduc, C., 2009. Land clearing, climate variability, and water resources increase in semiarid southwest Niger: A review. Water Resour. Res. 45. https://doi.org/10.1029/2007WR006785
Fawley, A., 1955. Geology and Underground Water Resources of the Makutupora Depression. Rec. Geol. Surv. Tanganyika, Engineering Geology 5.
Fawley, A.P., 1958. Evaporation rate at Dodoma, Tanganyika. Rec Geol Surv Tanganyika.
Feyen, L., Vázquez, R., Christiaens, K., Sels, O., Feyen, J., 2000. Application of a distributed physically-based hydrological model to a medium size catchment. Hydrol Earth Syst Sci 4, 47–63. https://doi.org/10.5194/hess-4-47-2000
Fischer, E.M., Knutti, R., 2016. Observed heavy precipitation increase confirms theory and early models. Nat. Clim. Change 6, 986–991. https://doi.org/10.1038/nclimate3110
Foley, J.A., Levis, S., Costa, M.H., Cramer, W., Pollard, D., 2000. Incorporating Dynamic Vegetation Cover Within Global Climate Models. Ecol. Appl. 10, 1620–1632. https://doi.org/10.1890/1051-0761(2000)010[1620:IDVCWG]2.0.CO;2
Foster, S., 1998. Groundwater recharge and pollution vulnerability of British aquifers: a critical overview. Geol. Soc. Lond. Spec. Publ. 130, 7–22. https://doi.org/10.1144/GSL.SP.1998.130.01.02
Foster, S., Loucks, D.P., 2006. Non-renewable groundwater resources: A guidebook on Socially-sustainable Management for Water-policy Makers. Unesco.
Foxx, T.S., Tierney, G.D., Williams, J.M., 1984. Rooting depths of plants relative to biological and environmental factors. Los Alamos National Lab., NM (USA).
Fricke, H.C., O’Neil, J.R., 1999. The correlation between 18O/16O ratios of meteoric water and surface temperature: its use in investigating terrestrial climate change over geologic time. Earth Planet. Sci. Lett. 170, 181–196. https://doi.org/10.1016/S0012-821X(99)00105-3
Gan, T.Y., Dlamini, E.M., Biftu, G.F., 1997. Effects of model complexity and structure, data quality, and objective functions on hydrologic modeling. J. Hydrol. 192, 81–103. https://doi.org/10.1016/S0022-1694(96)03114-9
Gat, J.R., 1971. Comments on the stable isotope method in regional groundwater investigations. Water Resour. Res. 7, 980–993. https://doi.org/10.1029/WR007i004p00980
Gat, J.R., Mook, W.G., Meijer, H.A., 2001. Environmental isotopes in the hydrological cycle. International Atomic Energy Agency and United Nations Educational, Scientific and Cultural Organization.
Gates, J.B., Edmunds, W.M., Ma, J., Scanlon, B.R., 2008. Estimating groundwater recharge in a cold desert environment in northern China using chloride. Hydrogeol. J. 16, 893–910. https://doi.org/10.1007/s10040-007-0264-z

Gautam, M., 2006. Managing drought in sub-Saharan Africa: Policy perspectives. Invit. Pap. Prep. Present. Int. Assoc. Agric. Econ. Gold Coast Aust.
Giordano, M., 2009. Global Groundwater? Issues and Solutions. Annu. Rev. Environ. Resour. 34, 153–178. https://doi.org/10.1146/annurev.environ.030308.100251
Gleick, P.H., 1989. Climate change, hydrology, and water resources. Rev. Geophys. 27, 329–344. https://doi.org/10.1029/RG027i003p00329
Gonfiantini, R., 1986. Environmental isotopes in lake studies. Handb. Environ. Isot. Geochem. Terr. Environ. 113–168. https://doi.org/10.1016/B978-0-444-42225-5.50008-5
Gonfiantini, R., Roche, M.-A., Olivry, J.-C., Fontes, J.-C., Zuppi, G.M., 2001. The altitude effect on the isotopic composition of tropical rains. Chem. Geol. 181, 147–167. https://doi.org/10.1016/S0009-2541(01)00279-0
Graham, D.N., Butts, M.B., 2005. Flexible, integrated watershed modelling with MIKE SHE. Watershed Models 849336090, 245–272. https://doi.org/10.1201/9781420037432.ch10
Grey, D., Sadoff, C.W., 2007. Sink or swim? Water security for growth and development. Water Policy 9, 545. https://doi.org/10.2166/wp.2007.021
Groisman, P.Y., Knight, R.W., Easterling, D.R., Karl, T.R., Hegerl, G.C., Razuvaev, V.N., 2005. Trends in Intense Precipitation in the Climate Record. J. Clim. 18, 1326–1350. https://doi.org/10.1175/JCLI3339.1
Grönwall, J., 2016. Self-supply and accountability: to govern or not to govern groundwater for the (peri-) urban poor in Accra, Ghana. Environ. Earth Sci. 75, 1163. https://doi.org/10.1007/s12665-016-5978-6
GST, 1955. Geological Survey of Tanganyika., Geological Survey of Tanganyika., Tanzania., Bundesanstalt für Bodenforschung., & V.O. Technoexport. (1953). [Geological map of Tanganyika, scale 1:125,000]: Quarter degree sheet. Dodoma, Tanzania: Mineral Resources Division. [WWW Document].
Hargreaves, G.H., Samani, Z.A., 1982. Estimating potential evapotranspiration. J. Irrig. Drain. Div. 108, 225–230.
Hassan, R., 2005. Ecosystems and Human Well-Being: Current State and Trends: Findings of the Condition and Trends Working Group. Island Press.
Havnø, K., Madsen, M.N., Dørge, J., 1995. MIKE 11–a generalized river modelling package. Comput. Models Watershed Hydrol. 733–782.
Hayashi, M., Chiba, H., 1994. Identification of groundwater components by CI- and stable isotope signatures: a case study in a semi-arid basin in Tanzania. Jap Groundw. Hydrol. 36, 259–275.
Hayuma, A.M., 1980. Dodoma: The planning and building of the new capital city of Tanzania. Habitat Int. 5, 653–680. https://doi.org/10.1016/0197-3975(80)90007-7
Healy, R.W., 2010. Estimating Groundwater Recharge. Cambridge University Press.
Healy, R.W., Cook, P.G., 2002. Using groundwater levels to estimate recharge. Hydrogeol. J. 10, 91–109. https://doi.org/10.1007/s10040-001-0178-0
Heath, R.C., 1983. Basic ground-water hydrology. US Geological Survey.
Hegerl, G.C., Black, E., Allan, R.P., Ingram, W.J., Polson, D., Trenberth, K.E., Chadwick, R.S., Arkin, P.A., Sarojini, B.B., Becker, A., Dai, A., Durack, P.J., Easterling, D., Fowler, H.J., Kendon, E.J., Huffman, G.J., Liu, C., Marsh, R., New, M., Osborn, T.J., Skliris, N., Stott, P.A., Vidale, P.-L., Wijffels, S.E., Wilcox, L.J., Willett, K.M., Zhang, X., 2015. Challenges in Quantifying Changes in the Global Water Cycle. Bull. Am. Meteorol. Soc. 96, 1097–1115. https://doi.org/10.1175/BAMS-D-13-00212.1
Holman, I.P., Tascone, D., Hess, T.M., 2009. A comparison of stochastic and deterministic downscaling methods for modelling potential groundwater recharge under climate change in East Anglia, UK: implications for groundwater resource management. Hydrogeol. J. 17, 1629–1641. https://doi.org/10.1007/s10040-009-0457-8
Houghton, J.T., Ding, Y., Griggs, D.J., Noguer, M., Linden, P.J. van der, Dai, X., Maskell, K., Johnson, C.A. (Eds.), 2001. Climate Change 2001: The Scientific Basis: Contribution of Working Group I to the Third Assessment Report of the Intergovernmental Panel on Climate Change. Cambridge University Press, Cambridge ; New York.
Houze, R.A., Cheng, C.-P., 1977. Radar characteristics of tropical convection observed during GATE: Mean properties and trends over the summer season. Mon. Weather Rev. 105, 964–980. https://doi.org/10.1175/1520-0493(1977)105<0964:RCOTCO>2.0.CO;2
Hunter, P.R., MacDonald, A.M., Carter, R.C., 2010. Water Supply and Health. PLoS Med 7, e1000361. https://doi.org/10.1371/journal.pmed.1000361
Huntington, T.G., Richardson, A.D., McGuire, K.J., Hayhoe, K., 2009. Climate and hydrological changes in the northeastern United States: recent trends and implications for forested and aquatic ecosystemsThis article is one of a selection of papers from NE Forests 2100:

A Synthesis of Climate Change Impacts on Forests of the Northeastern US and Eastern Canada. Can. J. For. Res. 39, 199–212. https://doi.org/10.1139/X08-116
IAEA, 2014. IAEA/GNIP precipitation sampling guide.
IAEA/WMO, 2018. Global Network of Isotopes in Precipitation. The GNIP Database. [WWW Document]. URL https://nucleus.iaea.org/wiser (accessed 2.1.18).
Jacobsen, M., Webster, M., Vairavamoorthy, K., 2012. The future of water in African cities: Why waste water?, Directions in development;environment and sustainable development. The World Bank.
Jarvis, A., Reuter, H.I., Nelson, A., Guevara, E., 2008. Hole-filled SRTM for the globe Version 4. Available CGIAR-CSI SRTM 90m Database Httpsrtm Csi Cgiar Org 15.
Jasechko, S., Taylor, R.G., 2015. Intensive rainfall recharges tropical groundwaters. Environ. Res. Lett. 10, 124015. https://doi.org/10.1088/1748-9326/10/12/124015
Jiménez Cisneros, B.E., Oki, T., Arnell, N.W., Benito, G., Cogley, J.G., Doll, P., Jiang, T., Mwakalila, S.S., 2014. Freshwater resources, in: Climate Change 2013: The Physical Science Basis, IPCC AR5. Cambridge University Press, Cambridge, United Kingdom and New York, NY, USA, pp. 229–269.
Johnson, A.I., 1967. Specific yield: compilation of specific yields for various materials (USGS Numbered Series No. 1662- D), Water Supply Paper. U.S. Government Printing Office, Washington, D.C.
Jones, I.C., Banner, J.L., 2003. Estimating recharge thresholds in tropical karst island aquifers: Barbados, Puerto Rico and Guam. J. Hydrol. 278, 131–143. https://doi.org/10.1016/S0022-1694(03)00138-0
Jones, I.C., Banner, J.L., Humphrey, J.D., 2000. Estimating recharge in a tropical Karst Aquifer. Water Resour. Res. 36, 1289–1299. https://doi.org/10.1029/1999WR900358
Jones, J.P., Sudicky, E.A., McLaren, R.G., 2008. Application of a fully-integrated surface-subsurface flow model at the watershed-scale: A case study. Water Resour. Res. 44. https://doi.org/10.1029/2006WR005603
Jyrkama, M.I., Sykes, J.F., 2007. The impact of climate change on spatially varying groundwater recharge in the grand river watershed (Ontario). J. Hydrol. 338, 237–250. https://doi.org/10.1016/j.jhydrol.2007.02.036
Kangalawe, R.Y.M., 2009. Land use/cover changes and their implications on rural livelihoods in the degraded environments of central Tanzania. Afr. J. Ecol. 47, 135–141. https://doi.org/10.1111/j.1365-2028.2008.01060.x
Kashaigili, J., 2010. Assessment of groundwater availability and its current and potential use and impacts in Tanzania. Rep. Prep. Int. Water Manag. Inst. IWMI Sokoine Univ. Agric. Morogoro Tanzan.
Kashaigili, J., Mashauri, D., Abdo, G., 2003. Groundwater management by using mathematical modeling: Case of the Makutupora groundwater basin in Dodoma Tanzania. Botsw. J. Technol. 12. https://doi.org/10.4314/bjt.v12i1.15342
Keese, K.E., Scanlon, B.R., Reedy, R.C., 2005. Assessing controls on diffuse groundwater recharge using unsaturated flow modeling. Water Resour. Res. 41. https://doi.org/10.1029/2004WR003841
Kharin, V.V., Zwiers, F.W., Zhang, X., Hegerl, G.C., 2007. Changes in Temperature and Precipitation Extremes in the IPCC Ensemble of Global Coupled Model Simulations. J. Clim. 20, 1419–1444. https://doi.org/10.1175/JCLI4066.1
Kharin, V.V., Zwiers, F.W., Zhang, X., Wehner, M., 2013. Changes in temperature and precipitation extremes in the CMIP5 ensemble. Clim. Change 119, 345–357. https://doi.org/10.1007/s10584-013-0705-8
Kristensen, K.J., Jensen, S.E., 1975. A model for estimating actual evapotranspiration from potential evapotranspiration. Hydrol. Res. 6, 170–188. https://doi.org/10.2166/nh.1975.0012
Kundzewicz, Z.W., Mata, L.J., Arnell, N.W., Döll, P., Jimenez, B., Miller, K., Oki, T., Şen, Z., 2009. Water and climate projections. Hydrol. Sci. J. 54, 406–415. https://doi.org/10.1623/hysj.54.2.406
Kundzewicz, Z.W., Mata, L.J., Arnell, N.W., Doll, P., Kabat, P., Jimenez, B., Miller, K., Oki, T., Zekai, S., Shiklomanov, I., 2007. Freshwater resources and their management, in: Climate Change 2007: Impacts, Adaptation and Vulnerability. Contribution of Working Group II to the Fourth Assessment Report of the Intergovernmental Panel on Climate Change. Cambridge University Press, pp. 173–210.
Lachniet, M.S., Patterson, W.P., Burns, S., Asmerom, Y., Polyak, V., 2007. Caribbean and Pacific moisture sources on the Isthmus of Panama revealed from stalagmite and surface water δ18O gradients. Geophys. Res. Lett. 34. https://doi.org/10.1029/2006GL028469

Lapworth, D.J., Nkhuwa, D.C.W., Okotto-Okotto, J., Pedley, S., Stuart, M.E., Tijani, M.N., Wright, J., 2017. Urban groundwater quality in sub-Saharan Africa: current status and implications for water security and public health. Hydrogeol. J. 25, 1093–1116. https://doi.org/10.1007/s10040-016-1516-6

Leblanc, M.J., Favreau, G., Massuel, S., Tweed, S.O., Loireau, M., Cappelaere, B., 2008. Land clearance and hydrological change in the Sahel: SW Niger. Glob. Planet. Change 61, 135–150. https://doi.org/10.1016/j.gloplacha.2007.08.011

Lerner, D.N., Issar, A., Simmers, I., 1990. Groundwater Recharge: A Guide to Understanding and Estimating Natural Recharge. Heise.

MacDonald, A.M., Bonsor, H.C., Dochartaigh, B.É.Ó., Taylor, R.G., 2012. Quantitative maps of groundwater resources in Africa. Environ. Res. Lett. 7, 024009. https://doi.org/10.1088/1748-9326/7/2/024009

MacDonald, A.M., Calow, R.C., 2009. Developing groundwater for secure rural water supplies in Africa. Desalination 248, 546–556. https://doi.org/10.1016/j.desal.2008.05.100

MacDonald, A.M., Calow, R.C., Macdonald, D.M.J., Darling, W.G., Dochartaigh, B. é. ó., 2009. What impact will climate change have on rural groundwater supplies in Africa? Hydrol. Sci. J. 54, 690–703. https://doi.org/10.1623/hysj.54.4.690

MacDonald, A.M., Davies, J., Calow, R., Chilton, J., 2005. Developing groundwater: a guide for rural water supply. ITDG Publishing, Rugby, UK.

MacDonald, A.M., Taylor, R.G., Bonsor, H.C., 2013. Groundwater in Africa : is there sufficient water to support the intensification of agriculture from “land grabs”?, in: Allan, J., Keulertz, M., Sojamo, S., Warner, J. (Eds.), Handbook of Land and Water Grabs in Africa. Routledge, London, UK, pp. 376–383.

Maurice, L., Taylor, R.G., Tindimugaya, C., MacDonald, A.M., Johnson, P., Kaponda, A., Owor, M., Sanga, H., Bonsor, H.C., Darling, W.G., Gooddy, D., 2018. Characteristics of high-intensity groundwater abstractions from weathered crystalline bedrock aquifers in East Africa. Hydrogeol. J. https://doi.org/10.1007/s10040-018-1836-9

McCarthy, J.J., 2001. Climate change 2001: impacts, adaptation, and vulnerability: contribution of Working Group II to the third assessment report of the Intergovernmental Panel on Climate Change. Cambridge University Press.

McMahon, T.A., Vogel, R.M., Pegram, G.G., Peel, M.C., Etkin, D., 2007. Global streamflows–Part 2: Reservoir storage–yield performance. J. Hydrol. 347, 260–271. https://doi.org/10.1016/j.jhydrol.2007.09.021

Meinzer, O.E., 1923. The occurrence of ground water in the United States with a discussion of principles. Govt. Print. Off.

Mileham, L., Taylor, R., Todd, M., Tindimugaya, C., Thomson, J., 2009. The impact of climate change on groundwater recharge and runoff in a humid, equatorial catchment: sensitivity of projections to rainfall intensity. Hydrol. Sci. J. 54, 727–738. https://doi.org/10.1623/hysj.54.4.727

MOF, N.B.S., 2012. Population and housing census: population distribution by administrative areas. Minist. Finance Dar Es Salaam.

Moriasi, D.N., Arnold, J.G., Van Liew, M.W., Bingner, R.L., Harmel, R.D., Veith, T.L., 2007. Model evaluation guidelines for systematic quantification of accuracy in watershed simulations. Trans. ASABE 50, 885–900. https://doi.org/10.13031/2013.23153

Mosha, A.C., 2004. The planning of the new capital of Tanzania: Dodoma, an unfulfilled dream. University of Botswana.

Muir, A., Anderson, B., Stephen, I., 1957. Characteristics of Some Tanganyika Soils. J. Soil Sci. 8, 1–18. https://doi.org/10.1111/j.1365-2389.1957.tb01863.x

Murray, R., Louw, D., van der Merwe, B., Peters, I., 2018. Windhoek, Namibia: from conceptualising to operating and expanding a MAR scheme in a fractured quartzite aquifer for the city’s water security. Sustain. Water Resour. Manag. 4, 217–223. https://doi.org/10.1007/s40899-018-0213-0

Myneni, Knyazikhin, Park, 2015. MOD15A2H MODIS/Terra Leaf Area Index/FPAR 8-Day L4 Global 500m SIN Grid V006 [LEAF AREA INDEX (1 MONTH - TERRA/MODIS)]. NASA EOSDIS Land Processes DAAC. https://doi.org/10.5067/MODIS/MOD15A2H.006

Nash, J.E., Sutcliffe, J.V., 1970. River flow forecasting through conceptual models part I — A discussion of principles. J. Hydrol. 10, 282–290. https://doi.org/10.1016/0022-1694(70)90255-6

Neumann, R., Jung, G., Laux, P., Kunstmann, H., 2007. Climate trends of temperature, precipitation and river discharge in the Volta Basin of West Africa. Int. J. River Basin Manag. 5, 17–30. https://doi.org/10.1080/15715124.2007.9635302

Niang, I., Ruppel, O.C., Abdrabo, M.A., Essel, A., Lennard, C., Padgham, J., Urqhart, P., 2014. Africa. In: Climate Change 2014: Impacts, Adaptation, and Vulnerability. Part B: Regional

Aspects. Contribution of Working Group II to the Fifth Assessment Report of the Intergovernmental Panel on Climate Change [Barros, V.R., C.B. Field, D.J. Dokken, M.D. Mastrandrea, K.J. Mach, T.E. Bilir, M. Chatterjee, K.L. Ebi, Y.O. Estrada, R.C. Genova, B. Girma, E.S. Kissel, A.N. Levy, S. MacCracken, P.R. Mastrandrea, and L.L. White (eds.)]. Cambridge University Press, Cambridge, United Kingdom and New York, NY, USA, pp. 1199-1265.

Nicholson, S., 2000. The nature of rainfall variability over Africa on time scales of decades to millenia. Glob. Planet. Change, Paleomonsoon variations and terrestrial environmental change 26, 137–158. https://doi.org/10.1016/S0921-8181(00)00040-0

Nicholson, S., 1998. Interannual and interdecadal variability of rainfall over the African continent during the last two centuries, in: Water Resources Variability in Africa during the XXth Century. IAHS, pp. 107–116.

Nicholson, S., 1996. A review of climate dynamics and climate variability in Eastern Africa, in: The Limnology, Climatology and Paleoclimatology of the East African Lakes. pp. 25–56.

Nimmo, J.R., Healy, R.W., Stonestrom, D.A., 2006. Aquifer Recharge, in: Encyclopedia of Hydrological Sciences. American Cancer Society. https://doi.org/10.1002/0470848944.hsa161a

Nimmo, J.R., Horowitz, C., Mitchell, L., 2015. Discrete-storm water-table fluctuation method to estimate episodic recharge. Ground Water 53, 282–292. https://doi.org/10.1111/gwat.12177

Nkotagu, H., 1996a. Application of environmental isotopes to groundwater recharge studies in a semi-arid fractured crystalline basement area of Dodoma, Tanzania. J. Afr. Earth Sci. 22, 443–457. https://doi.org/10.1016/0899-5362(96)00022-X

Nkotagu, H., 1996b. Origins of high nitrate in groundwater in Tanzania. J. Afr. Earth Sci., Hydrogeochemical Studies in Sub-Saharan Africa 22, 471–478. https://doi.org/10.1016/0899-5362(96)00021-8

Okotto, L., Okotto-Okotto, J., Price, H., Pedley, S., Wright, J., 2015. Socio-economic aspects of domestic groundwater consumption, vending and use in Kisumu, Kenya. Appl. Geogr. 58, 189–197. https://doi.org/10.1016/j.apgeog.2015.02.009

Onodera, S., 1993. Estimation of a Rapid Recharge Mechanism in the Semi-arid Upland, Tanzania, Using Soil Water 18O and Cl-. IAHS Publ. 151–151.

Onodera, S., Kitaoka, K., Hayashi, M., Shindo, S., Kusakabe, M., 1995a. Evaluation of the groundwater recharge process in a semiarid region of Tanzania, using delta D and delta 18O. Int. Assoc. Hydrol. Sci. Publ. 383–391.

Onodera, S., Kitaoka, K., Shindo, S., 1995b. Stable isotopic compositions of deep groundwater caused by partial infiltration into the restricted recharge area of a semiarid basin in Tanzania. IAHS Publ.-Ser. Proc. Rep.-Intern Assoc Hydrol. Sci. 227, 75–84.

Owor, M., Taylor, R.G., Tindimugaya, C., Mwesigwa, D., 2009. Rainfall intensity and groundwater recharge: empirical evidence from the Upper Nile Basin. Environ. Res. Lett. 4, 035009. https://doi.org/10.1088/1748-9326/4/3/035009

Page, J., 2008. The Diversification Challenge in Africa’s Resource-Rich Economies. Brook. Inst., Global Working Papers.

Pavelic, P., 2012. Groundwater availability and use in Sub-Saharan Africa: a review of 15 countries. International Water Management Institute (IWMI).

Peel, M.C., McMahon, T.A., Finlayson, B.L., Watson, F.G.R., 2001. Identification and explanation of continental differences in the variability of annual runoff. J. Hydrol. 250, 224–240. https://doi.org/10.1016/S0022-1694(01)00438-3

Refsgaard, Storm, 1995. Computer models of watershed hydrology, in: Singh, V.P. (Ed.), Computer Models of Watershed Hydrology. Water Resources Publications Highlands Ranch, CO.

Richey, A.S., Thomas, B.F., Lo, M.-H., Reager, J.T., Famiglietti, J.S., Voss, K., Swenson, S., Rodell, M., 2015. Quantifying renewable groundwater stress with GRACE. Water Resour. Res. 51, 5217–5238. https://doi.org/10.1002/2015WR017349

Risi, C., Bony, S., Vimeux, F., Descroix, L., Ibrahim, B., Lebreton, E., Mamadou, I., Sultan, B., 2008. What controls the isotopic composition of the African monsoon precipitation? Insights from event-based precipitation collected during the 2006 AMMA field campaign. Geophys. Res. Lett. 35. https://doi.org/10.1029/2008GL035920

Robins, N.S., Davies, J., Farr, J.L., Calow, R.C., 2006. The changing role of hydrogeology in semi-arid southern and eastern Africa. Hydrogeol. J. 14, 1483–1492. https://doi.org/10.1007/s10040-006-0056-x

Rockstrom, J., Karlberg, L., 2009. Zooming in on the global hotspots of rainfed agriculture in water-constrained environments. SEI.

Rozanski, K., Araguás-Araguás, L., Gonfiantini, R., 1993. Isotopic patterns in modern global precipitation. Clim. Change Cont. Isot. Rec. 1–36. https://doi.org/10.1029/GM078p0001
Salama, R., Hatton, T., Dawes, W., 1999. Predicting land use impacts on regional scale groundwater recharge and discharge. J. Environ. Qual. 28, 446–460. https://doi.org/10.2134/jeq1999.00472425002800020010x
Scanlon, B.R., Healy, R.W., Cook, P.G., 2002. Choosing appropriate techniques for quantifying groundwater recharge. Hydrogeol. J. 10, 18–39. https://doi.org/10.1007/s10040-001-0176-2
Scanlon, B.R., Keese, K.E., Flint, A.L., Flint, L.E., Gaye, C.B., Edmunds, W.M., Simmers, I., 2006a. Global synthesis of groundwater recharge in semiarid and arid regions. Hydrol. Process. 20, 3335–3370. https://doi.org/10.1002/hyp.6335
Scanlon, B.R., Keese, K.E., Flint, A.L., Flint, L.E., Gaye, C.B., Edmunds, W.M., Simmers, I., 2006b. Global synthesis of groundwater recharge in semiarid and arid regions. Hydrol. Process. 20, 3335–3370.
Schaap, M.G., Leij, F.J., van Genuchten, M.Th., 2001. rosetta: a computer program for estimating soil hydraulic parameters with hierarchical pedotransfer functions. J. Hydrol. 251, 163–176. https://doi.org/10.1016/S0022-1694(01)00466-8
Scholl, M.A., Shanley, J.B., Zegarra, J.P., Coplen, T.B., 2009. The stable isotope amount effect: new insights from NEXRAD echo tops, Luquillo Mountains, Puerto Rico. Water Resour. Res. 45. https://doi.org/10.1029/2008WR007515
Sellers, P.J., Bounoua, L., Collatz, G.J., Randall, D.A., Dazlich, D.A., Los, S.O., Berry, J.A., Fung, I., Tucker, C.J., Field, C.B., Jensen, T.G., 1996. Comparison of Radiative and Physiological Effects of Doubled Atmospheric CO2 on Climate. Science 271, 1402–1406. https://doi.org/10.1126/science.271.5254.1402
Senguji, F.H., 1999. Importance of isotope hydrology techniques in water resources management: A case study of the Makutupora basin in Tanzania.
Shiklomanov, I.A., Rodda, J.C., 2004. World water resources at the beginning of the twenty-first century. Cambridge University Press.
Shindo, S., 1989. Study on the recharge mechanism and development of groundwater in the inland area of Tanzania: Interim report of Japan-Tanzania Joint Research, 92p. Unpubl. Rep.
Shindo, S., Kongola, L., Kondo, A., Sato, Y., Sakura, Y., Matsumoto, E., 1990. Study on the Recharge Mechanism and Development of Groundwater in the Inland area of Tanzania (2) [WWW Document]. KAKEN. URL https://kaken.nii.ac.jp/grant/KAKENHI-PROJECT-01041013/ (accessed 2.1.18).
Shindo, S., Kongola, L., Kondo, A., Sato, Y., Sakura, Y., Matsumoto, E., 1989. Study on the Recharge Mechanism and Development of Groundwater in the Inland area of Tanzania [WWW Document]. KAKEN. URL https://kaken.nii.ac.jp/grant/KAKENHI-PROJECT-01041013/ (accessed 2.1.18).
Siebert, S., Burke, J., Faures, J.M., Frenken, K., Hoogeveen, J., Döll, P., Portmann, F.T., 2010. Groundwater use for irrigation – a global inventory. Hydrol Earth Syst Sci Discuss 7, 3977–4021. https://doi.org/10.5194/hessd-7-3977-2010
Simmers, I., 2003. Understanding water in a dry environment: hydrological processes in arid and semi-arid zones. AA Balkema Publisher.
Simmers, I., Hendrickx, J.M.H., Kruseman, G.P., Rushton, K.R. (Eds.), 1997. Recharge of Phreatic Aquifers in (Semi-) Arid Areas: IAH International Contributions to Hydrogeology 19, 1 edition. ed. CRC Press, Rotterdam ; Brookfield, VT, USA.
Sishodia, R.P., Shukla, S., Graham, W.D., Wani, S.P., Jones, J.W., Heaney, J., 2017. Current and future groundwater withdrawals: Effects, management and energy policy options for a semi-arid Indian watershed. Adv. Water Resour. 110, 459–475. https://doi.org/10.1016/j.advwatres.2017.05.014
Somaratne, N., Smettem, K.R.J., 2014. Theory of the generalized chloride mass balance method for recharge estimation in groundwater basins characterised by point and diffuse recharge. Hydrol Earth Syst Sci Discuss 2014, 307–332. https://doi.org/10.5194/hessd-11-307-2014
Steiger, J.H., 1980. Tests for comparing elements of a correlation matrix. Psychol. Bull. 87, 245–251. https://doi.org/10.1037/0033-2909.87.2.245
Stoll, S., Hendricks Franssen, H.J., Butts, M., Kinzelbach, W., 2011. Analysis of the impact of climate change on groundwater related hydrological fluxes: a multi-model approach including different downscaling methods. Hydrol Earth Syst Sci 15, 21–38. https://doi.org/10.5194/hess-15-21-2011

Taylor, R.G., Howard, K., 2000. A tectono-geomorphic model of the hydrogeology of deeply weathered crystalline rock: evidence from Uganda. Hydrogeol. J. 8, 279–294. https://doi.org/10.1007/s100400000069
Taylor, R.G., Howard, K., 1999. The influence of tectonic setting on the hydrological characteristics of deeply weathered terrains: evidence from Uganda. J. Hydrol. 218, 44–71. https://doi.org/10.1016/S0022-1694(99)00024-4
Taylor, R.G., Howard, K., 1996. Groundwater recharge in the Victoria Nile basin of east Africa: support for the soil moisture balance approach using stable isotope tracers and flow modelling. J. Hydrol. 180, 31–53. https://doi.org/10.1016/0022-1694(95)02899-4
Taylor, R.G., Koussis, A., Tindimugaya, C., 2009. Groundwater and climate in Africa—a review. Hydrol. Sci. J. 54, 655–664. https://doi.org/10.1623/hysj.54.4.655
Taylor, R.G., Scanlon, B., Döll, P., Rodell, M., van Beek, R., Wada, Y., Longuevergne, L., Leblanc, M., Famiglietti, J.S., Edmunds, M., Konikow, L., Green, T.R., Chen, J., Taniguchi, M., Bierkens, M.F.P., MacDonald, A., Fan, Y., Maxwell, R.M., Yechieli, Y., Gurdak, J.J., Allen, D.M., Shamsudduha, M., Hiscock, K., Yeh, P.J.-F., Holman, I., Treidel, H., 2013a. Ground water and climate change. Nat. Clim. Change 3, 322–329. https://doi.org/10.1038/nclimate1744
Taylor, R.G., Tindimugaya, C., Barker, J., Macdonald, D., Kulabako, R., 2010. Convergent radial tracing of viral and solute transport in gneiss saprolite. Ground Water 48, 284–294. https://doi.org/10.1111/j.1745-6584.2008.00547.x
Taylor, R.G., Todd, M.C., Kongola, L., Maurice, L., Nahozya, E., Sanga, H., MacDonald, A.M., 2013b. Evidence of the dependence of groundwater resources on extreme rainfall in East Africa. Nat. Clim. Change 3, 374–378. https://doi.org/10.1038/nclimate1731
Tebaldi, C., Hayhoe, K., Arblaster, J.M., Meehl, G.A., 2006. Going to the Extremes. Clim. Change 79, 185–211. https://doi.org/10.1007/s10584-006-9051-4
The Citizen, 2014. Construction of Farkwa Dam, is it the death of Bahi? [WWW Document]. URL http://www.thecitizen.co.tz/News/Plan-to-build-Farkwa-Dam-worries-Bahi/1840374-2245384-c1qh71/index.html (accessed 11.27.17).
The East African, 2017. Magufuli set to relocate to Dodoma by 2019 [WWW Document]. East Afr. URL http://www.theeastafrican.co.ke/news/Magufuli-set-to-relocate-to-Dodoma-by-2019/2558-4128464-gtyy5v/index.html (accessed 4.7.18).
Theis, C.V., 1935. The relation between the lowering of the piezometric surface and the rate and duration of discharge of a well using ground-water storage. Eos Trans. Am. Geophys. Union 16, 519–524. https://doi.org/10.1029/TR016i002p00519
Thompson, J., Porras, I.T., Wood, E., Tumwine, J.K., Mujwahuzi, M.R., Katui-Katua, M., Johnstone, N., 2000. Waiting at the tap: changes in urban water use in East Africa over three decades. Environ. Urban. 12, 37–52. https://doi.org/10.1177/095624780001200204
Thompson, J.R., 2012. Modelling the impacts of climate change on upland catchments in southwest Scotland using MIKE SHE and the UKCP09 probabilistic projections. Hydrol. Res. 43, 507–530. https://doi.org/10.2166/nh.2012.105
Thompson, J.R., Green, A.J., Kingston, D.G., Gosling, S.N., 2013. Assessment of uncertainty in river flow projections for the Mekong River using multiple GCMs and hydrological models. J. Hydrol. 486, 1–30. https://doi.org/10.1016/j.jhydrol.2013.01.029
Thompson, J.R., Sørenson, H.R., Gavin, H., Refsgaard, A., 2004. Application of the coupled MIKE SHE/MIKE 11 modelling system to a lowland wet grassland in southeast England. J. Hydrol. 293, 151–179. https://doi.org/10.1016/j.jhydrol.2004.01.017
Trenberth, K.E., 1999. Conceptual Framework for Changes of Extremes of the Hydrological Cycle with Climate Change. Clim. Change 42, 327–339. https://doi.org/10.1023/A:1005488920935
Trenberth, K.E., Dai, A., Rasmussen, R.M., Parsons, D.B., 2003. The changing character of precipitation. Bull. Am. Meteorol. Soc. 84, 1205–1217. https://doi.org/10.1175/BAMS-84-9-1205
UN, 2018a. The Sustainable Development Goals Report 2018. United Nations Pubn.
UN, 2018b. SDG 6 Synthesis Report 2018 on Water and Sanitation. UN-Water. URL http://www.unwater.org/publications/highlights-sdg-6-synthesis-report-2018-on-water-and-sanitation-2/ (accessed 8.9.18).
UN, 2017. World Population Prospects The 2017 Revision (No. ESA/P/WP/248).
UN, 2015a. World Population Prospects: The 2015 Revision, Key Findings and Advance Tables.
UN, 2015b. Millennium Development Goals Report: 2015. United Nations Publications.
UN, 2014. World Urbanisation Prospects: the 2014 Revision, Highlights (ST/ESA/SER. A/352). Department of Economic and Social Affairs. Popul. Div. N. Y. U. N.

UN, 2013. Water security and the global water agenda: a UN-water analytical brief. Hamilt. UN Univ.
UNECA, 2008. Africa review report on agriculture and rural development: (summary).
UNECA/AU/AfDB, 2003. The Africa water vision for 2025: Equitable and sustainable use of water for socioeconomic development. Addis Ababa Ethiop. Econ. Comm. Afr.
UNEP, 2010. Africa Water Atlas. UNEP/Earthprint.
UNEP, 2002. Africa Environment Outlook: Past, Present and Future Perspectives. Earthprint for and.
Van Genuchten, M.T., 1980. A closed-form equation for predicting the hydraulic conductivity of unsaturated soils 1. Soil Sci. Soc. Am. J. 44, 892–898. https://doi.org/10.2136/sssaj1980.03615995004400050002x
Vázquez, R.F., Feyen, L., Feyen, J., Refsgaard, J.C., 2002. Effect of grid size on effective parameters and model performance of the MIKE-SHE code. Hydrol. Process. 16, 355–372. https://doi.org/10.1002/hyp.334
Vogel, J.C., Van Urk, H., 1975. Isotopic composition of groundwater in semi-arid regions of southern Africa. J. Hydrol. 25, 23–36. https://doi.org/10.1016/0022-1694(75)90036-0
Wades, F.B., Oates, F., 1938. An explanation of degree sheet no. 52, Dodoma-Geological Survey of Tanganyika, Tanganyika Territory. Department of Lands and Mines. Geological Division. Government Printer, South Africa.
Wang, G., Wang, D., Trenberth, K.E., Erfanian, A., Yu, M., Bosilovich, M.G., Parr, D.T., 2017. The peak structure and future changes of the relationships between extreme precipitation and temperature. Nat. Clim. Change 7, 268–274. https://doi.org/10.1038/nclimate3239
Wang, H., Wang, T., Zhang, B., Li, F., Toure, B., Omosa, I.B., Chiramba, T., Abdel-Monem, M., Pradhan, M., 2014. Water and Wastewater Treatment in Africa – Current Practices and Challenges. CLEAN – Soil Air Water 42, 1029–1035. https://doi.org/10.1002/clen.201300208
Wani, Suhas Pralhad, Rockström, J., Oweis, T.Y., 2009. Rainfed agriculture: unlocking the potential. CABI.
Wani, S. P., Sreedevi, T.K., Rockström, J., Ramakrishna, Y.S., 2009. Rainfed agriculture–past trends and future prospects. Rainfed Agric. Unlocking Potential 7, 1. https://doi.org/10.1079/9781845933890.0001
Westra, S., Alexander, L.V., Zwiers, F.W., 2012. Global Increasing Trends in Annual Maximum Daily Precipitation. J. Clim. 26, 3904–3918. https://doi.org/10.1175/JCLI-D-12-00502.1
Wheater, H.S., Mathias, S.A., Li, X., 2010. Groundwater modelling in arid and semi-arid areas. Cambridge University Press.
WHO/UNICEF, 2017. Progress on drinking-water sanitation and hygiene: 2017 update and SDG baselines, 1 edition. ed. World Health Organization, S.l.
WHO/UNICEF, 2008. WHO | Progress on Drinking-water and Sanitation: [WWW Document]. WHO. URL http://www.who.int/water_sanitation_health/monitoring/jmp2008/en/ (accessed 3.2.16).
Willmott, C.J., 1981. On the Validation of Models. Phys. Geogr. 2, 184–194. https://doi.org/10.1080/02723646.1981.10642213
WMO, 2018. World Weather Information Service [WWW Document]. World Weather Inf. Serv. URL http://worldweather.wmo.int/en/city.html?cityId=667 (accessed 6.18.18).
WMO, 2014. EL NIÑO/LA NIÑA UPDATE.
Wood, W.W., 1999. Use and Misuse of the Chloride-Mass Balance Method in Estimating Ground Water Recharge. Groundwater 37, 2–3. https://doi.org/10.1111/j.1745-6584.1999.tb00949.x
World Bank, 2018. Urban population (% of total) | Data [WWW Document]. URL https://data.worldbank.org/indicator/SP.URB.TOTL.IN.ZS (accessed 8.13.18).
WWP, U., 2017. The United Nations World Water Development Report 2017. Wastewater: The Untapped Resource. Paris, UNESCO.
XinhuaNet, 2017. UN bodies in Tanzania completes shift to capital Dodoma - Xinhua | English.news.cn [WWW Document]. URL http://www.xinhuanet.com/english/2017-12/08/c_136809400.htm (accessed 4.7.18).
Yang, L., Qi, Y., Zheng, C., Andrews, C.B., Yue, S., Lin, S., Li, Y., Wang, C., Xu, Y., Li, H., 2018. A Modified Water-Table Fluctuation Method to Characterize Regional Groundwater Discharge. Water 10, 503. https://doi.org/10.3390/w10040503
Yurtsever, Y., 1975. Worldwide survey of stable isotopes in precipitation, Isotope Hydrology Section. IAEA.
Zhang, L., Dawes, W.R., Hatton, T.J., Reece, P.H., Beale, G.T.H., Packer, I., 1999. Estimation of soil moisture and groundwater recharge using the TOPOG_IRM model. Water Resour. Res. 35, 149–161. https://doi.org/10.1029/98WR01616

Zhang, X., Zwiers, F.W., Hegerl, G.C., Lambert, F.H., Gillett, N.P., Solomon, S., Stott, P.A., Nozawa, T., 2007. Detection of human influence on twentieth-century precipitation trends. Nature 448, 461–465. https://doi.org/10.1038/nature06025

Appendices

Appendix A

A map showing the calculation of the area above 1400 mamsl in the Makutapora Basin.

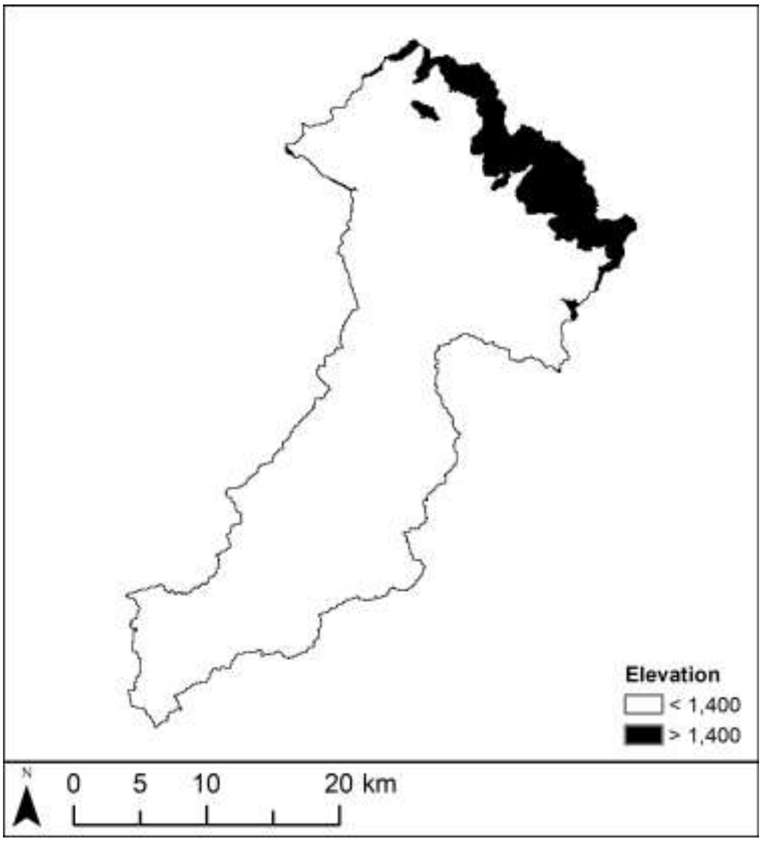

Figure B.1 Elevation of the Makutapora Basin highlighting the area more than 1400 mamsl.

Appendix B

Synthesised groundwater abstraction record of individual wells.

BH37/53

BH17/53

BH36/57

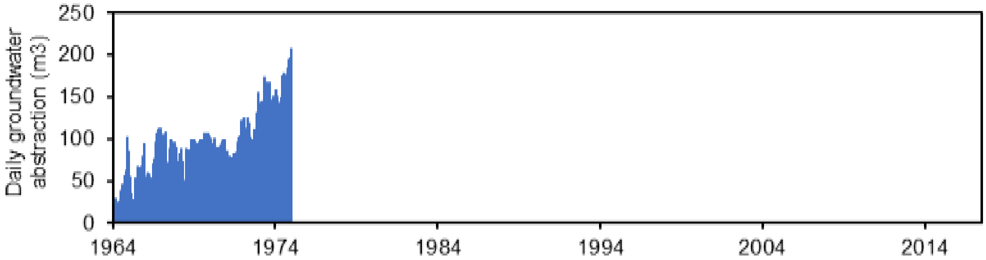

BH97/70

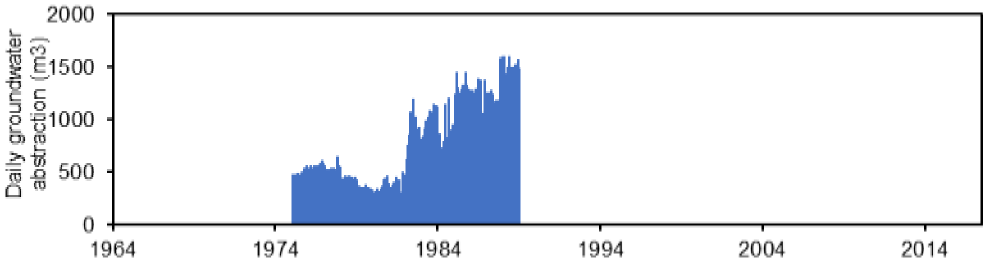

BH217/73

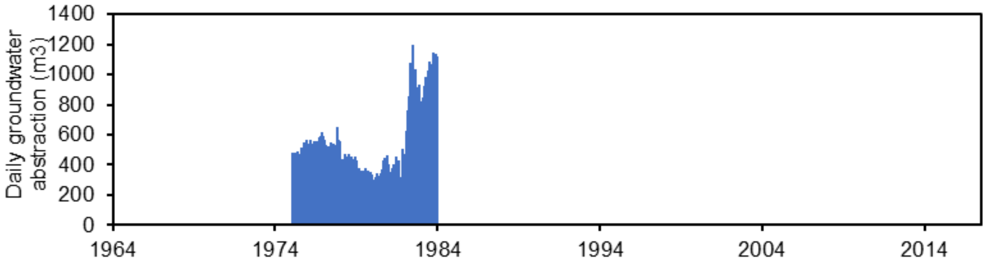

BH8/54

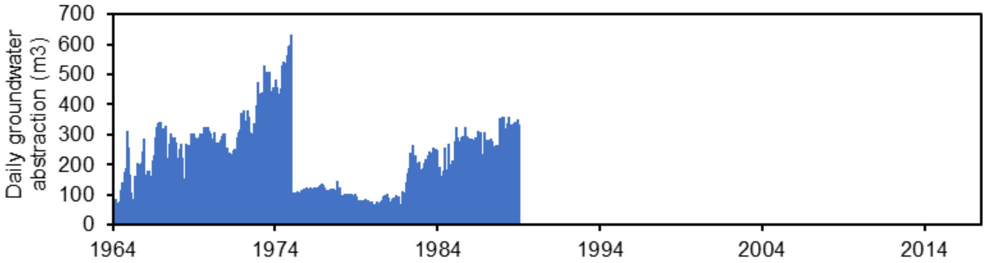

BH10/59

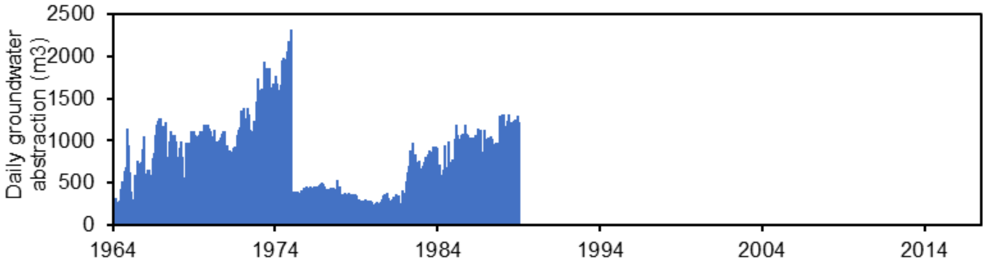

BH117/75

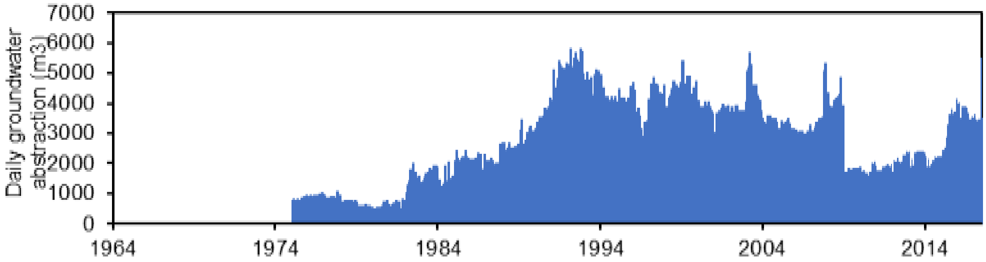

BH118/75

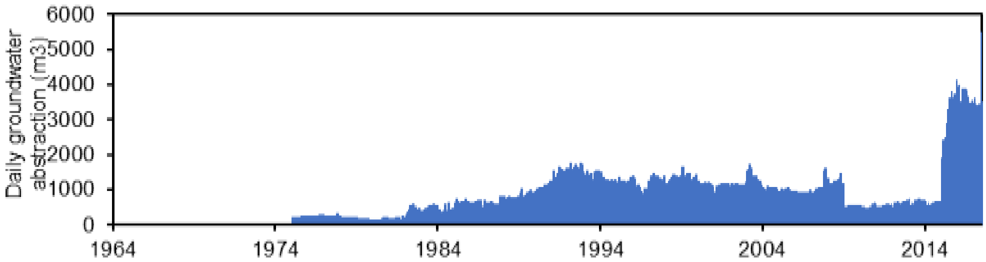

BH119/75

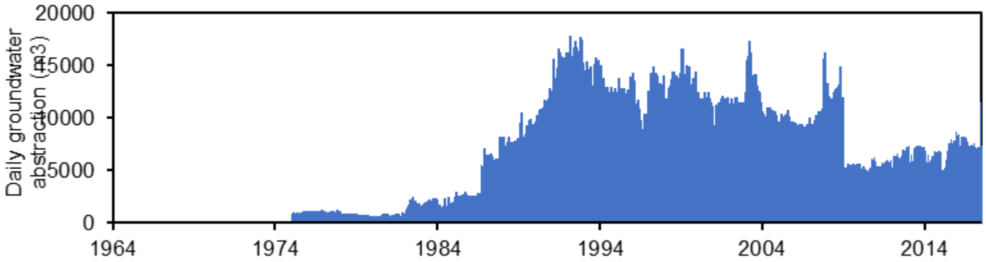

BH131/75

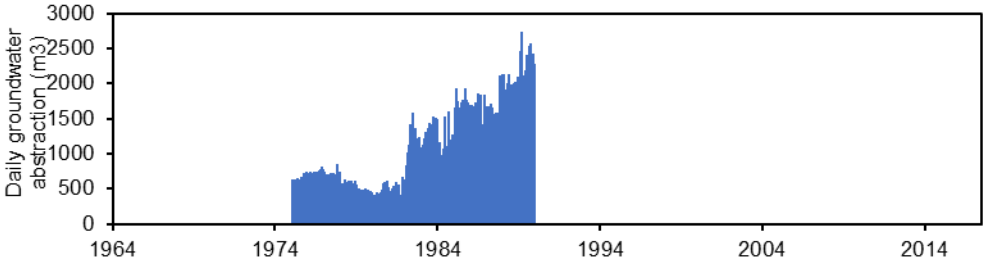

BH147/78

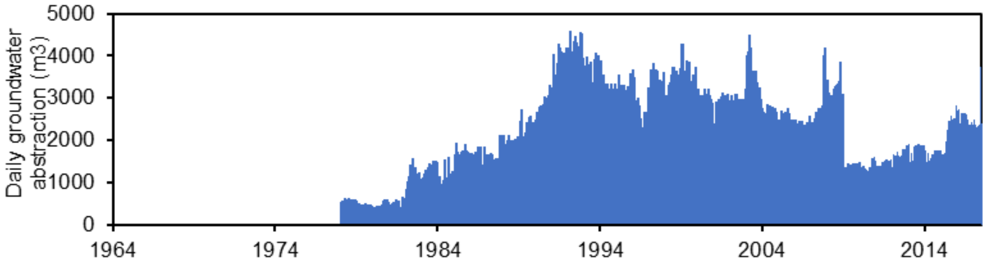

BH26/79

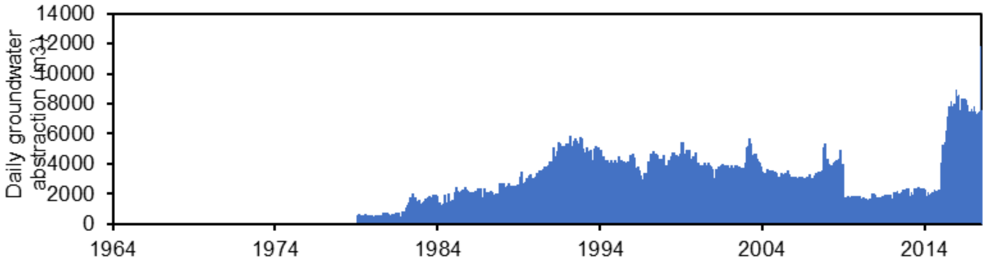

C3

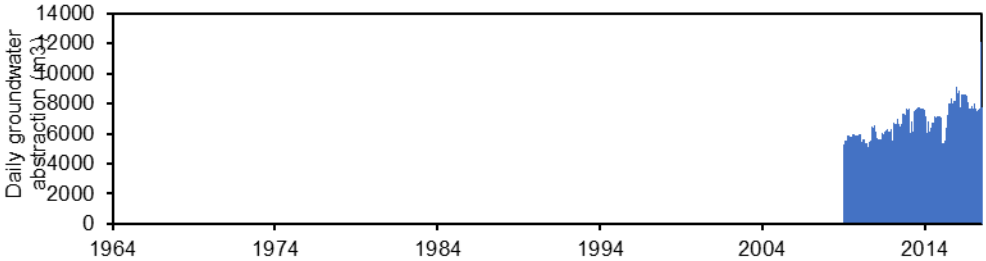

C1


Daily groundwater abstraction (m3)
12000
10000
8000
6000
4000
2000
0
1964
1974
1984
1994
2004
2014

C9


Daily groundwater abstraction (m3)
10000
8000
6000
4000
2000
0
1964
1974
1984
1994
2004
2014

C8


Daily groundwater abstraction (m3)
6000
5000
4000
3000
2000
1000
0
1964
1974
1984
1994
2004
2014

C4


Daily groundwater abstraction (m3)
5000
4000
3000
2000
1000
0
1964
1974
1984
1994
2004
2014

S2


Daily groundwater abstraction (m3)
4000
3000
2000
1000
0
1964
1974
1984
1994
2004
2014

Appendix C

Details of precipitation data available near Makutapora, and the dataset used by Taylor et al. (2013b).

There are several precipitation datasets deriving from either Makutapora or Dodoma. They are detailed below:

- '**Dodoma'** data from 1932-present. This daily data was recorded at Dodoma Airport Meteorological station. This dataset has been verified as real at the meteorological station itself and by Hydrosciences Montpellier.
- **'Makutapora Maji'** – Monthly data 1937-1989 the exact provenance of this data is unclear. The Swahili word "maji" means water, so it does not signify a location of collection. This data came from Hydrosciences Montpellier with no indication of location.
- '**Makutapora 1**' – A precipitation record received from DUWASA containing monthly data from 1921 to 2003. This data was supposedly recorded in the Makutapora Basin.
- "**Makutapora 2**" – A precipitation record received from DUWASA containing monthly data from 1998 to 2012. This data was supposedly recorded in the Makutapora Basin.
- **Makutapora Meteorological Station** – Daily data recorded at the Makutapora Meteorological station from 2007 to present.

1) It appears that the "Makutapora 1" record is based on the Dodoma record from **1937 to 1974**. During this period, the correlation of monthly rainfall is 0.99. There is no systematic difference in that one is always greater than the other, but the values are suspiciously consistently +/- 1mm. During the same period, the Maji record is similar to both Dodoma and Makutapora (as you'd expect from proximate rain gauges), but one does not seem derived from the other.

2) Between **1974 and 1989** (Maji ends in 1989), the "Makutapora 1" and Maji record become a lot more similar. The difference seems less systematic than between Dodoma and "Makutapora 1" in the previous period, but the time series become conspicuously more similar.

3) Between **1989 and 1998**, the Dodoma and "Makutapora 1" records seem fairly different. The "Makutapora 1" record does not seem to be derived from the Dodoma record during this time. Presumably, the "Makutapora 1" record derives from Makutapora data.

4) **1998 – 2003** – We have overlapping records from DUWASA, “Makutapora 1” and “Makutapora 2”. These records do not match in parts, yet neither are based on Dodoma data. These are potentially different records from within the Makutapora Basin, however, that seem unlikely.

5) **2003 – 2007** – The Dodoma data and the “Makutapora 2” record are not derived from one another.

6) **2007 – 2012** – The Makutapora Meteorological Station data matches the “Makutapora 2” data. It was therefore assumed that “Makutapora 2” comprises data from the Makutapora Meteorological Station.

From this, it is assumed that the precipitation data published by Taylor et al. (2013b) was a composite record consisting of some data recorded in Dodoma and some in Makutapora. This suspicion was later confirmed by Emmanuel Nahozya of the Ministry of Water and Irrigation.

Appendix D

C10

Lithology	Bottom
Clay	60.0
Weathered Granite	-

Construction	
Total depth (m)	86.2
Screened depth (mbgl)	61.3 - 69.8
	70.6 - 79.2
Depth to water table (m)	-

C11

Lithology	Bottom
Clay	65.0
Calcrete	73.0
Weathered Granite	-

Construction	
Total depth (m)	104.2
Screened depth (mbgl)	73.5 - 82.1
	91.1 - 96.7
Depth to water table (m)	-
Casing diameter (mm)	180 from 0.4 - 70.2
	127 from 70.2 - 104

C12

Lithology	Bottom
Clay	45.0
Calcrete	52.0
Weathered Granite	79.0
Basement Granite	-

Construction	
Total depth (m)	131.2
Screened depth (mbgl)	62.8 - 125.5
Depth to water table (m)	-
Casing diameter (mm)	325 from 0.3 - 60.0
	127 from 60.0 - 130.0

C5

Lithology	Bottom
Calcrete	16.0
Weathered Granite	-

Construction	
Total depth (m)	121.7
Screened depth (mbgl)	65.8 - 82.9
	92.7 - 104.1
Depth to water table (m)	-
Casing diameter (mm)	325 from 0.3 - 65.6
	180 from 65.6 - 107.4

C6

Lithology	Bottom
Clay	66.0
Calcrete	72.0
Weathered Granite	-

Construction	
Total depth (m)	119.8
Screened depth (mbgl)	70.5 - 73.3
	75.3 - 101.0
	112.0 - 114.9
Depth to water table (m)	-
Casing diameter (mm)	325 from 0.3 - 75.3
	180 from 75.3 - 119.8

C7

Lithology	Bottom
Clay	49.5
Weathered Granite	-

Construction	
Total depth (m)	108.6
Screened depth (mbgl)	64.0 - 81.1 85.9 - 101.1
Depth to water table (m)	-
Casing diameter (mm)	325 from 0.1 - 63.6 180 from 63.6 - 105.0

C8

Lithology	Bottom
Clay	59.0
Calcrete	82.0
Weathered Granite	-

Construction	
Total depth (m)	107.9
Screened depth (mbgl)	88.6 - 102.8
Depth to water table (m)	-
Casing diameter (mm)	325 from 0.3 - 88.5 180 from 88.5 - 106.8

C9

Lithology	Bottom
Clay	6.0
Calcrete	24.0
Weathered Granite	-

Construction	
Total depth (m)	100.0
Screened depth (mbgl)	-
Depth to water table (m)	-
Casing diameter (mm)	325 from 0.2 - 60.0 180 from 60.0 - 98.0

10/59

Lithology	Bottom
Mbuga Clay	35.1
Calcrete	64.6
Sand	86.7
Weathered Granite	-

Construction	
Total depth (m)	91.0
Screened depth (mbgl)	-
Depth to water table (m)	-

103/78

Lithology	Bottom
Mbuga Clay	6.8
Sand	15.7
Clay	20.1
Sand Gravel	25.1
Calcrete	26.4
Weathered Granite	35.9
Clay	46.1
Calcrete	55.6
Clay	63.1
Weathered Granite	-

Construction	
Total depth (m)	66.0
Screened depth (mbgl)	-
Depth to water table (m)	22.8 - 57.9

107A/72

Lithology	Bottom
Mbuga Clay	9.3
Sand	25.0
Clay	44.1
Calcrete	62.1
Sand	65.0
Weathered Granite	76.0
Basement Granite	-

Construction	
Total depth (m)	92.0
Screened depth (mbgl)	-
Depth to water table (m)	-

108/70

Lithology	Bottom
Mbuga Clay	16.3
Clay	58.1
Calcrete	66.8
Sand Gravel	83.6
Weathered Granite	-

Construction	
Total depth (m)	87.0
Screened depth (mbgl)	-
Depth to water table (m)	-

117/75

Lithology	Bottom
Mbuga Clay	2.6
Silt	28.4
Clay	31.5
Sand	59.1
Clay	64.0
Sand Gravel	87.9
Basement Granite	-

Construction	
Total depth (m)	119.0
Screened depth (mbgl)	-
Depth to water table (m)	-

118/75

Lithology	Bottom
Silt	22.7
Clay	39.9
Sand	59.5
Weathered Granite	65.1
Basement Granite	-

Construction	
Total depth (m)	119.7
Screened depth (mbgl)	-
Depth to water table (m)	-

119/75

Lithology	Bottom
Silt	8.3
Sand	14.6
Silt	40.6
Sand	60.2
Basement Granite	-

Construction	
Total depth (m)	119.7
Screened depth (mbgl)	-
Depth to water table (m)	-

122/75

Lithology	Bottom
Mbuga Clay	19.3
Calcrete	30.6
Mbuga Clay	33.2
Sand	51.5
Weathered Granite	54.0
Basement Granite	-

Construction	
Total depth (m)	97.9
Screened depth (mbgl)	-
Depth to water table (m)	18.9 - 26.4

123/75

Lithology	Bottom
Mbuga Clay	55.5
Clay	63.2
Calcrete	74.5
Weathered Granite	82.8
Basement Granite	-

Construction	
Total depth (m)	98.0
Screened depth (mbgl)	-
Depth to water table (m)	-
Casing diameter (mm)	250 from 0.0 - 76.0 165 from 76.0 - 98.0

131/75

Lithology	Bottom
Clay	59.0
Calcrete	71.0
Clay	74.8
Weathered Granite	84.3
Basement Granite	-

Construction	
Total depth (m)	110.9
Screened depth (mbgl)	-
Depth to water table (m)	-

147/75

Lithology	Bottom
Mbuga Clay	4.6
Calcrete	27.7
Sand Gravel	35.3
Weathered Granite	-

Construction	
Total depth (m)	85.5
Screened depth (mbgl)	-
Depth to water table (m)	-
Casing diameter (mm)	305 from 0.0 - 58.0
	273 from 58.0 - 68.2
	260 from 68.2 - 74.3

163/75

Lithology	Bottom
Mbuga Clay	1.6
Clay	26.9
Sand	30.0
Sand Gravel	33.2
Weathered Granite	40.8
Basement Granite	-

Construction	
Total depth (m)	104.7
Screened depth (mbgl)	-
Depth to water table (m)	-

169/75

Lithology	Bottom
Mbuga Clay	13.8
Clay	28.4
Calcrete	40.4
Sand	43.6
Sand Gravel	46.1
Basement Granite	-

Construction	
Total depth (m)	101.9
Screened depth (mbgl)	-
Depth to water table (m)	-

170/75

Lithology	Bottom
Mbuga Clay	8.4
Clay	18.1
Sand	35.7
Weathered Granite	45.2
Basement Granite	-

Construction	
Total depth (m)	119.8
Screened depth (mbgl)	-
Depth to water table (m)	-
Casing diameter (mm)	197 from 0.0 - 36.0
	180 from 36.0 - 50.0
	165 from 50.0 - 119.8

182/75

Lithology	Bottom
Mbuga Clay	11.9
Sand	22.1
Clay	34.1
Calcrete	46.8
Weathered Granite	56.9
Basement Granite	-

Construction	
Total depth (m)	120.8
Screened depth (mbgl)	-
Depth to water table (m)	-
Casing diameter (mm)	219 from 0.0 - 64.0
	165 from 64.0 - 100.0

193/75

Lithology	Bottom
Silt	9.1

Construction	
Total depth (m)	92.0

Clay	17.3	**Screened depth (mbgl)**	-
Sand	25.5	**Depth to water table (m)**	-
Sand Gravel	35.7		
Weathered Granite	-		

196/75

Lithology	Bottom	Construction	
Clay	19.7	**Total depth (m)**	120.7
Sand	27.9	**Screened depth (mbgl)**	-
Weathered Granite	53.4	**Depth to water table (m)**	-
Basement Granite	-		

207/75

Lithology	Bottom	Construction	
Mbuga Clay	11.0	**Total depth (m)**	116.1
Clay	23.8	**Screened depth (mbgl)**	-
Calcrete	40.6	**Depth to water table (m)**	-
Sand Gravel	58.1		
Weathered Granite	77.8		
Basement Granite	-		

220/75

Lithology	Bottom	Construction	
Mbuga Clay	1.7	**Total depth (m)**	123.1
Clay	11.0	**Screened depth (mbgl)**	-
Sand Gravel	23.7	**Depth to water table (m)**	-
Mbuga Clay	53.2		
Sand Gravel	60.7		
Weathered Granite	75.1		
Basement Granite	-		

234/75

Lithology	Bottom	Construction	
Silt	5.5	**Total depth (m)**	142.2
Calcrete	15.0	**Screened depth (mbgl)**	-
Sand Gravel	56.2	**Depth to water table (m)**	24.5 - 33.0
Clay	61.2		
Weathered Granite	96.7		
Basement Granite	-		

30A/53

Lithology	Bottom	Construction	
Mbuga Clay	40.4	**Total depth (m)**	86.4
Calcrete	55.8	**Screened depth (mbgl)**	-
Sand	57.6	**Depth to water table (m)**	17.9 - 25.9
Calcrete	75.4		
Sand	81.5		
Weathered Granite	-		

34/51A

Lithology	Bottom	Construction	
Mbuga Clay	6.9	**Total depth (m)**	57.8
Clay	24.9	**Screened depth (mbgl)**	-
Sand	38.7	**Depth to water table (m)**	-
Weathered Granite	54.3		

Basement Granite	-

34/68

Lithology	Bottom
Mbuga Clay	8.7
Clay	57.5
Calcrete	81.9
Weathered Granite	-

Construction	
Total depth (m)	98.7
Screened depth (mbgl)	-
Depth to water table (m)	-

35/53

Lithology	Bottom
Mbuga Clay	12.1
Clay	-

Construction	
Total depth (m)	34.2
Screened depth (mbgl)	-
Depth to water table (m)	18.0 - 23.2

36/57

Lithology	Bottom
Mbuga Clay	17.4
Clay	53.6
Calcrete	63.4
Sand Gravel	72.0
Weathered Granite	-

Construction	
Total depth (m)	143.8
Screened depth (mbgl)	-
Depth to water table (m)	-

39/53

Lithology	Bottom
Mbuga Clay	7.8
Clay	39.1
Sand Gravel	46.4
Weathered Granite	56.2
Basement Granite	-

Construction	
Total depth (m)	58.7
Screened depth (mbgl)	-
Depth to water table (m)	18.2 - 24.9

8/54

Lithology	Bottom
Mbuga Clay	46.3
Calcrete	63.5
Sand	67.8
Calcrete	73.3
Sand	75.8
Weathered Granite	-

Construction	
Total depth (m)	86.2
Screened depth (mbgl)	-
Depth to water table (m)	-

86/78

Lithology	Bottom
Mbuga Clay	40.6
Calcrete	63.4
Basement Granite	-

Construction	
Total depth (m)	206.2
Screened depth (mbgl)	-
Depth to water table (m)	17.6 - 33.2

88/75

Lithology	Bottom
Mbuga Clay	44.8
Calcrete	49.1
Sand	65.7
Weathered Granite	71.2
Basement Granite	-

Construction	
Total depth (m)	94.5
Screened depth (mbgl)	-
Depth to water table (m)	-

89/75

Lithology	Bottom
Mbuga Clay	50.8
Sand	62.4
Calcrete	86.4
Sand	97.4
Basement Granite	-

Construction	
Total depth (m)	105.4
Screened depth (mbgl)	-
Depth to water table (m)	18.9 - 29.3

97/70

Lithology	Bottom
Mbuga Clay	38.7
Clay	60.8
Calcrete	74.9
Sand	81.1
Basement Granite	-

Construction	
Total depth (m)	84.1
Screened depth (mbgl)	-
Depth to water table (m)	-

97/75

Lithology	Bottom
Mbuga Clay	42.1
Sand	43.9
Clay	53.1
Sand	76.4
Calcrete	78.2
Sand	82.5
Basement Granite	-

Construction	
Total depth (m)	107.1
Screened depth (mbgl)	-
Depth to water table (m)	-

98/2009

Lithology	Bottom
Mbuga Clay	2.0
Clay	30.0
Weathered Granite	-

Construction	
Total depth (m)	125.0
Screened depth (mbgl)	-
Depth to water table (m)	-

Appendix E

Soil zone profiles

In the MIKE SHE/MIKE 11 model, there are 4 zones defined by their soil zone profiles (figure XXX), labelled according to the top layer, Mbuga clay, decomposed granite, weathered granite or granite. Soil zones associated with each area are listed below.

Mbuga clay

	Top (mbgl)	Bottom (mbgl)
Mbuga clay	0	3
Decomposed granite	3	78
Weathered granite	78	153
Granite	153	1500

Decomposed granite

	Top (mbgl)	Bottom (mbgl)
Decomposed granite	0	75
Weathered granite	75	150
Granite	150	1500

Weathered granite

	Top (mbgl)	Bottom (mbgl)
Weathered granite	0	75
Granite	75	1500

Granite

	Top (mbgl)	Bottom (mbgl)
Granite	0	1500

Vertical discretisation

The unsaturated zone is vertically discretised throughout the model domain as follows:

Top (mbgl)	Bottom (mbgl)	Cell height	Number of cells
0	1	0.1	10
1	3	0.2	10
3	6	0.3	10
6	10	0.4	10

10	50	0.5	80
50	1500	10	145

As elevations within the basin are highly varied, the soil zones are defined to a depth of 1500 m below ground to ensure the full range of possible water table elevations are covered.

Soil parameters

Van Guntchen model parameters for each textural class used in the MIKE SHE model are listed below.

Textural Class	θ_s	θ_r	**α**	**n**	**Bulk density**	**K**
Mbuga clay	0.5	0.4	0.005	1.1	1200	1.0×10^{-10}
Decomposed granite	0.4	0.05	0.067	2.68	1650	1.0×10^{-2}
Weathered granite	0.3	0.02	0.145	2.68	1650	1.0×10^{-4}
Granite	0.01	0.001	0.34	1.4	2700	1.0×10^{-7}

θ_s is saturated water content [L^3L^{-3}], θ_r is residual water content [L^3L^{-3}], α is related to the inverse of the air entry suction, $\alpha > 0$ [L^{-1}], n is a measure of the pore-size distribution, $n > 1$ (dimensionless), bulk density is given in units of [Kgm^{-3}], and K is hydraulic conductivity [ms^{-1}].

Appendix F

LAI values for each of the three types of vegetation, grassland, shrubland and forest, are cyclical at an annual scale. Below are the monthly values for each vegetation type.

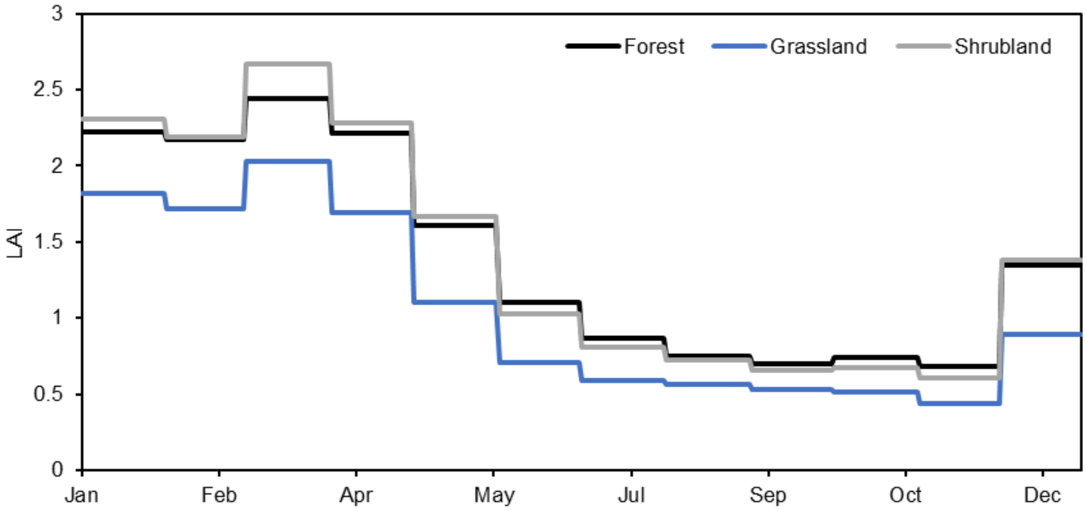

RD values for grassland, shrubland and forest are constant at 0.5 m, 0.1 m and 0.75 m, respectively.